Microarray investigation of the role of *Pax6* at the PSPB using a novel tauGFP-Pax6 reporter mouse

By

Catherine Carr

Thesis submitted for the degree of doctor of philosophy at the University of Edinburgh

2008

Disclaimer

I, Catherine Carr, performed all of the experiments presented in this thesis unless otherwise clearly stated. In particular I would like to acknowledge the work of Alan Ross and Thorsten Forster for their assistance with the microarray hybridizations and data analysis described in chapter 4. I would also like to acknowledge the help of Mi Da in carrying out the *in situ* hybridizations in chapter 6. No part of this work has been or is being submitted for any other degree or qualification.

Signed:

Date:

Acknowledgements

There are many people without whom this project would have faltered and died long before it reached its conclusion. I would like to thank Dave Price and John Mason for being such excellent supervisors and for their unfailing patience and support throughout my time in Edinburgh.

There are many people without whose invaluable technical support and advice the microarray experiment could not have succeeded. I would like to thank Shonna Johnston, Jan Vrana and Simon Monard for all their help with cell sorting and flow cytometry. I owe a dept of gratitude to Jan in particular for sorting all of the samples used in the microarray experiment and for his constant good humour and patience in spite of many last minute cancellations on my part. I would also like to thank Austin Smith and Brian Hendrich for providing me with a bit of bench space for RNA extractions. The technical expertise of the members of the CGTI was critical to the success of this experiment. Special thanks go to Alan Ross, who carried out the array hybridizations, Thorsten Forster for normalisation and statistical analysis and Gary Rubin for helping to coordinate it all.

I would like to thank Linda Wilson and Trudi Gillespie for help with confocal microscopy. I am also very grateful to the BRR staff who looked after the animals, especially Peter, Scott, Adrian, Neil, Louise and Duncan.

The members of DBUG, past and present, have been instrumental in creating a working environment that is second to none in terms of friendliness and the ready availability of help, both in terms of technical assistance and more general support. In particular I would like to thank Ian Simpson, Katy Gillies, Mike Molinek, Mark Barnett, Tom Pratt and Vassiliki Fotaki for sharing their expertise in a variety of areas. The *in situs* shown in chapter 6 could not have been completed without the very generous help of Mi Da to whom I am greatly indebted.

Chris, Tammy, JohnD and Lasani – the writers' lunches were a wonderful haven in which to moan and share ideas; I hope there are many more lunches with less stressful themes! The members of the Spears' coffee club: Norah, Alison, Rowena, Katy, Louise, Mike, Jane, Tammy, Pan, JohnD, Dominic, Derek, Viv and Grace; for understanding that coffee time should be written in stone and that life is better when there's time for a chat. Petrina, Natasha, Leah and various others (too many to mention, but many of them mentioned above), for pints and poker and many other social occasions. What would life be without wigs and hats and dancing on tables?

Gordon, Fanney, Simon, and Tom provided a superb escape from the trials of research into the weird and wonderful world of anatomy teaching – there are so few workplaces where no one bats an eye if you want to waltz with a skeleton! I would also like to thank Iain for all the bizarre conversations, not least about 'guy fawking of the leg' – I won't forget that excuse!

I would like to thank my dear and wonderful sisters Cella and Mary for telephone dinners, the long distance sharing of bottles of wine and the relentless pursuit of that last elusive answer in the cryptic crossword. May the three graces be reunited often in beautiful places the world over. My magnificent brothers too, Patrick, Jim and Ambi, for phone calls and get-togethers along the way. Most importantly I would like to thank my parents Ambrose and Bríd for their continued support and their unwavering belief that I could achieve whatever I set my mind to.

Ní neart a cur le chéile.

Abstract

Pax6 encodes a highly conserved transcriptional regulator that is widely expressed during development of the eye, olfactory bulbs and central nervous system. *Pax6*$^{-/-}$ mice exhibit severe brain defects, lack eyes and nasal structures, and die at birth. Included among the functions of *Pax6* are cell adhesion, cell cycle progression, axon guidance and boundary formation. The pallial-subpallial boundary (PSPB) is both a physical and gene expression boundary separating dorsal and ventral telencephalon. Pax6 is required for this boundary to develop. In *Pax6*$^{-/-}$ embryos, genes which normally have a sharp border of expression at the PSPB become ectopically expressed and the radial glial fasicles that make up the physical component of the boundary fail to form. There is also an increase in the number of interneurons migrating dorsally across the boundary to enter the cortex while corticofugal axons struggle to cross the PSPB and enter the ventral telencephalon. Here a novel tauGFP-Pax6 reporter mouse, *DTy54*, is described in which cells capable of expressing *Pax6* are tauGFP positive. In general the expression pattern of tauGFP corresponds well with the known Pax6 expression pattern in the eye and forebrain and the gradient of cortical Pax6 expression from high rostro-laterally to low caudo-medially is also recapitulated by tauGFP. The cytoskeletal localisation of the tauGFP also labels cellular processes and the axons projecting from Pax6 positive cells such as those forming the optic nerve can be clearly seen. At E10.5 the forebrain expression patterns of tauGFP and Pax6 correspond exactly, but at later stages tauGFP expression can be seen in areas negative for Pax6. This can be seen at E12.5 in the ventral telencephalon and in both the dorsal and ventral telencephalon at E15.5. Pax6 and tauGFP expression colocalise more closely in the diencephalon. *In situ* hybridization analysis of *Pax6* and *tauGFP* transcripts suggests that many of the discrepancies in expression seen at the protein level are due to a longer protein half-life for tauGFP than for Pax6. The expression of tauGFP allows the PSPB to be accurately dissected. The cells from this region can then be sorted by FACS to isolate cells expressing high levels of tauGFP and enrich for the Pax6 positive population. Microarray analysis of gene expression is this population of cells in *Pax6*$^{+/+}$*.DTy54*$^{+}$ and *Pax6*$^{sey/sey}$*.DTy54*$^{+}$ embryos is described here. This analysis identified many genes that show a significant change in expression at the PSPB in the absence of Pax6 expression including *Ngn2*, *Lhx6*, *Neurod6* and *CyclinD1* and *2*. The biological processes and molecular functions in which these genes are involved were examined to provide insight into the role of *Pax6* in this population of cells. Several processes previously reported to be regulated by *Pax6* were identified together with a number of novel processes with which *Pax6* has not formerly been associated. Some of these include cell cycle, neurogenesis, transcription and metabolic and signalling pathways. This study has also identified many novel downstream targets of *Pax6*, such as *Sema3G* and *PlexinA4*, which will help to elucidate the genetic basis for the *Pax6*$^{sey/sey}$ phenotype at the PSPB. The changes in expression levels of *Ngn2*, *Lhx6* and *Gsh2*, identified by microarray, were validated by *in situ* hybridization, which showed a good correspondence with the microarray results.

Abbreviations

ANR – anterior neural ridge

AP – anterior-posterior

BAC – bacterial artificial chromosome

cDNA – complementary deoxyribonucleic acid

ChIP – chromatin immunoprecipitation

CNS – central nervous system

DamID – DNA adenine methyltransferase identification

DNA – deoxyribonucleic acid

DV – dorsoventral

E – embryonic day

EBSS – Earle's balanced salt solution

FACS – fluorescence activated cell sorting

GFP – green fluorescent protein

GO – Gene Ontology

IZ – intermediate zone

KEGG – Kyoto Encyclopaedia of Genes and Genomes

LCS – lateral cortical stream

LGE – lateral ganglionic eminence

MGE – medial ganglionic eminence

mRNA – messenger ribonucleic acid

p – prosomere

pA – polyadenylation

PBS – phosphate buffered saline

PC – posterior commissure

PCR – polymerase chain reaction

PSPB – pallial-subpallial boundary

r – rhombomere

RIN – RNA integrity number

RNA – ribonucleic acid

RT-PCR – reverse transcriptase-coupled polymerase chain reaction

SAGE – serial analysis of gene expression

Sey – small eye

SVZ – subventricular zone

TPOC – tract of the postoptic commissure

VZ – ventricular zone

YAC – yeast artificial chromosome

Table of Contents

Chapter 1 – General Introduction

1.1 Early development of the brain

The brain develops from the broad cranial end of the neural plate, which is composed of a thick layer of pesudostratified columnar neuroectoderm cells. Indentations in this region mark out the three presumptive primary brain vesicles; the prosencephalon, mesencephalon and rhombencephalon. Beginning on embryonic day 7.5 (E7.5) in mice, the neural plate undergoes a process called neurulation in which it folds along the craniocaudal axis so that its lateral edges meet in the dorsal midline, forming the hollow neural tube. Neurulation is completed by the closing of the cranial and caudal neuropores (Rossant and Tam, 2002). The space enclosed by the neural tube is the neural canal, which gives rise to the ventricles of the brain and persists as the central canal of the spinal cord. Along its entire length the neural tube is divided into four longitudinal divisions; the floor, basal, alar and roof-plates. The telencephalon develops at the most rostral end of the neural tube and from early stages can be seen to be divided into dorsal and ventral regions. The doral part of the telencephalon is the pallium and gives rise to the cerebral cortex, while the ventral telencephalon is composed of the subpallium and this gives rise to the basal ganglia (Rossant and Tam, 2002; Fig. 1.1).

At E9 swellings of the brain vesicles divide them into neuromeres, with neuromeric boundaries defined both by morphological structures and gene expression patterns (Puelles and Rubenstein, 1993; Rubenstein *et al.,* 1994). The prosomeric model uses these neuromeric divisions to describe the developing brain in terms of distinct segments. According to this model the three primary brain vesicles are subdivided as follows: The prosencephalon is divided into six prosomeres, numbered p1-6, with p6 being the most rostral. Within the rhombencephalon nine rhombomeres are formed; r1-8 and the rostral isthmus. R8 is the most caudal of the rhombomeres. The mesencephalon remains undivided. These divisions are defined by morphological landmarks combined with gene expression patterns; with sharp borders of expression corresponding with the divisions of the model. From E12 the five secondary brain vesicles can be distinguished. The telencephalon and diencephalon are prosencephalic derivatives with p1-3 making up the diencephalon and p4-6 the

telencephalon (Bulfone *et al.,* 1993). The mesencephalon remains unchanged and the rhombencephalon gives rise to the metencephalon (r1) and myelencephalon (r2-7).

A number of problems have been encountered in applying the prosomeric model to the rostral forebrain. In this region gene expression patterns do not clearly define the the boundaries between the putative prosomeres. In order for a boundary to truly delimit one prosomere from another it must completely traverse the neural tube from roof- to floor-plate and this is not the case with the putative boundaries in the rostral forebrain (Puelles and Rubenstein, 2003). There are also patterning effects seen here, which are not found elsewhere in the developing brain, and that result in the formation of oblique boundaries unique to the rostral forebrain. To account for this, a simplified model has been suggested (Puelles and Rubenstein, 2003). In this model p1-3 remain essentially unaltered with p1 comprising the pretectum, p2 the dorsal thalamus and epithalamus and p3 the ventral thalamus and eminentia thalami. P4-6 are no longer classified as 3 distinct prosomeres, instead the secondary prosencephalon is regarded as a single histogenetic field comprising the telencephalon and hypothalamus (Puelles and Rubenstein, 2003). The longitudinal divisions of the neural tube, the floor, basal, alar and roof-plates, remain unchanged. The neuromeric divisions of the developing brain as defined by this modified model are outlined in Figure 1.2.

1.2 Regulation of forebrain development by signalling molecules

Patterning occurs along three axes of the developing brain; the anterior-posterior (AP) axis, medial-lateral axis and the dorso-ventral (DV) axis (Fig. 1.3). The major signalling centres and the signalling molecules they produce are shown in Figure 1.3 A. Signalling centres for medial-lateral patterning most likely lie along the edges of the cortex. The cortical hem, for example, which comprises the medial edge of the cortex, has been shown to express members of the *Wnt* and BMP gene families (Furuta *et al.,* 1997; Grove *et al.,* 1998). Putative signalling centres for patterning along the AP axis include the anterior neural ridge (ANR) and anteromedial telencephalon (Shimamura and Rubenstein, 1997; McWhirter *et al.,* 1997).

Figure 1.1: Dorso-ventral division of the telencephalon

Schematic diagram of a coronal section through the left telencephalic vesical of the mouse forebrain at E12.5 showing the division into dorsal and ventral regions. The dorsal pallium will give rise to the cerebral cortex while the ventrally lying subpallium gives rise to the basal ganglia.

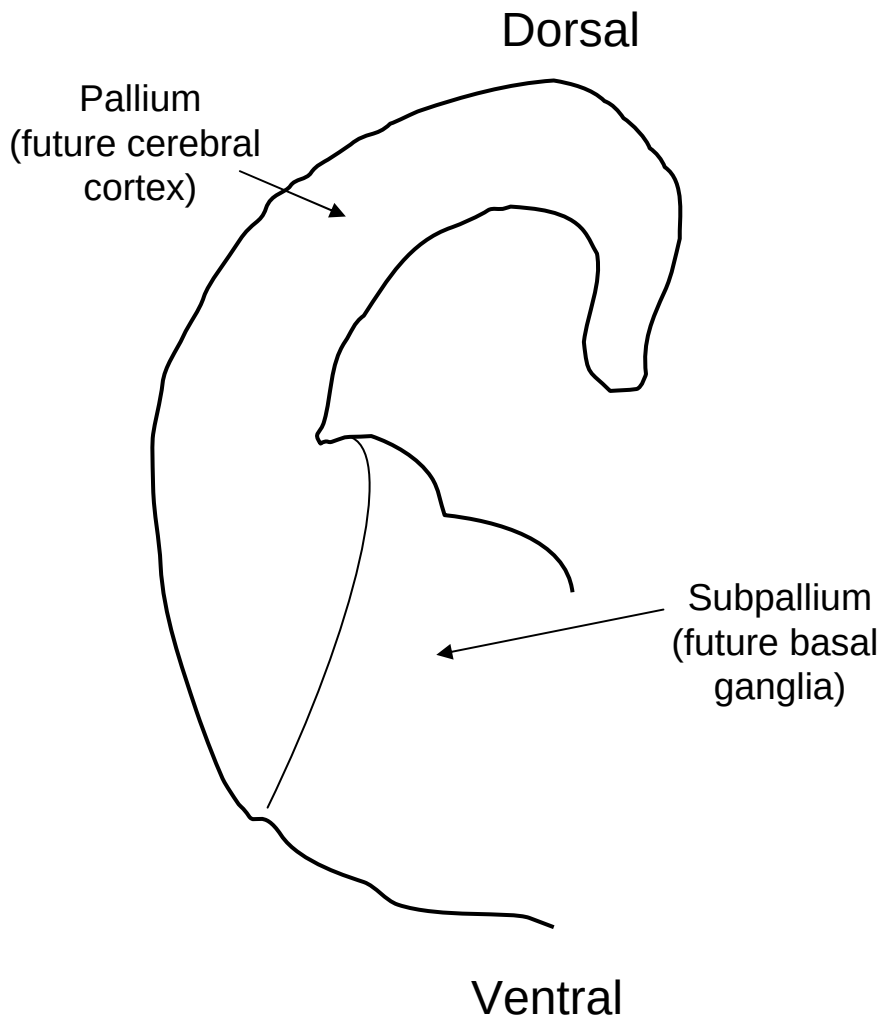
Dorsal
Pallium
(future cerebral
cortex)
Subpallium
(future basal
ganglia)
Ventral

Figure 1.1

Figure 1.2: Neuromeric divisions of the developing brain

Schematic medial view of the embryonic mouse brain at E12.5 showing the prosomeric divisions. Transverse and longitudinal boundaries are shown in blue. Acx, archicortex; cge, lge, mge, caudal, lateral and medial ganglionic eminences; dt, dorsal thalamus; et, epithalamus; emt, eminentia thalami; is, isthmus; m, mesencephalon; ncx, neocortex; ob, olfactory bulb; pt, pretectum; vt, ventral thalamus. (Adapted from Bulfone *et al.,* 1993)

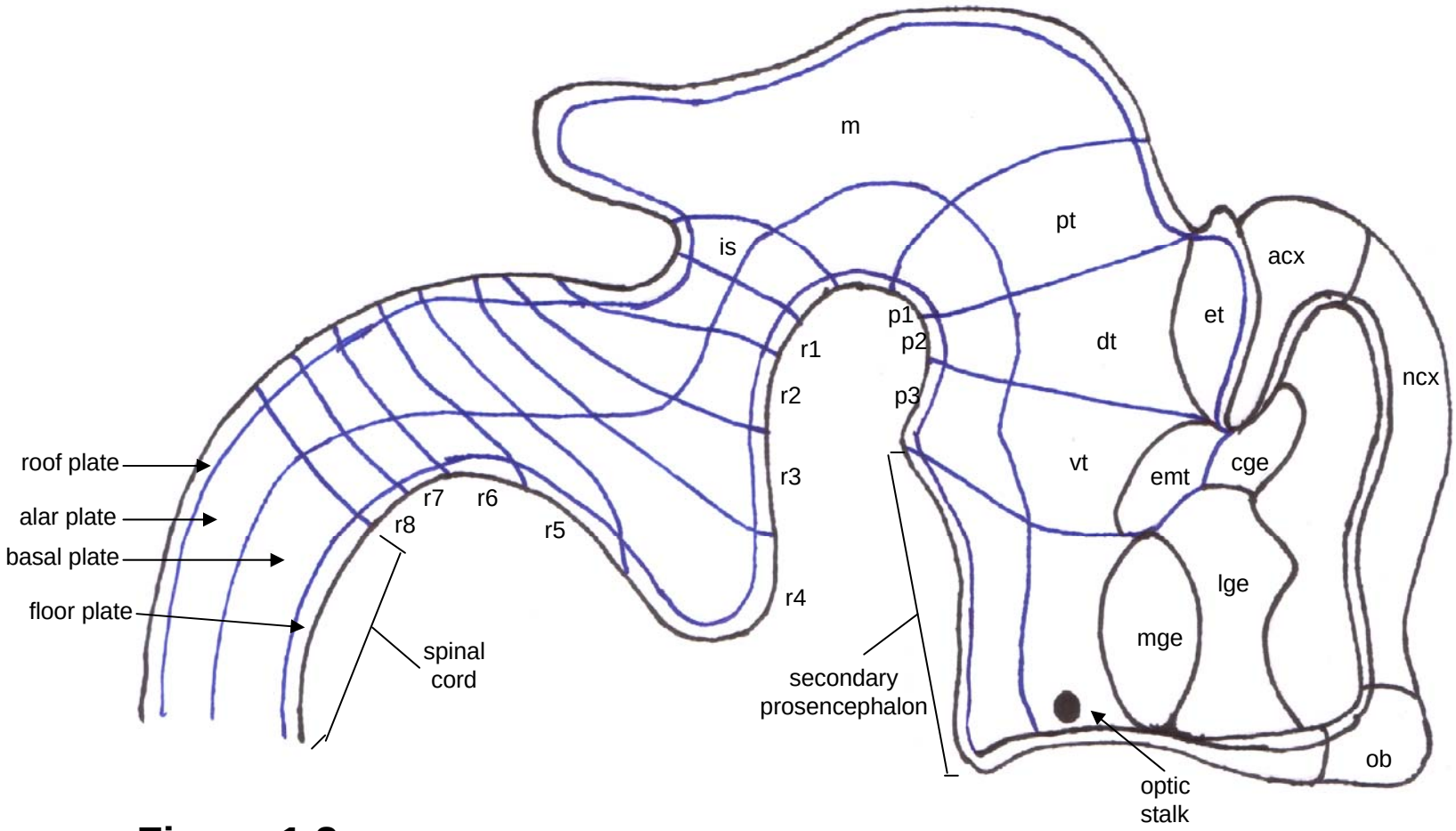
m
pt
is
acx
et
p1
p2
dt
r1
ncx
r2
p3
roof plate
r3
vt
emt
cge
alar plate
r7
r6
r8
r5
basal plate
lge
r4
floor plate
mge
spinal
cord
secondary
prosencephalon
ob
optic
stalk

Figure 1.2

Figure 1.3: Schematic representation of forebrain signalling centres and the dorso-ventral divisions of the telencephalon

(A) Schematic diagram of the mouse forebrain at E11.5, viewed from the dorsal side, anterior is up. Signalling centers, the signalling molecules they produce and their likely directions of diffusion are shown. FGFs (black arrows) are expressed in the anterior neural ridge and then in the anteromedial telencephalon. Wnts and BMPs (hatched arrows) are expressed in the cortical hem at the caudomedial edge of the cortex. Dotted arrows indicated possible cortical patterning signals from lateral and posterior sources, which may include TGF-α and Shh. The red arrow indicates the anterior-posterior axis of development. (A was adapted from Ragsdale and Grove 2001). (B) shows a coronal section cut through the left telencephalic vesical at E11.5-E12.5. The dorso-ventral divisions of the telencephalon are labelled and the locations of the cortical angle and pallial-subpallial boundary are indicated. Red arrows indicate the medial-lateral and dorso-ventral axes of developmental patterning.

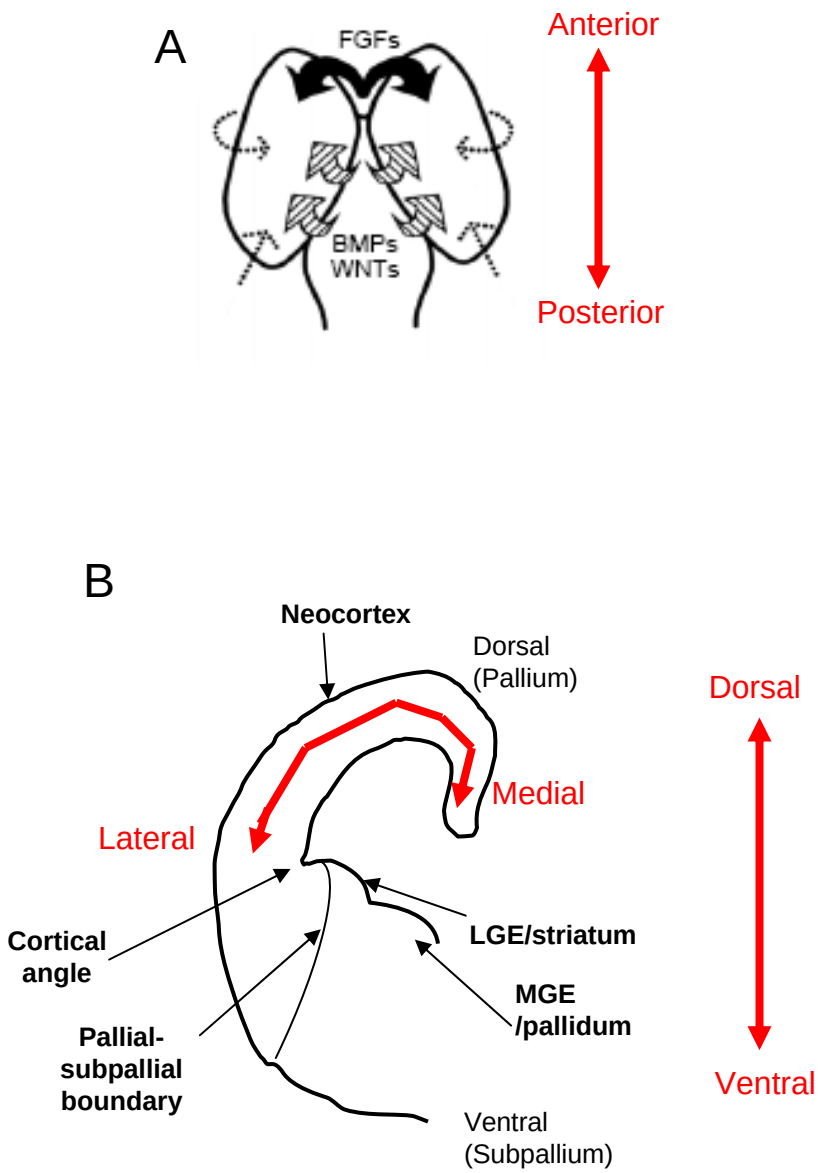
A
FGFs
BMPs
WNTs
Anterior
Posterior
B
Neocortex
Dorsal
(Pallium)
Medial
Lateral
Cortical
angle
LGE/striatum
MGE
/pallidum
Pallial-
subpallial
boundary
Ventral
(Subpallium)
Dorsal
Ventral

Figure 1.3

DV patterning occurs after the AP pattern has been laid down. The DV axis is patterned by signalling molecules produced initially in the adjacent ectoderm and axial mesoderm and later in the roof and floor plates of the neural tube (Ericson *et al.,* 1995; Furuta *et al.,* 1997; Monuki *et al.,* 2001). Dorsal cell fates are induced by *transforming growth factor-β* (*Tgfβ*) family members, while ventral fates are induced by *sonic hedgehog* (*Shh*) (Ericson *et al.,* 1995; Hébert *et al.,* 2002; for review see Wilson and Rubenstein 2000; Ragsdale and Grove, 2001; Campbell, 2003).

1.2.1 Medial-Lateral Patterning

The cortical hem at the medial edge of the cortex expresses multiple *Wnt* genes as well as members of the BMP and *Msx* gene families (Furuta *et al.,* 1997; Grove *et al.,* 1998). It is located between the developing hippocampus and choroid plexus, making it an ideal source of patterning signals for the development of both these structures. The delineation of the cortical hem by the expression of *Wnt* genes can be seen from E12.5 (Grove *et al.,* 1998). Wnt signalling has been shown to be required for the specification of hippocampal cells and in *Wnt3a* mutant embryos the hippocampus fails to develop (Lee *et al.,* 2000*)*. The signalling molecules of the cortical hem also have a role in establishing gene expression patterns along the medial-lateral axis of the dorsal telencephalon. The transcription factor *Emx2*, which is expressed in a graded high posteromedial to low anterolateral pattern across the neocortex (Bishop *et al.,* 2000, 2002; Muzio *et al.,* 2002) has an enhancer that is a direct target of BMP and Wnt signalling and these signalling pathways act together to regulate the gradient of *Emx2* expression (Theil *et al.,* 2002). At E8.5 canonical Wnt signalling occurs through much of the dorsal telencephalon but from E10.5 this activity retracts caudomedially so that by E12.5 it is only present in the cortical hem (Machon *et al.,* 2007). The progression of neurogenesis in the dorsal telencephalon is complementary to this retraction of Wnt signalling (Machon *et al.,* 2007).

A further source of signalling molecules is the cortical antihem which lies along the lateral edge of the developing cortex at the junction between the dorsal and ventral telencephalon. The curve of the antihem mirrors the curve of the cortical hem and together they demarcate the medial and lateral limits of the cortical ventricular zone

(Assimacopoulos *et al.,* 2003). The antihem expresses the epidermal growth factor (EGF) family members *Tgfα*, *Neuregulin 1* (*Nrg1*), and *Nrg3* along with *Fgf7* and the Wnt antagonist *secreted frizzled-related protein 2* (*Sfrp2*). The expression of EGFs is not confined to the antihem; they are expressed in graded patterns, with the antihem showing the highest level of expression for each of the three genes. The location of the antihem at the pallial-subpallial boundary (PSPB) allows it to influence medial-lateral patterning of the developing cortex as well as the DV patterning of telencephalon as a whole (Fig. 1.3 B). The EGFs expressed in the antihem may also be involved in the regulation of migration of cortical interneurons from their source in the ventral telencephalon to the cortex (Assimacopoulos *et al.,* 2003).

1.2.2 Dorso-Ventral Patterning

Along the DV axis the telencephalon is divided into a ventral subpallial and dorsal pallial region. These regions give rise to the basal ganglia and the cerebral cortex respectively. The neuroepithelium of the pallium is the source of the cortical projection neurons while most interneurons migrate into the cortex from the subpallium (Porteus *et al.,* 1994; DeCarlos *et al.,* 1996; Tamamaki *et al.,* 1997; Zhu *et al.,* 1999). As the DV pattern is established, different regions become characterised by distinct gene expression patterns. For example dorsal telencephalic progenitor cells express members of the *Emx* gene family while ventral telencephalic progenitors express *Nkx2.1* and *Dlx* family members (Wilson and Rubenstein, 2000). The PSPB, defined by gene expression patterns, does not lie at the cortical angle where the pallium and lateral ganglionic eminence (LGE) meet (Fig. 1.3 B). Instead it is located in the dorsal-most part of the LGE and is marked by the restricted expression of transcription factors such as *Pax6* and *Dbx* on the pallial side and *Gsh2* and *Nkx2.1* on the subpallial side (Toresson *et al.,* 2000; Yun *et al.,* 2001). These patterns of gene expression are established by members of the *Tgfβ* and *hedgehog* (HH) families of signalling molecules, which are critical in patterning the DV axis.

The *Tgfβ* family members involved in DV patterning are BMPs. BMPs are expressed in the roof plate of the developing neural tube and confer a dorsal identity

on cells (Furuta *et al.,* 1997; Hébert *et al.,* 2002). They are required for the formation of the dorsal midline structures such as the choroid plexus and the hippocampus. In the absence of BMP signalling these structures fail to form, although other aspects of dorsal patterning, such as the establishment of the cortical hem, still occur suggesting a role for other signalling molecules in the generation of dorsal cells (Hébert *et al.,* 2002). Further evidence of the importance of BMP signalling for the development of the dorsal midline is provided by the phenotype of mice lacking BMP receptors 1a and 1b. These mice suffer from holoprosencephaly, with dorsal midline structures completely absent and impaired specification of ventral telencephalic cells (Fernandes *et al.,* 2007). *Wnt* family members are expressed in the dorsal midline and also in the VZ of the pallium and at the PSPB (Grove *et al.,* 1998; Kim *et al.,* 2001). Together BMPs and *Wnts* act to regulate the expression of dorsal-specific transcription factors such as *Emx1*, *Emx2* and *Lhx2* (Monuki *et al.,* 2001; Theil *et al.,* 2002). Expression of *Wnt7b* and its inhibitor *Sfrp2* at the PSPB suggests that Wnt signalling may be involved in the formation of this boundary (Kim *et al.,* 2001).

Specification of ventral cell types at all AP levels of the neural tube occurs in response to *Shh* signalling (Fuccillo *et al.,* 2004). Shh, produced in the mesoderm beneath the neural tube and in the ventromedial cells of the forebrain, acts in a concentration dependent manner to induce specific cell types at different positions along the DV axis (Ericson *et al.,* 1995). This can be most clearly seen in the developing spinal cord where cells express floor plate marker genes in response to high levels of Shh, while at much lower levels Shh induces the differentiation of cells into motor neurons (Roelink *et al.,* 1995). The medial ganglionic eminences (MGEs) fail to form in the absence of *Shh* and *Nkx2.1* expression is lost. Development of the lateral ganglionic eminences (LGEs) still occurs however, suggesting that in the telencephalon *Shh* is essential for ventromedial patterning while more lateral fates can be produced in its absence (Rallu *et al.,* 2002).

In *Shh* null mutants the development of the telencephalon is extremely abnormal and by birth it cannot be recognised without the use of telencephalic-specific markers

(Rallu *et al.,* 2002; Fuccillo *et al.,* 2004). In mammals the *Gli* transcription factors are the only known mediators of the HH signalling pathway, and of these the repressor form of Gli3 is the only one that has been shown to be involved in DV patterning (Rallu *et al.,* 2002). The interaction between Shh and Gli3 is mutually antagonistic with Shh repressing Gli3 in ventral regions of the neural tube and Gli3 repressing Shh in dorsal regions.

The importance of this interaction can be inferred by the phenotype of *Shh/Gli3* double mutants which is less severe than that of mutants for either gene on its own. *Nkx2.1* expression (lost in the *Shh* mutant) is restored in the double mutant and a morphologically distinct MGE can be identified (Rallu *et al.,* 2002). Compared with the *Gli3* single mutant the improved phenotype of the double mutant also suggests that the patterning defects seen in the *Gli3* mutant are caused, in part at least, by increased Shh signalling. The fact that DV patterning can be established in the absence of both *Gli3* and *Shh* indicates that a second pathway, that is independent of *Shh*, must be involved in patterning the telencephalon along the DV axis.

A potential signalling molecule for *Shh*-independent DV patterning is Fgf8. *Fgf8* expression is lost in *Shh* mutants, but is upregulated in *Gli3* mutants (Kuschel *et al.,* 2003). *Gli3* mutants show ventralisation of the dorsal telencephalon with the loss or reduction of *Emx1* and *Emx2* transcription. In vitro, in the absence of *Shh*, *Fgf8* has been shown to induce ventral marker genes such as *Mash1* and *Dlx2* in dorsal telencephalic explants and to suppress *Emx1* expression (Kuschel *et al.,* 2003). The signalling centres that pattern the forebrain have been shown to interact and FGF signals are normally antagonised by BMP signalling (Shimogori *et al.,* 2004; Storm *et al.,* 2006). The loss of BMP expression in *Gli3* mutants allows *Fgf8* to cause the development of rostroventral structures at the expense of the dorsomedial telencephalon (Kuschel *et al.,* 2003).

1.2.3 Anterior-Posterior Patterning

AP patterning of the neural tube is largely established through the actions of FGFs. *Fgf8* is expressed in the ANR and anteromedial telencephalon while the FGF

receptors *Fgfr1*, *2* and *3* are expressed in a graded pattern along the AP axis of the developing neocortex (Fukuchi-Shimogori and Grove, 2001). *Fgf8* induces the development of the rostral telencephalon and its overexpression in the ANR causes the anterior neocortical domain to increase in size by shifting boundaries, defined by cadherin expression, posteriorly along the AP axis. This expansion occurs at the expense of the more posterior occipital domains, which contract so that the total AP length remains unchanged (Fukuchi-Shimogori and Grove, 2001). Conversely if *Fgf8* expression is reduced there is a decrease in the frontal domain with a corresponding increase in the size of more posterior regions, as their boundaries are shifted anteriorly.

1.3 Regulation of forebrain development by transcription factors

The signalling molecules that establish the pattern of the forebrain do so by regulating the expression of different transcription factors in specific areas of the forebrain. These transcription factors in turn control the expression patterns of other genes, allowing distinct areas of the forebrain to express unique subsets of genes. This generates the genetic diversity seen in areas of the forebrain that are programmed to perform different functions. Examples of some of the diverse roles of specific transcription factors are given below.

Gli3 expression is essential for maintaining the molecular identity of the dorsal telencephalon. Gli3 is a mediator of the Shh signalling pathway and has long been thought to prevent the ventralisation of dorsal regions of the telencephalon by Shh (Rallu *et al.,* 2002). More recent work by Rash and Grove (2007), however, suggests that the loss of dorsal fates seen in the absence of *Gli3* is due to the effects of FGF signalling which is increased in *Gli3* mutants. There is also evidence to suggest that *Gli3* expression is critical for the development of the boundary between diencephalon and telencephalon (Fotaki *et al.,* 2006). These two structures are joined abnormally in *Gli3* mutants with diencephalic tissue present in a region that one might expect to be dorsal telencephalon. This gives the appearance of ventralisation of this tissue as many ventral telencephalic marker genes are also expressed in the diencephalon (Fotaki *et al.,* 2006).

The loss of the dorsomedial telencephalon in *Gli3* mutants also results in the loss of the expression of BMPs and Wnts from the signalling centres in this tissue (Tole *et al.,* 2000). This results in a failure to correctly pattern the dorsal telencephalon with the early loss of *Emx1* expression (Tole *et al.,* 2000). This in turn affects *Pax6* expression which by E14.5 is greatly reduced (Kuschel *et al.,* 2003).

As BMPs and *Shh* are confined to dorsomedial and ventromedial regions respectively, other factors must be involved in mediating the patterning of more lateral aspects of the DV axis. *Pax6* and *Gsh2* have complementary expression patterns in the developing telencephalon, where they act to repress each other. *Pax6* is expressed in the cortical VZ and in the lateralmost part of the LGE to the level of the PSPB. On the subpallial side of this boundary *Gsh2* is expressed in the VZ of both the LGE and MGE (Toresson *et al.,* 2000; Yun *et al.,* 2001). Both genes are expressed in graded patterns with the highest levels of expression at the PSPB. In the absence of Pax6 the PSPB doesn't form correctly and a number of signalling molecules expressed at this boundary, including *Wnt7b* and *Sfrp2*, are lost (Kim *et al.,* 2001; Assimacopoulos *et al.,* 2003). The antihem signalling centre is thereby completely lost in *Pax6* mutants. *Pax6* mutants also show ectopic expression of ventral markers such as *Mash1* and *Dlx* genes in the developing cortex, where they are normally repressed through the maintained expression of *neurogenin 1* and *2* by *Pax6* (Toresson *et al.,* 2000).

1.4 *Pax6* and its role in eye and forebrain development

1.4.1 The *Pax6* gene

Pax6 is a member of the paired-box family of transcription factors and therefore has two DNA binding domains – the paired-domain and the homeodomain. These domains are separated by a glycine-rich linker sequence and can bind DNA both independently and cooperatively (Callaerts *et al.,* 1997; Jun and Desplan, 1996; for reviews of *Pax6* see Simpson and Price 2002; Manuel and Price 2005). The paired box domain, which characterises the *Pax* gene family, was first discovered in the *Drosophila* gene *paired* and was found to be conserved in a number of functionally

related genes including *gooseberry-proximal* and *-distal*, *Pox meso* and *Pox neuro* (Bopp *et al.,* 1986, 1989). The paired box was subsequently found to be conserved across a wide variety of species from turtle and zebrafish to mammals. The first murine *Pax* gene, *Pax1*, was identified in 1988 by Deutsch et al. using the paired box of *gooseberry-distal* to probe two mouse genomic libraries. Nine members of the *Pax* gene family have since been identified in both mouse and human (for review see Lang *et al.,* 2007).

Pax6 expression is first seen as early as embryonic day 8.5 (E8.5) in the mouse. It is widely expressed in the developing CNS including the forebrain, hindbrain, cerebellum and ventral neural tube (Grindley *et al.,* 1995; Walther and Gruss, 1991). It is also expressed in pancreatic islet cells (Sander *et al.,* 1997; St-Onge *et al.,* 1997), the developing olfactory system, and in the lens, cornea and retina of the developing eye (Grindley *et al.,* 1995; Quinn *et al.,* 1996). *Pax6* expression is critical for survival and *Pax6* null mice die immediately after birth. In these mice the eyes and nasal structures are absent and the diencephalon fails to innervate a severely malformed cerebral cortex (Hogan *et al.,* 1986; Hill *et al.,* 1991; Schmahl *et al.,* 1993; Pratt *et al.,* 2000).

1.4.2 Phenotypes of mutations in *Pax6*

The human condition aniridia and its homologous mouse phenotype, *small eye* (*Sey*), were long believed to be caused by mutations in the same gene. Analysis of a candidate gene for aniridia predicted that its protein product would have the characteristics of the paired box family of transcription factors (Ton *et al.,* 1991) and a murine cDNA was subsequently found that was 92% homologous to the candidate aniridia gene at the nucleotide level and produced an almost identical amino acid sequence (Ton *et al.,* 1992). Analysis of the *Pax6* gene in mice with a variety of *Sey* alleles confirmed that *Pax6* is the gene responsible for this phenotype (Hill *et al,* 1991). Identification of the *Drosophila* homolog of *Pax6*, *eyeless*, which is critical for eye formation in the fly, shows the high degree of functional conservation of this gene across species (Quiring *et al.,* 1994).

The conservation of *Pax6* function and the importance of its regulatory role during development are evident from the phenotypes caused by mutations in this gene. In mice, heterozygosity results in a decrease in eye size and ocular abnormalities including iris hypoplasia, corneal opacification and cataracts (Hogan *et al.,* 1988). Humans with heterozygous mutations in *PAX6* suffer from aniridia, displaying a variable eye phenotype similar to that seen in heterozygous mice, and so *Sey* mice provide a good model in which to study aniridia (Glaser *et al.,* 1990; van der Meer-de Jong *et al.,* 1990). There is also a variety of structural brain abnormalities associated with *PAX6* haploinsufficiency in humans. The pineal gland is frequently absent or abnormal. In a study of 24 subjects, only 4 had a pineal gland which was structurally normal (Mitchell *et al.,* 2003). The anterior commissure is often absent or hypoplastic and the corpus callosum may also be reduced in size (Sisodiya *et al.,* 2001). This decrease in the callosal area is possibly due to a decrease in the number of interhemispheric projection fibres. The anterior commissure also plays an important role in interhemispheric transfer, particularly of olfactory and auditory fibres. Studies have shown that aniridia patients frequently have reduced olfaction (Sisodiya *et al.,* 2001). There is also evidence of deficient auditory interhemispheric transfer in aniridia patients often, but not always, associated with an absent/hypoplastic anterior commissure and/or a reduced corpus callosum (Bamiou *et al.,* 2004).

1.4.3 *Pax6* and the dorso-ventral specification of the telencephalon

The telencephalon is divided into a ventral subpallial and dorsal pallial region and these give rise to the basal ganglia and the cerebral cortex respectively (Fig. 1.1). *Pax6* is expressed in dorsal regions of the telencephalon, throughout the population of cells dividing at the ventricular edge, and helps to delineate the PSPB, the earliest division to occur within this structure. Expression is much more limited to smaller groups of cells in the ventral telencephalon (Puelles *et al.,* 1999). Figure 1.4 shows the expression pattern of *Pax6* in the developing mouse forebrain between E11.5 and E15.5. As mentioned previously, the PSPB is located in the dorsal-most part of the LGE and is marked by higher/restricted expression of transcription factors such as

Figure 1.4: Schematic representation of the expression profile of *Pax6* in the wild-type developing forebrain from E11.5 to E15.5

(A and B) Coronal sections cut through the left telencephalic vesicle at E11.5–E12.5 and E15.5, respectively. Low levels of *Pax6* in the ventricular zone of the LGE are represented by the dotted area. (C and D) Parasagittal sections through the forebrain at E12.5 and E14.5 showing *Pax6* expression in the telencephalon and diencephalon, but not in the mesencephalon. In the cortex, *Pax6* is expressed in a rostro-lateral^{high} to caudio-medial^{low} gradient. Di, diencephalon; m, mesencephalon; t, telencephalon. (Adapted from Manuel and Price, 2005)

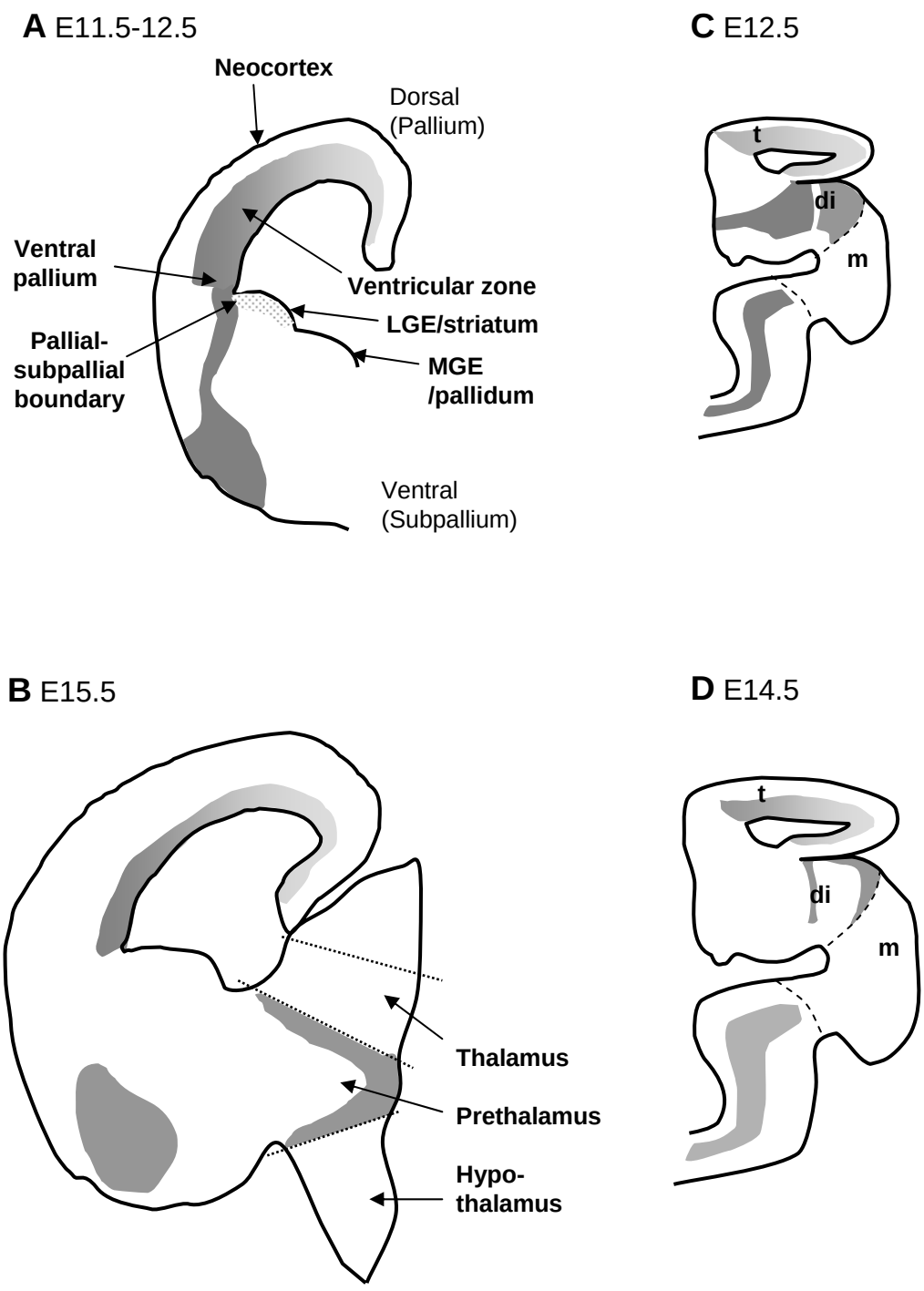
A E11.5-12.5
Neocortex
Dorsal
(Pallium)
Ventral
pallium
Ventricular zone
LGE/striatum
Pallial-
subpallial
boundary
MGE
/pallidum
Ventral
(Subpallium)
C E12.5
t
di
m
B E15.5
Thalamus
Prethalamus
Hypo-
thalamus
D E14.5
t
di
m

Figure 1.4

Pax6 and *Dbx* on the pallial side and *Gsh2* and *Nkx2.1* on the subpallial side (Stoykova *et al.,* 1996; 2000; Toresson *et al.,* 2000; Yun *et al.,* 2001). This boundary is marked by gene expression patterns as early as E9.5 (Toresson *et al.,* 2000; Yun *et al.,* 2001). A physical boundary also develops in this region in the form of radial glial fascicles which are most prominent at E16.5 in mice (Neyt *et al.,* 1997; Stoykova *et al.,* 1997). In the absence of Pax6 protein, both the physical and the gene expression boundaries are lost.

Cells from either side of the boundary have different adhesive properties due to the expression of different cadherins. Cells of the LGE, ventral to the PSPB, express *cadherin-6* while the cells of the developing cortex, dorsal to the boundary, express *R-cadherin* (Matsunami and Takeichi, 1995; Inoue *et al.,* 2001). The expression of *R-cadherin* is regulated in part by *Pax6*, with which its expression overlaps. In $Pax6^{Sey/Sey}$ embryos, *R-cadherin* expression is reduced in areas where the two genes are normally co-expressed, although levels are unaltered in other areas (Stoykova *et al.,* 1997). These differences in cadherin expression are important in maintaining the PSPB by restricting the mixing of pallial and subpallial cells, as shown by aggregation experiments (Stoykova *et al.,* 1997). Cortical and striatal cells, from mice aged between E12.5 and E14.5, tend to segregate if they are mixed *in vitro*. By E15.5 this region-specific adhesion is lost. In $Pax6^{Sey/Sey}$ mice the PSPB fails to form and cells from cortical and striatal regions in these animals fail to segregate if they are mixed between E12.5 and E14.5 (Stoykova *et al.,* 1997). This is due to an alteration in the adhesive properties of $Pax6^{Sey/Sey}$ cortical cells, as these cells segregate from wild-type cortical cells while striatal cells from wild-type and $Pax6^{Sey/Sey}$ mice still form mixed cell clusters.

Pax6 is only one of a large number of genes, both pallial and subpallial, whose expression is delimited by the PSPB. Other dorsal markers whose expression patterns have a sharp border at the PSPB include *Ngn2* and *Tbr1*, while ventral markers include *Gsh2*, *Dlx1*, *Vax1*, *Mash1* and *Six3* (Stoykova *et al.,* 2000). At E9.5, *Gsh2*, *Dlx1* and *Mash1* are expressed in progenitor cells of the LGE and MGE and by E10.5 they can be seen to be expressed most strongly adjacent to the PSPB (Toresson

et al., 2000; Yun *et al*., 2001). *Pax6* overlaps with *Gsh2* expression in the dorsal-most part of the LGE where it is expressed at low levels (Stenman *et al.,* 2003; Toresson *et al.,* 2000; Yun *et al.,* 2001), but it is very strongly expressed in the ventral pallium, on the dorsal side of the boundary, where it coincides with the strong expression of *Ngn2*.

Pax6 is critically important in establishing the PSPB. The PSPB fails to form in *Pax6*$^{-/-}$ mutant mice and marker genes no longer have a sharp expression boundary in this region (Stoykova *et al.,* 1996; Stoykova *et al.,* 2000). Several of these marker genes play complementary or cooperative roles to that of *Pax6* in establishing the PSPB, as is demonstrated by the phenotype of animals with various combinations of mutations in these genes. In the absence of Pax6 there is a dorsal expansion of subpallial markers which coincides with a downregulation of pallial marker genes. By E12.5 *Gsh2*, *Dlx* and *Mash1* are all ectopically expressed in the progenitor cells of the ventrolateral cortex (Toresson *et al.,* 2000; Yun *et al.,* 2001). This ectopic expression continues to expand dorsally so that by E14.5 it includes the ventricular zone (VZ) of the dorsolateral cortex (Toresson *et al.,* 2000). *Ngn 2* expression is lost in the areas of ectopic *Gsh2* expression and is downregulated in the remainder of the cortical VZ (Stoykova *et al.,* 2000; Toresson *et al.,* 2000; Kroll and O'Leary, 2005).

Gsh2 protects the ventral telencephalon from becoming dorsalised by repressing *Pax6* in the LGE (Toresson *et al.,* 2000; Yun *et al*., 2001). *Gsh2*$^{-/-}$ mice show a phenotype that is opposite to that of *Pax6*$^{Sey/Sey}$ embryos, with ectopic expression of the pallial markers *Tbr2*, *Ngn1* and *2* and *Pax6* in striatal progenitor cells at E10.5 (Toresson *et al.,* 2000; Yun *et al*., 2001). This ventral expansion of dorsally-expressed genes coincides with the loss of *Dlx* and *Mash1* from much of the LGE, where they are expressed at high levels in the wildtype. The misspecification of these cells is less pronounced at E12.5 and by E14.5 pallial genes are no longer ectopically expressed, possibly due to the effect of ectopic *Gsh1* expression (Yun *et al.,* 2001). *Gsh1* is normally only expressed in ventral parts of the LGE, but it is expressed more strongly in the *Gsh2* mutant and at later stages it expands into the dorsal LGE where it is thought to compensate for *Gsh2*, thereby reducing the

molecular abnormalities in the LGE. These mutants also have abnormalities in the differentiation of striatal cells and the developing olfactory bulb is reduced in size (Yun *et al.,* 2001).

In *Pax6*$^{-/-}$/*Gsh2*$^{-/-}$ double mutants, striatal development is improved compared with the *Gsh2*$^{-/-}$ single mutants. Cortical progenitors remain misspecified and continue to express ventral marker genes, as in *Pax6*$^{-/-}$ mice, although the double mutants do show an improvement in cortical plate formation. Neuronal migration, from the VZ to the cortical plate, is guided by the processes of radial glial cells (Anton *et al.,* 1996). Ectopic expression of *Gsh2* in more dorsal regions of the telencephalon may be involved in the alteration of radial glial cell morphology seen in *Pax6* mutants, thereby having a direct effect on the manifestation of migration defects seen in these embryos (Carić *et al.,* 1997; Toresson *et al.,* 2000). This may also account for the failure of the radial glial fascicles to form at the PSPB in the *Pax6* mutant.

Tlx is another gene that cooperates with *Pax6* in the formation of the PSPB. Although *Tlx* is expressed in VZ cells on both sides of the PSPB, *Tlx* loss-of-function mutants show a misspecification of the ventral pallium that is similar to, but less severe than, that seen in the *Pax6*$^{-/-}$ mutant (Stenman *et al.,* 2003). *Gsh2* expression is expanded dorsally so that its region of overlap with *Pax6* expression is wider than in wildtypes (Stenman *et al.,* 2003). A stream of migrating *Pax6*-positive cells, which appear to originate from the region of overlapping *Pax6* and *Gsh2* expression, extends out along the PSPB from the subventricular zone (SVZ) towards the pial surface as part of the lateral cortical stream (LCS). In the *Tlx* mutant, where this overlapping region is increased, a much wider stream of cells can be seen (Stenman *et al.*, 2003), while there is a marked decrease in these cells in the *Gsh2* mutant (Toresson *et al.*, 2000). *Ngn2* expression retracts dorsally, corresponding to the dorsal expansion of *Mash1*, while both *Dbx1* and *Sfrp2* expression are lost from the VZ of the ventral pallium. Heterozygous mutations in either *Pax6* or *Tlx* do not appear to have any effect on the development of the PSPB; however, compound heterozygotes display a mild phenotype with some ectopic *Gsh2* and *Mash1* positive cells present in the ventral pallium. The loss of one copy of *Pax6* on the *Tlx*$^{-/-}$

background results in a phenotype that, while worse than *Tlx*$^{-/-}$ on its own, is less severe than that of *Pax6*$^{-/-}$ mice (Stenman *et al.,* 2003). However, the loss of one or both copies of *Tlx* on the *Pax6*$^{-/-}$ background does not affect the patterning defects seen in *Pax6* mutants. This is probably due to a much broader requirement for *Pax6* than for *Tlx* in patterning the dorsal telencephalon.

1.4.4 *Pax6* in cortical development and neurogenesis

The neocortex develops from the prosencephalon at the rostral end of the neural tube. Its six-layered structure is formed by the migration of differentiated cells from the proliferative ventricular and subventricular zones. It develops from the inside out, with later born neurons migrating past earlier born neurons to form the outer layers (Angevine and Sidman, 1961; Rakic, 1974). When the earliest neurons are produced they become organised as the preplate, within which the cortical plate proper is laid down. As more and more cortical neurons migrate towards the pial surface, the preplate becomes divided into the superficial marginal zone and the deep subplate, with the developing cortical plate lying between these two layers (Marin-Padilla, 1978). As soon as they are generated, postmitotic neurons migrate away from the ventricular zone towards the developing cortical plate where they bypass older cortical plate neurons to take up more superficial positions, just deep to the marginal zone (Angevine and Sidman, 1961; Rakic, 1974). The neurons then associate into layers, with each layer containing neurons of a similar birth date (Rakic, 1974). In this way the six-layered structure of the neocortex is established with layer 2 composed of the latest born neurons. By birth the VZ has been lost, along with most of the cells of the subplate and marginal zone (Estivill-Torrus *et al.,* 2002).

In mice cortical neurogenesis begins around E11 (Levers *et al.,* 2001). The progenitor cells that produce the majority of the different cell types found in the cortex are located in the ventricular and subventricular zones. There are two main types of progenitor cells – radial glia and intermediate progenitor cells. Intermediate progenitor cells are also called basal progenitors as they divide away from the ventricular surface (Miyata *et al.,* 2004; Noctor *et al.,* 2004). They are derived from radial glial cells and can only give rise to neurons. Radial glia, on the other hand, are

multipotent precursors that divide at the ventricular surface and can give rise to both neurons and glia (Götz *et al.,* 1998; Heins *et al.,* 2002; Noctor *et al.,* 2001; 2002). Along with their role as progenitor cells, radial glial cells have other important functions in the developing brain. They are involved in neuronal migration and also in boundary formation and patterning of the cortex.

In the absence of functional Pax6 a number of defects occur during cortical neurogenesis. These result in the formation of a thin and disorganised cortical plate and the accumulation of neurons in the SVZ and IZ, where they from dense clusters (Schmahl *et al.,* 1993; Carić *et al.,* 1997). This phenotype results in part from migrational defects in late-born neurons (from E15). Early born neurons can migrate normally to the cortical plate (Schmahl *et al.,* 1993) and it is during the late stages of neurogenesis that cells can be seen to accumulate in the SVZ and IZ (Schmahl *et al.,* 1993; Carić *et al.,* 1997). These migrational problems are caused by a defect in the mutant environment rather than by a cell autonomous requirement for *Pax6* in late-born neurons and can be rescued by transplantation into a wildtype cortex (Carić *et al.,* 1997). The underlying defect is likely to be the changes in the morphology of radial glial cells that occur in the absence of Pax6 (Götz *et al.,* 1998). During normal corticogenesis the radial migration of neurons is guided by radial glial cells with which they form cell junctions and this method of migration becomes more important at later stages of cortical development (Anton *et al.,* 1996).

Pax6 is important not only for the correct migration of neurons to the cortical plate but also for the regulation of cell cycle parameters in the progenitor cell population (Götz *et al.,* 1998; Estivill-Torrus *et al.,* 2002; Manuel *et al.,* 2007; Quinn *et al.,* 2007). A shortening of the cell cycle at E12.5, early in corticogenesis, has been reported (Estivill-Torrus *et al.,* 2002), but a more recent study by Quinn *et al.* (2007) found no significant difference between wildtype and mutant progenitors at this age, probably due to the use of a different method to measure cell cycle length. Between E12.5 and E15.5 there is a more rapid increase in the proportion of cells dividing asymmetrically (to produce neurons) as opposed to symmetrically (to self-renew) in the *Pax6* mutant compared to wildtype (Estivill-Torrus *et al.,* 2002). This

observation corresponds well with the decrease in the number of cells re-entering S-phase at this age in *Pax6*$^{-/-}$, seen by Quinn *et al.* (2007). Concurrent with the decrease in S-phase re-entry is an increase in the proportion of differentiating neurons, suggesting that in the absence of functional Pax6 cortical progenitor cells exit the cell cycle early (Quinn *et al.,* 2007). Early cell cycle exit would also explain the decrease in neurogenic potential observed in cortical radial glial cells isolated from E14 *Pax6* mutant embryos (Heins *et al.,* 2002).

There is not only a requirement for *Pax6* expression in the proliferative cells of the developing cortex, the correct level of expression is also important, with changes in cell cycle kinetics observed both in the absence of Pax6 and when is expressed at higher than normal levels (Talamillo *et al.,* 2003; Manuel *et al.,* 2007; Quinn *et al.,* 2007). Analysis of *Pax6*$^{-/-}$↔*Pax6*$^{+/+}$ chimeric embryos shows that *Pax6*$^{-/-}$ cells segregate from wildtype cells by E10.5 (Talamillo *et al.,* 2003). In addition to this there is an under-representation of these cells in the hippocampus, cortex and dorsal LGE in chimeras at E12.5 (Quinn *et al.,* 2007). Over-expression of *Pax6* also affects corticogenesis causing a decrease in the thickness of the superficial cortical layers (Manuel *et al.,* 2007). *Pax77*$^{+}$ mice carry 5-7 copies of the human *PAX6* gene in YAC Y593 and show an increase in Pax6 protein levels specifically in the normal *Pax6* expression pattern. At E15.5 *Pax77*$^{+}$ embryos show a reduction in the proportion of S-phase cells and in the density of cells undergoing mitosis specifically in rostral and central parts of the cortex but not in caudal areas (Manuel *et al.,* 2007). In *Pax77*$^{+}$↔*Pax6*$^{+/+}$ chimeras there is an under-representation of *Pax77*$^{+}$ cells at all rostro-caudal levels of the cortical VZ and in the rostral IZ. This emphasises the importance of maintaining the correct level of *Pax6* expression if normal corticogenesis is to occur.

1.4.5 *Pax6* in the regulation of cortical arealisation

Pax6 and *Emx2* are expressed in opposing patterns along the medial-lateral axis of the developing cortex, with high levels of *Pax6* in rostro-lateral regions and of *Emx2* in caudo-medial areas (Bishop *et al.,* 2000; 2002). Emx2 and Pax6 proteins are required to establish this graded expression pattern and they also act to down-

regulate each other's activity (Muzio *et al.,* 2002). In this way *Emx2* and *Pax6* help to regulate the early regionalisation of the neocortex, although the importance of *Pax6* in this process is disputed by Manuel *et al.* (2007).

Emx2 and *Pax6* preferentially impart caudo-medial and rostro-lateral identities respectively. The expression patterns of the areal markers *Cadherin6* (*Cad6*) and *Cadherin8* (*Cad8*) show complementary changes in *Emx2* and *Pax6* mutants. *Cad6* marks the somatosensory and auditory areas while *Cad8* labels the more rostrally located motor area (Bishop *et al.,* 2000). In the *Emx2* mutant the expression pattern of these marker genes is shifted caudo-medially resulting in an expansion of rostro-lateral areas at the expense of caudo-medial regions which, while present, are greatly reduced in size. An opposite shift in cadherin expression patterns occurs in the *Pax6* mutant (Bishop *et al.,* 2000). If *Pax6* and *Emx2* were equally important in this process one might expect to see a caudo-medial shift in cortical patterning in *Pax6* over-expressing animals. Contrary to expectations however the position of the somatosensory area was unaltered in these animals compared to wildtype (Manuel *et al.,* 2007).

Emx2 and *Pax6* are also involved in establishing the expression patterns of *Wnt* genes in the cortical hem and this signalling centre is distorted in both *Emx2* and *Pax6* mutants (Muzio *et al.,* 2002). *Emx2* mutants also show down-regulation of *Wnt3a* and restriction of *Wnt8b* expression to a small region at the medial boundary of the cortex (Muzio *et al.,* 2002). In contrast *Wnt8b* expression is expanded along the medial-lateral axis of *Pax6* mutants, although the expression of *Wnt3a* remains unaltered.

A cortex specific knockout of *Pax6* allowed the effect of loss of Pax6 on cortical arealisation to be analysed at postnatal stages as these animals survive to adulthood, unlike $Pax6^{sey/sey}$ animals which die a birth. Expression analysis of regional markers in *Pax6* cortical knockout animals showed a rostral shift in the boundary between visual and somatosensory areas (Piñon *et al.,* 2008). The boundary between the

somatosensory and motor areas was also shifted rostrally and there was a severe decrease in the size of the frontoorbital/motor area (Piñon *et al.,* 2008).

1.4.6 The involvement of Pax6 in the development of forebrain axonal connections

Pax6 is important for the correct development of a number of the axonal tracts that connect different areas of the brain. The posterior commissure (PC) and the tract of the postoptic commissure (TPOC) are among the earliest tracts to develop and can be identified from E10.5. *Pax6* expression is required for the correct development of both these tracts (Grindley *et al.,* 1997; Mastick *et al.,* 1997; Andrews and Mastick 2003; Nural and Mastick 2004). The PC crosses the dorsal midline at the p1/mesencephalic boundary and is severely reduced in size in *Pax6* mutant embryos (Grindley *et al.,* 1997; Mastick *et al.,* 1997). In wildtype embryos at E10.5 a number of axon bundles can be seen crossing the midline in this region. These bundles are completely absent in *Pax6* mutants, although by E11.5 some axons can be seen crossing the midline in this area (Mastick *et al.,* 1997). The cells which do project to the PC in *Pax6* mutants are located in the ventral part of p1, suggesting that *Pax6* is only required for the projection of a subset of PC cells, those located in dorsal p1 (Mastick *et al.,* 1997).

At E9.5 cells at the base of the optic stalk begin to send out axons that will form the TPOC (Easter *et al.,* 1993). The course of the TPOC at E10.5 correlates well with the pattern of *Pax6* expression. Initially a tight axon bundle, the tract widens in p3 as axons fan out over an area defined by strong *Pax6* expression before narrowing again to cross the p2/p3 boundary (Mastick *et al.,* 1997). Axons of the TPOC display pathfinding errors in *Pax6* mutant embryos, specifically when navigating through p3 where they would normally encounter strong *Pax6* expression. Many axons wrongly enter the cerebral vesicle while others form loops or project ventral to the tract. Of the axons that reach the p2/p3 boundary, very few manage to cross it with the majority turning to run dorsally along the boundary (Mastick *et al.,* 1997). It seems likely that the role of *Pax6* in guiding the navigation of TPOC axons is mediated through *R-cadherin*. In *Pax6* mutants *R-cadherin* expression is lost from regions

where its expression overlaps with *Pax6*, including p3 where TPOC pathfinding errors occur. Electroporation of an *R-cadherin* expression construct into the *Pax6* mutant forebrain at E10.5 is sufficient to rescue the defects in TPOC navigation (Andrews and Mastick, 2003).

Two other major tracts disrupted in *Pax6* mutants are the thalamocortical and corticothalamic tracts. The axons of the thalamocortical tract begin to emerge from the dorsal thalamus at E13. The tract passes through the ventral thalamus then turns sharply to avoid the hypothalamus and enter the ventral telencephalon. In the ventral telencephalon axons pass through the internal capsule and arrive at the cortex around E15 (Braisted *et al.,* 1999). Formation of the thalamocortical tract is disrupted in *Pax6* mutants. Although the dorsal thalamus is present, and the tract does begin to project, it doesn't extend far into the ventral telencephalon and so never reaches its target cells in the cortex (Kawano *et al.,* 1999; Pratt *et al.,* 2000; Hevner *et al.,* 2002; Jones *et al.,* 2002). Co-culture experiments combined with analysis of $Pax6^{-/-} \leftrightarrow Pax6^{+/+}$ chimeras suggests that there is a cell autonomous requirement for *Pax6* in the dorsal thalamic cells whose axons form the thalamocortical tract (Pratt *et al.,* 2002). Cortical expression of *Pax6* is not required for the correct navigation of these axons as the thalamocortical tract forms normally in cortex specific *Pax6* knockout mice (Piñon *et al.,* 2008).

Corticothalamic axons navigate along the same pathway as thalamocortical axons, but in the opposite direction. In the absence of *Pax6* these axons also fail to reach their targets (Hevner *et al.,* 2002; Jones *et al.,* 2002). Corticothalamic axons have difficulties crossing the PSPB with most axons becoming displaced laterally when they encounter this boundary. In caudal regions some axons are able to cross the PSPB but they do so in abnormal fasciculations (Jones *et al.,* 2002). At E18.5 cortical axons can be seen forming an abnormal bundle in the basal forebrain, but these axons do not enter the thalamus (Hevner *et al.,* 2002). Difficulties crossing the PSPB may be due to changes in the cellular arrangement at this boundary. In the absence of *Pax6* the neuroepithelium of the PSPB is broad and irregular with cells more tightly packed than in wildtype (Jones *et al.,* 2002).

The expression of a number of axon guidance molecules is altered in the dorsal telencephalon in the absence of *Pax6* and this may contribute to the navigation difficulties of the thalamocortical and corticothalamic axons. The semaphorins *Sema3c* and *Sema5a* are both expressed in the pallium with highest expression seen adjacent to the PSPB. In *Pax6*$^{-/-}$ embryos pallial expression of *Sema3c* is abolished while *Sema5a* expression is lost at the PSPB, although it is still expressed at lower levels in more dorsal parts of the pallium (Jones *et al.,* 2002).

1.4.7 The role of Pax6 in the regulation of migration

The correct migration of neurons from the area in which they are produced to their final location in the cortex is a critical part of normal brain development with some neurons travelling significant distances from the area in which they are produced. Migration takes place along migratory pathways which are generally either radially or tangentially oriented. The projection neurons that populate the cortex of the telencephalon migrate radially from the ventricular and subventricular zones in which they are produced to the developing cortical plate where they come to rest in layers formed by cells of similar birthdates (Rakic, 1974). The majority of cortical interneurons are produced not in the cortical VZ but in the VZ of the ganglionic eminences (Anderson *et al.,* 1997; deCarlos *et al.,* 1996). These interneurons migrate tangentially across the PSPB, with cells originating in the MGE travelling in the intermediate zone before moving radially into the cortical plate while cells from the LGE pass initially into the cortical proliferative zone (Anderson *et al.,* 2001). Interneurons also migrate tangentially to the striatum and along the rostral migratory stream to populate the olfactory bulb.

Radial migration occurs either by somal translocation or by locomotion. Early born neurons that will go on to form the marginal zone, subplate and early cortical plate migrate mainly by somal translocation. These cells have their cell body located in the VZ and a leading process that extends to the pial surface, spanning more that half the depth of the cerebral wall. They migrate by shortening the leading process, causing the continuous advancement of the cell body (Nadarajah *et al.,* 2001).

During later developmental stages however, locomotion becomes more common perhaps due to the increase in the distance that must be travelled. The migration of locomotive cells is guided by radial glia with which they make specialised junctions (Anton *et al.,* 1996). Radial glial cells are bipolar cells whose cell bodies lie in the VZ with a short process extending to the ventricular surface and a much longer process spanning the depth of the cortex to reach the pial surface. This morphology allows them to guide the radial migration of newborn neurons away from the VZ to the correct layer of the developing cortical plate (Naradjah *et al.,* 2001). Locomotion is slower than translocation as movement is discontinuous with rapid forward movement alternated with periods of relatively slow progress (Nadarajah *et al.,* 2001). Many locomotive neurons complete their migrations by somal translocation. Once their leading process makes contact with the marginal zone their cell body moves to its correct location within the cortical plate by the shortening and thickening of this process (Nadarajah *et al.,* 2001).

Radial glia express different transcription factors depending on the region of brain in which they are located. Cortical radial glia, for example, express *Pax6* which is critical for the correct patterning of the telencephalon. Ectopic expression of *Gsh2* in more dorsal regions of the telencephalon may be involved in the alteration of radial glial cell morphology seen in *Pax6* mutants; thereby having a direct effect on the manifestation of the migration defects seen in these embryos (Carić *et al.,* 1997; Toresson *et al.,* 2000). Their processes become wavy with small branches, making them appear more like the radial glia of the ganglionic eminences where *Pax6* is not normally expressed (Götz *et al.,* 1998).

Tangentially migrating neurons in the proliferative zones on either side of the PSPB slow down as they approach the boundary region, probably in response to a short-range inhibitory signal (Neyt *et al.,* 1997). This role in limiting migration is not restricted to proliferative regions. The number of MGE/LGE derived GABAergic interneurons that enter the cortex is controlled by the PSPB and there is a significant increase in the number of dorsally migrating cells when the PSPB is lost in *Pax6* mutant mice (Chapouton *et al.,* 1999).

Sfrp2 is a *Wnt* antagonist which, in the region of the PSPB, appears to have a complementary expression pattern to *Wnt-7b* (Kim *et al.,* 2001). *Sfrp2* expression is confined to the cortical neuroepithelium where it overlaps with *Pax6* while *Wnt7b* is expressed in the LGE, closely apposed to the PSPB. In the *Pax6* mutant *Sfrp2* and *Wnt7b* expression at the PSPB is lost (Kim *et al.,* 2001). Given these expression patterns, and their change in response to a loss of *Pax6*, it is possible that *Wnt* signalling may play a role in the migration of interneurons across the PSPB. Indeed, Sfrp2 has been shown to inhibit migration of malignant glioma cells *in vitro* (Roth *et al.,* 2000) and so may have a role in limiting dorsal migration at the PSPB.

Much of the increase in the number of cortical interneurons in $Pax6^{sey/sey}$ embryos may be due not to increased migration across the PSPB, but rather to dorsal cells acquiring a ventral fate. In the absence of Pax6 there is a gradual expansion of expression of ventral marker genes into the dorsal telencephalic VZ. By E14.5 *Mash1* is expressed throughout the VZ of the dorsal telencephalon, while there is *Dlx1/2* expression superficial to *Mash1* expression (Kroll and O'Leary, 2005; Quinn *et al.,* 2007). As well as aberrantly expressing ventral markers, these dorsal cells show a change in fate, producing GABAergic interneurons that would normally be produced by progenitor cells of the LGE. Within the $Pax6^{Sey/Sey}$ cortex numerous ectopias can be seen which are composed mainly of interneurons. These ectopias are linked by streams of cells that connect them to misspecified dorsal progenitor cells. Lineage tracing confirms that the cells forming these streams and ectopias are of an *Emx1* lineage that would normally produce the *Emx1*-positive cortical plate neurons (Kroll and O'Leary, 2005).

Another population of migratory cells to show defects in the absence of Pax6 is the lateral cortical stream (LCS). These cells are produced from progenitor cells at the PSPB and then migrate ventrally towards the amygdaloid region of the ventral telencephalon where they contribute to specific nuclei in this structure. The LCS is composed of a mixture of *Pax6*- and *Dlx2*-positive cells along with a significant number of cells that express both *Pax6* and *Dlx2*. The *Pax6*-positive cells start to

migrate before the *Dlx2*-positive cells with large numbers of both cell types contributing to the migratory stream by mid-neurogenesis (Carney *et al.,* 2006). Although the LCS still forms in the absence of *Pax6*, the cells that form this migratory stream do not stop migrating when they reach the amygdaloid area but instead continue towards the pial surface where they form an aberrant accumulation (Brunjes *et al.,* 1998).

It is clear that *Pax6* has a wide range of activities during forebrain development from regulating the cell cycle to influencing migration and axon guidance. As these activities have been well characterised in the literature the time is now ripe to identify the molecular targets of this important transcription factor in order to fully understand how *Pax6* exerts its effect.

1.5 Identifying transcription factor targets

The controlled expression of genes in specific spatio-temporal patterns is critical during development. Transcription factors play an important role in regulating gene expression patterns so there is much interest in identifying their downstream targets. Where information is available on potential candidate genes these can be investigated by reverse transcriptase-coupled polymerase chain reaction (RT-PCR) and *in situ* hybridization to see if expression of the target gene changes when the transcription factor is mutated. A variety of techniques have been developed to identify potential transcription factor targets and a number of these are described below.

Chromatin immunoprecipitation (ChIP) and DNA adenine methyltransferase identification (DamID) allow the identification of the genomic binding sites of transcription factors. ChIP involves the *in vivo* cross-linking of proteins to chromatin with formaldehyde followed by the isolation of protein-DNA complexes by immunoprecipitation using an antibody to the protein of interest. Reversal of the cross-linking step allows the immunoprecipitated DNA to be analysed (for review see Orlando, 2000). The DamID technique involves fusing the bacterial protein DNA adenine methylase (Dam) to the protein of interest, causing methylation of adenine residues in the region of the protein binding site. The restriction enzyme

DpnI can then be used to isolate methylated DNA fragments for investigation (for review see Orian, 2006). Both ChIP and DamID can be combined with genomic DNA microarray techniques to allow the rapid analysis of many binding sites at once (for examples see Ren *et al.,* 2000; van Steensel *et al.,* 2001).

Subtractive hybridization allows the comparison of two conditions, such as mutant and wildtype, to identify transcripts present in one but not the other. Labelled cDNA derived from mutant mRNA is hybridized repeatedly to plasmid DNA from a cDNA library of wildtype transcripts. This removes cDNA from transcripts present in both populations, thereby enriching for transcripts unique to, or at higher levels in, the mutant situation. These enriched transcripts can then be cloned and sequenced or used as probes to screen a cDNA library of mutant transcripts. This technique was first used by Scott *et al* (1983) to identify genes differentially expressed in a mouse cell line transformed with the tumour virus SV40.

Another way of generating clones of transcripts present/up-regulated in one mRNA population compared with another is by differential display, a method described by Liang and Pardee in 1992. This technique uses a combination of reverse transcription and PCR to amplify a subset of cDNA fragments from the pools of mRNA to be compared. The cDNA fragments are then resolved side by side on a polyacrilamide gel and fragments showing differential expression can be excised and investigated. Not only is this method quicker than subtractive hybridization, it has the added advantage of allowing more than two conditions to be compared at the same time.

A further method for the identification of transcription factor targets is serial analysis of gene expression (SAGE; Velculescu *et al.,* 1995). This involves the generation of short nucleotide tags that can uniquely identify a transcript. cDNA is synthesised from mRNA using a biotinylated oligo (dT) primer and then cut with a restriction enzyme. The 3' ends of the cDNAs are then isolated by binding to streptavidin beads and a linker sequence containing a type IIS restriction site is ligated to the 5' end. Type IIS enzymes will cleave DNA a short but defined distance away from their

recognition site (Szybalski, 1985). Cleavage with a type IIS enzyme therefore produces short nucleotide tags with a known sequence at its 5' end corresponding to the recognition site of the restriction enzyme used to cut the cDNA. Pairs of tags, or ditags, can be generated by blunt end ligation. Concatenation of these ditags followed by cloning allows sequencing of multiple tags within a single clone. The known restriction enzyme recognition site, located at either end of a ditag, acts as punctuation to identify sequences that belong to different transcripts. In this manner transcripts for different populations can be compared (Velculescu *et al.,* 1995; for review see Taverner *et al.,* 2004).

These techniques are very labour intensive and require a substantial amount of time spent generating clones of transcripts before potential targets can be identified. Differential display in particular also suffers from a poor signal to noise ratio, which makes the identification of target genes difficult. As a result, the use of these techniques has been largely superseded by the microarray approach to identifying transcription factor targets which allows efficient screening of the entire transcriptome.

1.5.1 Microarray approach to identifying transcription factor targets

The first DNA array studies were performed using macroarrays consisting of up to several hundred cDNA probes bound to a nylon membrane. Target RNA was labelled with a radioisotope, hybridized to the membrane and the signal intensity for each probe measured. The first data generated from such a study was published by Schena *et al.* (1995). Technical advances led to the design of microarrays with numbers of probes in the tens of thousands. A microarray, or DNA chip, consists of a glass slide to which arrays of probes have been attached in an ordered grid so that each probe can be identified by its location (Luo and Geschwind, 2001). The probes are either short oligonucleotides or cDNAs. Early microarrays contained, at most, several hundred probes, but technological advances mean that probes can now be arrayed at high densities (Lipshutz *et al.,* 1999). This coupled with the completion of the sequencing of many genomes means that microarrays with probes covering the entire transcriptome are available for many organisms (Slonim, 2002; Elvidge,

2006). In most microarray experiments 2 samples to be compared are labelled with different fluorescent dyes, either Cy3 or Cy5, and then the samples are mixed and hybridized to the same DNA chip (Simon *et al.,* 2003). Affymetrix microarrays are an exception to this with each sample hybridized to separate DNA chip (Luo and Geschwind, 2001). After hybridization the microarray is scanned and the fluorescent intensity of bound target from each sample is measured for each probe. This gives a measure of the abundance of any given transcript in a sample.

The development of efficient methods of linear mRNA amplification has also meant that gene expression in small populations of cells, or even in single cells, can be investigated (for examples see Kamme *et al.,* 2003; Torres-Munoz *et al.,* 2004; Marsh *et al.,* 2008). This is particularly useful for the study of complex tissues such as the brain where the heterogeneous cell composition may mask changes in gene expression, occurring only in a specific cell type, when measurements are made from whole tissue samples. Isolation of the cells of interest prior to RNA extraction allows a more accurate picture of gene expression levels to be produced (Morris and Wilson, 2004). One recent study, for example, used fluorescence activated cell sorting (FACS) to isolate GFP labelled cortical interneurons from E14.5 mouse cortices, where they are present in relatively low abundance, to determine the genes involved in the development of this cell type (Marsh *et al.,* 2008).

1.6 Aims of this thesis

- To characterise a novel *Pax6* reporter mouse line, *DTy54*, in which cells expressing *Pax6* also express *tau.GFP* and are neomycin resistant
- To examine gene expression in *Pax6* positive cells at the PSPB, as identified by tauGFP expression, in $Pax6^{+/+}$*.DTy54* and $Pax6^{sey/sey}$*.DTy54* embryos at E12.5 using a microarray experiment
- To analyse the microarray data and compare it with known alterations in gene expression in this area and with published microarray data on dorsal and ventral telencephalon
- To validate by *in situ* hybridization some of the changes in gene expression identified by microarray

Chapter 2 – Materials and Methods

2.1 Animals

The *DTy54* mouse line (Tyas *et al.,* 2006) was hemizygous for the tauGFP-Pax6 reporter transgene and was maintained on a CD1 background. The *Sey* line was maintained on a Swiss background. *Sey* mice are heterozygous for the $Pax6^{SeyEd}$ allele. This allele has a premature stop codon caused by a point mutation, which prevents the production of functional Pax6 protein (Hill *et al.,* 1991). *DTy54* and *Swiss Sey* lines were intercrossed to produce a *DTy54-Sey* line of compound heterozygotes. The *DTy54-Sey* line was used to generate embryos carrying the *DTy54* transgene on all *Pax6* backgrounds. *Sey* animals and embryos older than E14.5 were identified by eye phenotype. Embryos younger than E14.5 were identified by polymerase chain reaction (PCR) for *Pax6* followed by DdeI digestion of the PCR product to allow differentiation between the *Pax6* wildtype and *Sey* alleles. *DTy54* animals were identified by PCR for the reporter transgene and embryos were identified by GFP fluorescence. Where embryos were being collected, the day of vaginal plug following mating was designated E0.5 and pregnant females were killed at various ages by cervical dislocation.

2.2 Genomic DNA Extraction and Polymerase Chain Reaction

Genomic DNA was extracted from ear clips or from embryonic limb tissue. Tissue was lysed in 50µl hotshot lysis buffer (25mM NaOH; 0.2mM EDTA) at 95ºC for 30 minutes and then cooled to 4ºC. 50µl of neutralizing buffer (40mM Tris-HCl) was then added to stop the reaction. 1µl of this solution was added to 19µl of PCR reaction mix:

10x Reaction buffer	2.0µl
Forward Primer (10µM)	1.0µl
Reverse Primer (10µM)	1.0µl
dNTPs (10mM each)	0.4µl
H_2O	13.8µl
$MgCl_2$ (50mM)	0.6µl
Taq polymerase	0.2µl

Table 2.1: Primers for Genotyping by PCR

Allele	Primer Sequence	Product Size (bp)
DTy54 construct	Forward: 5' CCGTGTGCCTCAACCGTA 3' Reverse: 5' CACGGTTTACTGGGTCTGG 3'	283
Pax6	Forward: 5' TTAGGAAGGCTTTGTGGAGGC 3' Reverse: 5' CTTTCTCCAGAGCCTCAATCTG 3'	282

For *DTy54* primers, cycle conditions were as follows:
96ºC for 2 minutes
[96ºC for 30 seconds, 57.5ºC for 30 seconds and 72ºC for 45 seconds] for 30 cycles

For *Pax6* primers, cycle conditions were as follows:
95˚C for 2 minutes
[95˚C for 1 minute, 56.5˚C for 1 minute and 72˚Cfor 1 minute] for 43 cycles
5µl of the PCR product was then incubated with DdeI enzyme for 3 hours at 37˚C. DdeI cleaves the wildtype allele of *Pax6* once to give products of 199 and 83 base pairs. The *Sey* allele of *Pax6* is cleaved a second time at its point mutation giving products of 180, 83 and 19 base pairs. This allows wildtype, heterozygous and homozygous mutant samples to be distinguished.

2.3 Histology

Embryos were collected in ice cold phosphate buffered saline (PBS), decapitated and the heads fixed overnight in ice cold 4% paraformaldehyde (PFA). After fixation tissue was rinsed in PBS before processing for vibratome or wax sectioning.

2.3.1 Vibratome sectioning

Heads were embedded in 4% low melting point agarose. Vibratome sections were cut at 100 or 200µm and collected in 1:1 glycerol:PBS containing TOPRO3 (1:5000; Molecular Probes). After 24 hours sections were transferred to 9:1 glycerol:PBS, allowed to equilibrate and then mounted on glass slides.

2.3.2 Wax Sectioning

Tissue was dehydrated through graded alcohols and embedded in paraffin wax. Microtome sections (10µm) were cut and mounted on superfrost positively charged glass slides (VWR). Sections were allowed to air dry and were then incubated overnight at 37ºC prior to use.

2.3.3 Cryostat Sectioning

Embryos for cryostat sectioning were collected in ice cold PBS, decapitated and frozen on dry ice. OCT embedding medium (RA Lamb) was used to attach the tissue to the chuck at -20˚C. Cryostat sections (15µm) were cut at between -20˚C and -25˚C and mounted on superfrost positively charged glass slides. Tissue was sectioned and reacted on the day of collection.

2.3.4 Immunofluorescence

Cryostat sections were dried at room temperature and fixed for 10 minutes in 1:1 methanol/acetone at -20ºC. Sections were then dried for 15 minutes at room temperature, rehydrated in PBS for 5 minutes and incubated for 15 minutes in blocking solution containing 2% bovine serum albumin, 2% sheep serum, 7% glycerol and 0.2% Tween 20 in PBS. Sections were then incubated overnight at room temperature with primary antibodies. Sections were washed three times in PBS/Tween $20^{0.2\%}$ and incubated with secondary antibodies for 1 hour at room temperature.

Table 2.2: Details of Antibodies

1ºAntibody	Raised	Dilution	2ºAntibody	Dilution
Pax6 AD1.5.6 and AD2.35 (Engelkamp *et al.,* 1999)	Mouse	each at 1:50	Goat anti-mouse Alexa fluor 568 (Molecular Probes)	1:150
GFP (Abcam)	Rabbit	1:8000	Goat anti-mouse Alexa fluor 488 (Molecular Probes)	1:150

2.3.5 *In situ* Hybridization

In situ hybridization was performed on 10µm wax sections. Sections were dewaxed and rehydrated through xylene and graded alcohols, washed in PBS and digested in

20µg/ml Proteinase K in PBS at 37ºC for 5 minutes. Sections were then washed first in 0.2% Glycine/PBS and then in PBS, followed by post-fixing in 4% PFA/0.2% glutaraldehyde for 20 minutes. Sections were washed again in PBS before incubation with prehyb solution for 2 hours and were then hybridized overnight with 1ng/µl probe in prehyb solution. Following hybridization sections were rinsed in 2xSSC, pH4.5 and then washed at 5˚C below the hybridization temperature in 50% Formamide/2xSSC. Sections were then washed in PBS/Tween$^{0.1\%}$, incubated for 1 hour at room temperature in Boehringer blocking solution containing 10% sheep serum followed by incubation at 37ºC with anti-DIG for 2 hours. Sections were washed overnight in PBS/Tween$^{0.1\%}$, and finally washed in NTM and stained with NBT/BCIP.

Prehyb Solution

Formamide	5.0ml
20xSSC, pH4.5	2.5ml
Boehringer Block	100mg
ddH_2O	2.0ml
Dissolve in waterbath at 65˚C	
0.5M EDTA	100µl
10% Tween-20	100µl
10% CHAPS	100µl
Heparin (50mg/ml)	4µl
tRNA (50mg/ml)	200µl

20xSSC

NaCl	87.66g
Tri-soduim Citrate	44.12g

In 500ml ddH_20; pH4.5

NTM

1M Tris-HCl, pH9.5	25.0ml
5M NaCl	5.0ml
1M $MgCl_2$	12.5ml

Make up to 250ml with distilled water.

2.4 Generation of RNA probes for *in situ* hybridization

Five probes were used for *in situ* hybridization. Plasmid templates for 3 of these were available in the lab. The *GFP* and *Gsh2* probes were synthesised from plasmid DNA containing the full length coding region for *mGFP* and *Gsh2* respectively. The *Pax6* probe contained a 1.2kb segment of the *Pax6* coding region, including exon 5a.

DNA templates for the generation of RNA probes for *Ngn2* and *Lhx6* were amplified by PCR from the 3' end of the gene of interest in genomic DNA, ligated into a plasmid vector and transfected into competent cells.

PCR Reaction Mix

10x Reaction buffer	5.0µl
Forward Primer (10µM)	2.5µl
Reverse Primer (10µM)	2.5µl
dNTPs (10mM each)	1.0µl
H_2O	35.5µl
Pfu polymerase	0.2µl
DNA	3.0µl

Table 2.3: Primers to amplify sequences for cloning

Probe	Primer Sequences	Product size
Lhx6	Forward: 5' AGGTACCCATGGCTTCAGTG 3' Reverse: 5' GGAGACGTCTGACTGCAACA 3'	829bp
Ngn2	Forward: 5' CCCTCTCTCGTCCTCTACCC 3' Reverse: 5' ATGAAGCAATCCTCCCTCCT 3'	822bp

Cycle conditions for *Lhx6* primers:

95ºC for 2 minutes

[95ºC for 30 seconds, 57ºC for 30 seconds and 72ºC for 2 minutes] for 30 cycles

72ºC for 5 minutes

4ºC holding step

Cycle conditions for *Ngn2* primers:

95ºC for 2 minutes

[95ºC for 30 seconds, 55ºC for 30 seconds and 72ºC for 2 minutes] for 30 cycles

72ºC for 5 minutes

4ºC holding step

2.4.1 Purification of PCR products

PCR products were purified using a QIAquick gel extraction kit (Qiagen) for column purification of DNA from enzymatic reactions. The protocol was followed

according to manufacturer's instructions using a bench top microcentrifuge. DNA was eluted in 30µl ddH_2O.

2.4.2 A-tailing modification of blunt-ended PCR fragments and ligation into vectors

A-tails were added to the blunt-ended PCR fragments generated using Pfu polymerase by incubation for 30 minutes at 70ºC in the following solution:

Purified PCR fragment	1µl
10x Taq reaction buffer with $MgCl_2$	1µl
1mM ATP (final conc. 0.2mM)	2µl
Taq DNA polymerase (5units/µl)	1µl
H_2O	5µl

A-tailed PCR fragments were then ligated into pGEM®-T Easy vectors (Promega). Ligation reactions were set up as follows:

	Standard Reaction	Positive Control	Background Control
2x rapid ligation buffer, T4 DNA ligase	5µl	5µl	5µl
pGEM®-T Easy vector (50ng)	1µl	1µl	1µl
PCR product	2µl	---	---
Control Insert DNA	---	2µl	---
T4 DNA Ligase (3units/µl)	1µl	1µl	1µl
H_2O	1µl	1µl	3µl

Ligation reactions were incubated either for 1 hour at room temperature or overnight at 4˚C before transfection into JM109 competent cells (Promega). JM109 cells were thawed on ice for 5 minutes. 50µl of cells was then added to 2µl ligation reaction in a 10ml serile tube on ice, mixed by flicking and left on ice for 20 minutes. Cells were heat-shocked in a water bath at exactly 42˚C for 45 seconds and then returned to ice for 2 minutes. 950µl SOC medium (Invitrogen) was added to the cells which were then incubated for 1.5 hours at 37˚C in a shaking incubator. 100µl and 900µl of

these cultures were plated onto LB/ampicillin agar plates and incubated overnight at 37˚C.

LB Medium

Tryptone 5.0g

Yeast extract 2.5g

NaCl 2.5g

In 500ml ddH2O, pH7.0; autoclave

For LB/ampicillin for agar plates 7.5g agar was added before autoclaving and allowed to cool to 50ºC. Ampicillin was then added to a final concentration of 100µg/ml. Agar was poured into 85mm petri dishes and allowed to set. Plates were stored upside down at 4ºC.

10 colonies from each ligation reaction were grown overnight in 1.5ml LB medium at 37˚C with shaking. Plasmid DNA was recovered by miniprep using a QIAprep kit (Qiagen) according to manufacturer's protocol and eluted in 50µl ddH_2O. Plasmid DNA was digested with EcoRI to liberate the PCR product. Colonies identified as having been successfully transfected with the PCR product were grown overnight in 150ml LB medium at 37˚C with shaking. Plasmid DNA was recovered using a HiSpeed Plasmid Midi Kit (Qiagen) and protocol provided by the manufacturer. Plasmid DNA was eluted in 1ml ddH_2O.

2.4.3 Synthesis of RNA probes

Plasmid DNA was linearised using the appropriate enzyme and the linearised DNA purified and used as template for the synthesis of RNA probes.

Table 2.4: Details of probes

Probe	Plasmid	Restriction Enzyme antisense	RNA polymerase antisense	Probe Size	Hybridization Temperature
GFP	pBluescript II KS+	KpnI	T7	745bp	70ºC
Pax6	pCR-Blunt II-TOPO	BamHI	T7	1.2kb	70 ºC
Gsh2	pBluescript II KS-	NotI	T3	951bp	65 ºC
Lhx6	pGEM®-T Easy	SacII	SP6	829bp	70 ºC
Ngn2	pGEM®-T Easy	SacII	SP6	822bp	65 ºC

Reaction Mix using T7/T3	
DNA	1.0µg
10x Reaction buffer	2.0µl
DIG-labelled dNTPs	2.0µl
RNase Inhibitor	0.5µl
T7/T3 RNA polymerase	2.0µl
ddH_2O to 20µl	Xµl
Total	20µl

Reaction Mix using SP6	
DNA	1.0µg
5x Reaction buffer	4.0µl
DIG-labelled dNTPs	2.0µl
DDT	2.0µl
RNase Inhibitor	0.5µl
SP6 RNA polymerase	2.0µl
ddH_2O to 20µl	Xµl
Total	20µl

Reactions were incubated in a water bath at 37ºC for 2 hours. 2µl DNaseI, RNase free (10 units/µl) was then added and incubated for a further 15 minutes at 37ºC. 2µl 0.2M EDTA was added to stop the reaction. 2.5µl 4M LiCl and 75µl chilled EtOH were then added and the probe was precipitated overnight at -20ºC. The probe was pelleted by centrifugation at 13,000rpm for 15 minutes and the supernatant removed. The probe was rinsed in 70% EtOH, centrifuged again and the supernatant removed. Tubes were covered with pierced parafilm and probes left to dry for 1 hour at room temperature before being re-suspended in 100µl RNase free ddH_2O.

2.5 Dissection of Telencephalic Tissue

E12.5 embryos were collected in ice-cold, oxygenated Earle's balanced salt solution (EBSS). *Pax6*$^{+/+}$*.DTy54*$^{+}$ embryos were identified by GFP fluorescence, *Pax6*$^{sey/sey}$*.DTy54*$^{+}$ embryos were identified by the absence of eyes and GFP fluorescence. The telencephalic lobes were isolated and flattened to show the ventricular surface. The strong expression of GFP at the pallial-subpallial boundary (PSPB) was then used as a guide to dissect each lobe into dorsal, lateral and ventral regions, with the lateral portion including the PSPB. A more detailed description of the dissection technique is given in Chapter 4.

2.6 Cell Dissociation and FACS

Dissected telencephalic tissue was dissociated using the papain dissociation system (Worthington Biochem). Briefly, tissue was triturated with 1ml papain solution,

containing DNase (20 units of papain; 100 units of DNase), and incubated at 37ºC for 10 minutes, followed by centrifugation at 300g for 7 minutes. The cell pellet was resuspended in 1ml low concentration albumin-ovomucoid inhibitor and gently pipetted onto 1.5ml high concentration albumin-ovomuciod inhibitor to create a density gradient. This was centrifuged at 70g for 7 minutes and cells were resuspended in 1% goat serum in PBS. Cells were sorted for GFP by fluorescence activated cell sorting (FACS) using a DakoCytomation MoFlo MLS high speed sorter. If cells were to be analysed but not sorted, the analysis was carried out on a Beckman-Coulter XL flow cytometer (10,000-20,000 cells were analysed per sample). Telencephalic cells dissociated from non-transgenic littermates were used as negative controls to position the gates for both sorting and analysis.

2.7 Immunocytochemistry on sorted cells

After sorting cells were fixed in 500µl of 70% ethanol and stored at -70ºC. 5% goat serum in PBS (PBSG) was added to 1.5ml in an eppendorf tube. Cells were centrifuged for 6 minutes at 6500rpm in a bench top microcentrifuge and the supernatant removed by pipetting. Mouse anti-Pax6 primary antibody (1:200; DSHB) was added in 200µl PBSG, mixed by pipetting and incubated for 1 hour at room temperature. PBSG was added to 1.5ml, inverted to mix and left for 2-3 minutes to rinse. Cells were centrifuged for 6 minutes at 6500rpm and the supernatant removed by pipetting. Secondary antibody, goat anti-mouse alexa fluor 647 (1:150; Molecular Probes), was added in 150µl PBSG, mixed by pipetting and incubated for 45 minutes in the dark at room temperature. Cells were rinsed as before and resuspended in 500µl PBSG. Cells were analysed using a BD Biosciences FACSCalibur® flow cytometer. Telencephalic cells from a non-transgenic littermate and incubated without primary antibody were used as a negative control. Data was analysed and images generated using WinMDI 2.8 software (available from http://facs.scripps.edu/software.html).

2.8 RNA extraction

RNA was extracted from either dissected telencephalic tissue or FACS sorted cells using a Qiagen RNeasy kit. Membranes were disrupted and the lysate homogenized on a QIAshredder spin column. 70% ethanol was added to facilitate binding of RNA to the silica-gel membrane of the RNeasy spin column. Any traces of genomic DNA were removed by on-column DNase digestion. Contaminants were removed by washing and then the RNA was eluted in RNase-free water. RNA was stored at -80ºC.

2.9 Real time RT-PCR

RNA from dorsal, lateral and ventral telencephalic tissue was reverse transcribed to cDNA as follows: ~0.5µg RNA was made up to a final volume of 20.1µl in RNase-free H_2O, incubated at 75ºC for 5 minutes and then held on ice for 2 minutes. 7.9µl of RT reaction mix was added to each sample and samples were then incubated at 42ºC for 1 hour, with 2µl of RT added after the first 5 minutes, and then at 95ºC for 5 minutes. If the cDNA was not to be used immediately it was stored at -20ºC.

1µl of cDNA was added to 24µl of real time RT-PCR reaction mix.

RT Reaction Mix		Real time RT-PCR Reaction Mix	
Random hexamers	1.0µl	Primer mix (12.5µM each)	1.0µl
10x reaction buffer	3.0µl	H_2O	10.5µl
$MgCl_2$ (50mM)	1.8µl	SYBR® PCR Master Mix	12.5µl
dNTPs (10mM each)	1.5µl		
RNase inhibitor (50u/µl)	0.6µl		

Cycle conditions for real time RT-PCR for all primers were as follows:

96ºC for 3minutes

[96ºC for 30 seconds, 55ºC for 1 minute and 72ºC for 1 minute] for 30 cycles

72ºC for 5 minutes

Table 2.5: PCR primers for real time RT-PCR

Gene	Primer Sequence	Product Size (bp)
Dbx1	Forward: 5' CAACAGACCCACCACCTTCT 3' Reverse: 5' TGGCTCACAGTAAGCACTGG 3'	226
Dlx2	Forward: 5' CCAAAAGCAGCTACGACCT 3' Reverse: 5' GGCCAGATACTGGGTCTTCT 3'	224
Mash1	Forward: 5' GGGATCCTACGACCCTCTTA 3' Reverse: 5' TAGTGAAGGTGCCCCTGTAG 3'	238
Ngn2	Forward: 5' CAAACTTTCCCTTCTTGATG 3' Reverse: 5' CATTCAACCCTTACAAAAGC 3'	250
Sfrp2	Forward: 5' AAGTTCCTGTGCTCGCTCTT 3' Reverse: 5' TGTCGTTGTCGTCCTCATTC 3'	309

2.10 Statistical Analysis

Statistical analysis of any data, other than the microarray data, was carried out using Microsoft Excel. Statistical analysis of the microarray data is described below and in chapter 4.

2.11 Microarray Experiment

As microarrays are a highly specialised technique help and advice on the design and implementation of the microarray experiment was sought from Prof. Peter Ghazal at the Scottish Centre for Genomic Technology and Informatics (CGTI; now the Division of Pathway Medicine), University of Edinburgh Medical School. The amplification, labelling and hybridization of the RNA samples to the microarrays were carried out by Alan Ross at the CGTI. Thorsten Forster, also at the CGTI, carried out the initial quality control checks, normalisation and statistical analysis of the array data.

2.11.1 RNA Amplification and Labelling

RNA extracted from FACS sorted lateral telencephalic cells was amplified and labelled with cyanine dyes. Before amplification, RNA quality was assessed using the Agilent bioanalyser which measures the degree of RNA degradation and assigns

each sample with an RNA integrity number (RIN) between 1 and 10, where 10 is high quality, intact RNA. The Agilent low RNA input linear amplification kit was then used to amplify the RNA samples and to produce cRNA, labelled with either Cyanine 3 (Cy3) or Cyanine 5 (Cy5) fluorescent labels. Briefly; a poly dT primer with a T7 polymerase promoter was annealed to the poly A^+ RNA. Reverse transcriptase was then added to the reaction and double stranded cDNA was synthesised. Using T7 RNA polymerase, cRNA, incorporating either cyanine 3- or cyanine 5-labelled CTP, was synthesised from the cDNA. Using this protocol approximately 1μg cRNA is produced from 50ng of starting material.

2.11.2 Microarray Hybridization

Fluorescently labelled cRNA samples were hybridized to Agilent dual-dye whole mouse genome arrays (G4122A) in accordance with Agilent protocols. 750ng of cyanine 3- and 750ng of cyanine 5-labelled cRNA were hybridized at 60ºC for 17 hours in a rotating oven.

2.11.3 Imaging Software

After hybridization arrays were scanned in an Agilent scanner for Cy3 and Cy5 and images analysed using Agilent's feature extraction software (version 7.1).

2.11.4 Normalisation and Statistical Analysis

Normalisation and statistical analysis of the microarray data was performed using R-based software (www.R-project.org) and is described in detail in Chapter 4.

2.11.5 Gene Ontology Analysis

Gene ontology analysis of genes found to be significantly up- or down-regulated in *Pax6*$^{sey/sey}$*.DTy54*$^+$ compared to *Pax6*$^{+/+}$*.DTy54*$^+$ was carried out using two free, web-based packages. These were WebGestalt (WEB-based GEne SeT AnaLysis Toolkit; http://bioinfo.vanderbilt.edu/webgestalt/) and FunNet, Transcriptional Networks Analysis (www.funnet.info). Both of these packages analyse sets of genes on the basis of how the individual genes in the set are annotated in the Gene Ontology (GO;

www.geneontology.org) and Kyoto Encyclopedia of Genes and Genomes (KEGG; www.genome.jp/kegg) databases.

Chapter 3 – Validation of DTy54 Reporter Mouse

3.1 Introduction

Neurogenesis in normal development of the mouse forebrain takes place from embryonic day 11 (E11) to E17 (Levers *et al.*, 2001). *Pax6* is one of the first members of the Pax family to be expressed, with expression in the dividing cells of the neuroepithelium of the forebrain and hindbrain seen as early as E8.0 (Walther and Gruss, 1991). *Pax6* plays a wide variety of roles in brain development. These roles include regulation of cell adhesion, regulation of cell cycle progression in progenitor cells, arealisation, and neuron specification and axon guidance (for review see Simpson and Price, 2002; Manuel and Price, 2005). *Pax6* is also involved in cell migration; however this is most likely a secondary function as the migrational defects of $Pax6^{Sey/Sey}$ cells can be rescued by transplantation into a wild-type environment (Carić *et al.,* 1997). Another role for *Pax6* can be seen in the formation of boundaries in the developing CNS, where it is involved in establishing the di-mesencephalic boundary and boundaries along the dorso-ventral axis (Matsunaga *et al.,* 2000).

The diverse functions of *Pax6* in the development of the mammalian brain mean that a reliable tool for the investigation of this gene would be extremely useful. Here, a recently derived *Pax6* reporter mouse, *DTy54*, is described (Tyas *et al.,* 2006). The reporter cassette of the *Pax6* transgene consists of tauGFP-IRESKozak-Neo^R-pA-C2MAZ. It has been inserted in exon 4 of the *PAX6* gene in yeast artificial chromosome (YAC) Y593 and its expression is therefore under the control of *PAX6* regulatory elements. Y593 contains the entire human *PAX6* locus and sufficient surrounding genomic material to recapitulate the normal *Pax6* expression pattern in mice (Schedl *et al.,* 1996), emphasising the high degree of conservation between mouse and human not only in the coding region of *Pax6* but also in its regulatory sequences. It has also been shown to be capable of rescuing the *small eye* (*Sey*) phenotype in mice. The IRESKozak component of the construct contains an internal ribosome entry site (IRES). These sites allow the 40S ribosome subunit to bind internally to the mRNA enabling the translation of two genes, in this case *tauGFP* and the *neomycin resistance* gene, from a single mRNA transcript (for review see

Vagner *et al.,* 2001). This means that every cell capable of expressing *Pax6* should also express GFP and be neomycin resistant, thereby allowing cell dissociation and subsequent isolation of Pax6 positive cells to be carried out, either by fluorescence activated cell sorting (FACS) or by selection for G418 antibiotic resistance. The pA (polyadenylation) site is necessary for the production of fully functional mRNA in eukaryotic cells. C2MAZ is a binding site for the transcription factor MAZ, located downstream of the human *C2* gene and it has been shown to pause transcription by RNA polymerase II (Ashfield *et al.,* 1991, 1994; Yonaha and Proudfoot, 2000). It is used here as a strong stop site to prevent loss of the construct by the splicing of exon 3 to downstream exons by slowing down RNA polymerase II and pausing transcription. The generation of the *DTy54* mouse line is described in detail in Tyas *et al.,* 2006.

3.2 Results

In order for mice carrying the *DTy54* reporter transgene to act as a useful tool for studying *Pax6*, the *tauGFP* expression pattern must be clearly defined in relation to the known pattern of *Pax6* expression. Any differences between the two expression patterns must be highlighted in order to prevent the erroneous interpretation of future results generated using these mice. To investigate if tauGFP expression in *DTy54* mice was consistent with the known expression pattern of Pax6, embryos were collected at E10.5, 12.5, 14.5 and 15.5. *Pax6* is normally expressed in the forebrain, hindbrain, cerebellum and the developing eye. Here the focus is on the expression pattern of the tauGFP reporter in the forebrain and eye; however this reporter has also been shown to recapitulate the Pax6 expression pattern in the hindbrain and the cerebellum (Tyas *et al.,* 2006).

3.2.1 Expression of tauGFP in the developing eye

Pax6 is critical for the development of the eye where it is expressed in the cornea, lens epithelium, and retina (Grindley *et al.,* 1995; Davis *et al.,* 2003). At all ages examined tauGFP expression was seen in those parts of the eye where Pax6 is normally found. Examples are shown at E12.5 (Fig. 3.1 A and B) and E14.5 (Fig. 3.1 C and D).

Figure 3.1: Coronal sections showing tauGFP expression in the developing eye

A)-D) show tauGFP expression in the retina, lens and cornea of the eye at E12.5. (A and B) and at E14.5 (C and D). TauGFP can also be seen in retinal ganglion cell axons as they leave the eye (B and C), in the optic nerves (E) and at the optic chiasm (F). Images were converted to greyscale to allow the GFP labelling to be seen more clearly. Co, cornea; le, lens; oc, optic chiasm; on, optic nerve and re, retina. Scale bars: 100μm in A, B and D; 200μm in C, E and F.

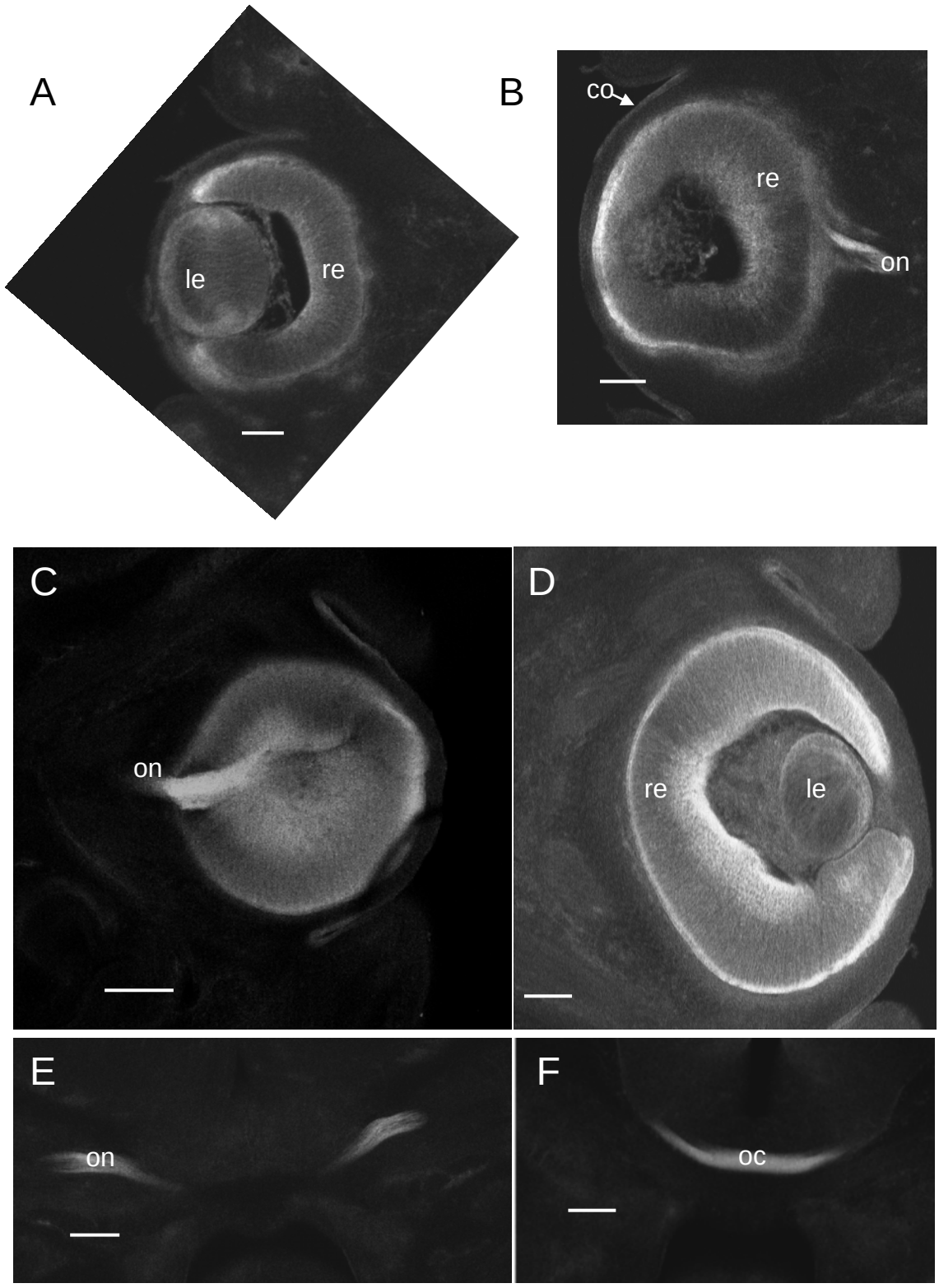

Figure 3.1

3.2.2 Expression of tauGFP in cellular processes

The cytoplasmic localisation of tauGFP allows cellular processes to be visualised. This is most strikingly demonstrated in the axons of retinal ganglion cells. These axons are labelled along their length with tauGFP and can be seen leaving the eye to form the optic nerve and at the optic chiasm (Fig. 3.1 E and F). Other axon tracts are also labelled including the posterior commissure, shown here at E12.5 (Fig. 3.2 A). The processes of radial glial cells are labelled along their length by tauGFP and can be seen extending out towards the pial surface of the cortex (Fig. 3.2 F).

3.2.3 Expression of tauGFP in the developing forebrain

Within the developing cortex Pax6 is expressed in a high rostro-lateral to low caudo-medial gradient (Walther and Gruss, 1991; Stoykova *et al.,* 1997; Puelles *et al.,* 1999) and this gradient is mirrored in the expression levels of tauGFP. The medio-lateral component of this gradient is shown here in coronal sections at both E12.5 and E14.5 where expression of tauGFP can be seen to increase from medial to lateral regions of the developing cortex with highest expression at the pallial-subpallial boundary (PSPB) (Fig. 3.2 A, B and D). The rostro-caudal component of the gradient is demonstrated in Tyas *et al.,* 2006. A population of GFP positive cells can be seen ventral to this region of strong expression (arrows in Fig. 3.2 C). These are most likely part of the population of Pax6 positive cells that are known to migrate from the PSPB to contribute to the amygdala (Carney *et al.,* 2006). In the diencephalon at E12.5 tauGFP can be seen in the ventral thalamus in a pattern characteristic of Pax6 expression in this region (Fig. 3.2 A) (Stoykova *et al.,* 1996; Jones *et al.,* 2002). Pax6 has been shown to be expressed in the pineal gland, and is required for the formation of this structure (Estivill-Torrús *et al.,* 2001). In caudal regions at E14.5 the pineal gland is clearly labelled by tauGFP expression (Fig. 3.2 E).

3.2.4 Co-localisation of Pax6 and tauGFP protein

Immunofluorescence was carried out to determine whether Pax6 and tauGFP proteins co-localise. At E10.5 their expression patterns can be seen to overlap exactly (Fig. 3.3). In the telencephalon the boundary of expression between pallium

Figure 3.2: Coronal sections showing tauGFP expression in the developing forebrain

A) and B) show tauGFP expression in the developing cortex at E12.5, with strongest expression seen at the pallial-subpallial boundary (indicated by the dashed red line in B). In A) expression can also be seen in the ventral thalamus and eye and in the axons of the developing optic chiasm and the posterior commissure. C) is a high magnification of the boxed area in B), showing GFP positive cells (arrows) in the ventral telencephalon; these are most likely part of the population of Pax6 positive cells known to migrate to the ventral telencephalon from the pallial-subpallial boundary. The graded expression of tauGFP in the cortex, with highest expression at the pallial-subpallial boundary (dashed red line), is still evident at E14.5 (D). Expression in the pineal gland is shown in E). Labelling of radial glial processes extending towards the pial surface of the cortex can be seen in F). Images were converted to greyscale to allow the GFP labelling to be seen more clearly. Cge, caudal ganglionic eminence; ctx, cortex; lge, lateral ganglionic eminence; mge, medial ganglionic eminence; oc, optic chiasm; pc, posterior commissure; pi, pineal gland and vt, ventral thalamus. Scale bars: 200µm in A, B, D and E; 50µm in C and 25µm in F.

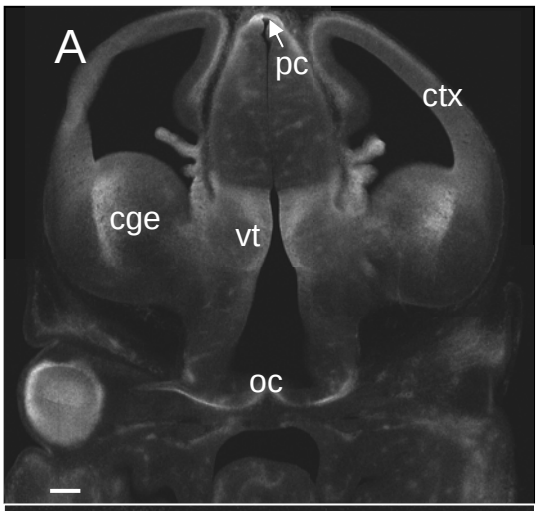

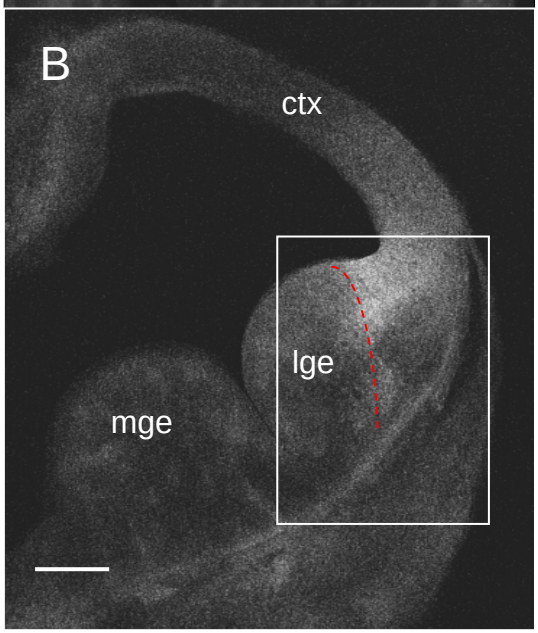

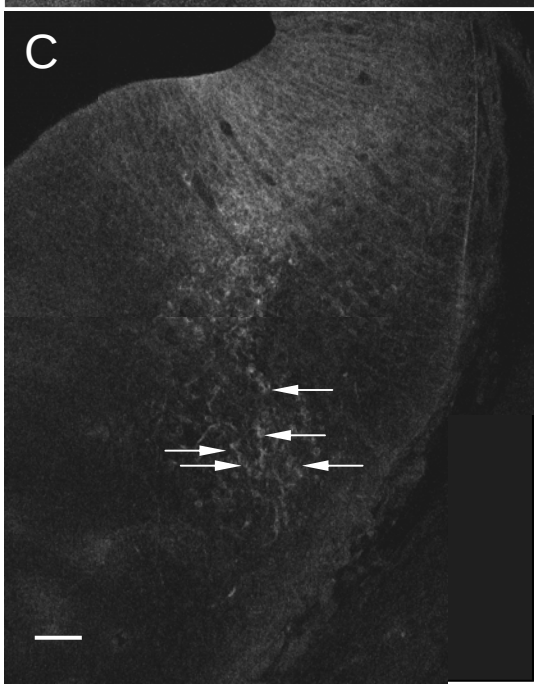

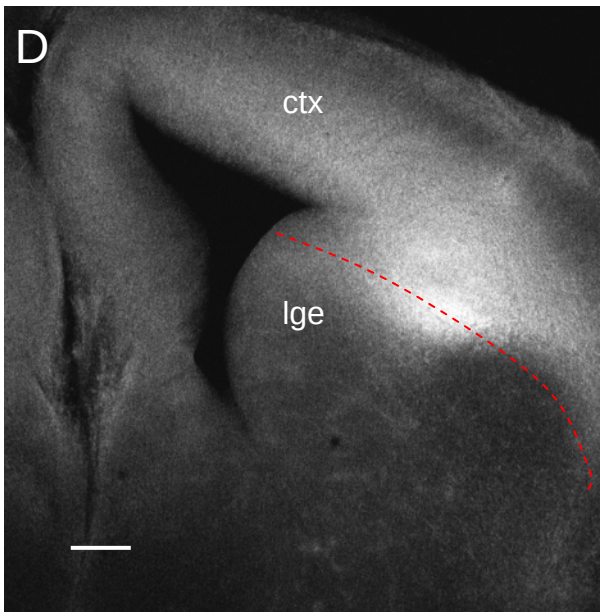

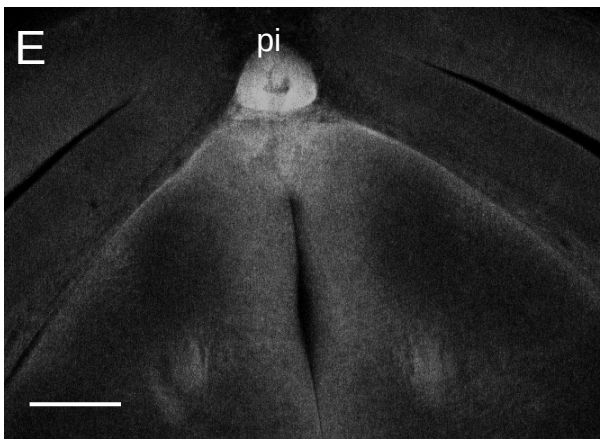

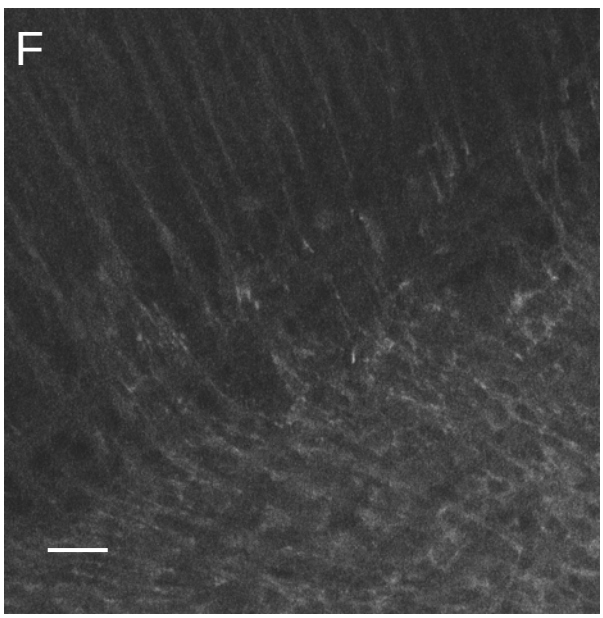

Figure 3.2

Figure 3.3: Immunofluorescence to show co-localisation of Pax6 and GFP at E10.5

Immunofluorescence for Pax6 and GFP on 15μm coronal sections at E10.5. A) and D) show Pax6 expression, GFP expression is shown in B) and E) and overlays of both genes are shown in C) and F). At E10.5 there is an exact correspondence between Pax6 and GFP expression, with a clear decrease in expression of both proteins moving from pallium to subpallium. The E10.5 thalamus is shown in D)-F), demonstrating the much wider expression of Pax6/GFP at this age compared with later stages when expression becomes more restricted in this tissue. Dt, dorsal thalamus; p, pallium; sp, subpallium; vt, ventral thalamus. Scale bars: 50μm.

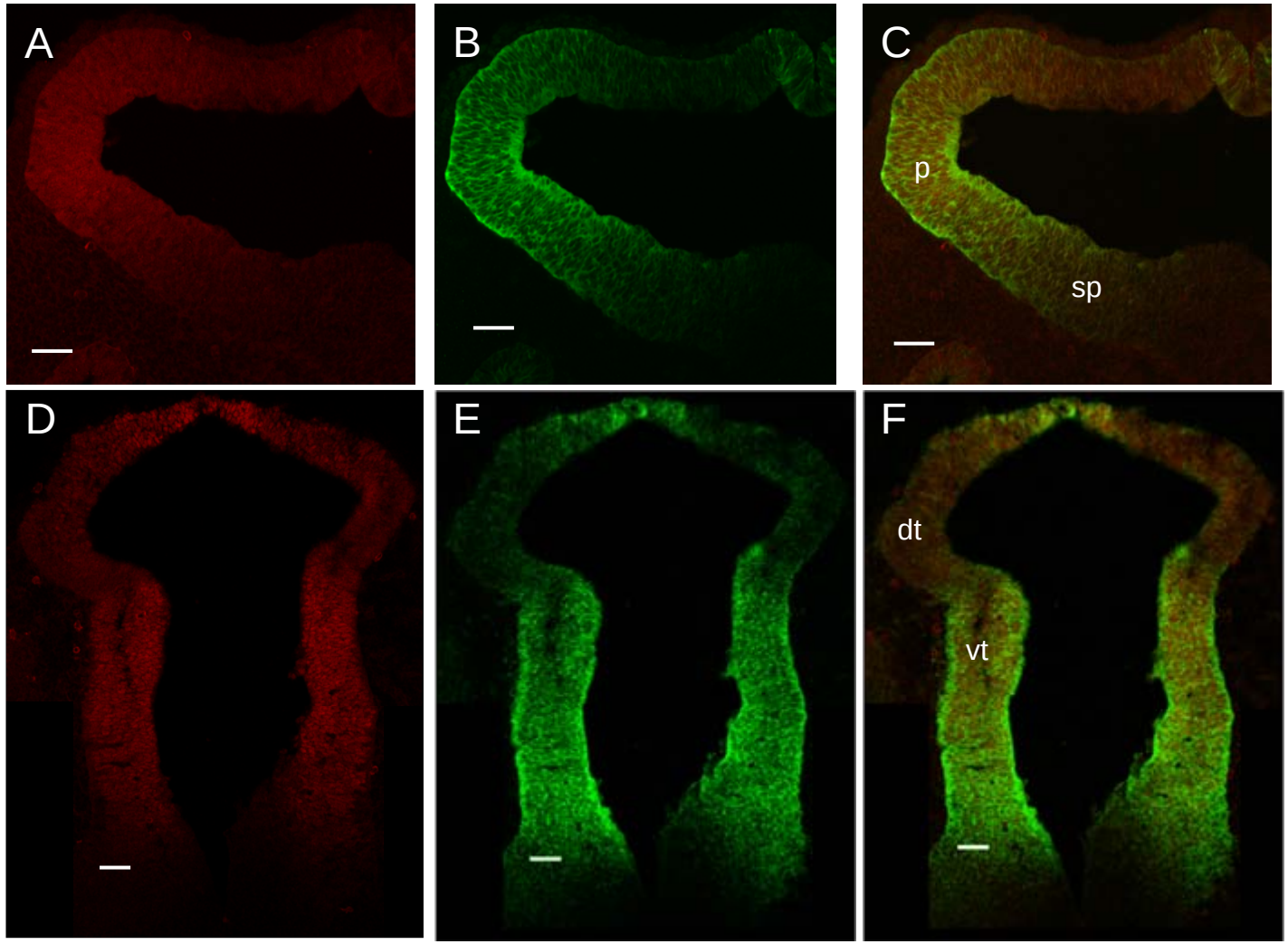

Figure 3.3

and subpallium can be clearly seen (Fig. 3.3 A-C). Pax6 is expressed throughout both the dorsal and ventral thalamus at E10.5. TauGFP can also be seen throughout this structure at this age, showing a close correspondence to the Pax6 expression pattern (Fig. 3.3 D-F).

At later stages however, there is an increasing discrepancy between the expression patterns of the two genes at the protein level. At E12.5 the expression patterns of Pax6 and tauGFP can be seen to diverge increasingly moving from dorsal to ventral telencephalon (Fig. 3.4). In the dorsal pallium Pax6 and tauGFP expression patterns are identical (Fig. 3.4 B-B") but, approaching the PSPB, tauGFP positive/Pax6 negative cells can be seen in the area between the ventricular zone (VZ) and the pial surface (Fig. 3.4 C-C"; area to the left of broken line in C"). Cells double labelled for Pax6 and tauGFP can be seen adjacent to the PSPB, but these are surrounded by a large area of tissue that is tauGFP positive/Pax6 negative (Fig. 3.4 D-E"; arrows in D" and E"). Further ventrally in the amygdaloid area a discrete population of tauGFP negative/Pax6 positive cells can be seen (Fig. 3.4 F-F"). By E15.5 the differences between Pax6 and tauGFP expression have become more marked (Fig. 3.5). This is especially noticeable in the developing cortex where a band of tauGFP expression can be seen surrounding the double labelled VZ (Fig. 3.5 B-C"; area to the right of broken line in B"). In the ventral telencephalon tauGFP positive/Pax6 positive cells can again be seen in a much wider area that is tauGFP positive/Pax6 negative (Fig. 3.5 D-D"; arrows in D"). There is also strong tauGFP labelling of the internal capsule where only a few Pax6 positive cells can be seen (Fig. 3.5 E-E"; arrows in E).

In the thalamus at E15.5 the expression patterns of both Pax6 and tauGFP have become more restricted. Pax6 expression, which was throughout the diencephalon at E10.5, is now confined to a highly distinctive pattern of expression in the ventral thalamus (Stoykova *et al.,* 1996; Jones *et al.,* 2002). The expression of tauGFP more closely recapitulates the changes in diencephalic Pax6 expression over time. By E15.5 the domain of tauGFP expression has become greatly restricted and has also acquired the butterfly shape characteristic of Pax6 expression at this age. There are,

Figure 3.4: Co-localisation of Pax6 and GFP in the telencephalon at E12.5

Immunofluorescence for Pax6 and GFP on 15µm coronal sections at E12.5. a) is a schematic showing the outline of the tissue in A)-A''). The arrow indicates the cortical angle and the dashed line shows the position of the pallial-subpallial boundary. A)-F) show Pax6 expression. GFP expression is shown in A')-F') and overlays of both genes are shown in A'')-F''). Low power images are shown in A)-A''). The boxed areas labelled B-F in A'') indicate the areas shown at high power in B)-F''). B)-B'') shows a very tight correspondence between Pax6 and GFP expression in the dorsal pallium. Moving ventrally towards the cortical angle GFP positive cells start to appear outside the ventricular zone (dashed white line in C''), where Pax6 is not being expressed C)-C''). An increasing discrepancy can be seen between the expression of Pax6 and GFP as you move from dorsal to ventral telencephalon. D)-E'') show Pax6 positive/GFP positive cells (some of which are indicated by arrows) in the ventral telencephalon surrounded by a wider area of Pax6 negative/GFP positive tissue. A discrete population of Pax6 positive/GFP negative cells in the most ventral part of the telencephalon is shown in F)-F''). Lge, lateral ganglionic eminence; mge, medial ganglionic eminence; p, pallium; vz, ventricular zone. Scale bars: 25µm in A-A'' and 5µm in B-F''.

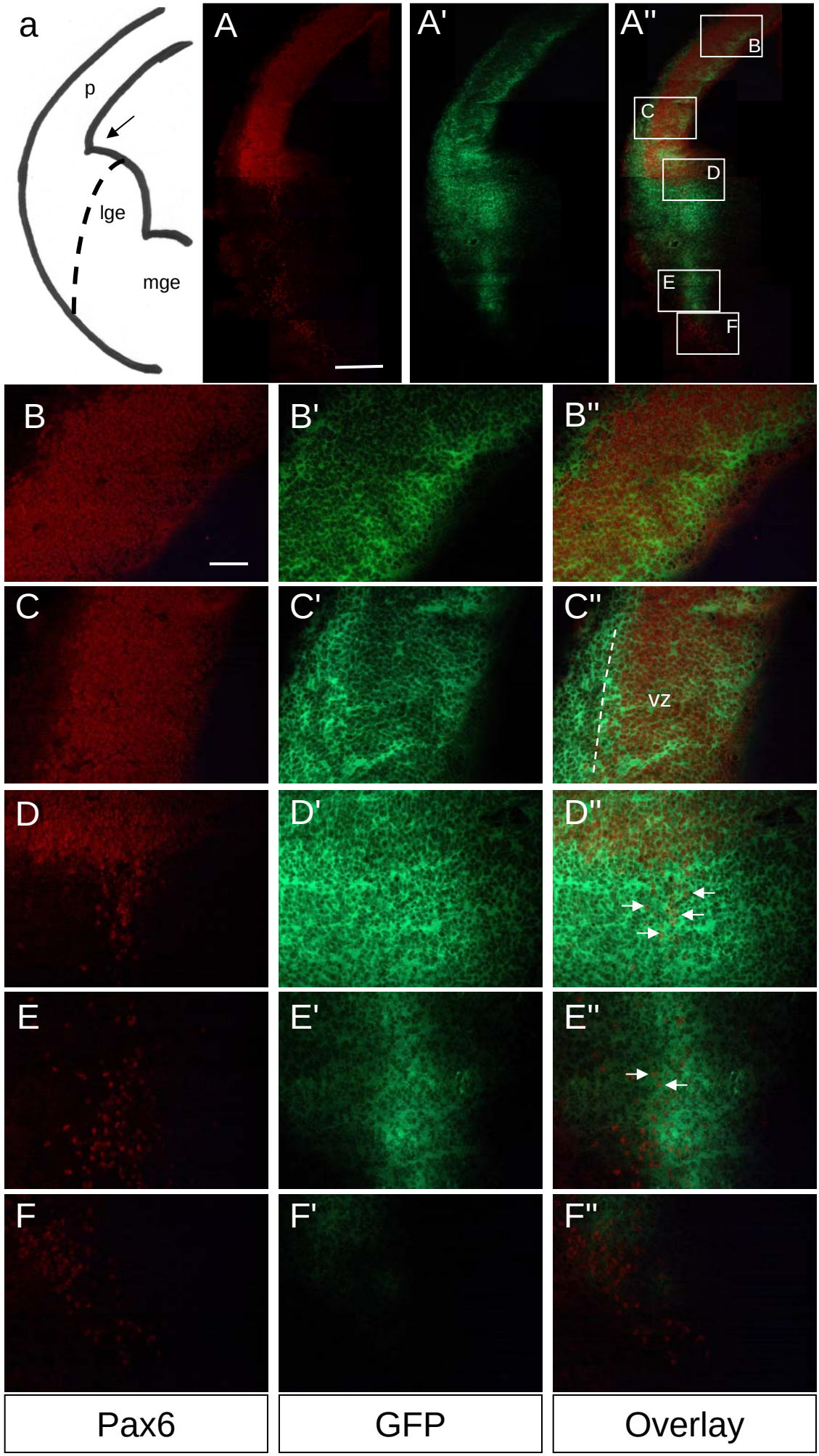

Figure 3.4

Figure 3.5: Immunofluorescence to show co-localisation of Pax6 and GFP at E15.5

Immunofluorescence for Pax6 and GFP on 15µm coronal sections at E15.5. a) is a schematic showing the outline of the tissue in A)-A''). The position of the pallial-subpallial boundary is indicated by the dashed line and the blue lines show the location of the internal capsule. A)-F) show Pax6 expression. GFP expression is shown in A')-F') and overlays of both genes are shown in A'')-F''). Low power images are shown in A)-A''). The boxed areas labelled B-F in A'') indicate the areas shown at high power in B)-F''). B)-B'') shows expression in the cortical ventricular zone where Pax6 and GFP co-localise. GFP expression can also be seen in the subventricular zone where Pax6 in not expressed. The expression pattern moving away from the ventricular zone, towards the pial surface, is shown in C)-C''). Pax6 expression is absent from this region and the area adjacent to the pia can be seen to be negative for both proteins. Pax6 positive/GFP positive cells (examples marked with arrows) in the ventral telencephalon can be seen to be surrounded by a wider are of Pax6 negative/GFP positive tissue in D)-D''). The internal capsule is shown in E)-E''). Strong GFP label can be seen in this area (E'), but Pax6 expression is limited to just a few cells (arrows in E). Thalamic expression of Pax6 and GFP is shown in F)-F''). The two proteins co-localise well in the ventral thalamus, although there are areas which are Pax6 negative/GFP positive (see boxed area in F''). Ctx, cortex; dt, dorsal thalamus; ic, internal capsule; svz, subventricular zone; vt, ventral thalamus; vz, ventricular zone. Scale bars: 25µm in A-A'' and 5µm in B-F''.

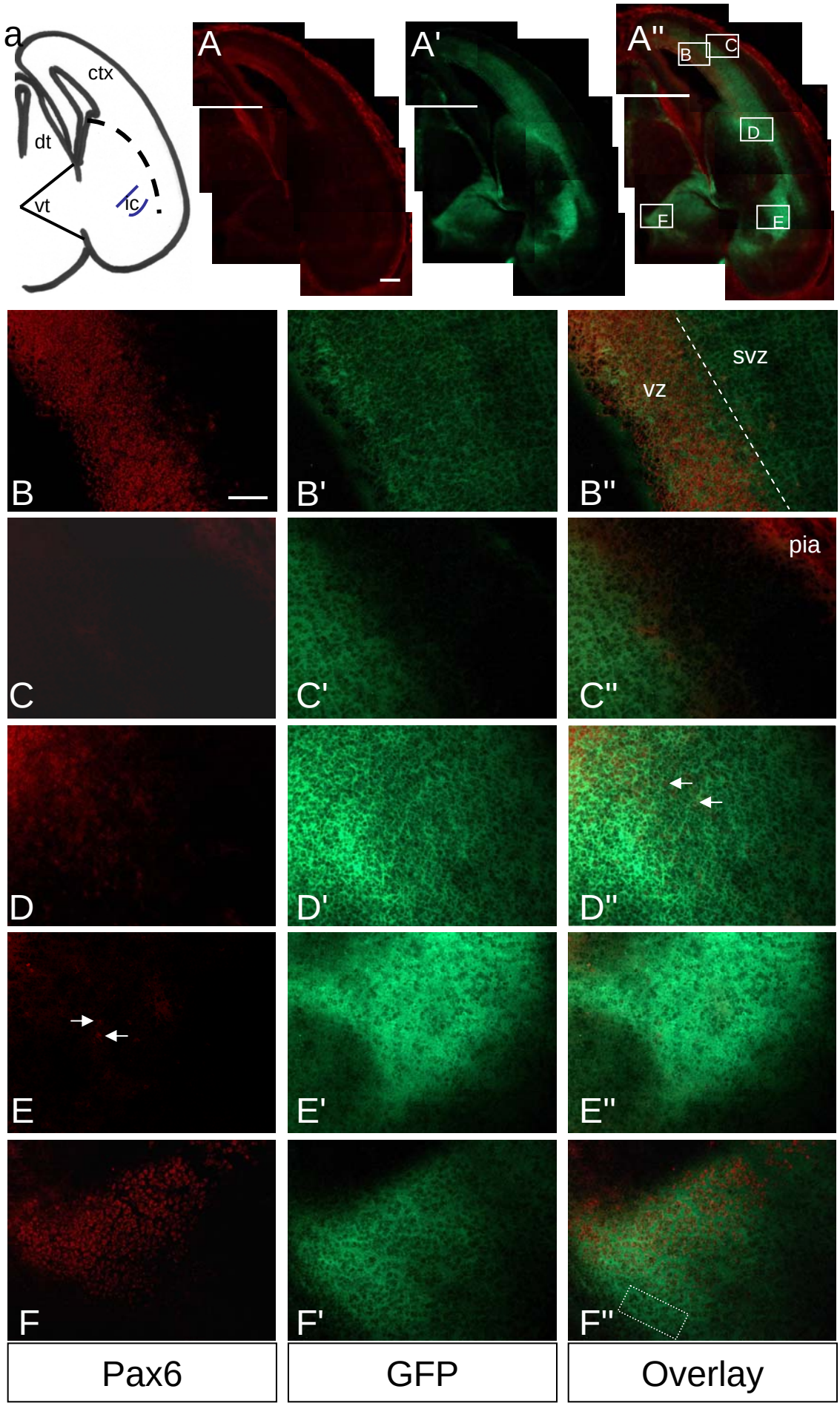
a
ctx
dt
vt
lc
A
A'
A''
B
C
D
E
B
B'
B''
svz
vz
C
C'
C''
pia
D
D'
D''
E
E'
E''
F
F'
F''
Pax6
GFP
Overlay

Figure 3.5

however, regions that are tauGFP positive/Pax6 negative (Fig. 3.5 F-F") although in these areas tauGFP staining appears more diffuse and may be present in cellular processes rather than in cell bodies.

3.2.5 Co-localisation of *Pax6* and *tauGFP* transcripts

As there were some discrepancies between the expression of Pax6 and tauGFP proteins it was decided to use *in situ* hybridization to determine if there was a greater degree of co-localisation at the RNA level. In order to carry out an accurate comparison, adjacent sections were hybridized with either a *Pax6* or a *GFP* probe. At E12.5 the transcription pattern in the dorsal pallium is identical for both genes (Fig. 3.6 A, B, E and F). Moving ventrally towards the PSPB, to where the differences in protein expression begin to appear, transcription of the two genes continues to be confined to the VZ (Fig. 3.6 C and G). In the ventral telencephalon, however, there is a much larger population of *Pax6* positive cells than *GFP* positive cells (compare Fig3.6 D and H) which corresponds with the tauGFP negative/Pax6 positive population seen in the amygdaloid region by immunofluorescence.

At E15.5, the patterns of expression of *Pax6* and *GFP* are highly similar (Fig. 3.7 A and E), particularly in the cortex where there is a dramatic difference in protein expression at this stage. In the cortex both *Pax6* and *GFP* expression are clearly confined to the VZ (Fig. 3.7 B and F). In the thalamus, although the general pattern of *GFP* transcription is the same as for *Pax6*, *GFP* is not as strongly expressed as *Pax6* in this region (Fig. 3.7 C and G). *GFP* may also be less widely expressed than *Pax6* in the thalamus but due to the high levels of background staining it is difficult to be certain if this is the case. The internal capsule which was strongly labelled for GFP by immunofluorescence can be seen to be surrounded by *GFP* positive cells, although *Pax6* expression is noticeably absent in this region (compare Fig. 3.7 D and H).

Figure 3.6: *In situ* hybridization for *Pax6* and *GFP* on coronal sections at E12.5

Adjacent 10μm coronal sections hybridized with a probe for *Pax6* (A-D) or *GFP* (E-H). Background levels of staining are indicated in I)-K) which show non-transgenic tissue hybridized with the *GFP* probe. Boxed areas in A), E) and I) indicate the areas shown at high power in B)-D), F)-H) and J) and K) respectively. B) and F) show *Pax6* and *GFP* expression throughout the cortical depth in the dorsal pallium. At the cortical angle expression of both genes can be seen to be restricted to the ventricular zone (C and G; dashed red line indicates the limit of the VZ). In the ventral telencephalon a population of *Pax6* positive cells can be seen (D). There is a similar, but smaller, population of cells positive for *GFP* (H); it is likely that these cells are also positive for *Pax6*. The most ventral cells of the *Pax6* positive group (boxed area in D) are in a region that is *GFP* negative. Vz, ventricular zone. Scale bars: 25μm in A, E and I; 5μm in B-D, F-H, J and K.

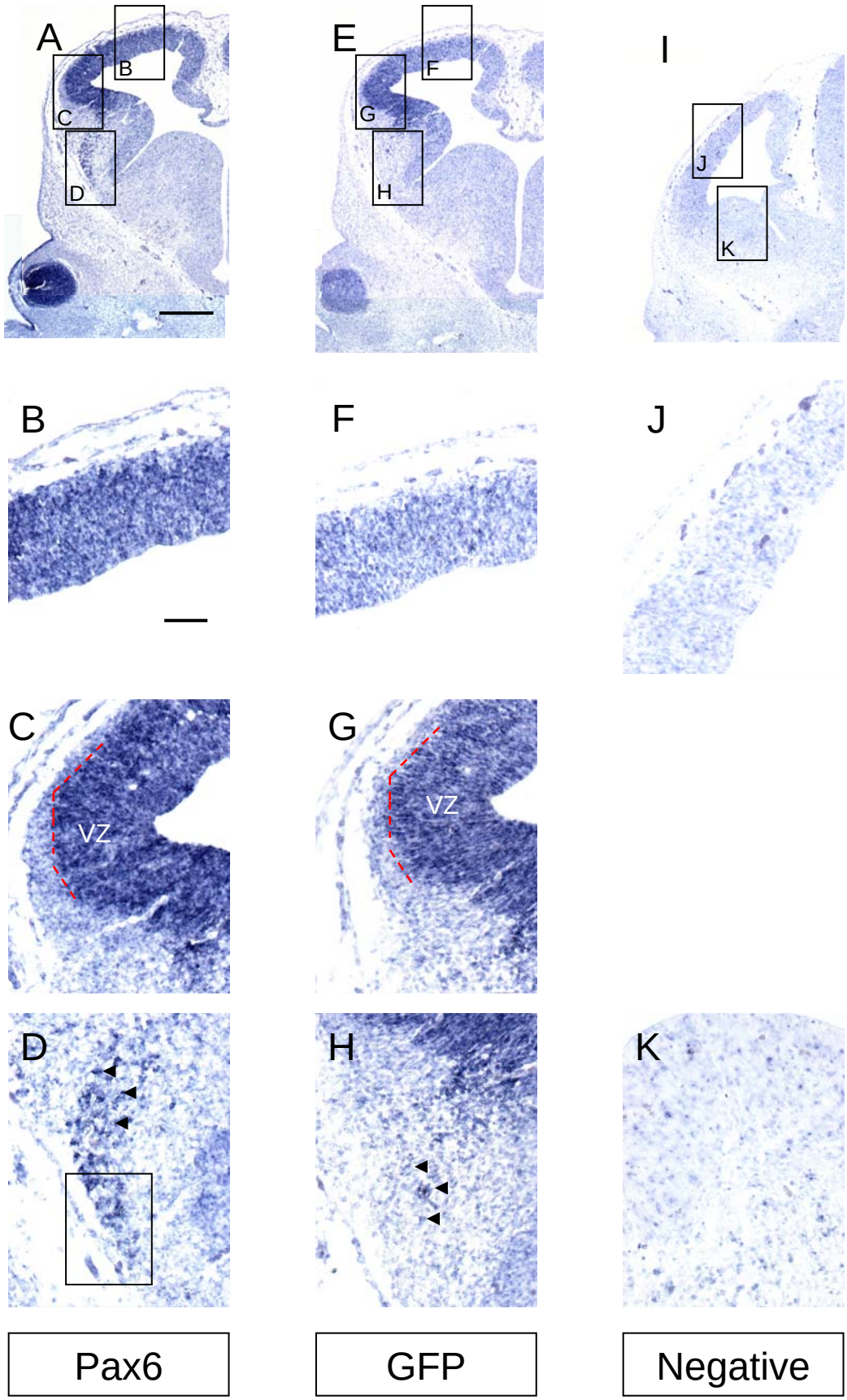

Figure 3.6

Figure 3.7: *In situ* hybridization for *Pax6* and *GFP* on coronal sections at E15.5

Adjacent 10μm coronal sections hybridized with a probe for *Pax6* (A-D) or *GFP* (E-H). Background levels of staining are indicated in I) and J) which show non-transgenic tissue hybridized with the *GFP* probe. Boxed areas in A), E) and I) indicate the areas shown at high power in B)-D), F)-H) and J) respectively. In the cortex *Pax6* (B) and *GFP* (F) expression are confined to the ventricular zone. Thalamic expression of *Pax6* and *GFP* appear similar particularly in the ventricular zone. In post-mitotic cells *Pax6* appears more strongly expressed than *GFP* and is possibly also more widely expressed (compare C and G). The region of the internal capsule can be seen to be surrounded by many *GFP* positive cells (H), but *Pax6* expression in this region is absent (D). Images were converted to greyscale to allow the signal from the *GFP* probe to be more easily distinguished from background noise. Ic, internal capsule; vz, ventricular zone. Scale bars: 50μm in A, D and G; 5μm in B, C, F, G, I and J; 10μm in D and H.

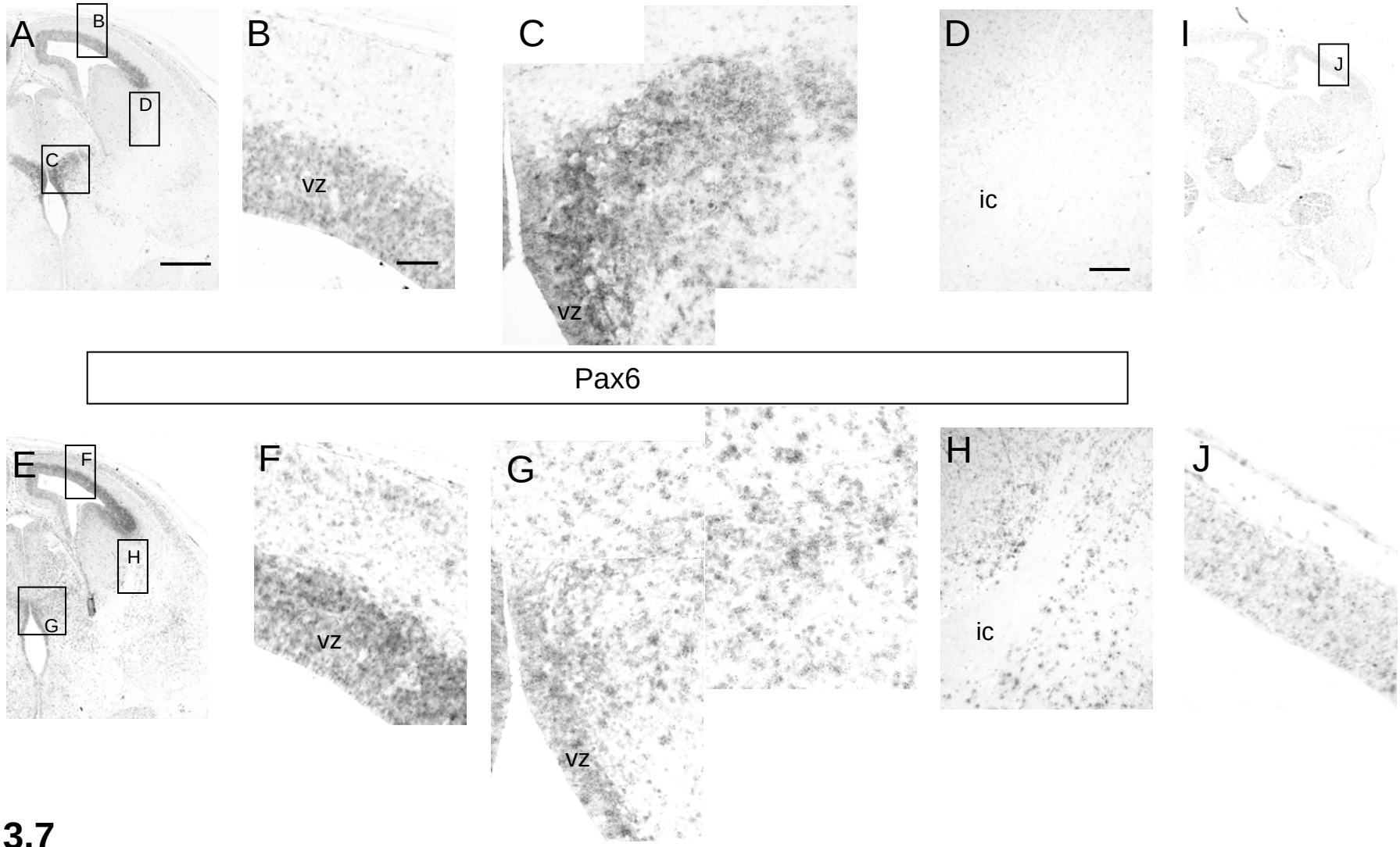

Figure 3.7

3.3 Discussion

Pax6 is expressed in a range of regions in the developing brain where some of its functions include cell adhesion, cell cycle progression, axon guidance and cortical patterning. Due to its wide variety of functions there is a lot of interest in characterising its expression pattern and in examining the effect of loss of function mutations on brain development. The development of a reliable tool for studying *Pax6* would therefore be of great benefit to this area of research. The results shown here allow an assessment of the reliability of the recently derived *DTy54* reporter mouse as a marker for *Pax6* expression.

3.3.1 Expression of tauGFP in the developing eye and forebrain

The tauGFP expression pattern seen in coronal sections of *DTy54* embryos closely resembles the known Pax6 expression pattern at both E12.5 and E14.5. One obvious difference between the two patterns, however, is the strong GFP labelling of cellular processes caused by the cytoskeletal rather than nuclear localisation of tauGFP. This is particularly striking in axon bundles such as the optic nerve and the posterior commisure and could potentially provide a useful tool for studying the development of axonal tracts where the projecting cells are *Pax6* positive.

3.3.2 Co-localisation of *Pax6* and *tauGFP* expression

The discrepancy between the expression of Pax6 and tauGFP proteins, and the fact that this discrepancy increases over time, suggests that there may be a difference in the half-lives of the two proteins. The expression pattern seen in the developing cortex in particular supports this, as here all the cells that are GFP positive/Pax6 negative are derived from Pax6 positive progenitors. This is backed up by evidence from *in situ* hybridization, as in the developing cortex there is a much closer correspondence between expression of *Pax6* and *GFP* mRNA. This is particularly striking at E15.5.

The labelling of cellular processes by tauGFP also seems likely to be making a significant contribution to the areas that are GFP positive/Pax6 negative especially in the ventral telencephalon. The band of GFP expression seen extending ventrally

from the VZ along the PSPB is most likely within the processes of the radial glial cells which are known to form a pallisade at this boundary (Stoykova *et al.,* 1997). Although the radial glial fascicles cannot be clearly identified on the thin sections used here for immunofluorescence, tauGFP labelling of radial glial processes in the developing cortex can be clearly seen in thicker vibratome sections and as these radial glial cells are Pax6 positive, their labelling with tauGFP is to be expected. This could be shown definitively by performing double immunofluorescene for GFP and a radial glial marker such as RC2.

There does, however, appear to be some uncoupling of the expression of the transgene from *Pax6* expression in the ventral telencephalon. At E15.5 tauGFP labelling can be seen in the region of the internal capsule where there are next to no Pax6 positive cells. This tauGFP staining is very diffuse in appearance and seems likely to be present in cellular processes rather than cell bodies. Cells in nuclei of the midbrain and hindbrain have been shown to project axons through the internal capsule to reach cortical targets (van der Kooy and Kuypers, 1979; Galindo-Mireles *et al.,* 1985; Waterhouse *et al.,* 1986; Deng *et al.,* 2007; for review see Hornung, 2003). Given that *Pax6* is expressed in the hindbrain, where it is required for the development of a number of brainstem nuclei, it is likely that the GFP positive axons seen traversing the internal capsule may have Pax6 positive cell bodies that lie within these nuclei (Engelkamp *et al.,* 1999; Landsberg *et al.,* 2005; Schmid *et al.,* 2007). A detailed analysis of the expression patterns of Pax6 and tauGFP in the hindbrain might help to clarify this. *In situ* hybridization at E15.5 clearly shows the presence of *GFP* mRNA in many cells surrounding the internal capsule where *Pax6* transcripts appear to be completely absent. These cells are negative for tauGFP protein however suggesting that there may be some form of post-transcriptional regulation preventing the translation of tauGFP is these cells.

There is also a population of Pax6 positive/GFP negative cells in the most ventral part of the telencephalon. If these cells express GFP at all it is at levels below detection by either immunofluorescence or *in situ* hybridization. This could be due to a difference in how expression is regulated in post-mitotic as opposed to

progenitor cells. *Pax6* has been shown to regulate its own transcription via a feedback mechanism (Kleinjan *et al.,* 2004; Manuel *et al.,* 2007). When *DTy54* is crossed onto the *Pax6* overexpressing line *Pax77*$^{+}$, which shows a 1.5-3 fold increase in Pax6 protein levels, production of tauGFP from the transgene is significantly reduced (Manuel *et al.,* 2007). Similarly there is a significant increase in tauGFP levels in *Pax6*$^{sey/sey}$*.DTy54*, suggesting that the level of tauGFP may be inversely proportional to level of production of functional Pax6 (Manuel *et al.,* 2007). If, due to its region of insertion, the transgene is more sensitive to this feedback mechanism in post-mitotic cells than the endogenous locus this could result in a down-regulation of transcription from the transgene. A difference in the regulation of expression between progenitors and post-mitotic cells could also help explain the expression pattern seen in the thalamus. In the E15.5 thalamus, GFP can be seen in areas where Pax6 is not expressed but the diffuse appearance of the staining suggests that the GFP is present in cellular processes rather than in cell bodies. By *in situ* hybridization however, both genes show similar expression patterns but with *Pax6* expressed more strongly and also perhaps more widely. Unfortunately high levels of background staining make it difficult to be certain of the exact extent of *GFP* labelling. Interestingly, in the progenitor cells of the thalamus, the expression of both genes corresponds very closely, although a difference in the level of expression can still be seen. This would also support the argument that *Pax6* expression is regulated differently between post-mitotic and progenitor cells.

Another possible explanation for the presence of Pax6 positive/GFP negative cells in the ventral telencephalon is that *Pax6* is not being transcribed by these cells and the Pax6 protein is present as a result of cell-cell transfer. Cell-cell transfer of the homeodomain transcription factor *Engrailed* has been demonstrated *in vitro* (Joliot *et al.,* 1998). There is also compelling evidence to suggest that such transfer may occur *in vivo*. *Engrailed* has been shown to have access to a subcellular compartment *in vivo* that would allow it to be exported from the cell (Joliot *et al.,* 1997). Two overlapping sequences in the homeodomain (one for cellular export, the other for cellular uptake) that are highly conserved between homeodomain containing proteins have also been identified as necessary for cell-cell transfer (Joliot *et al.,* 1998;

Maizel, *et al.,* 1999; 2002). Computer modelling of this mechanism of protein transfer has also demonstrated how it could be used to produce expression gradients and the sharp boundaries of expression seen between pairs of homeodomain transcription factors that can regulate their own and each others transcription (Holcman *et al.,* 2007). A recent paper by Sugiyama *et al.,* (2008) demonstrates *in vivo* the transfer of Otx2 from retinal cells to parvalbumin cells in the visual cortex where it plays an important role in visual cortical plasticity. Given this, cell-cell transfer cannot be ruled out as a possible explanation for the Pax6 positive/GFP negative population of cells seen here in the ventral telencephalon.

Chapter 4 – Microarray Experiment

4.1 Introduction

4.1.1 Previous Analyses of the development of *Pax6*$^{sey/sey}$ animals

There is a large body of literature examining the role of *Pax6* in the developing mouse brain (for review see Simpson and Price 2002; Manuel and Price 2005). *Pax6* is known to play an important role in many of the developmental processes of the forebrain. The correct navigation of thalamocortical and corticofugal axons requires *Pax6* expression (Mastick *et al.,* 1997; Pratt *et al.,* 2000; Jones *et al.,* 2002) and neuronal migration is disrupted in the absence of Pax6 (Carić *et al.,* 1997; Talamillo *et al*., 2003). *Pax6* is also important in regulating cell adhesion in the forebrain (Stoykova *et al.,* 1997; Tyas *et al.,* 2003) and in controlling aspects of the cell cycle in cortical progenitor cells (Warren *et al.,* 1999; Estivill-Torrus *et al.,* 2002; Quinn *et al.,* 2007).

As a transcription factor *Pax6* can regulate the expression of a range of other genes. A number of *Pax6* target genes have been identified by *in situ* hybridization including *Ngn2*, *Emx1*, *Mash1* and *Gsh2* (Stoykova *et al.,* 1996; 2000). In order to gain a more complete insight into the genes whose expression is controlled by *Pax6*, however, a high throughput approach looking at the expression of many genes at once is required.

4.1.2 How this study will add to our understanding of the role of *Pax6*

A number of microarray studies have been carried out to investigate gene expression changes in the developing forebrain in response to the loss of functional Pax6 protein in both mouse and rat (Faedo *et al.* 2004; Arai *et al.* 2005; Holm *et al.* 2007). The microarray experiment described here aims to build on the knowledge obtained from previous array studies by using a more refined technique to isolate the cells of interest for analysis. The *DTy54* mouse line makes it possible to isolate a population of cells, enriched for cells expressing *Pax6*, from the developing forebrain by fluorescence activated cell sorting (FACS). This allows us to investigate more detailed questions as to the role of *Pax6* in different populations of cells and to focus

more narrowly on the possible cell autonomous changes in gene expression in response to the loss of functional Pax6.

The PSPB plays an important role in the development of the telencephalon and *Pax6* expression is critical for the normal formation of this structure (Stoykova *et al.,* 1997). In order to better understand the role of *Pax6* at the PSPB it was decided to carry out a microarray experiment to compare gene expression in cells of the lateral telencephalon, including the PSPB, that are being activated to express *Pax6* in $Pax6^{+/+}$ and $Pax6^{Sey/Sey}$ embryos at E12.5. This would allow large numbers of genes to be analysed simultaneously and should identify any genes whose expression at the PSPB has been up- or down-regulated in $Pax6^{Sey/Sey}$ compared to wildtype embryos. It was decided to use E12.5 embryos as this is the earliest stage at which dissection of the PSPB seemed feasible.

Before the microarray analysis could be carried out, however, it was necessary to devise a dissection strategy that would allow the cells of interest to be isolated in a completely reproducible manner. *GFP* expression in *DTy54* not only reports where *Pax6* is expressed, it also mirrors the gradient of expression seen in the developing dorsal telencephalon (Tyas *et al.,* 2006). As *Pax6* is most highly expressed at the PSPB, this region can be easily identified in *DTy54* embryos by the high level of GFP. This region can be dissected under a fluorescence microscope, the cells dissociated and the GFP positive cells isolated by FACS. As the reporter construct is independent of the endogenous *Pax6* locus it can also be crossed onto *small eye* mice to generate $Pax6^{Sey/Sey}.DTy54^{+}$ embryos for comparison. The accuracy and reproducibility of the dissection was assessed in $Pax6^{+/+}.DTy54^{+}$ embryos by real-time RT-PCR and FACS analysis of dorsal, lateral and ventral telencephalic tissue. This strategy allows the role of *Pax6* to be investigated in a well defined population of cells from an area of the telencephalon for which *Pax6* expression is critical to its development.

4.2 Results

4.2.1 Developing a method to isolate the cells of interest

In order to look at gene expression specifically in *Pax6* expressing cells at the PSPB it was necessary to dissect out this region of the telencephalon accurately and consistently, before dissociating the cells and isolating those expressing the *DTy54* reporter by FACS. GFP is highly expressed at the PSPB as this is the region of highest Pax6 expression in the telencephalon and so this region can be readily visualised under fluorescence, aiding accurate dissection.

4.2.1.1 Dissection Technique for isolating the PSPB

First the brain was isolated by an incision between the eye and the base of the brain and the skin and membranes were removed (Fig. 4.1 A). The telencephalic lobes were dissected away from the rest of the brain by an incision on either side of the diencephalon and the two lobes were then separated (Fig. 4.1 B). A small incision was made, just dorsal to the PSPB, at the rostral end of each lobe and another at the caudal end (dashed lines in Fig. 4.1 B). These incisions allowed the lobes to be flattened, by folding back the dorsal telencephalon (in direction of arrows in Fig. 4.1 B), so that the ventricular surface was uppermost. In this orientation the stripe of intense GFP expression at the PSPB could be clearly seen (Fig. 4.1 C-E). The tissue could then be divided into three pieces with cuts being made on either side of the PSPB as labelled by GFP expression (Fig. 4.1 F-H). The same dissection technique was also used to isolate the equivalent areas from $Pax6^{sey/sey}.DTy54^{+}$ embryos (Fig. 4.1 I-P).

4.2.1.2 FACS analysis of dissection

In order to check the accuracy of the dissection, cells from dorsal, lateral (including the PSPB) and ventral regions of the $Pax6^{+/+}.DTy54^{+}$ telencephalon were dissociated and analysed by FACS. As the GFP expression pattern recapitulates the gradient of Pax6 expression in the developing cortex, with strongest expression at the PSPB, one would expect to see more cells with a higher level of GFP expression in samples from lateral compared with dorsal telencephalon. Samples from the ventral telencephalon would be expected to have very few GFP positive cells as the Pax6

Figure 4.1: Dissection of telencephalon from *Pax6$^{+/+}$.DTy54^{+}* and *Pax6$^{sey/sey}$.DTy54^{+}* embryos at E12.5, into dorsal, lateral and ventral regions

Dissection of the telencephalon from E12.5 *Pax6$^{+/+}$.DTy54^{+}* (A-H) and *Pax6$^{sey/sey}$.DTy54^{+}* (I-P) embryos. A) and I) show GFP fluorescence overlaid on a bright-field image of the whole brain, viewed from above, after skin and membranes have been removed. Broken red lines indicate where incisions were made to isolate the telencephalic lobes. B) and J) show the cut medial surface of the telencephalic lobe with GFP fluorescence overlaid on a bright-field image, broken red lines indicate where incisions were made at the rostral and caudal ends of the lobe. The tissue was flattened by folding back the dorsal telencephalon in the direction of the arrows in B) and J). The flattened telencephalic lobe with the ventricular surface uppermost is shown under bright-field (C and K) and GFP fluorescence (D and L). An overlay of bright-field and GFP is shown in E and M. Broken red lines indicate where incisions were made to divide the tissue into dorsal, lateral and ventral regions. The dissected tissue is shown under bright-field (F and N), GFP fluorescence (G and O). An overlay of bright-field and GFP is shown in H and P. Rostral is to the right in all images and dorsal is up in all images except A and I.

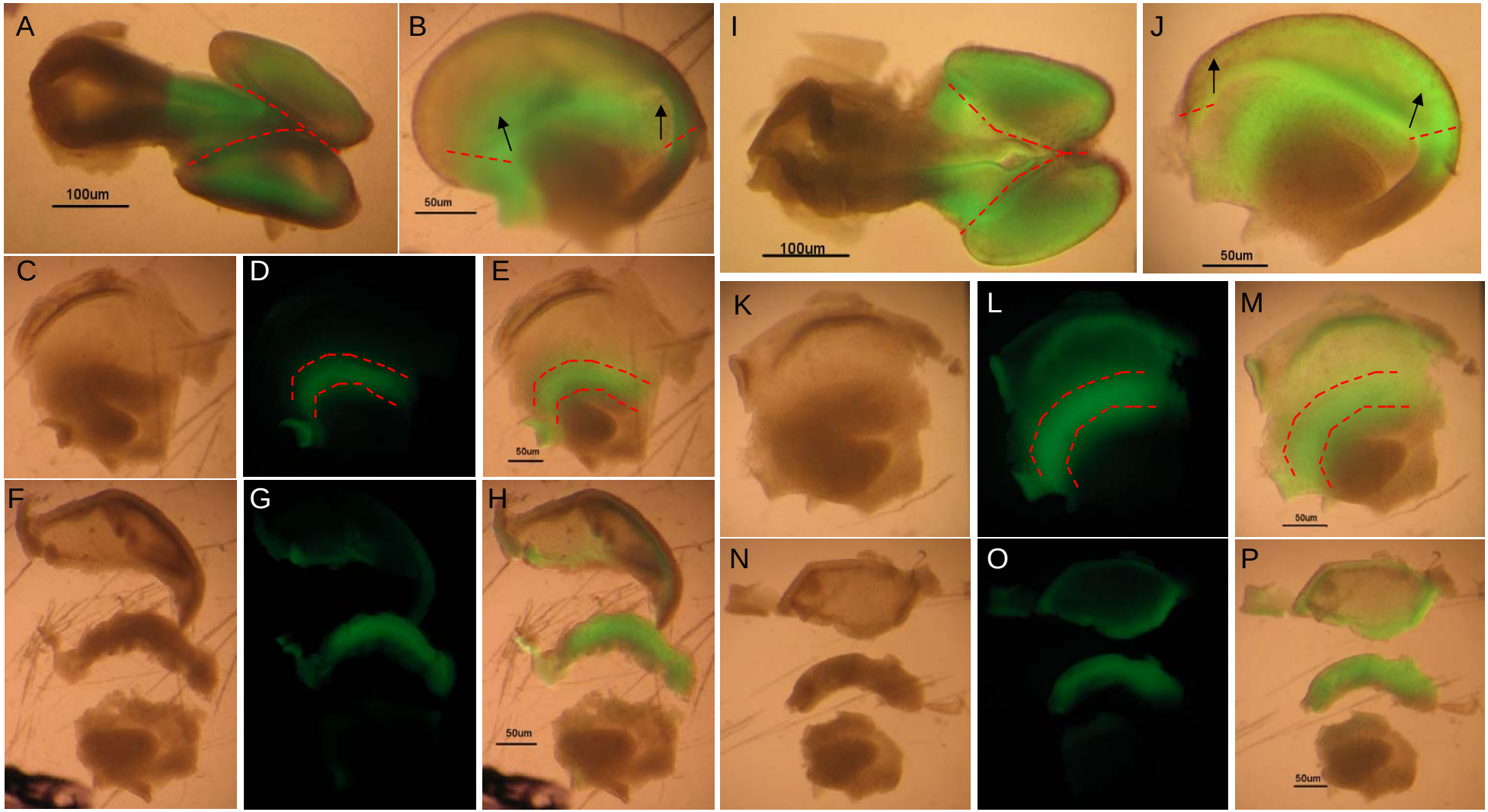
A
100um
B
50um
I
100um
J
50um
C
D
E
50um
K
L
M
50um
F
G
H
50um
N
O
P
50um
Pax6+/+.DTy54
Pax6sey/sey.DTy54

Figure 4.1

Figure 4.2: FACS analysis of dorsal, lateral and ventral telencephalic cells

Frequency histograms of cell number against GFP fluorescence for samples of cells from A) the telencephalon of non-transgenic controls and (B-D) the dorsal, lateral and ventral parts of the DTy54 telencephalon. Cells from the lateral telencephalon show a higher average expression of GFP than cells in the dorsal telencephalon, with the GFP positive peak shifted to the right compared with dorsal samples (B and C). GFP positive cells are almost completely absent in the ventral telencephalon (D).

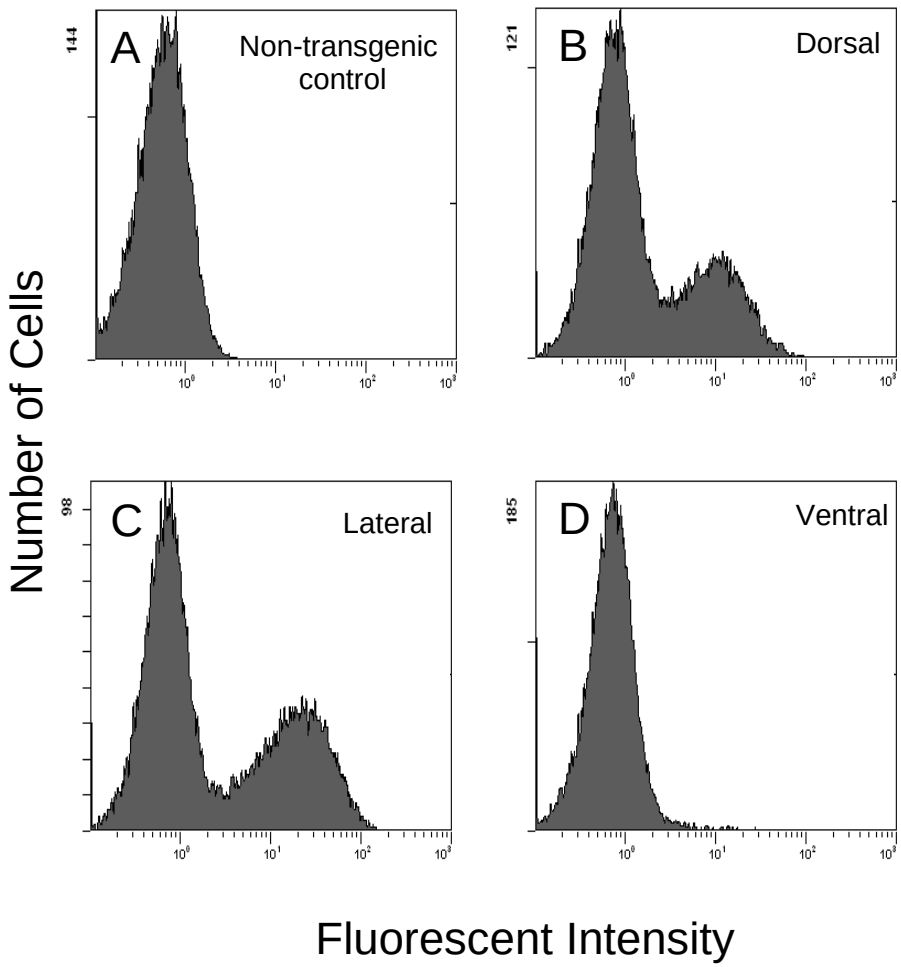
A
Non-transgenic control
B
Dorsal
C
Lateral
D
Ventral
144
121
98
185
Number of Cells
Fluorescent Intensity

Figure 4.2

positive population in this region is very small. FACS analysis showed the profiles of GFP expression to be as expected in the different tissue samples (Fig. 4.2). The lateral telencephalon not only contained a greater proportion of GFP positive cells but these cells also expressed GFP at a higher level. This is shown by the shift to the right of the peak of the GFP expressing population (compare Fig. 4.2 B and C). Only a tiny proportion of cells from the ventral telencephalon were GFP positive (Fig. 4.2 D) which is unsurprising as this region is largely negative for Pax6.

4.2.1.3 RT-PCR analysis of dissection

To further ensure that the dissections were as accurate as possible RNA was extracted from dorsal, lateral and ventral tissue samples for analysis by real time RT-PCR. The expression of a number of marker genes for dorsal, lateral and ventral regions was compared between samples. The expression of the dorsal marker gene *Ngn2* was significantly higher in tissue samples from dorsal regions compared with ventral tissue samples (Student's t-test, $p<0.01$), where expression was almost entirely absent (Fig. 4.3 A). The level of *Ngn2* was also significantly higher in lateral than in ventral tissue samples (Student's t-test, $p<0.01$). Although expression levels in the lateral telencephalon were slightly lower than dorsal regions, this difference was not statistically significant.

Expression of the ventral markers *Mash1* and *Dlx2* showed a pattern that was almost the exact opposite of that seen for *Ngn2*, with the highest level of expression seen in ventral tissue for both genes (Fig. 4.3 B and C). For *Mash1* the difference in expression between ventral and dorsal samples was statistically significant (Student's t-test, $p<0.01$). The expression level of *Mash1* in the lateral telencephalon was almost halfway between that seen in dorsal and ventral regions. Although the difference in *Mash1* expression between ventral and lateral telencephalon was not statistically significant, the level of *Mash1* was significantly higher in lateral compared to dorsal regions (Fig. 4.3 B, Student's t-test, $p<0.05$). *Dlx2* was highly expressed in ventral regions and expression was only slightly lower in lateral compared to ventral samples. *Dlx2* expression in dorsal regions was all but absent (Fig. 4.3 C). The only

statistically significant difference in *Dlx2* expression was between dorsal and ventral regions (Student's t-test, $p<0.01$).

The expression of *Sfrp2* and *Dbx1*, which were used as markers of the lateral telencephalon, showed only slight differences in expression in different parts of the telencephalon. For *Sfrp2*, dorsal and lateral telencephalon showed almost identical levels of expression with slightly lower expression in the ventral telencephalon (Fig. 4.3 D). However, there were no statistically significant changes in *Sfrp2* expression between any of the regions of the telencephalon. *Dbx1* was most highly expressed in the ventral telencephalon (Fig. 4.3 E). The level of *Dbx1* in the lateral telencephalon was about half that seen in ventral regions, with slightly lower levels of expression seen in dorsal tissue. Again however, these changes in expression levels were not statistically significant.

4.2.2 Carrying out the Microarray Experiment

Having established that the PSPB could be accurately dissected from $DTy54^{+}$ embryos, a microarray experiment was carried out to identify the downstream targets of *Pax6* in this region. The design of the microarray experiment was as follows: *Pax6* expressing cells of the PSPB were isolated by dissection followed by FACS. RNA was then extracted from the cells of interest, fluorescently labelled and hybridized to the microarray chip. A schematic illustration of the experimental protocol is shown in Figure 4.4.

4.2.2.1 Collection of Microarray Samples

To identify changes in gene expression at the PSPB in the absence of functional Pax6, specifically in a population of cells enriched for *Pax6* expression, this region was isolated by dissection from E12.5 embryos that were either $Pax6^{+/+}.DTy54^{+}$ or $Pax6^{sey/sey}.DTy54^{+}$ as described above (Fig. 4.1). The cells were then dissociated and sorted by FACS (Fig. 4.5). Before experimental samples were sorted, dissociated telencephalic cells from a non-transgenic embryo were used to position the gate for collection so that no non-transgenic cells were within the gated region (Fig. 4.5 A). This was a very stringent cut-off that eliminated both GFP-negative cells and cells

Figure 4.3: Gene expression levels measured by real-time RT-PCR

The expression of *Ngn2*, *Mash1*, *Dlx2*, *Sfrp2*, and *Dbx1* is shown relative to levels of *Gapdh* as measured by real-time RT-PCR in the dorsal, lateral and ventral telencephalon. *Ngn2* is expressed at relatively high levels in dorsal and lateral telencephalon but is almost absent from ventral regions (A). *Mash1* and *Dlx2* are expressed at very low levels dorsally with higher expression seen in lateral and ventral tissue (B and C). *Sfrp2* shows similar expression levels in all samples, with a slight decrease in expression from dorsal to ventral regions (D). *Dbx1* is also expressed in all regions with highest expression seen ventrally and slightly lower levels of expression in dorsal and lateral regions. Differences in expression were examined by t-test and statistically significant differences are indicated as follows: * = $p < 0.05$, ** = $p < 0.01$. (n = 6 for *Sfrp2*; 4 for *Ngn2*, *Dbx1* and *Mash1* and 2 for *Dlx2*)

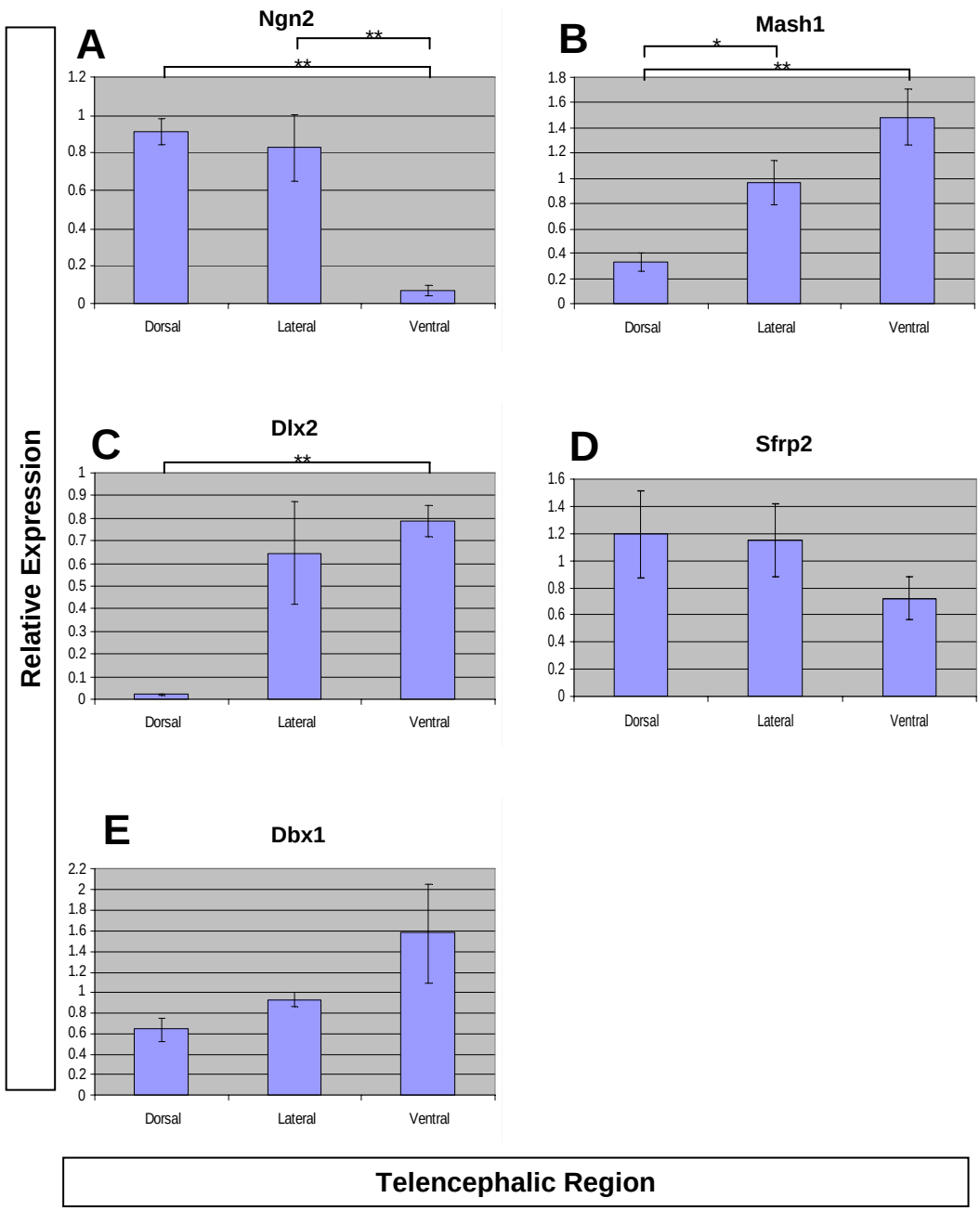
A
Ngn2
**
**
1.2
1
0.8
0.6
0.4
0.2
0
Dorsal
Lateral
Ventral
B
Mash1
*
**
1.8
1.6
1.4
1.2
1
0.8
0.6
0.4
0.2
0
Dorsal
Lateral
Ventral
C
Dlx2
**
1
0.9
0.8
0.7
0.6
0.5
0.4
0.3
0.2
0.1
0
Dorsal
Lateral
Ventral
D
Sfrp2
1.6
1.4
1.2
1
0.8
0.6
0.4
0.2
0
Dorsal
Lateral
Ventral
E
Dbx1
2.2
2
1.8
1.6
1.4
1.2
1
0.8
0.6
0.4
0.2
0
Dorsal
Lateral
Ventral
Relative Expression
Telencephalic Region

Figure 4.3

Figure 4.4: Schematic outline of microarray experiment

The basic steps of the microarray experiment are outlined for both *Pax6*$^{+/+}$*.DTy54* samples (left) and *Pax6*$^{sey/sey}$*.DTy54* samples (right). GFP expression at the ventricular surface of the telencephalic lobes is shown (top) with the area to be dissected indicated by broken red lines. Cells were then dissociated and the GFP positive cells isolated by FACS. RNA was extracted from these cells, amplified and labelled with Cy5 (red) or Cy3 (green) fluorescent dyes. The two RNA samples were then combined and hybridized to an Agilent® G4122A whole mouse genome array. PSPB, pallial-subpallial boundary.

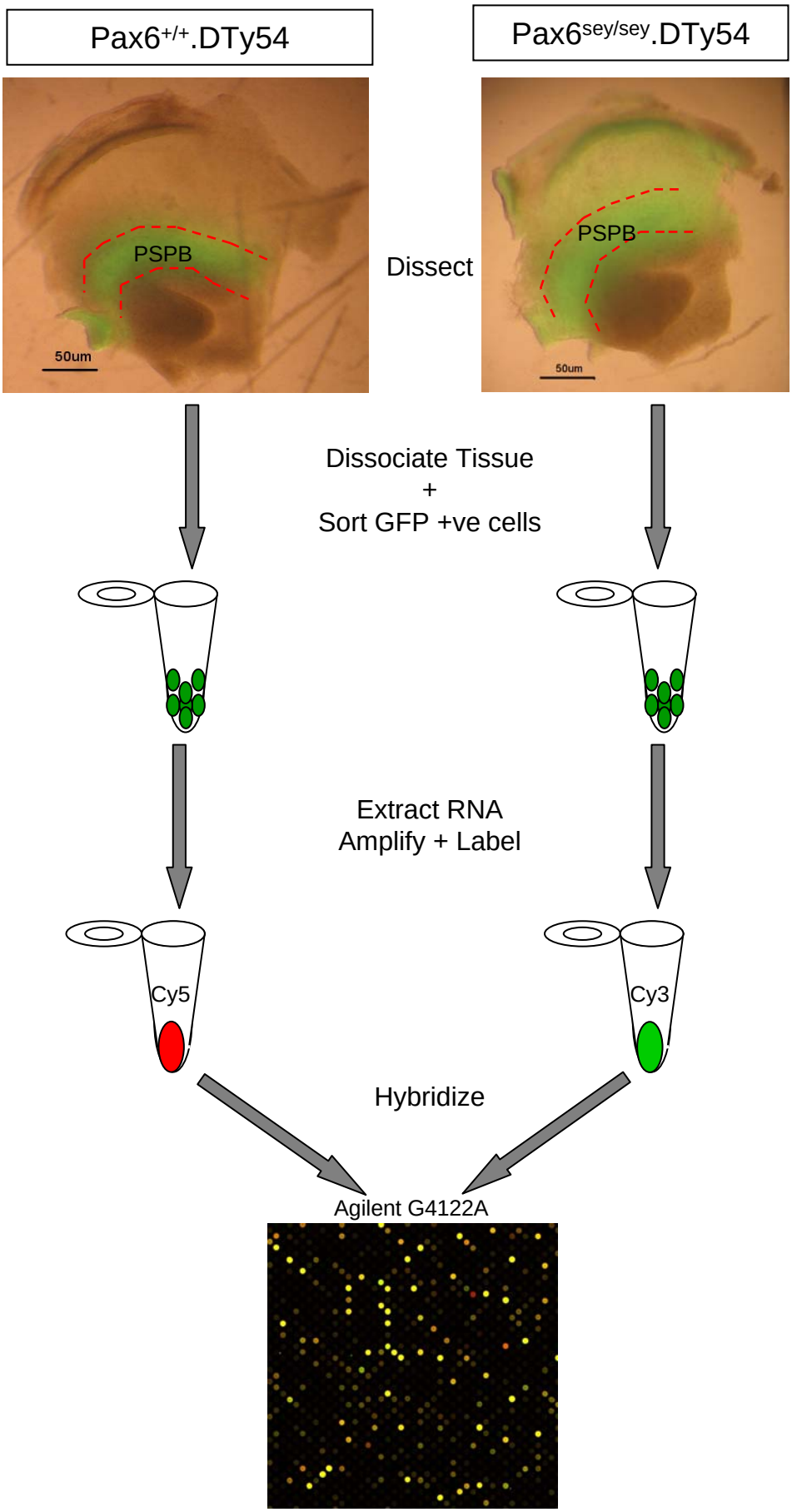
Pax6+/+.DTy54
Pax6sey/sey.DTy54
PSPB
50um
Dissect
PSPB
50um
Dissociate Tissue
+
Sort GFP +ve cells
Extract RNA
Amplify + Label
Cy5
Cy3
Hybridize
Agilent G4122A

Figure 4.4

with low levels of GFP when the experimental samples were sorted (Fig. 4.5 B and C). For samples from *Pax6*$^{+/+}$.*DTy54*$^{+}$ embryos almost 70% of cells expressed high levels of GFP and were included in the gated region, around 75% of cells were within the gated region for *Pax6*$^{sey/sey}$.*DTy54*$^{+}$ samples. In order to ensure that no technical errors occurred while sorting was being carried out the purity of the GFP positive cell population was checked by analysing a small number of cells from this population for levels of GFP fluorescence (Fig. 4.5 D and E). If sorting has occurred as expected then the proportion of cells falling within the sort gate should be close to 100%. The samples used for the microarray experiment all had a purity of 97% or higher when this analysis was carried out.

To ensure that the GFP positive population isolated for analysis by microarray was indeed enriched for *Pax6* expressing cells, immunocytochemistry for Pax6 was carried out on both the GFP positive and GFP negative populations of cells (Fig. 4.6 A). Cells were then analysed by flow cytometry. This proved to be a very difficult experiment technically and due to misidentified plug dates and the degradation of cells during the experimental procedure only one sample, from E13.5 embryos, gave usable results (Fig. 4.6). Telencephalic cells from a GFP negative littermate, incubated without primary antibody were used as a negative control (Fig. 4.6 B and C). Almost all cells in the GFP positive cell population were also positive for Pax6 (Fig. 4.6 D and E; cells to the right of the line in E are Pax6 positive). The GFP negative cell population contained a mixture of Pax6 positive and negative cells, but the proportion of Pax6 positive cells in the population was lower than for the GFP positive cell population (Fig. 4.6 F and G; cells to the right of the line in G are Pax6 positive) and these cells were more likely to be expressing Pax6 at a lower level than Pax6 positive cells from the GFP positive population (compare Fig. 4.6 E and G).

Pax6$^{sey/sey}$.*DTy54*$^{+}$ embryos were easily identifiable due to absence of eyes, but as the *Pax6*$^{sey/+}$ phenotype is not evident until E14.5 it was impossible to distinguish between *Pax6*$^{sey/+}$.*DTy54*$^{+}$ and *Pax6*$^{+/+}$.*DTy54*$^{+}$ embryos at E12.5. This meant that the *Pax6*$^{+/+}$.*DTy54*$^{+}$ littermates of *Pax6*$^{sey/sey}$.*DTy54*$^{+}$ embryos could not be used as they could not be identified without genotyping by PCR and so embryos for the

Figure 4.5: FAC sorting of samples for microarray

Graphs of fluorescent intensity plotted against cell number. The fluorescent profile of telencephalic cells from a non-transgenic embryo is shown in A. This was used to establish where the gate should be placed. The fluorescent profile of cells from the E12.5 lateral telencephalon of *Pax6*$^{+/+}$.*DTy54*$^{+}$ and *Pax6*$^{sey/sey}$.*DTy54*$^{+}$ embryos are shown in B) and C) respectively. The population of cells falling within the gated region were collected for analysis by microarray. The percentage of cells falling within the gated region is indicated on the graph. D) and E) show the fluorescent profile, after sorting, of the gated cells in A) and B) respectively, demonstrating that sorting was carried out efficiently.

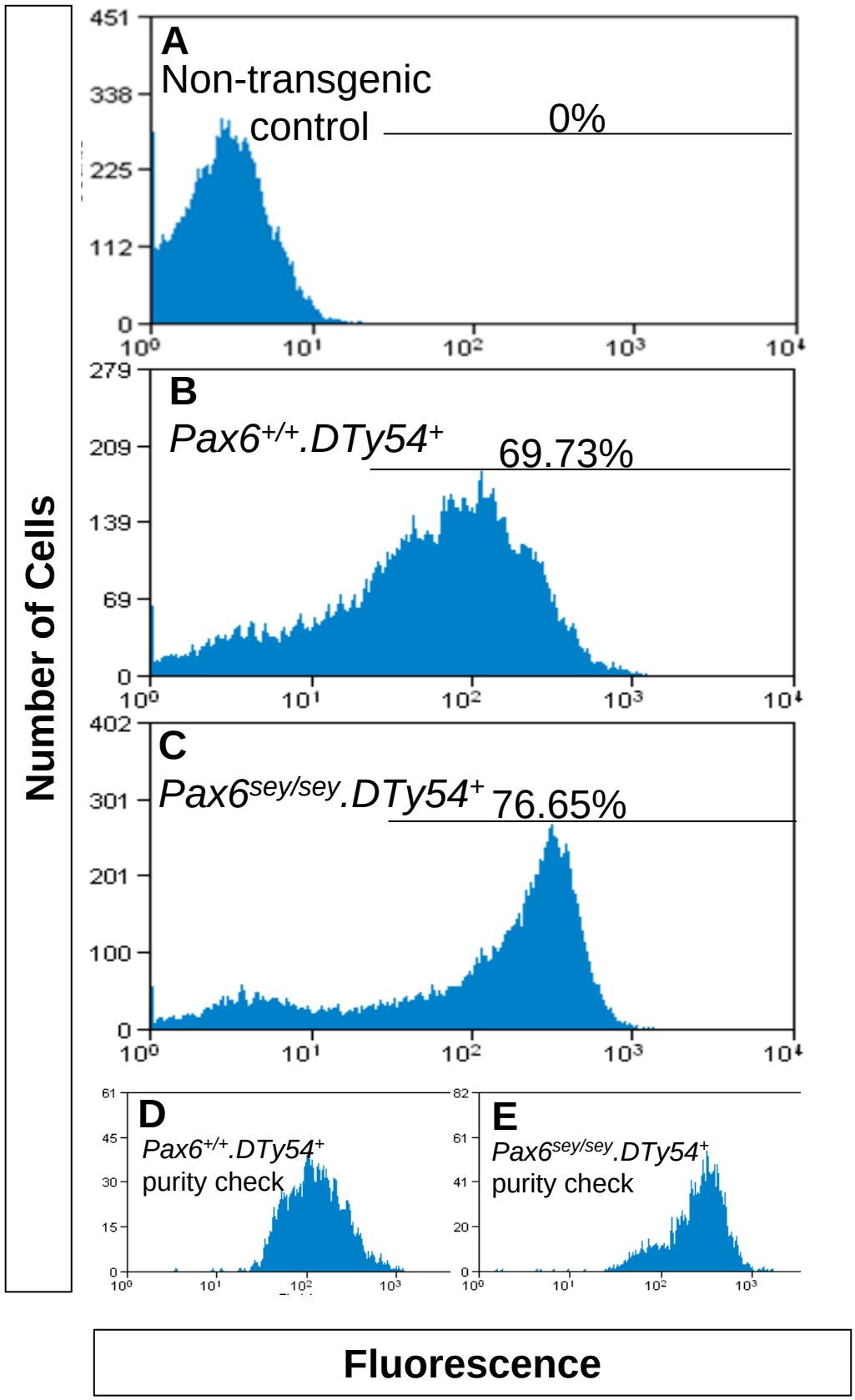
A
Non-transgenic
control
0%
B
Pax6+/+.DTy54+
69.73%
C
Pax6sey/sey.DTy54+
76.65%
D
Pax6+/+.DTy54+
purity check
E
Pax6sey/sey.DTy54+
purity check
Number of Cells
Fluorescence

Figure 4.5

Figure 4.6: Immunocytochemisty and flow analysis of FAC sorted cells

Cells from the lateral telencephalon on E13.5 embryos were sorted and both GFP positive (Population 1) and GFP negative (Population 2) cells were collected for analysis by immunocytochemistry (A). Data from non-transgenic telencephalic cells incubated without primary antibody is shown in B and C. Cells from Population 1 labelled with a Pax6 antibody are shown in D and E; similarly labelled cells from Population 2 are shown in F and G. B, D and F show forward and side scatter profiles of the cell populations. Events included in the region R1 are deemed intact cells and the Pax6 labelling of these cells, measured by A647 fluorescence, is shown in C, E and G respectively. Cells with a measured fluorescence to the left of the vertical line in C, E and G are deemed to be negative for Pax6 expression, while those to the right of the line are taken to be positive for Pax6.

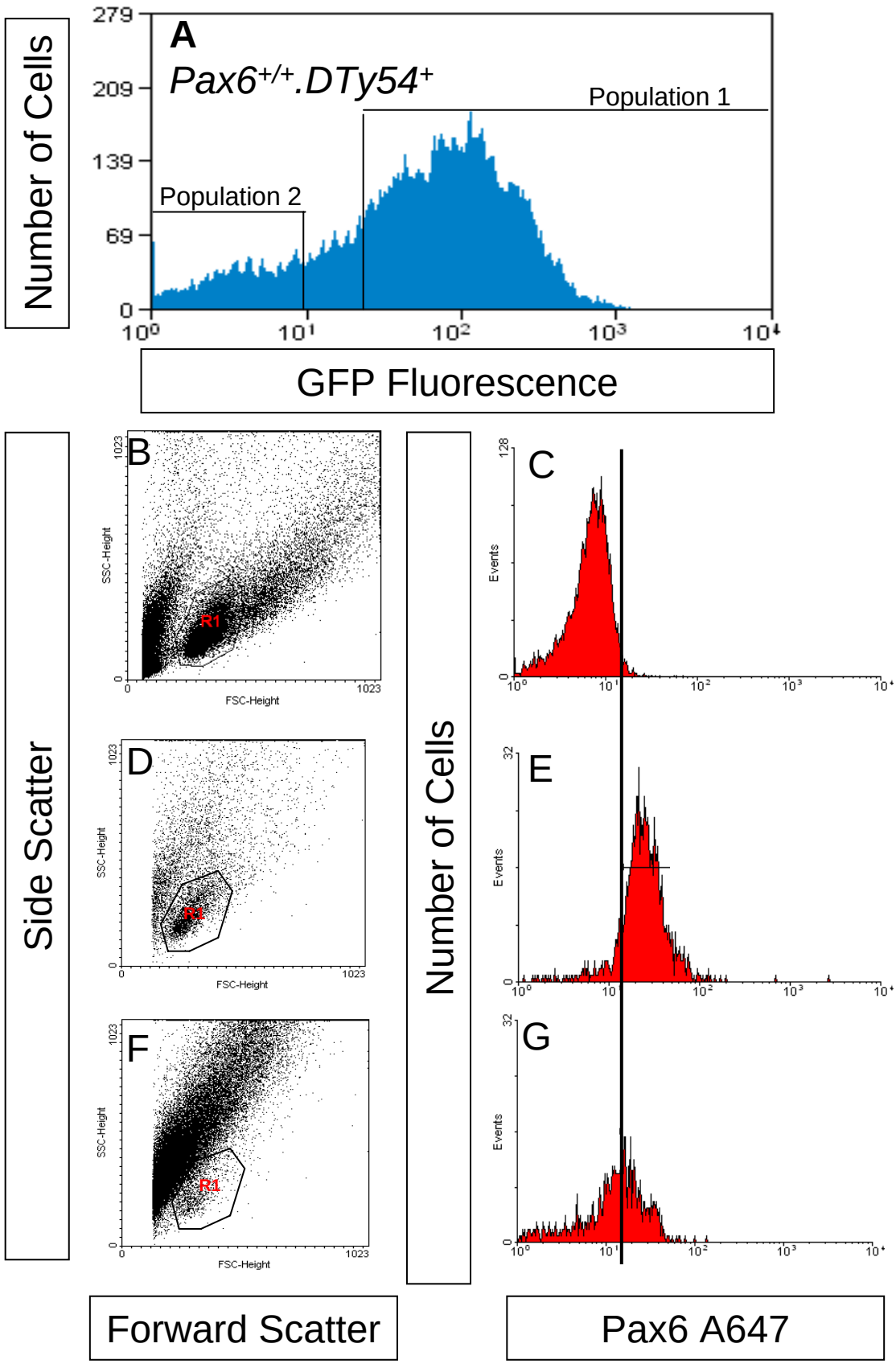
A
Pax6+/+.DTy54+
Population 1
Population 2
279
209
139
69
0
Number of Cells
10⁰
10¹
10²
10³
10⁴
GFP Fluorescence
B
C
D
E
F
G
SSC-Height
FSC-Height
R1
Events
Side Scatter
Number of Cells
Forward Scatter
Pax6 A647

Figure 4.6

Pax6$^{+/+}$.*DTy54*$^{+}$ microarray samples were generated separately. In order to collect enough GFP positive cells to provide a sufficient amount of RNA for a microarray experiment, it was necessary to pool tissue samples. Each microarray sample consisted of tissue pooled from four different embryos. Where possible the embryos in an individual sample were all littermates to help limit biological variation within samples. However, in most cases, especially for *Pax6*$^{sey/sey}$.*DTy54*$^{+}$ samples, embryos were collected from two or more litters. Collection of *Pax6*$^{sey/sey}$.*DTy54*$^{+}$ samples proved to be particularly challenging as this genotype was found less frequently than predicted by normal Mendelian inheritance (Table 4.1). Chi squared analysis showed a significant difference in the distribution of genotypes observed compared with the expected distribution (p-value<0.001). Interestingly this difference was only seen when the *DTy54* transgene was carried by the male (p-value<0.001; Table 4.2). When the female was transgenic there was no significant difference in the genotype distribution (p-value=0.125; Table 4.3).

RNA was extracted from the GFP positive cells immediately after sorting to minimise the amount of RNA degradation. To ensure that the RNA was of high quality each sample was analysed using the Agilent® Bioanalyser. This assigns an RNA integrity number (RIN) of between 1 and 10 to each RNA sample, where 10 indicates high quality, intact RNA and 1 indicates poor quality RNA that is almost totally degraded (Schroeder *et al.* 2006). The bioanalyser output for the samples used in the microarray experiment is shown in (Fig. 4.7). All but one of the RNA samples used for the microarray had RINs of 9.3 or higher (Table 4.4). The Bioanalyser was unable to generate an RIN for sample Sey19 as there was very little RNA in this sample.

4.2.2.2 Hybridization of the microarrays

There were 5 microarrays available to be hybridized, but due to a number of problems encountered in collecting the RNA samples it was not practical to hybridize all of the arrays on the same day. The RNA in many of the initial samples

Genotype	*Pax6*$^{+/+}$/*Pax6*$^{sey/+}$	*Pax6*$^{+/+}$/*Pax6*$^{sey/+}$.*DTy54*$^{+}$	*Pax6*$^{sey/sey}$	*Pax6*$^{sey/sey}$.*DTy54*$^{+}$
Observed numbers of embryos	315	318	71	64
Expected numbers of embryos	288	288	96	96

Table 4.1: Distribution of genotypes collected at E12.5, from all crosses, compared with the expected Mendelian distribution

Chi squared analysis shows a significant difference in the distribution of genotypes (p-value < 0.001).

Genotype	*Pax6*$^{+/+}$/*Pax6*$^{sey/+}$	*Pax6*$^{+/+}$/*Pax6*$^{sey/+}$.*DTy54*$^{+}$	*Pax6*$^{sey/sey}$	*Pax6*$^{sey/sey}$.*DTy54*$^{+}$
Observed numbers of embryos	142	144	24	24
Expected numbers of embryos	125.25	125.25	41.75	41.75

Table 4.2: Distribution of genotypes collected at E12.5, from crosses where the DTy54 transgene was carried by the male, compared with the expected Mendelian distribution

Chi squared analysis shows a significant difference in the distribution of genotypes (p-value < 0.001).

Genotype	*Pax6*$^{+/+}$/*Pax6*$^{sey/+}$	*Pax6*$^{+/+}$/*Pax6*$^{sey/+}$.*DTy54*$^{+}$	*Pax6*$^{sey/sey}$	*Pax6*$^{sey/sey}$.*DTy54*$^{+}$
Observed numbers of embryos	77	93	17	28
Expected numbers of embryos	80.625	80.625	26.875	26.875

Table 4.3: Distribution of genotypes collected at E12.5, from crosses where the DTy54 transgene was carried by the female, compared with the expected Mendelian distribution

Chi squared analysis shows no significant difference in the distribution of genotypes (p-value = 0.125).

Array	Samples	RINs
1	WT12; Sey11	9.8; 9.8
2	WT16; Sey14	10; 9.8
3	WT17; Sey18	9.7; 9.3
4	WT17; Sey18	9.7; 9.3
5	WT12; Sey19	9.8; na

Table 4.4: Samples hybridized to each array and their associated RNA integrity numbers (RIN)

Figure 4.7: Analysis of RNA quality

Graphical output from the bioanalyser for 6 of the 7 unique RNA samples used in the microarray experiment. A-C show WT samples 12, 16 and 17 respectively and D-F show Sey samples 11, 14 and 18. The 18S and 28S ribosomal peaks can be clearly seen in each graph. The RNA integrity number for each sample is shown on the appropriate graph.

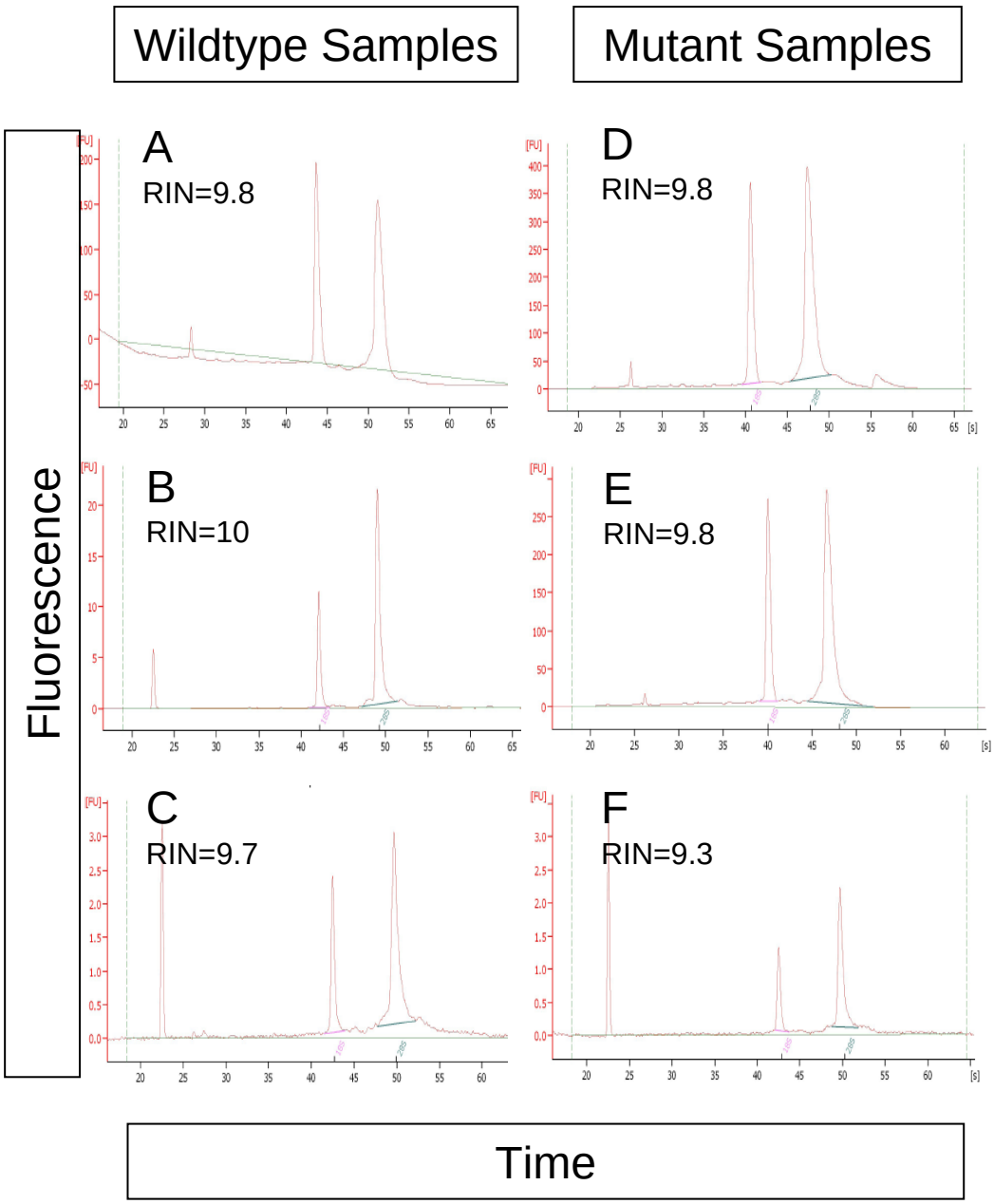
Wildtype Samples
Mutant Samples
Fluorescence
A
RIN=9.8
D
RIN=9.8
B
RIN=10
E
RIN=9.8
C
RIN=9.7
F
RIN=9.3
Time

Figure 4.7

collected was badly degraded when assessed on the bioanalyser and had to be discarded leaving only 2 samples of each genotype. Because of the length of time required to generate *Pax6*$^{sey/sey}$*.DTy54*$^{+}$ embryos, it was decided to hybridize the good quality samples and to hybridize the remaining samples as soon after collection as possible. This resulted in the arrays being hybridized in three batches as follows: Arrays 1 and 2 were hybridized together; array 3 was hybridized on its own; and finally arrays 4 and 5 were hybridized together. For reasons given below the same RNA samples were hybridized to both array 3 and array 4 and data from array 4 replaces the data from array 3 in the analysis.

While this strategy was not ideal, it did allow the initial normalisation and quality control of the first three datasets to be carried out before the final two arrays were hybridized. These quality control steps, described below, identified the dataset from array 3 as an outlier when compared to the data from arrays 1 and 2. As the collection of the last *Pax6*$^{sey/sey}$*.DTy54*$^{+}$ samples was taking far longer than was feasible, it was therefore decided to use one of the remaining arrays to repeat the hybridization of the samples hybridized to array 3. It was hoped that the array would prove to be a technical rather than a biological outlier and that the technical errors that had occurred during the initial hybridization would be eliminated, or at least reduced, on repetition of the experiment.

4.2.2.3 Quality control and normalisation

A number of quality control steps were carried out to assess the hybridization of the arrays. Scatterplots of the array data were used to ensure that the general appearance of the data was as expected, with most genes showing no change in expression between *Pax6*$^{+/+}$*.DTy54*$^{+}$ and *Pax6*$^{sey/sey}$*.DTy54*$^{+}$ samples. One would expect to see a graph in which most of the points rest on, or close to, a line representing no change in expression between the two samples. Apart from array 5, in which many genes with large changes in expression levels can be seen, scatterplots suggest that hybridization occurred as expected (Fig. 4.8). Scatterplots, however, only provide an overview of hybridization on a given array and give little indication of the quality of the individual samples hybridized to the array. In order to determine if any of the

Figure 4.8: Scatterplots of array data

Scatterplots of the data from arrays 1-5 are shown in A-E respectively. The fluorescent intensity measurement for each spot from the *Pax6*$^{sey/sey}$*.DTy54* sample (x-axis) is plotted against the fluorescent intensity of the *Pax6*$^{+/+}$*.DTy54* sample for that spot (y-axis).

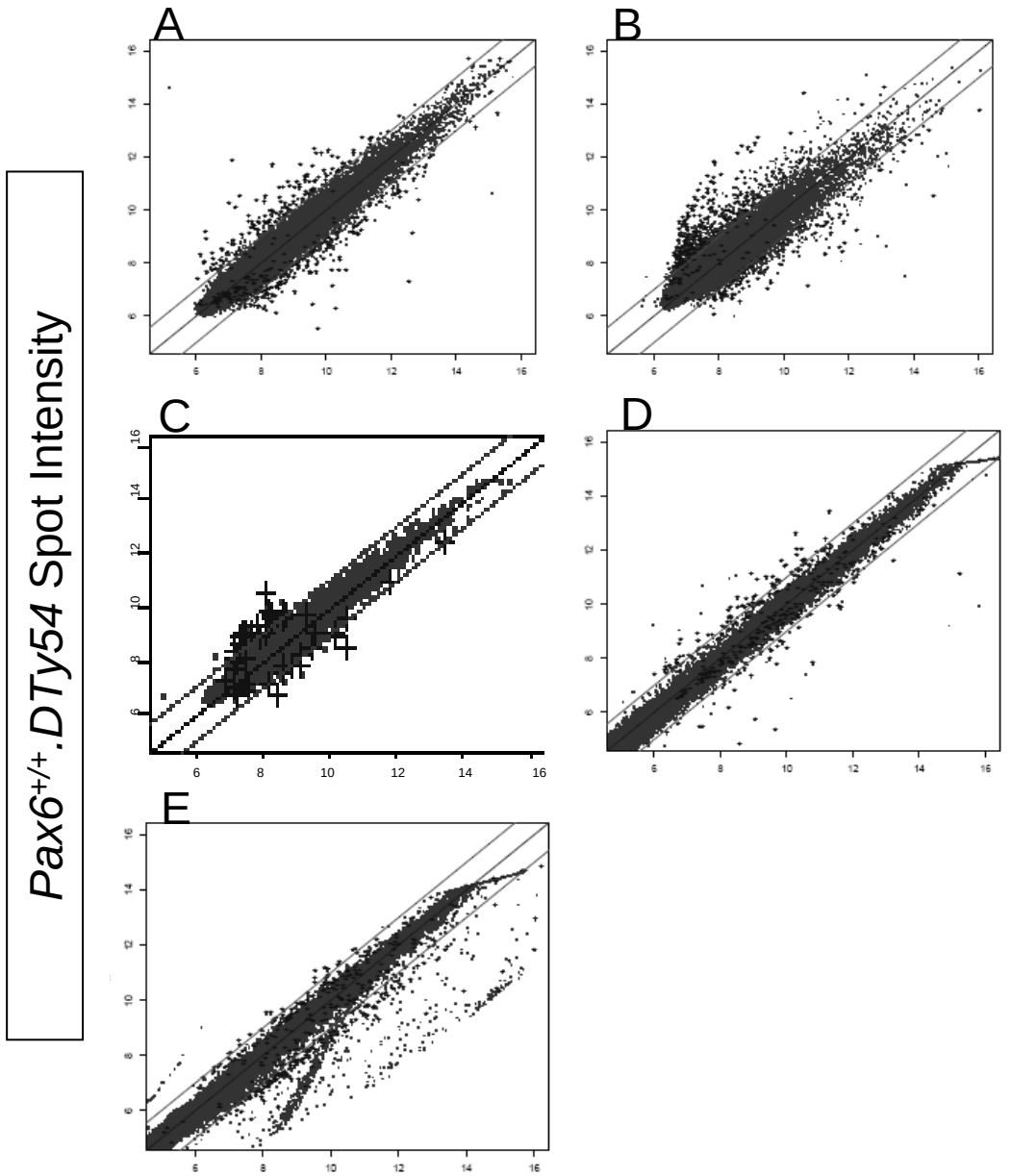
A
B
C
D
E
Pax6+/+.DTy54 Spot Intensity
Pax6sey/sey.DTy54 Spot Intensity

Figure 4.8

individual RNA samples were outliers, a comparison of the expression values measured for each sample was carried out, using a method called single dye pairs. This involved producing a series of graphs in which the intensity values measured for each sample was plotted against the expression values measured for every other sample (Fig. 4.9 and 4.10).

As with the scatterplots, one would expect to see a graph in which most of the points rest on, or close to, a line representing no change in expression between the two samples. When this analysis was done on the first three sets of array data, both samples hybridized to array 3 were identified as outliers. When data from either of these samples was plotted against data from any of the samples hybridized to arrays 1 and 2 the graphs produced showed a much wider spread of data-points than expected (Fig. 4.9). Data from any pairing of the samples hybridized to arrays 1 and 2 on the other hand produced a graph in which the data-points were tightly clustered around a relatively straight line.

After all arrays had been hybridized this analysis was repeated with data from arrays 1, 2, 4 and 5 (data from array 3 is replaced by data from array 4). This clearly identifies sample Sey19 as a problem sample as it produces a graph that deviates greatly from expected regardless of which other sample it is plotted against (Fig. 4.10). In summary, initial quality control checks on the array data suggest that in general hybridization occurred as expected, but data from arrays 3 and 5 should be treated with caution.

Data from all arrays was then normalised to minimise variation both within and between arrays. Firstly background noise was removed using Edwards' algorithm (Edwards, 2003). This is a non-linear method of removing background which uses a smoothing function rather than simply subtracting the background signal from the probe signal. This helps prevent the loss of data from regions where the background signal is high. Non-linear differences within arrays arise from differences in the efficiency of incorporation of the two dyes used to label the samples (Yang *et al.,* 2002). Loess normalisation was carried out to remove non-linear differences from

Figure 4.9: Single dye pairs (samples from 3 arrays)

Raw data from each individual sample hybridized to the first three arrays is plotted against every other sample to determine the general quality of the hybridizations. Graphs on the lower left hand side are mirror images of the graphs on the upper right hand side, with samples plotted on opposite axes. Both samples from array 3 (Sey18 and WT17) can be seen to be outliers as, apart from when they are plotted against each other, they produce a graph with a very wide spread in the data.

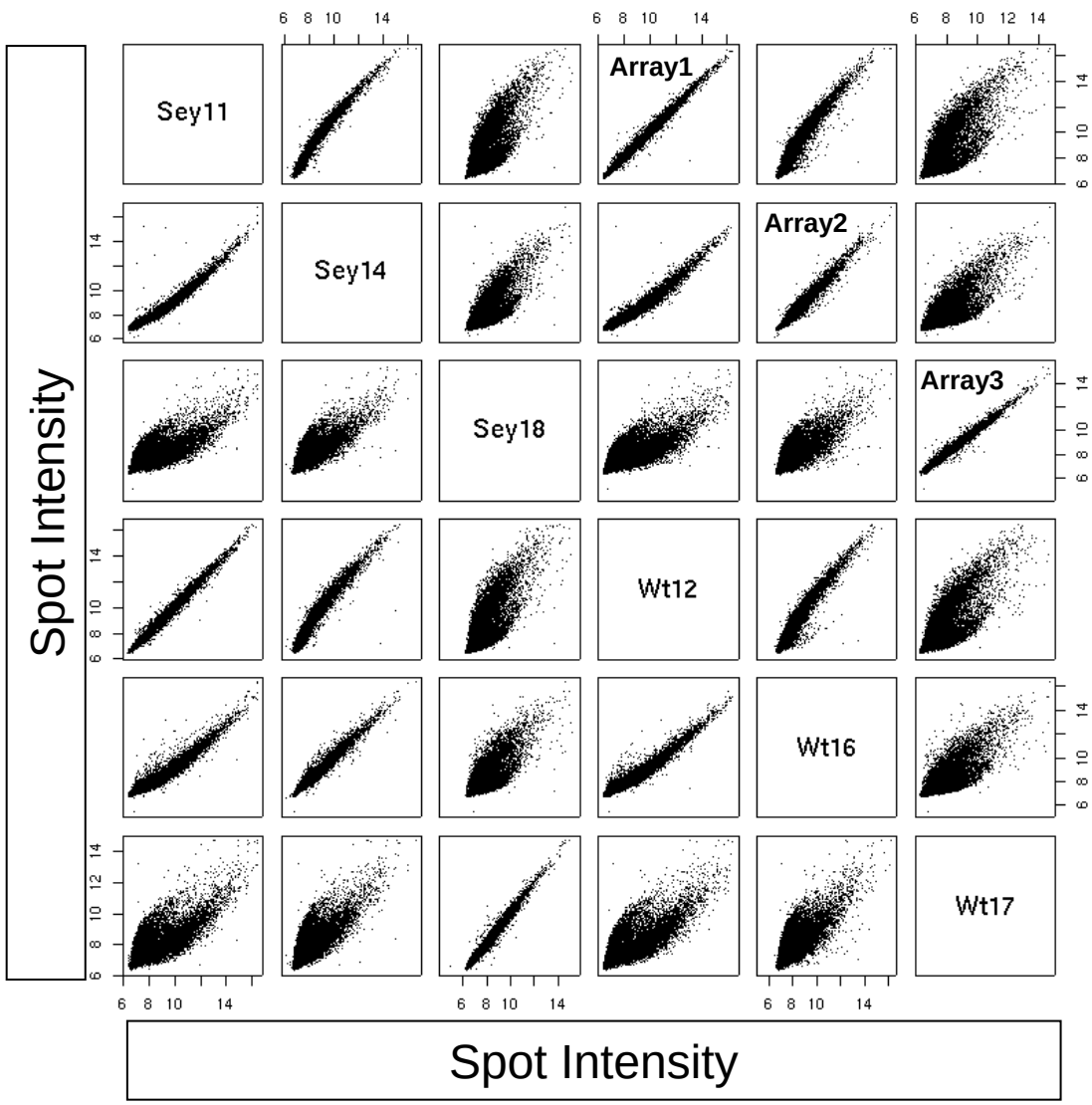
Spot Intensity
Sey11
Array1
Array2
Sey14
Array3
Sey18
Wt12
Wt16
Wt17
Spot Intensity

Figure 4.9

Figure 4.10: Single dye pairs

Raw data from each individual sample hybridized is plotted against every other sample to determine the overall quality of the dataset. Graphs on the lower left hand side are mirror images of the graphs on the upper right hand side, with samples plotted on opposite axes. Sample Sey19 can be identified as a problem sample due to the high proportion of spots that fail to cluster around the line of no change in expression, regardless of which other sample it is plotted against (graphs outlined in red).

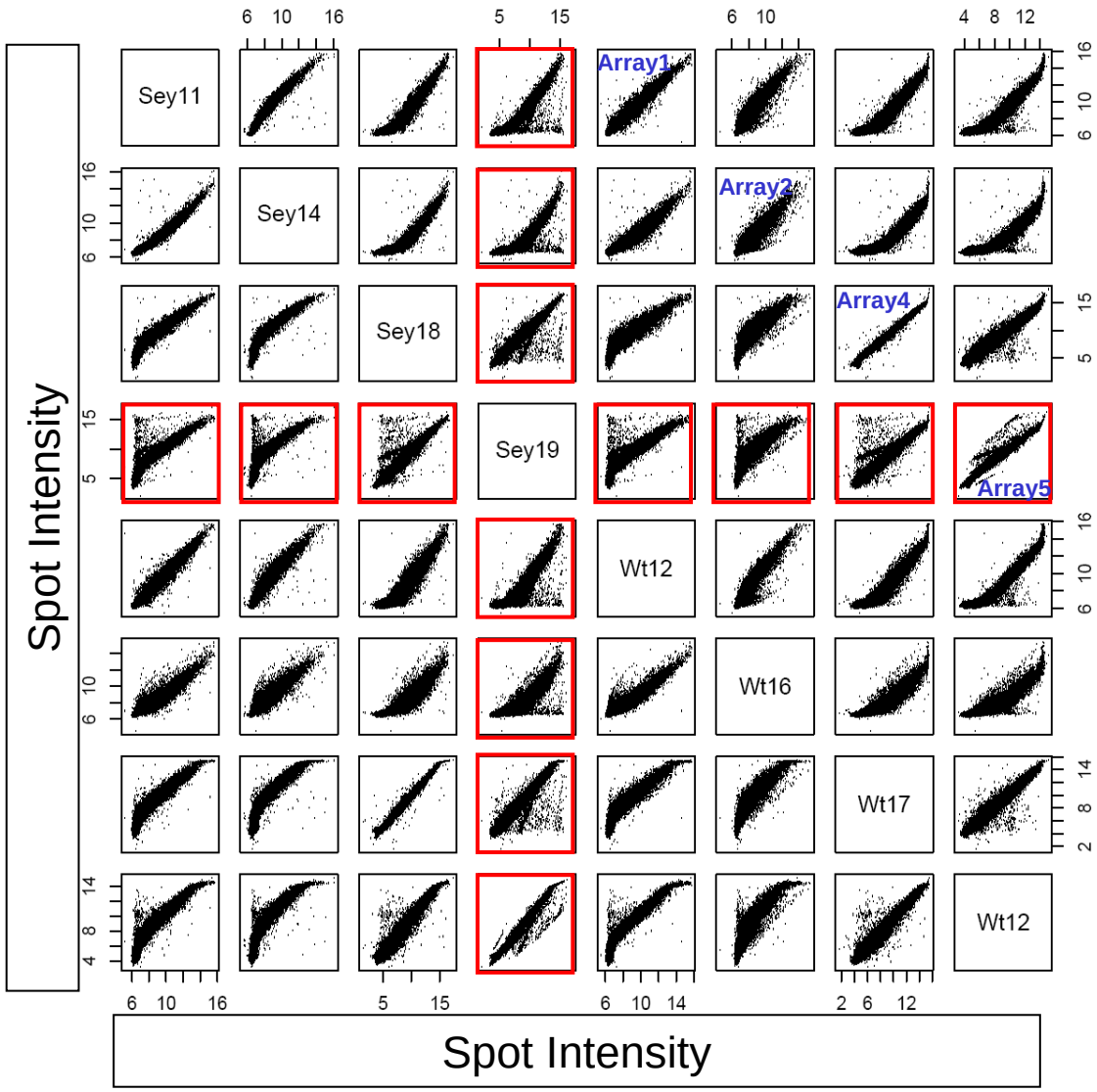
Spot Intensity
Sey11
Array1
Sey14
Array2
Sey18
Array4
Sey19
Array5
Wt12
Wt16
Wt17
Wt12
Spot Intensity

Figure 4.10

within each array (Cleveland, 1979; Yang *et al.,* 2002). For this the data was plotted on an MA plot, where M is the $\log_2$ expression ratio for *Pax6*$^{sey/sey}$.*DTy54*$^{+}$ compared with wildtype samples and A is the signal intensity from each spot on the array. Loess normalisation was used to linearise the data by applying a locally weighted regression model to the data, a subset at a time. The linearised data was then centred on a $\log_2$ expression ratio of zero, representing no change in expression for the majority of genes (Fig. 4.11). This normalisation step highlights the improvement in the quality of data when the hybridization of samples from array 3 was repeated (note the large number of genes with very low expression in Fig. 4.11 C' compared with D' and also the wider spread in the distribution of the data). It also identifies the dataset from array 5 as an outlier due to the large number of probes for which the hybridization signal was very low, or for which extreme fold changes were measured (boxed area in Fig. 4.11 E', compare with 4.11 A'-D').

In order to carry out comparisons between data from different arrays it was necessary to remove differences between arrays that were not due to biological variation. To do this the distribution of $\log_2$ ratios of expression for *Pax6*$^{sey/sey}$.*DTy54*$^{+}$ compared with wildtype samples was plotted on a boxplot for each array. These plots clearly show that the log ratio distributions of arrays 1 and 2 are much narrower than those of arrays 4 and 5 (Fig. 4.12). Any comparison between data from these 4 arrays would be skewed towards the results measured from array 4 and 5 due to the larger fold changes in the data from these arrays. To prevent the data being skewed in this manner and to allow accurate comparisons to be made between arrays it is necessary to normalise these differences in the distribution of $\log_2$ ratios. The distribution of data from each array was normalised to match the average distribution across all arrays using median absolute deviation measurements (Yang *et al.,* 2002). This method is based on the assumption that the differences in distribution are due to hybridization differences rather than to biological variation. This is a reasonable assumption as there were only small differences in distribution between arrays hybridized on the same day, while arrays hybridized on different days had large differences in the distribution of $\log_2$ ratios (compare data from arrays 1 and 2 with data from array 4 and 5 in Fig. 4.12).

Figure 4.11: MA plots

RNA abundance (A) plotted against $\log_2$ fold change in expression in *Pax6*$^{sey/sey}$.*DTy54*$^{+}$ samples compared to wildtype (M) is shown for all arrays before (A-E) and after (A'-E') Loess normalisation. The appearance of array 3 can be seen to be greatly improved on repetition of the hybridization (compare B and B' with C and C'). The problems with array 5 are only slightly improved on normalisation (see boxed areas in E') and so this array was excluded from further analysis.

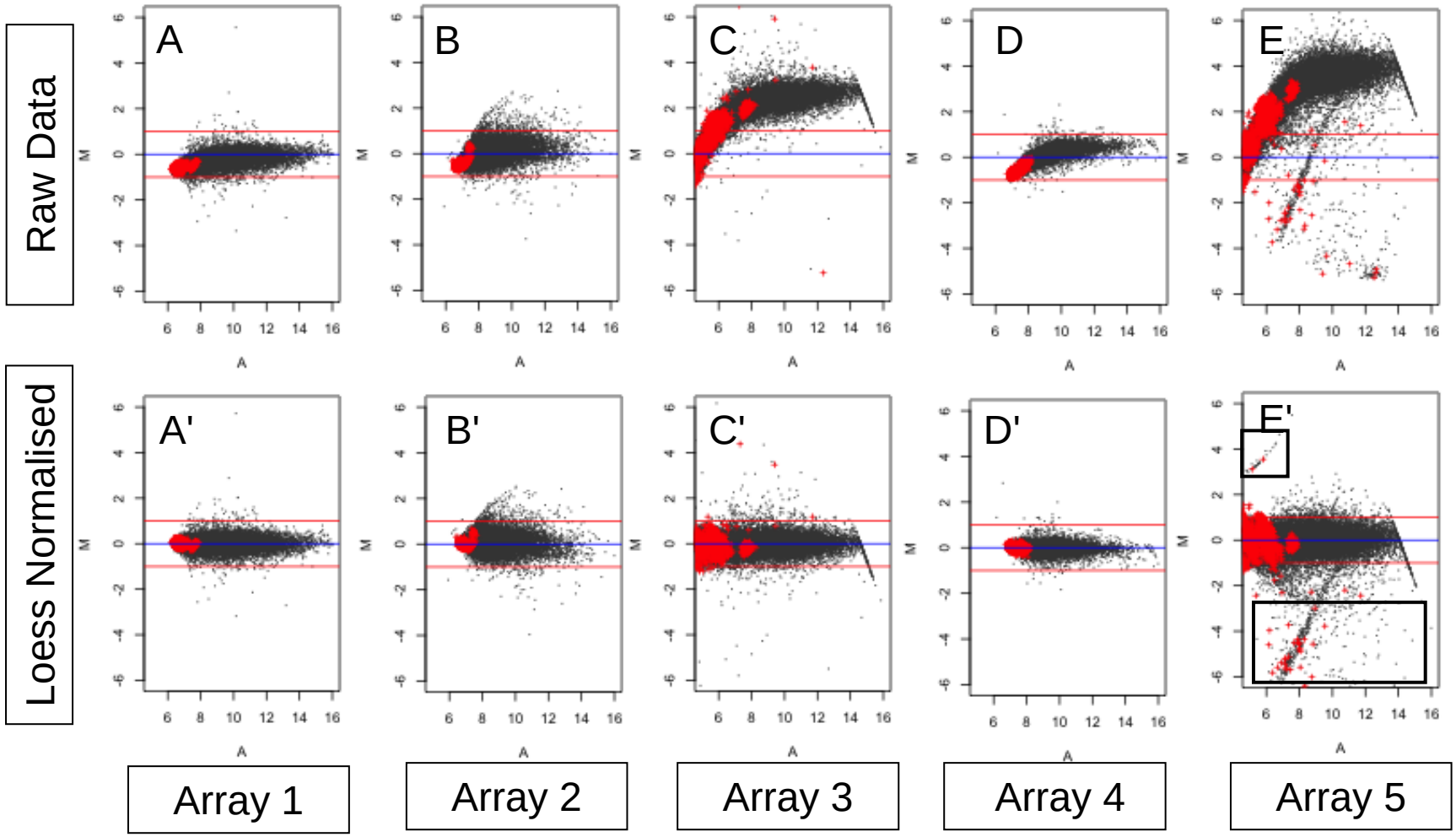
Raw Data
Loess Normalised
A
B
C
D
E
A'
B'
C'
D'
E'
M
A
Array 1
Array 2
Array 3
Array 4
Array 5

Figure 4.11

Figure 4.12: Boxplots of log-ratio distributions of raw data

The log-ratio distributions for each array, before normalisation, are shown. 50% of all spots fall within the boxed area for each array and the wide horizontal lines show the limits between which 75% of all spots fall. Arrays 3 and 4 can be seen to have a much wider range of log-ratios than arrays 1 and 2. Differences in log-ratio distribution were equalised using median absolute deviation measurements.

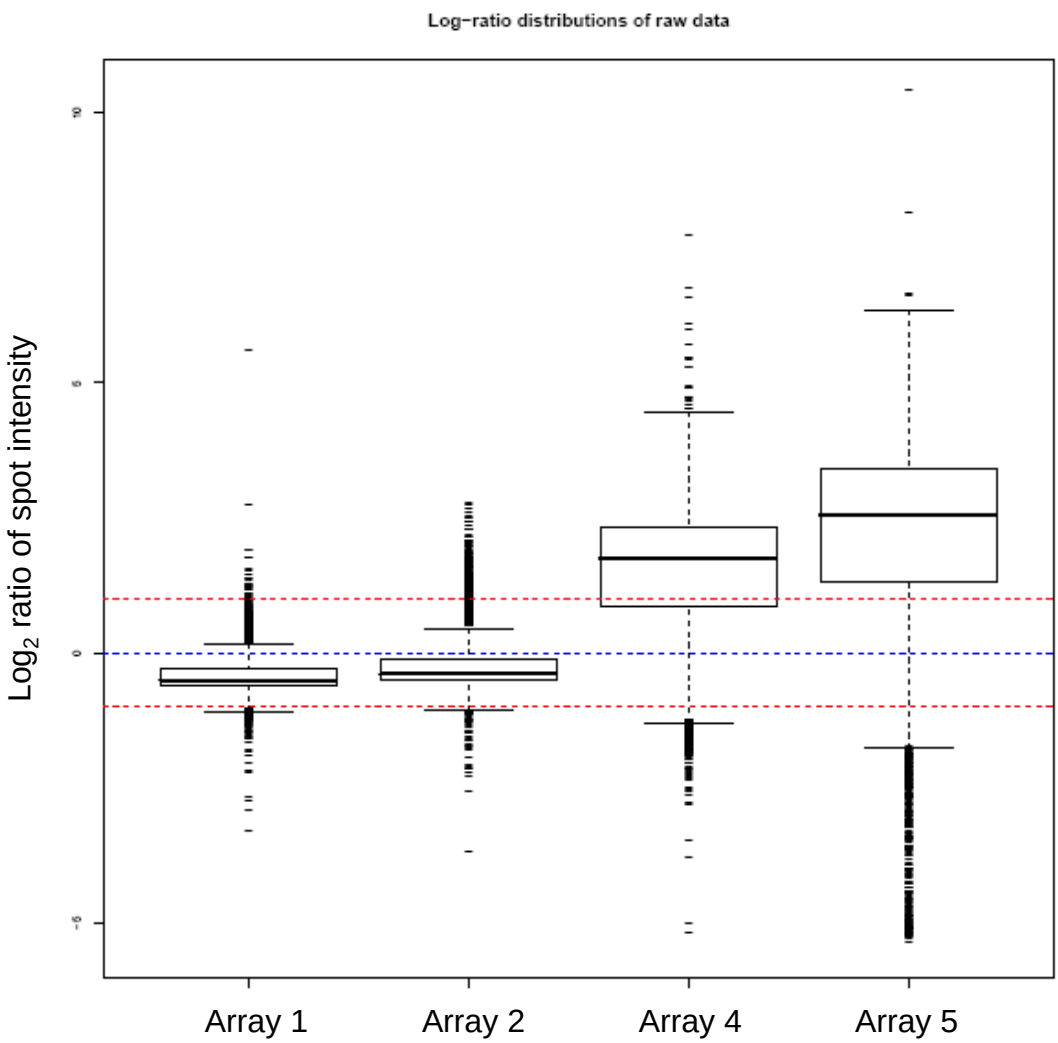
Log-ratio distributions of raw data
Log2 ratio of spot intensity
10
5
0
-5
Array 1
Array 2
Array 4
Array 5

Figure 4.12

Normalisation performed as expected, but did little to improve the appearance of data from array 5 (see the boxed areas in Fig 4.11 E'). The poor quality of the *small eye* sample hybridized to this array combined with the large number of outliers still present after normalisation seemed likely to bias the results. It was therefore decided to exclude array 5 from the analysis of the results. As the design of the microarray experiment did not include the use of a common reference sample, log ratios cannot be compared directly between different arrays as differences in the log ratio of a given gene could arise due to changes in the expression level of that gene in either of the samples hybridized to the array. Instead the comparison is made between three $Pax6^{+/+}.DTy54^{+}$ and three $Pax6^{sey/sey}.DTy54^{+}$ samples which are treated as array-independent biological replicates. Preliminary analysis assigned p-values to each $\log_2$ fold change value using an empirical Bayes moderated t-test (Efron and Tibshirani, 2002). This is a variation on the Students t-test which allows more accurate p-values to be estimated when the n-number is small, but there are a lot of other data available. In this case it takes advantage of the large number of probes present on each array and the fact that the expression of the majority of genes will remain unchanged to calculate p-values where there is only an n of 3 for each biological condition.

When statistical tests are repeated many times differences can be identified as being statistically significant just by chance. This is a particular problem with microarray data due to the large volume of data. If $p<0.05$ is taken as statistically significant then 5% of all tests carried out will give a significant result even where there is no significant difference (a false positive). In order to generate p-values for each probe on the microarray 43,000 t-tests were carried out. If 5% of these are identified as statistically significant just by chance then 2150 probes will be wrongly identified. It is therefore necessary to correct p-values to account for this effect of multiple testing (Smith *et al.,* 1987). P-values were adjusted using the Benjamini-Hochberg algorithm which increases the size of all p-values helping to minimise the number of false positives in the data (Benjamini and Hochberg, 1995). The effect of correcting for multiple testing is shown in figure 4.13, with a dramatic reduction in the number

Figure 4.13: Volcano plots showing effect of p-value adjustment

Log_2 fold change plotted against significance ($-log_{10}$ of p-value) before (A) and after (B) p-values were corrected for multiple testing. The vertical lines on the graph indicate a fold change of +/-2 and the horizontal line indicates a p-value of 0.1 (a p-value of 0.05 would lie slightly above this line). The genes of interest therefore are those genes in the upper left and right regions of the graph. The number of genes in these regions is greatly reduced after correction for multiple testing.

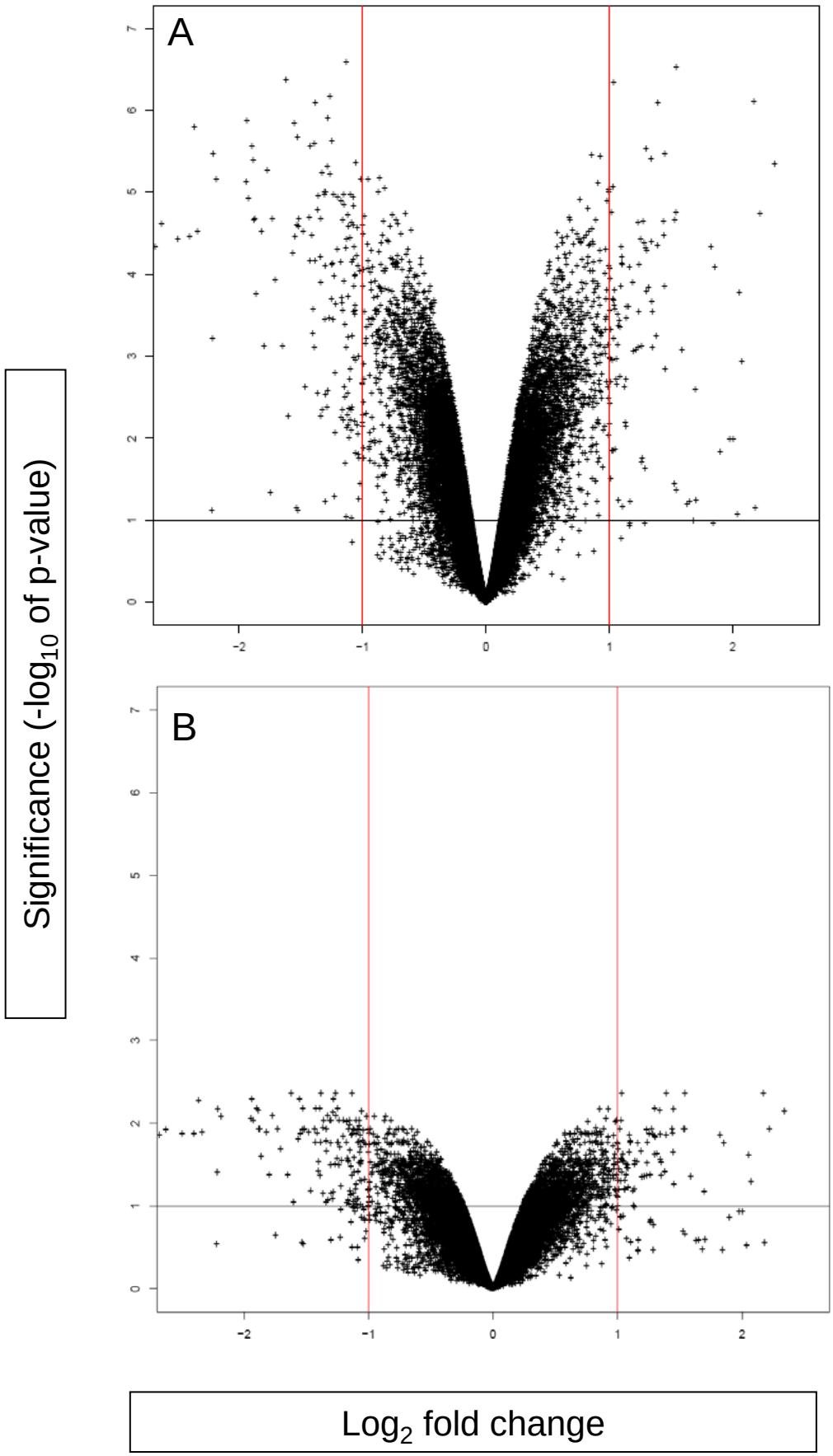

Figure 4.13

of probes with significant p-values, from 9096 to 943, after adjustment (compare Fig. 4.13 A and B).

4.3 Discussion

4.3.1 Validation of a dissection technique to isolate the PSPB

In order to develop a dissection strategy that would allow the accurate and consistent isolation of the lateral telencephalon, containing the PSPB, FACS analysis and real-time RT-PCR were carried out on dissected telencephali. The results of this analysis indicated that the region of the PSPB could indeed be accurately dissected. FACS analysis showed a high proportion of GFP positive cells in both dorsal and lateral cell populations as would be expected given that dorsal to the PSPB Pax6 is expressed throughout the VZ. Cells from the lateral telencephalon also express higher levels of GFP than those of the dorsal telencephalon. This corresponds well with the gradient of expression shown by both Pax6 and its GFP reporter with highest expression seen abutting the PSPB. The population of cells from the ventral telencephalon contained very few that were GFP positive, representing the small Pax6 positive population in a tissue that is mainly Pax6 negative.

The accuracy of the dissection was also supported by gene expression patterns as analysed by real-time RT-PCR. *Ngn2* is a marker of the developing cortex and has an expression boundary at the PSPB (Gradwhol *et al.,* 1996). It was therefore expected to be found at high levels in dorsal and lateral dissections and to be all but absent in ventral tissue; this was shown to be the case. *Mash1* and *Dlx2* have an opposite expression pattern to that of *Ngn2*, being expressed at high levels in the ventral telencephalon (Bulfone *et al.,* 1993; Guillemot and Joyner, 1993). These genes also have expression boundaries abutting the PSPB, and so their presence in the region defined here as lateral telencephalon is unsurprising. As expected, expression in the dorsal telencephalon is extremely low with *Dlx2* in particular being almost undetectable.

The results for the expression levels of *Dbx1* and *Sfrp2* were unexpected as they do not correspond with the previously published expression patterns of these genes at

E12.5. The telencephalic expression of *Sfrp2* at E12.5 has been shown by *in situ* hybridization to be largely confined to a small area of the VZ abutting the PSPB, although there is also some expression in the caudal ganglionic eminence (Kim *et al.,* 2001). This would explain the level of expression seen in ventral tissue samples. *Sfrp2* has not been shown to be expressed in the more dorsal parts of the pallium at E12.5 but the results shown here suggest that *Sfrp2* may be expressed throughout the pallium at this age with very similar levels of *Sfrp2* expression measured in both dorsal and lateral samples.

Telencephalic expression of *Dbx1* at E12.5 has been shown to be restricted to the VZ of the ventralmost part of the pallium (Medina *et al.,* 2004), yet the results shown here indicate a much wider expression pattern extending throughout the telencephalon. The high level of expression seen in the ventral telencephalon may be due, in part, to contamination from the adjacent eminentia thalami where *Dbx1* is highly expressed (Medina *et al.,* 2004). It is possible that *Dbx1* is expressed at low levels throughout the telencephalon and that this expression is being identified here due to the greater sensitivity of RT-PCR compared with *in situ* hybridization.

The fact that the expression patterns of *Ngn2*, *Mash1* and *Dlx2* were exactly as was expected and that the FACS results also suggest that the tissue was dissected accurately supports the idea that the differences seen here for expression of *Dbx1* and *Sfrp2* compared with published data are due more to the use of a more sensitive technique than to errors of dissection, although there may be some contamination of ventral samples as mentioned above. This could be tested for by measuring the levels of expression of genes expressed in the eminentia thalami but not in the ventral telencephalon. As the region of interest is the lateral telencephalon including the PSPB, contamination of ventral samples is not cause for concern. On the whole these results suggested that the dissection technique being used is sufficiently accurate and consistent to be reliably used to isolate the lateral telencephalon of E12.5 $Pax6^{+/+}.DTy54^{+}$ embryos for the collection of material for a microarray experiment. A comparable region, identified by anatomical landmarks and GFP expression, can be dissected from $Pax6^{sey/sey}.DTy54^{+}$ embryos.

4.3.2 Collecting sufficient material for the experiment

To investigate the specific roles of *Pax6* at the PSPB in the developing telencephalon a microarray experiment was designed to identify genes whose expression was significantly up- or down-regulated, in the *Pax6* expressing cells of this region, in embryos without functional Pax6 protein. This experiment relies on the use of the *Pax6*-GFP reporter mouse, *DTy54*, to enrich for the cells of interest by using the dissection strategy described in chapter 3 followed by cell dissociation and FACS. To ensure that there was indeed enrichment for the cells of interest; immunocytochemistry was performed on cells after sorting. This experiment suggests that the vast majority of cells in the GFP positive population are also Pax6 positive, but that not all Pax6 positive cells are included in this population. The proportion of GFP negative cells that were found to be Pax6 positive in this experiment seems surprisingly high. There were, however, a number of technical problems with the experiment. After sorting the cells began to degrade rapidly, significantly decreasing the number of cells available for analysis, and this was a particular problem with the GFP negative cells, probably because they were much fewer in number to begin with. The need to use a secondary antibody, due to the unavailability of a fluorescently conjugated Pax6 antibody, meant that there was an increased number of wash steps, with associated pipetting and centrifuging, which may have increased the degree of degradation of the samples. It is also possible that trapping of unbound antibody within cells may have artificially increased the measured levels Pax6 signal. In spite of this it seems clear that the GFP positive population is enriched for Pax6 expressing cells, particularly those expressing high levels of Pax6; but not all Pax6 positive cells are included in the GFP positive population. There are also a small number of Pax6 negative cells that are included in the GFP population, although these are minimal.

Each sample for the microarray was composed of tissue pooled from 4 embryos, from the same litter where possible. $Pax6^{+/+}.DTy54^{+}$ embryos were produced by crossing CD1 mice with $Pax6^{+/+}.DTy54^{+}$ animals. As the litters produced from this cross usually contained between 3 and 6 $Pax6^{+/+}.DTy54^{+}$ embryos, collecting these samples did not present a problem. Difficulties arose when collecting

Pax6$^{sey/sey}$.*DTy54*$^{+}$ samples however, as this genotype was under-represented in the litters collected. These embryos were generated by mating *Pax6*$^{sey/+}$.*DTy54*$^{+}$ to *Pax6*$^{sey/+}$ animals, with males and females of both genotypes being used. Due to the greater availability of *Pax6*$^{sey/+}$ females, however, in most cases the *DTy54* transgene was carried by the male. Although *Pax6*$^{sey/sey}$ animals die at birth there is no evidence in the literature to suggest that they have a reduced viability *in utero*, and so it seems likely that the *DTy54* transgene may be having a deleterious effect on the survival of these embryos. When chi-squared analysis was carried out, taking into account on which side of the cross the transgene was present, *Pax6*$^{sey/sey}$.*DTy54*$^{+}$ embryos were only under-represented when the male was transgenic and not when the transgene was carried by the female. In order to establish exactly what effect the *DTy54* transgene is having on the distribution of embryos in these litters it would have been necessary to genotype by PCR to distinguish between *Pax6*$^{+/+}$ and *Pax6*$^{sey/+}$ embryos. Unfortunately it was not feasible to collect tissue samples for PCR while attempting to collect samples for the microarray experiment and so it is not known if the number of *Pax6*$^{sey/+}$.*DTy54*$^{+}$ embryos is affected. It seems unlikely that the transgene has an effect on the number of *Pax6*$^{+/+}$.*DTy54*$^{+}$ embryos as there is no evidence of an under representation of this genotype in the *DTy54* mouse colony.

It is important to note that although the *DTy54* transgene is treated here as a null allele for *Pax6*, it can in fact produce a short form of the Pax6 protein lacking the paired domain (Kleinjan *et al*., 2006). Mice carrying 12 copies of the transgene have micropthalmia and, occasionally, cataracts but there is no apparent eye phenotype in mice carrying six copies of the transgene. Evidence from a similar reporter line, using a BAC transgene, suggests that expression of this Pax6 isoform is restricted to the eye and that it is not expressed in the brain (Kim and Lauderdale, 2006). Although it seems unlikely, given its very restricted expression pattern, that this protein could result in *Pax6*$^{sey/sey}$.*DTy54*$^{+}$ embryos being present at a lower than Mendelian ratio, an effect on viability caused by this protein cannot be ruled out. Another explanation, given that the under-representation is seen only when the transgene is carried by the male, may be that the production of *Pax6*^{sey}.*DTy54*$^{+}$ sperm is effected. This could be investigated by collecting younger embryos and

examining the distribution of genotypes. If *Pax6*$^{sey/sey}$*.DTy54*$^{+}$ embryos are under-represented because of a reduction in *Pax6*^{sey}*.DTy54*$^{+}$ sperm then one would expect them to be under-represented at all ages. If on the other hand they are under-represented because of impaired viability then at younger ages the distribution of genotypes should more closely resemble the Mendelian ratio.

4.3.3 Array Hybridization and Quality Control

The under-representation of *Pax6*$^{sey/sey}$*.DTy54*$^{+}$ embryos caused massive delays in the collection of the microarray samples. This resulted in RNA samples being stored for long periods at -70ºC, during which time the RNA in many samples began to degrade. The quality of a number of samples was so poor that they could not be used with any degree of confidence and so replacement samples had to be collected. To prevent further samples being lost by degradation during storage it was decided to hybridize samples as soon after collection as possible. This approach was less than ideal, increasing the risk of technical variation between arrays that were hybridized on different days and therefore not necessarily under identical conditions. It was preferable however to take this risk and to use high quality RNA samples than to hybridize all the arrays together using RNA of poorer quality.

In the end this hybridization strategy had a number of benefits as it was possible to carry out the initial normalisation steps on the first three arrays hybridized before the samples had been collected for the remaining two arrays. This allowed the dataset from array 3 to be identified as an outlier with both samples hybridized to the array showing very different data distributions compared to the samples on the other arrays. In general the level of expression seen across all genes was lower on array 3 making it more difficult to identify differentially expressed genes as it is difficult to accurately measure low levels of expression. The difference in the quality of data from this array compared to data from arrays 1 and 2 is probably due to problems during sample processing as array 3 was hybridized on a different day. Although statistically it would still have been better to collect 4 new samples for the remaining 2 arrays, due to time constraints and the scarcity of *Pax6*$^{sey/sey}$*.DTy54*$^{+}$ embryos, it was decided to repeat the hybridization of the samples hybridized to array 3. This

proved to be the right decision as the results from the second hybridization were much more comparable with the data from arrays 1 and 2.

Unfortunately the last array to be hybridized had to be excluded from the final analysis due to the poor quality of the data. Hybridization across the chip was very uneven, with localised areas of high over- and under-expression and a number of saturated spots. Analysis of the individual samples hybridized to this array indicated that the problems were most likely due to the *Pax6*$^{sey/sey}$.*DTy54*$^{+}$ sample. This was not altogether surprising as the yield of RNA in this sample was extremely low. After amplification and labelling only 500ng RNA was recovered. This falls a long way short of the 750ng RNA that Agilent® recommends should be hybridized to the array for each sample. The low quantity of RNA also meant that the bioanalyser was unable to generate a RIN for this sample and although both the 18S and 28S ribosomal peaks were present it is possible that the sample had already begun to degrade. Under more favourable circumstances this sample would not have been used, but due to time constraints it was not considered feasible to discard it and to attempt to collect a replacement sample. The need to exclude this array from the final analysis reduces the n number for each condition to 3, thereby reducing the statistical power of the experiment. This is not an insurmountable problem, it does mean however, that care must be taken to validate any conclusions drawn from the data by other means. A detailed analysis of the data from arrays 1, 2 and 4 will be described in the next chapter.

Chapter 5 – Analysis of Microarray Results

5.1 Introduction

One of the great advantages of a microarray based study is that theoretically it should be able to identify all genes whose level of expression changes under the conditions being investigated. Finding good ways to analyse this data, however, can prove challenging. Simple fold change analysis can be useful for narrowing down the list of candidate target genes; however, the selection of the fold change cut-off is very arbitrary and can lead to the exclusion of interesting, regulated genes from the analysis. With the rapid increase in the use of microarrays in recent years there has been a concurrent increase in the tools available to analyse the data generated from this research. A wide variety of software packages, many freely available on the internet, have been developed to convert the lists of genes produced by microarray experiments into useful biological information. These programmes allow large gene lists to be analysed efficiently, helping to circumvent the problems associated with the vast quantities of data arising from a microarray experiment. Many of these tools are based around the gene annotation systems of the Gene Ontology (GO) Consortium and the Kyoto Encyclopaedia of Genes and Genomes (KEGG). These databases classify genes in terms of their biological functions and the biological pathways in which they act. Analysis of a gene set in terms of these classifications allows long lists of genes to be broken down into groups of genes with common functions, thereby aiding the interpretation of the data.

The analysis of the microarray data generated from the comparison of gene expression at the PSPB between $Pax6^{+/+}.DTy54^{+}$ and $Pax6^{sey/sey}.DTy54^{+}$ embryos at E12.5 is described here. Firstly the data were examined to determine if the experiment accurately identified genes which were expected to show a change in expression by comparing them with genes previously reported to lie downstream of *Pax6*. Secondly a comparison was made with a recently published microarray study on changes in gene expression in the entire $Pax6^{sey/sey}$ telencephalon. Finally the data were analysed in terms of GO and KEGG annotations using a variety of more or less stringent fold change cut-offs to identify the biological functions of the regulated genes, and thus gain insight into the role of *Pax6* at the PSPB.

5.2 Results

Analysis of the microarray data identified 943 probes with a significant change in expression in *Pax6*$^{sey/sey}$.*DTy54*$^{+}$ compared with *Pax6*$^{+/+}$.*DTy54*$^{+}$. 411 of these were up-regulated (Appendix A) and 532 were down-regulated (Appendix B). Initially the complete dataset was compared with the published literature on *Pax6* and with a recent microarray experiment by Holm *et al.,* (2006). The functions and processes in which the regulated genes are involved were then analysed. This was done using a variety of different fold change cut-offs to select the genes of interest. The cut-offs used were genes with a significant fold change of >|1.5| (labelled red in Appendices A and B), genes with a significant fold change of >|2.0| (labelled green in Appendices A and B) and finally all genes with a significant change in expression were analysed, regardless of the magnitude of that change.

5.2.1 Comparison with previously published targets of *Pax6*

In order to investigate how well the microarray results recapitulate what is already known about downstream targets of *Pax6*, a list was compiled of genes that show a change in expression levels in the telencephalon of *Pax6* mutant mice, aged between E9.5 and E16.5, as identified by *in situ* hybridization or immunohistochemistry. The array data for these genes was then examined to determine if it concurred with the published data. Although some existing known targets might be expected to be found in the array data, the differences in the experimental paradigm used here compared to previous studies are such that complete agreement between the datasets is not expected. Overall there appears to be a good degree of correspondence between the published literature and the results presented here, particularly among the up-regulated gene set (Fig. 5.1). In the literature 16 genes have been identified as being up-regulated in response to a loss of *Pax6* expression (Table 5.1; Fig. 5.1 B). This study identified 10 of these genes (labelled blue in Appendix A) as having a significant up-regulation at the PSPB in *Pax6*$^{sey/sey}$.*DTy54*$^{+}$ and another 1 that was up-regulated and had a p-value approaching significance (*Arx*; fold change=1.736, p-value=0.061). Of the remaining 5 genes, 4 showed no statistically significant change in expression. The final gene, *Emx2*, was found to be significantly down-regulated (p-value=0.025), with a fold change of -1.594.

Table 5.1: Genes up-regulated in *Pax6*$^{sey/sey}$ in the literature

Genes previously identified as up-regulated in the telencephalon of *Pax6* mutant embryos aged between E9.5 and E16.5, by *in situ* hybridization or immunohistochemistry, compared with the observed fold change found in this microarray study. P-values as estimated by empirical Bayes t-test and corrected for multiple testing are also shown. Group A contains genes for which the change in expression measured by microarray was in agreement with published data. Group B are genes reported to show a change in expression in the literature but that were not found to be significantly altered in this study. Group C consists of *Emx2* which is reported to be up-regulated in the literature but was found to be significantly down-regulated by microarray.

Gene	Reference	Observed Fold Change	p-value	
Dlx1	Stoykova *et al.,* 1996; 2000; Hallonet *et al.,* 1998;	2.715	0.013	
Dlx	Toresson *et al.,* 2000	2.454 (*Dlx2*) 1.903 (*Dlx5*)	0.014 0.038	
Gsh2	Toresson *et al.,* 2000; Yun *et al.,* 2001; Stenman *et al.,* 2003	2.9	0.012	
Ki67	Toresson *et al.,* 2000	2.134	0.023	
Gad1	Yun *et al.,* 2001; Schuurmans *et al.,* 2004	1.677	0.025	
Lhx6	Stoykova *et al.,* 2000	15.439	0.008	**A**
Mash1	Toresson *et al.,* 2000; Stoykova *et al.,* 2000; Yun *et al.,* 2001; Muzio *et al.,* 2002; Heins *et al.,* 2002; Stenman *et al.,* 2003	2.88	0.012	
mEvf1 (Dlx6os1)	Faedo *et al.,* 2004	1.994	0.017	
Olig2	Heins *et al.,* 2002	1.542	0.029	
Vax1	Hallonet *et al.,* 1998; Stoykova *et al.,* 2000	1.483	0.025	
Arx	Visel *et al.,* 2007	1.736	0.061	
Fzd2	Visel *et al.,* 2007	1.327	0.106	
Er81	Yun *et al.,* 2001	1.237	0.329	**B**
mTsh	Caubit *et al.,* 2005	-1.59	0.099	
Six3	Stoykova *et al.,* 2000	-1.189	0.119	
Emx2	Muzio *et al.,* 2002	-1.594	0.025	**C**

Table 5.1: Genes up-regulated in *Pax6*$^{sey/sey}$ in the literature

Gene	Reference	Observed Fold Change	p-value	
Emx1	Toresson *et al.,* 2000; Muzio *et al.,* 2002	-1.584	0.03	
Neurod1	Visel *et al.,* 2007	-2.885	0.007	
Neurod6	Schuurmans *et al.,* 2004; Visel *et al.,* 2007	-6.816	0.009	
Ngn2	Toresson *et al.,* 2000; Stoykova *et al.,* 2000; Yun *et al.,* 2001; Heins *et al.,* 2002; Stenman *et al.,* 2003; Visel *et al.,* 2007	-10.201	0.014	
Pde1b	Visel *et al.,* 2007	-2.221	0.011	
R-Cad(Cdh4)	Stoykova *et al.,* 1997	-2.003	0.012	**A**
SDF1(Cxcl12)	Tiveron *et al.,* 2006	-2.129	0.012	
Sema5a	Jones *et al.,* 2002	-1.995	0.013	
Tbr1	Stoykova *et al.,* 2000;	-2.25	0.027	
Tbr2	Muzio *et al.,* 2002; Visel *et al.,* 2007	-4.549	0.009	
VGLUT2(Slc17a6)	Schuurmans *et al.,* 2004	-2.683	0.007	
Robo2	Jiménez *et al.,* 2002	-1.373	0.03	
Trim9	Visel *et al.,* 2007	-1.386	0.044	
Sema3c	Jones *et al.,* 2002	-1.199	0.137	
Neurod4	Visel *et al.,* 2007	-1.360	0.08	
Dbx1	Yun *et al.,* 2001	-1.215	0.16	
Delta-catenin	Duparc *et al.,* 2006	-1.308	0.094	
Lhx2	Yun *et al.,* 2001	-1.043	0.806	
Lrp5	Visel *et al.,* 2007	-1.016	0.945	
Nrg1	Assimacopoulos *et al.,* 2003	-1.107	0.278	
Tenascin-C	Stoykova *et al.,* 1997; Götz *et al.,* 1998	-1.181	0.179	**B**
VGLUT1(Slc17a7)	Schuurmans *et al.,* 2004	-1.173	0.210	
Wnt7b	Kim *et al.,* 2001	-1.266	0.131	
Odz	Visel *et al.,* 2007	1.754	0.064	
Ngn1	Visel *et al.,* 2007	1.034	0.804	
Sfrp2	Kim *et al.,* 2001; Muzio *et al.,* 2002	1.185	0.361	
Tgfα	Assimacopoulos *et al.,* 2003	1.055	0.564	
D930015E06Rik	Visel *et al.,* 2007	1.257	0.324	

Table 5.2: Genes down-regulated in *Pax6*$^{sey/sey}$ in the literature

Genes previously identified as down-regulated in the telencephalon of *Pax6* mutant embryos aged between E9.5 and E16.5, by *in situ* hybridization or immunohistochemistry, compared with the observed fold change found in this microarray study. P-values as estimated by empirical Bayes t-test and corrected for multiple testing are also shown. Group A contains genes for which the change in expression measured by microarray was in agreement with published data. Group B are genes reported to show a change in expression in the literature but that were not found to be significantly altered in this study.

Figure 5.1: Comparison with genes identified in the literature as downstream of *Pax6*

Venn diagrams showing the degree of overlap between genes previously identified as downstream of *Pax6* in the developing telencephalon and genes showing a significant regulation of >|1.5| fold at the PSPB. The number of genes identified from the literature is shown on the left and the number found in this study is shown on the right. A) shows data for all regulated genes, and this is divided into genes up-regulated or down-regulated in the literature in B) and C) respectively. Colour coding corresponds to the labelling of genes in Appendices A and B.

Figure 5.2: comparison with microarray data published by Holm *et al.*, (2007)

Venn diagrams showing the degree of overlap between genes identified by microarray as downstream of *Pax6* in the developing telencephalon at E12.5 and genes showing a significant regulation of >|1.5| fold at the PSPB. The number of genes identified by Holm *et al.,* (2007) is shown on the left and the number found in this study is shown on the right. A) shows data for all regulated genes, and this is divided into genes found to be up-regulated or down-regulated by Holm *et al.,* in B) and C) respectively. Colour coding corresponds to the labelling of genes in Appendices A and B.

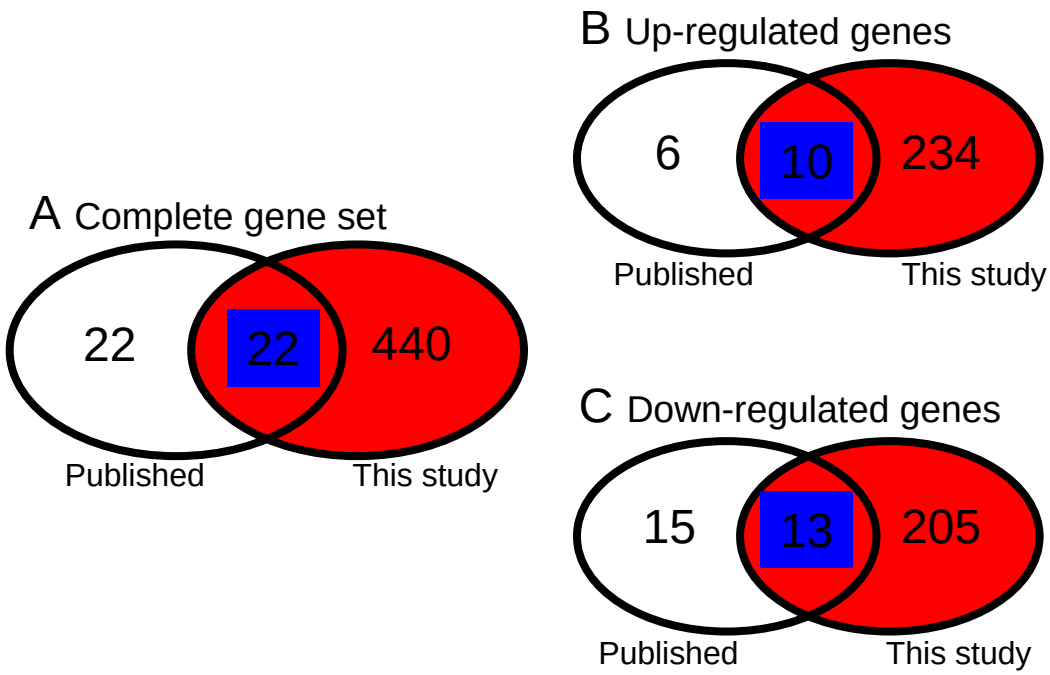

Figure 5.1

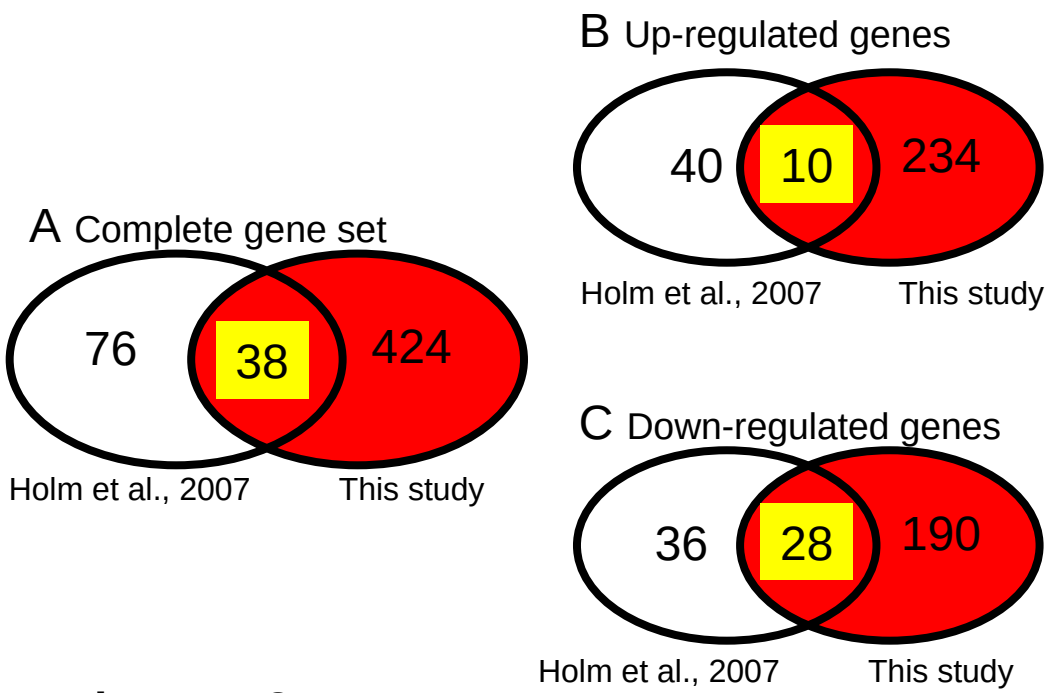

Figure 5.2

A similar trend was seen among genes previously identified as down-regulated in *Pax6* mutants (Table 5.2; Fig. 5.1 C). Of 28 genes reported to show a down-regulation in expression, 13 were found to be significantly down-regulated in this study (labelled blue in Appendix B). None of the remaining 15 genes were significantly regulated, although one of these genes, *Odz*, showed a reasonably large up-regulation (fold change=1.754) and this change in expression was approaching statistical significance (p=0.064).

5.2.2 Comparison with recently published microarray data

A recently published paper by Holm *et al.* (2007) described a microarray experiment comparing gene expression between wildtype and *small eye* cortex and ganglionic eminences at E12 and E15. (As Holm *et al.* defined the day of vaginal plug as E0 and for the purposes of this study it was defined as E0.5, their E12 embryos should be the same age as the embryos analysed here.) As the dissected region, containing the PSPB, analysed in this study contains cells from both cortex and LGE, microarray data was compared with changes in expression in both of these regions at E12 as found by Holm *et al.* (2007). A summary of this comparison is shown in tables 5.3 and 5.4.

Similar to the results of the comparison with regulated genes, identified by *in situ* hybridization or immunohistochemistry, there was a marked degree of overlap between the two datasets. Of the 114 genes found to be up- or down-regulated by >|1.5| fold by Holm *et al.,* 38 showed a similar statistically significant change in expression at the PSPB (Fig. 5.2). If these two sets of genes had been chosen randomly from the mouse genome, which contains ~23000 genes, then an overlap of only 2.3 genes would be expected between them[*]. Holm *et al.* identified 50 genes that were up-regulated by >1.5 fold; 10 of these were identified as significantly up-regulated in this study (Fig.5.2 B; genes labelled yellow in Appendix A) and a further 2 were up-regulated with p-values approaching significance (p=0.055 and 0.054). Of the remaining 38 genes, (one of which was represented twice in the Holm *et al.* data), none were significantly up-regulated at the PSPB. It is interesting to note

[*] Expected overlap was calculated as follows:
(Number of genes identified by Holm *et al.* × Number of genes identified in this study) / 23000

Gene	Data from Holm *et al.*, 2007		Data from this study		
	Fold Change Cortex	Fold Change GE	Fold Change	p-value	
Asb4	5.91	---	4.502	0.004	A
5031439A09Rik	2.88	1.77	5.06	0.007	
Mash 1	2.27	---	2.88	0.012	
Dlx1	2.01	---	2.715	0.013	
Dlx2	2.77	---	2.454	0.014	
Calb1	2.52	---	3.614	0.018	
Ccnd1	1.64	---	2.279	0.022	
Peg3	1.81	---	2.536	0.028	
Zic4	1.87	---	2.06	0.029	
Sulf2	1.61	---	2.053	0.029	
Dlk1	5.05	---	1.502	0.055	B
Kcnd2	1.93	---	1.279	0.054	
Rian	2.31	---	2.001	0.102	C
MBII-343 (Rian)	2.58	---	2.001	0.102	
Foxd1	2.48	---	1.524	0.233	
Fstl	1.85	---	1.428	0.156	
Gtl2	3.28	---	1.421	0.170	
Gpc3	2.41	---	1.260	0.097	
Otx2	3.24	---	1.303	0.111	
Igf2	1.64	---	1.282	0.122	
Cdh11	1.81	---	1.237	0.126	
Ogn	2.63	---	1.326	0.135	
Igf1	2.21	---	1.155	0.145	
Emb	1.93	---	1.143	0.196	
Col1a2	2	---	1.176	0.263	
Sepp1	1.54	---	1.106	0.271	
Id3	2.59	---	1.118	0.288	
Serpine2	1.94	---	1.114	0.306	
BCMP1	2.55	---	1.134	0.309	
Gsn	1.74	---	1.109	0.369	
Stx8	2.08	---	1.173	0.409	
Tex15	2.49	---	1.074	0.415	
Anxa5	1.59	---	1.081	0.546	
Anxa2	1.85	---	1.065	0.548	
1110004P15Rik (Ahnak)	2.28	---	1.109	0.582	
Id1	2.2	---	1.077	0.583	
Zfhx4	2.23	---	1.069	0.590	
Fgf17	2.33	---	1.035	0.739	
Cnn2	1.7	---	1.031	0.757	
Col5a2	1.76	---	1.002	0.988	

Gene	Data from Holm *et al.*, 2007		Data from this study		
	Fold Change Cortex	**Fold Change GE**	**Fold Change**	**p-value**	
Cxcl14	1.86	---	-1.237	0.109	**C**
Rgs16	1.57	---	-1.314	0.223	
Hbb-bh1	2.88	1.8	-1.181	0.231	
Lgals1	2.02	---	-1.123	0.418	
Wif1	2.7	---	-1.065	0.488	
S100a11	1.62	---	-1.038	0.780	
Lum	2.07	---	-1.022	0.88	
Bmp4	1.7	---	-1.014	0.908	
Crabp1	2.46	---	-1.013	0.949	
2610024A01Rik (Tmem163)	1.78	---	-2.121	0.039	**D**
Arl4	1.94	---	-1.465	0.034	

Table 5.3 Comparison of genes found to be up-regulated in *small eye* relative to wildtype by Holm *et al.*, (2007), along with the change in expression observed in this study. P-values have been adjusted for multiple testing. --- indicates where fold change data was not available for a particular tissue. Group A contains genes for which the change in expression measured in this study was in agreement with that measured by Holm *et al*. Group B are genes for which there is an agreement between the changes in expression, but this has not quite reached statistical significance in this study. Group C are genes reported to show a change in expression by Holm *et al.,* but that were not found to be significantly altered in this study. Group D are genes found to be significantly down-regulated in this study but up-regulated in the study by Holm *et al.*

Gene	Data from Holm *et al.*, 2007		Data from this study		
	Fold Change Cortex	Fold Change GE	Fold Change	p-value	
Uncx4.1	---	-2.66	-3.834	0.005	
NeuroD1	---	-3.85	-2.885	0.007	
Lhx9	---	-2.79	-4.633	0.007	
Slc17a6	---	-3.04	-2.683	0.007	
Epha3	-3.53	-2.04	-2.402	0.008	
NeuroD6	-4.18	-4.11	-6.816	0.009	
Tbr2	-2.75	-3.33	-4.549	0.009	
Pde1b	-3.43	-1.74	-2.221	0.011	
Cdh4	---	-2.06	-2.003	0.012	
NeuroD2	-2.00	---	-2.792	0.013	
Sema5a	-2.93	---	-1.995	0.013	
AP2-γ	-3.14	-2.00	-5.648	0.014	
Ngn2	-2.11	-8.75	-10.241	0.014	
Slc1a3	-2.22	---	-5.288	0.014	
9430059P22Rik (Shisa2; Tmem46)	-2.88	---	-2.925	0.014	**A**
Rlbp1	-3.55	-1.61	-2.368	0.017	
Serpini1	---	-1.82	-2.377	0.017	
Syt4	---	-1.96	-1.707	0.017	
2900026H06Rik (Ppp2r2b)	-1.71	---	-2.054 -2.09	0.017 0.031	
Bhlhb5	---	-1.95	-2.00	0.023	
Pcdh8	---	-1.83	-1.847	0.023	
9430077C05Rik (Etl4; BC026657)	-3.17	---	-2.169	0.026	
Tbr1	-1.61	-1.91	-2.25	0.027	
Nfia	-2.15	---	-1.898	0.032	
Tgfβ2	-2.05	---	-1.581	0.038	
Id4	-1.71	---	-1.706	0.043	
E130201N16Rik (Prr15)	-4.38	---	-1.378	0.024	**B**
Syn2	-1.65	---	-1.38	0.048	
Snca	---	-1.76	-1.626	0.055	**C**
Mab21l1	---	-2.74	-2.144	0.056	
Cyb561	---	-1.62	-1.355	0.061	
Dkk3	-1.80	---	-1.36	0.081	
Fhl1	-2.12	---	-1.34	0.089	
Catnd2 (Ctnnd2)	-3.26	---	-1.308	0.094	
Hnt	---	-1.85	-1.282	0.13	
Asph	---	-1.89	-1.194	0.136	**D**
Nr2f2	---	-2.22	-1.17	0.148	
2700033K02Rik (Nr2f2)	---	-2.91	-1.17	0.148	
Ppp1r1c	---	-1.92	-1.159	0.149	
Sorl1	-2.30	---	-1.185	0.161	

Gene	Data from Holm *et al.*, 2007		Data from this study		
	Fold Change Cortex	**Fold Change GE**	**Fold Change**	**p-value**	
TN-C	---	-2.03	-1.181	0.179	
Gria1	---	-1.66	-1.335	0.214	
1810020C19Rik (Alkbh3)	-2.04	---	-1.229	0.215	
Cav	-2.03	---	-1.171	0.22	
Hpca	-1.71	---	-1.116	0.237	
2010011I20Rik	-1.86	---	-1.18	0.269	
Nfib	-1.92	---	-1.165	0.38	
Aldo3 (Aldoc)	-5.52	---	-1.081	0.44	
Sfrp1	-2.61	---	-1.128	0.496	**D**
Inhbb	-1.86	---	-1.455	0.61	
Sez6	-1.92	---	-1.043	0.751	
Satb2	-2.12	---	-1.017	0.887	
Slc15a2	-2.62	---	2.015	0.064	
Plxna2	-2.11	---	1.358	0.097	
Bcl11b	-1.72	---	2.03	0.139	
Wnt7a	-3.04	---	1.176	0.251	
Epha5	-2.14	---	1.158	0.373	
Sox3	-2.34	---	1.081	0.396	
Ndr2	-2.04	---	1.093	0.429	
Mt3	-1.79	---	1.106	0.435	
Nfix	-2.08	---	1.067	0.449	
Ngn1	-2.20	-2.23	1.034	0.804	
Hs3st1	-1.94	---	1.018	0.91	
Sstr2	-2.60	---	---	---	

Table 5.4 Comparison of genes found to be down-regulated in *small eye* relative to wildtype by Holm *et al.,* (2007), along with the change in expression observed in this study. P-values have been adjusted for multiple testing. --- indicates where data was not available for a particular tissue. Group A contains genes for which the change in expression measured in this study was in agreement with that measured by Holm *et al*. Group B are genes for which there is an agreement between the changes in expression, but in this study it has not reached the |1.5| fold change cut off set by Holm *et al*. (2007). Group C are genes for which there is an agreement between the changes in expression, but this has not quite reached statistical significance in this study. Group D are genes reported to show a change in expression by Holm *et al.,* but that were not found to be significantly altered in this study. *Sstr2* has not been included in any of these groups as data on this gene was not available from this study.

however that 2 of these genes were significantly down-regulated with relatively large changes in expression (*Tmem163*: FC= -2.121; adjusted p-value=0.039 and *Arl4*: FC= -1.465; adjusted p-value=0.034; Table 5.3)

Among the 64 genes that Holm *et al.* found to show a greater than 1.5 fold down-regulation were 28 genes identified by this study as significantly down-regulated at the PSPB, with an absolute fold change of >1.5 (Table 5.4; Fig. 5.2 C; genes labelled yellow in Appendix B). A further 2 genes were found to be significantly down-regulated, but by <|1.5| fold. The expression of 33 of the remaining 34 genes was not significantly altered at the PSPB, although one gene, *Slc15a2*, showed a large up-regulation (2.015 fold) and had a p-value that was approaching significance (adjusted p-value=0.064). The final gene found to be downregulated by Holm *et al.* was *Sstr2* but data for this gene at the PSPB was unavailable. This was surprising as the microarray used (Agilent®, G4122A) is supposed to cover the whole mouse genome. *Sstr2* is a somatostatin receptor and other *Sstr* genes on the microarray showed no significant changes in expression.

5.2.3 Identification of over-represented themes in the microarray data

Having established that the microarray data generated in this study corresponds well both with previously published array data and with *Pax6* targets identified by other means, the dataset was then analysed as a whole. Microarray studies generally use an arbitrary fold change cut-off of between |1.5| and |2|, in conjunction with a statistically significant p-value, to identify genes of interest. Here genes with an absolute fold change of greater than 1.5 and an adjusted p-value less than 0.05 were identified as potential candidates for *Pax6* regulation (genes labelled red in Appendices A and B). Using these criteria 625 probes, representing 462 genes, were found to be significantly regulated in $Pax6^{sey/sey}.DTy54^{+}$ compared with $Pax6^{+/+}.DTy54^{+}$. Of these, 354 probes (representing 218 known genes) were downregulated and 271 probes (representing 244 known genes) were up-regulated. The 20 most up-regulated and 20 most down-regulated genes are listed in tables 5.5 and 5.6 respectively.

Gene	Fold Change	p-value	Adjusted p-value
Lhx6	15.439	5.82E-06	0.008
Smad2	9.677	4.26E-05	0.014
Titf1	7.406	1.02E-06	0.005
Mpped2	7.186	3.93E-05	0.014
Gpr177	5.060	4.51E-06	0.007
Btbd9	4.658	1.84E-05	0.012
Asb4	4.502	7.89E-07	0.004
Rbbp4	4.146	1.66E-04	0.025
Calb1	3.614	8.34E-05	0.018
Lhx8	3.538	4.55E-05	0.014
Ube2s	3.006	8.41E-04	0.045
Nkx6-2	2.910	3.02E-07	0.004
Gsh2	2.906	1.75E-05	0.012
Ascl1	2.888	2.22E-05	0.012
Arfl4	2.729	3.36E-06	0.007
B230215L15Rik	2.725	1.38E-04	0.023
Dlx1	2.715	3.35E-05	0.013
MGC73635	2.709	2.27E-05	0.012
Fxc1	2.623	8.08E-07	0.004
Hist1h1e	2.621	4.52E-05	0.014

Table 5.5 The 20 genes found to be most up-regulated at the PSPB with their associated fold change, p-value and the p-value after adjustment for multiple testing.

Gene	Fold Change	p-value	Adjusted p-value
Neurog2	-10.241	3.95E-05	0.014
Neurod6	-6.816	8.01E-06	0.009
BC020078	-6.408	4.59E-05	0.014
Prdm8	-6.185	2.47E-05	0.012
Tcfap2c	-5.648	3.71E-05	0.014
Slc1a3	-5.288	3.46E-05	0.014
Nhlh1	-5.151	1.61E-06	0.005
TC1651696	-5.053	3.03E-05	0.013
TC1574886	-4.645	6.06E-04	0.040
Lhx9	-4.633	3.41E-06	0.007
Eomes	-4.549	6.83E-06	0.009
Has2	-3.848	7.49E-06	0.009
Uncx4.1	-3.834	1.35E-06	0.005
Sema6d	-3.801	1.17E-05	0.009
Nrn1	-3.726	2.78E-06	0.007
Chst8	-3.696	4.07E-06	0.007
Slc17a6	-3.686	2.19E-05	0.012
Rabgap1l	-3.666	2.11E-05	0.012
Celsr1	-3.637	1.75E-04	0.025
3110035E14Rik	-3.531	3.06E-05	0.013

Table 5.6 The 20 genes found to be most down-regulated at the PSPB with their associated fold change, p-value and the p-value after adjustment for multiple testing.

This set of significantly regulated genes was further analysed to identify any themes in the biological function of genes regulated by *Pax6*. There are a number of annotation systems available that provide information on the biological function of genes. Two of the most commonly used are those of the Gene Ontology Consortium (GO) and the Kyoto Encyclopaedia of Genes and Genomes (KEGG). There are a number of programmes that use these annotation systems to analyse gene sets freely available on the internet. Two such programmes are WebGestalt (WEB-based GEne SeT AnaLysis Toolkit; Zhang *et al.,* 2005), and FunNet. These programmes both use GO and KEGG gene annotations to identify categories that are over-represented in a set of genes of interest. Analysis of those genes identified as being regulated by *Pax6* gave similar results when analysed with each of these programmes, however the graphs used here to illustrate these results were all generated using FunNet.

The GO database describes genes in terms of three ontologies – biological process, molecular function and cellular component. Within each of these ontologies are GO terms which are organised hierarchically in parent – child relationships (see Fig. 5.3 for example). Genes can be members of many different GO categories, allowing them to be described in more or less specific detail. Using this parent – child organisation FunNet is able to provide a variety of descriptions of the regulated gene-set. These range from detailed descriptions giving the most precise information available on the biological roles of the transcripts to much less specific overviews of the general functions of the gene-set as a whole.

Analysis of the biological processes in which the regulated genes are involved shows that transcription factors and genes involved more generally in the regulation of transcription are significantly over-represented in both the up-regulated and down-regulated transcripts (Fig. 5.4). This fits well with the role of *Pax6* as a high level transcription factor regulating many transcription pathways. Analysis of the up-regulated transcripts shows an over-representation of genes with a role in the cell cycle, and more specifically genes involved in DNA replication and repair, mitosis and cell division (Fig. 5.4). This increase in the expression of genes involved in the cell cycle would be compatible with the shortening of the cell cycle in $Pax6^{sey/sey}$

Figure 5.3: Example of the parent-child relationships used in the GO database

The term neuron migration (shown in red) is used as an example to demonstrate the organisation of the gene ontology database. Every term will have parent terms (shown in blue) and all genes associated with a specific term are also associated with the parent terms. In this example any genes involved in neuron migration will also be listed with genes involved in cell migration and the generation of neurons. Parent terms can have many child terms and examples of some of the other child terms for cell migration and the generation of neurons are shown in yellow. Genes involved in neuron migration can be divided into those involved either in the inward or outward migration of deep nuclear neurons. These are the two child terms of neuron migration (shown in green).

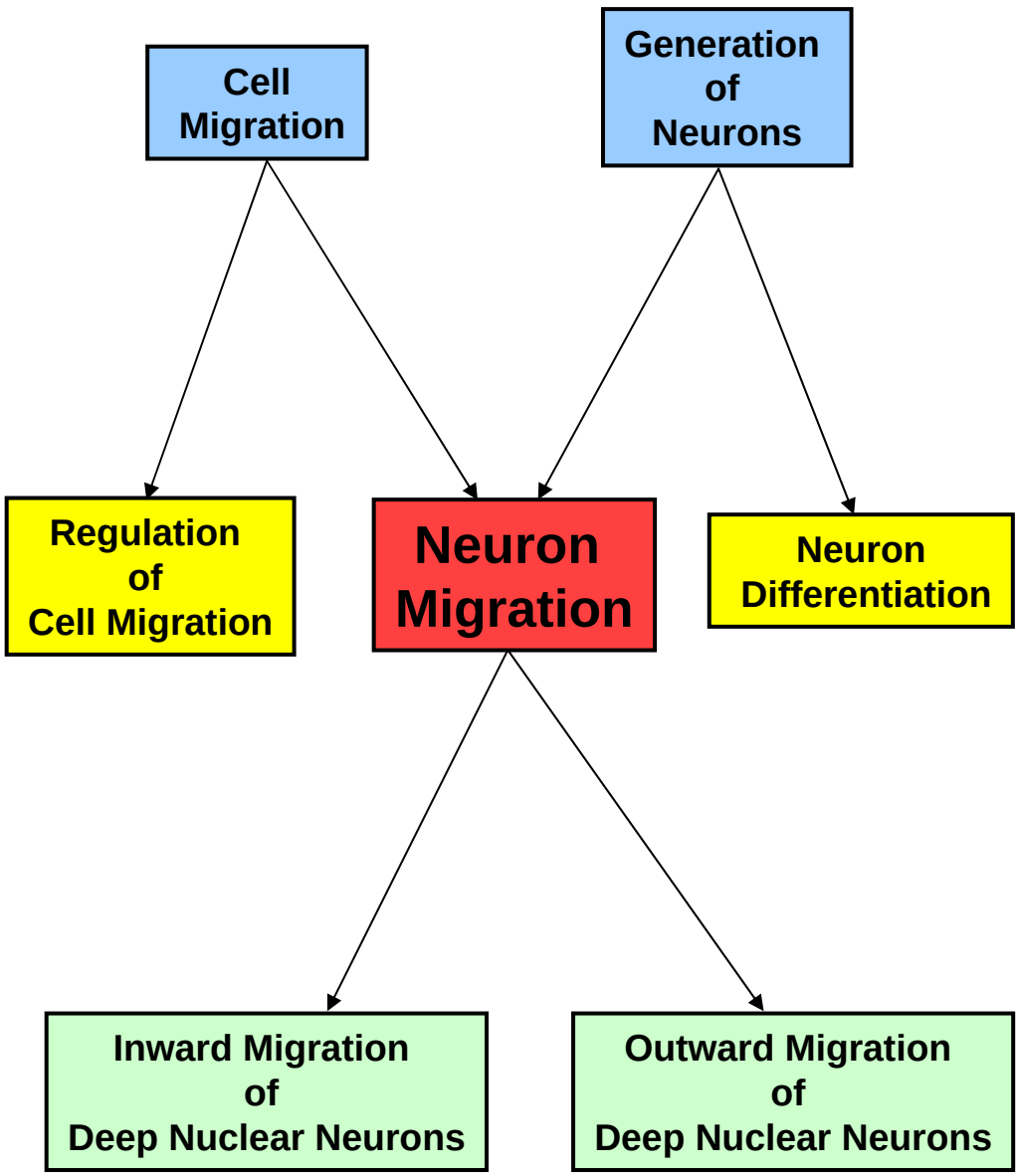
Cell Migration
Generation of Neurons
Regulation of Cell Migration
Neuron Migration
Neuron Differentiation
Inward Migration of Deep Nuclear Neurons
Outward Migration of Deep Nuclear Neurons

Figure 5.3

embryos at E12.5 reported by Estivill-Torrus *et al.* (2002). The processes that the down-regulated genes are involved in are more specifically associated with neuronal development. The general processes of forebrain, brain and nervous system development are all significantly over-represented, demonstrating the importance of *Pax6* as a potent neurogenic gene. The processes of neuron differentiation and migration along with axonogenesis and axon guidance are also over-represented in the down-regulated gene set (Fig. 5.4).

GO analysis into the molecular functions of the regulated gene list again emphasises the importance of *Pax6* in controlling the expression of other transcription factors, with transcription factor activity over-represented in both the up- and down-regulated gene sets (Fig. 5.5). The categories of DNA, nucleotide, protein and microtubule binding are all over-represented in the up-regulated transcripts. This fits well with the analysis of biological processes, complementing the processes of both transcription and cell division. The functions of the down-regulated transcripts are biased heavily towards transcription and the regulation of transcription (Fig. 5.5). This again supports the processes in which these genes are involved as many of the genes promoting neural differentiation and development do so by influencing transcription.

The KEGG database annotates genes in relation to the biological pathways and processes in which they are involved. Analysis of the regulated gene set based on KEGG annotations identified a number of pathways that were over-represented. The pathways over-represented in the down-regulated transcripts were the TGF-β signalling pathway and axon guidance pathways (Fig. 5.6). TGF-β signalling is very important in establishing correct patterns of gene expression in the developing forebrain (Shimagori *et al.,* 2004) and so the down-regulation of a number of its components in the absence of *Pax6* expression is perhaps unsurprising. Axon guidance pathways would also be expected to be down-regulated as axon navigation has been shown to be disrupted in $Pax6^{sey/sey}$ embryos (Mastick *et al.,* 1997; Pratt *et al.,* 2000; Jones *et al.,* 2002).

Figure 5.4: GO analysis of biological processes for genes with >|1.5| fold change

Graph showing the top 12 over-represented biological processes in the set of genes with a significant ($p<0.05$) fold change of >|1.5| in *Pax6*$^{sey/sey}$*.DTy54* compared with *Pax6*$^{+/+}$*.DTy54* for both up- and down-regulated genesets, as defined by the gene ontology database. Processes over-represented among the up-regulated gene set are mainly involved with the cell cycle and cell division while processes over-represented in the down-regulated gene set are more concerned with neuronal development. Transcription and its regulation are highly over-represented in both the up- and down-regulated gene sets. Transcriptional domain coverage is calculated as the number of transcripts in each significantly overrepresented theme expressed as a percentage of the number of transcripts annotated by at least one significantly over-represented theme. The number of genes in each category is given in bold.

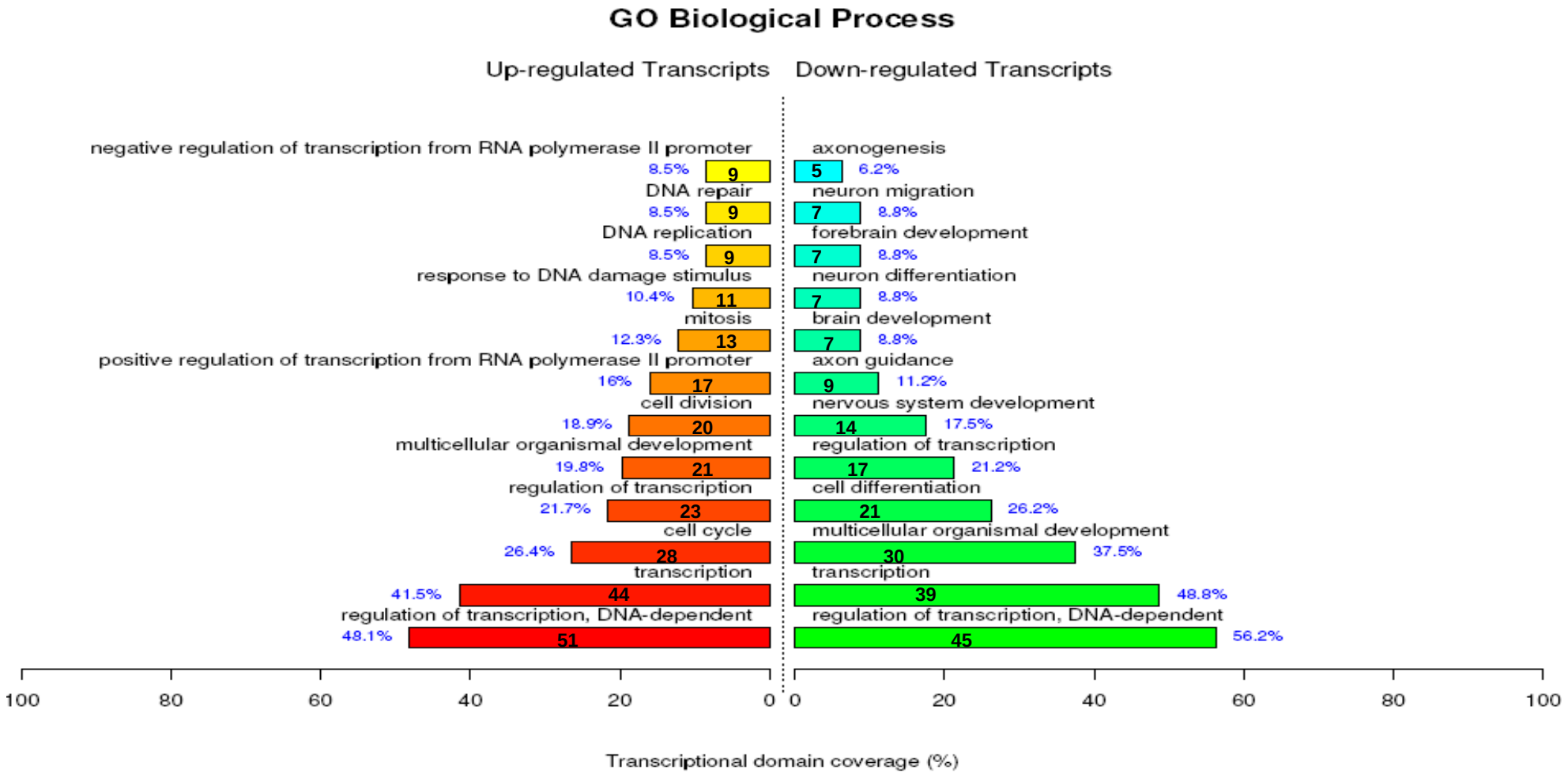
GO Biological Process
Up-regulated Transcripts
Down-regulated Transcripts
negative regulation of transcription from RNA polymerase II promoter
8.5%
9
DNA repair
8.5%
9
DNA replication
8.5%
9
response to DNA damage stimulus
10.4%
11
mitosis
12.3%
13
positive regulation of transcription from RNA polymerase II promoter
16%
17
cell division
18.9%
20
multicellular organismal development
19.8%
21
regulation of transcription
21.7%
23
cell cycle
26.4%
28
transcription
41.5%
44
regulation of transcription, DNA-dependent
48.1%
51
axonogenesis
5
6.2%
neuron migration
7
8.8%
forebrain development
7
8.8%
neuron differentiation
7
8.8%
brain development
7
8.8%
axon guidance
9
11.2%
nervous system development
14
17.5%
regulation of transcription
17
21.2%
cell differentiation
21
26.2%
multicellular organismal development
30
37.5%
transcription
39
48.8%
regulation of transcription, DNA-dependent
45
56.2%
100
80
60
40
20
0
0
20
40
60
80
100
Transcriptional domain coverage (%)

Figure 5.4

Figure 5.5: GO analysis of molecular functions for genes with >|1.5| fold change

Graph showing the molecular functions, as defined by the gene ontology database, over-represented in the set of genes with a significant ($p<0.05$) fold change of >|1.5| in *Pax6*$^{sey/sey}$*.DTy54* compared with *Pax6*$^{+/+}$*.DTy54*. Molecular functions over-represented among the up-regulated gene set include nucleotide and protein binding while the functions over-represented in the down-regulated gene set include metal ion binding. Transcription factor activity is highly over-represented in both the up- and down-regulated gene sets. Transcriptional domain coverage is calculated as the number of transcripts in each significantly overrepresented theme expressed as a percentage of the number of transcripts annotated by at least one significantly over-represented theme. The number of genes in each category is given in bold.

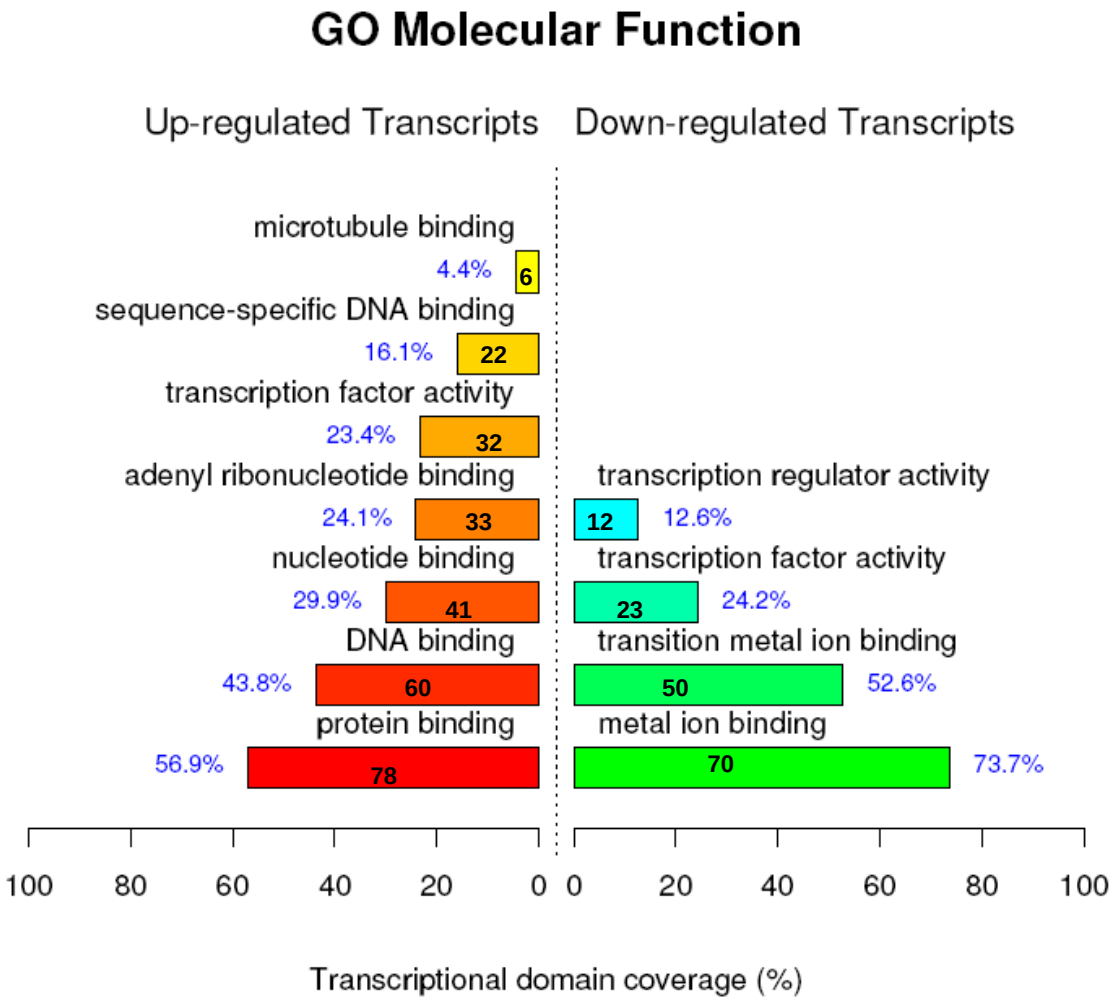
GO Molecular Function
Up-regulated Transcripts
Down-regulated Transcripts
microtubule binding
4.4%
6
sequence-specific DNA binding
16.1%
22
transcription factor activity
23.4%
32
adenyl ribonucleotide binding
24.1%
33
nucleotide binding
29.9%
41
DNA binding
43.8%
60
protein binding
56.9%
78
transcription regulator activity
12
12.6%
transcription factor activity
23
24.2%
transition metal ion binding
50
52.6%
metal ion binding
70
73.7%
100
80
60
40
20
0
0
20
40
60
80
100
Transcriptional domain coverage (%)

Figure 5.5

Figure 5.6: KEGG analysis for genes with >|1.5| fold change

Graph showing the processes and pathways, described in the Kyoto encyclopaedia of genes and genomes, over-represented in the set of genes with a significant ($p<0.05$) fold change of >|1.5| in *Pax6*$^{sey/sey}$*.DTy54* compared with *Pax6*$^{+/+}$*.DTy54*. Among the up-regulated themes are the cell cycle and the associated themes of DNA replication and the p53 signalling pathway. The down-regulated themes are axon guidance and TGF-ß signalling. Transcriptional domain coverage is calculated as the number of transcripts in each significantly overrepresented theme expressed as a percentage of the number of transcripts annotated by at least one significantly over-represented theme. The number of genes in each category is given in bold.

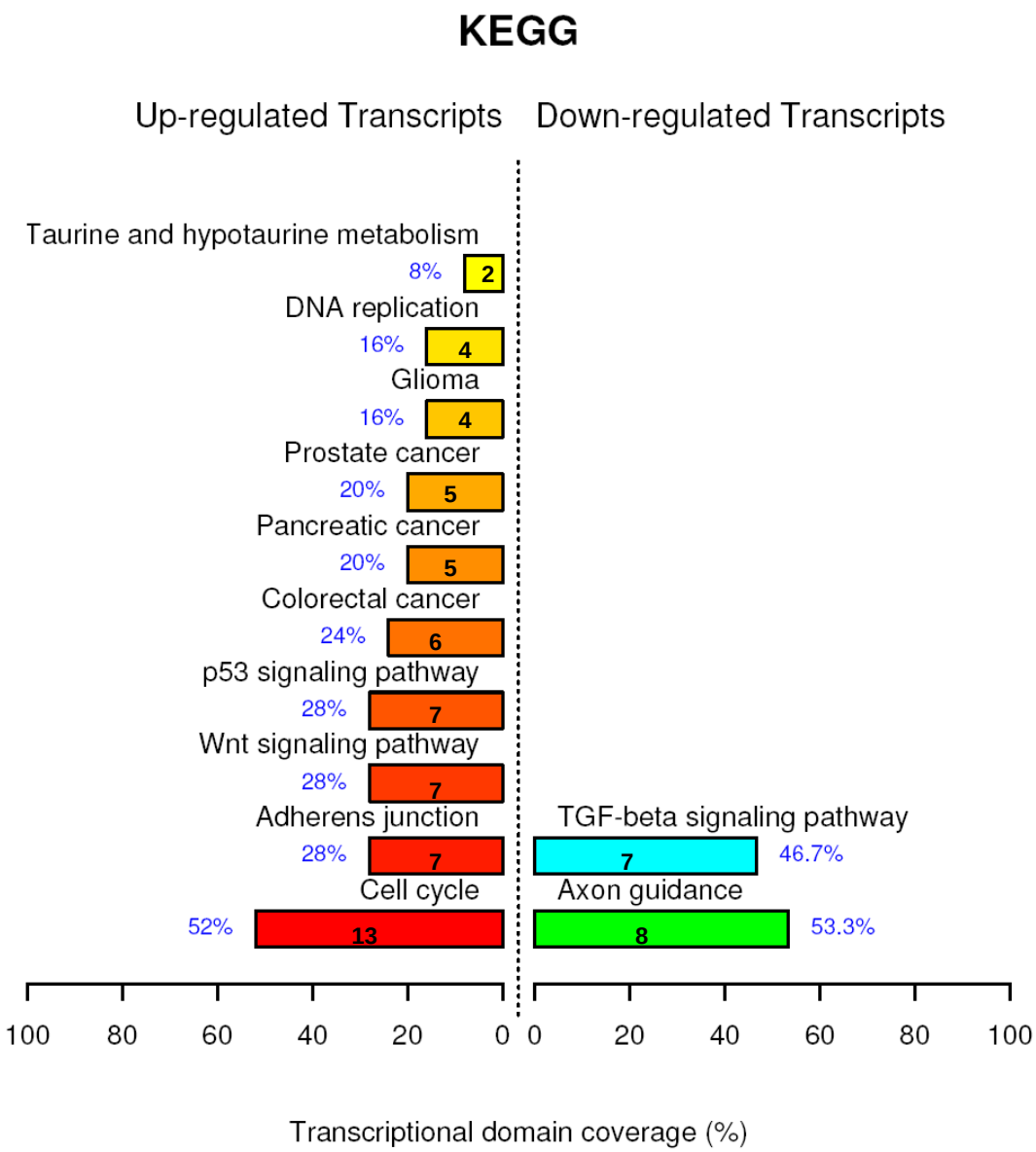
KEGG
Up-regulated Transcripts
Down-regulated Transcripts
Taurine and hypotaurine metabolism
8%
2
DNA replication
16%
4
Glioma
16%
4
Prostate cancer
20%
5
Pancreatic cancer
20%
5
Colorectal cancer
24%
6
p53 signaling pathway
28%
7
Wnt signaling pathway
28%
7
Adherens junction
28%
7
Cell cycle
52%
13
TGF-beta signaling pathway
7
46.7%
Axon guidance
8
53.3%
100
80
60
40
20
0
0
20
40
60
80
100
Transcriptional domain coverage (%)

Figure 5.6

The KEGG pathways over-represented by the up-regulated transcripts include the cell cycle and its associated pathways of DNA replication and the p53 signalling pathway, all of which would be expected to be identified given the results of the GO analysis. The Wnt signalling pathway and components of the adherens junction are also over-represented. Similar to TGF-β signalling, Wnt signalling is critically important in the development of the forebrain and so it is not surprising that *Pax6* regulates some of the components of this pathway; indeed *Sfrp2*, an inhibitor of *Wnt* signalling, has been shown to be downstream of *Pax6* (Kim *et al.,* 2001). The over-representation of components of the adherens junction is also to be expected as *Pax6* is known to play a role in cell adhesion, with altered cell adhesive properties seen in $Pax6^{sey/sey}$ embryos (Stoykova *et al.,* 1997; Tyas *et al.,* 2003). There are also a number of cancer pathways with an over-representation of gene members among the up-regulated gene-set.

5.2.4 Analysis of genes with a change in expression of >|2| fold

In order to determine if genes showing the largest changes in expression on the loss of *Pax6* are associated with the same themes identified above or if genes with large fold changes are associated with a specific subset of these themes, the analysis was repeated using a cut-off of +/- 2 fold change in expression to isolate the genes of interest (genes labelled green in Appendices A and B). In general the themes identified as over-represented were very similar between genes with >|1.5| fold change and those with >|2| fold change across the three categories of biological processes, molecular function and KEGG pathways; there were however some notable differences. The biological processes of pattern specification, neuron fate commitment and inner ear morphogenesis were over-represented among genes up-regulated >2 fold at the PSPB, but not in the set of genes up-regulated >1.5 fold (Fig. 5.7). Among down-regulated transcripts the processes of hindbrain development and synaptic vesicle endocytosis were found to be over-represented specifically in the set of genes down-regulated >2 fold.

The molecular functions over-represented among genes with larger fold changes are heavily biased towards functions involved in transcription regulation (Fig. 5.8). This

Figure 5.7: GO analysis of biological processes for genes with >|2.0| fold change

Graph showing the top 12 over-represented biological processes in the set of genes with a significant ($p<0.05$) fold change of >|2.0| in *Pax6*$^{sey/sey}$*.DTy54* compared with *Pax6*$^{+/+}$*.DTy54* for both up- and down-regulated genesets, as defined by the gene ontology database. Transcriptional domain coverage is calculated as the number of transcripts in each significantly overrepresented theme expressed as a percentage of the number of transcripts annotated by at least one significantly over-represented theme. The number of genes in each category is given in bold.

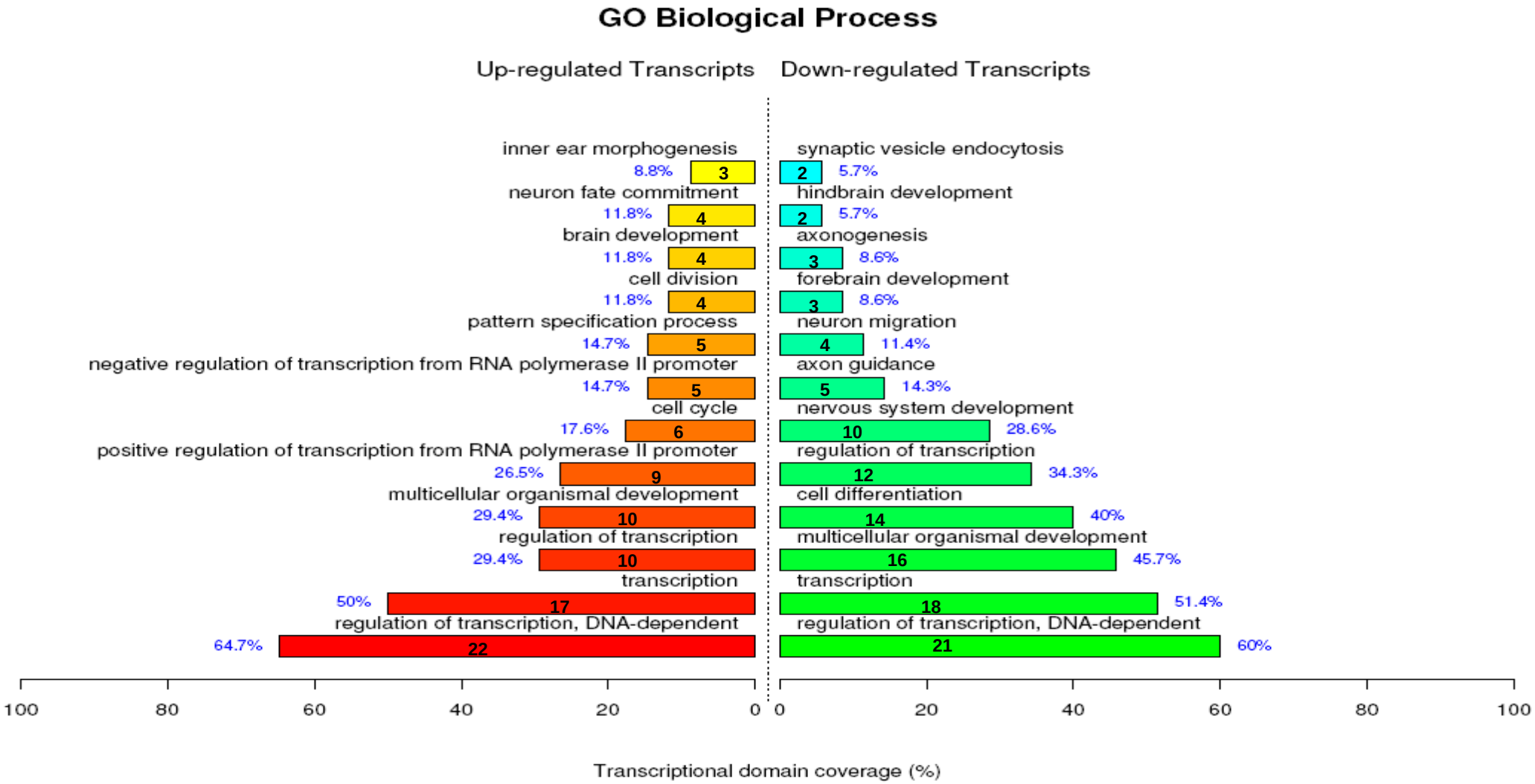
GO Biological Process
Up-regulated Transcripts
Down-regulated Transcripts
inner ear morphogenesis
8.8%
3
neuron fate commitment
11.8%
4
brain development
11.8%
4
cell division
11.8%
4
pattern specification process
14.7%
5
negative regulation of transcription from RNA polymerase II promoter
14.7%
5
cell cycle
17.6%
6
positive regulation of transcription from RNA polymerase II promoter
26.5%
9
multicellular organismal development
29.4%
10
regulation of transcription
29.4%
10
transcription
50%
17
regulation of transcription, DNA-dependent
64.7%
22
synaptic vesicle endocytosis
2
5.7%
hindbrain development
2
5.7%
axonogenesis
3
8.6%
forebrain development
3
8.6%
neuron migration
4
11.4%
axon guidance
5
14.3%
nervous system development
10
28.6%
regulation of transcription
12
34.3%
cell differentiation
14
40%
multicellular organismal development
16
45.7%
transcription
18
51.4%
regulation of transcription, DNA-dependent
21
60%
100
80
60
40
20
0
0
20
40
60
80
100
Transcriptional domain coverage (%)

Figure 5.7

Figure 5.8: GO analysis of molecular functions for genes with >|2.0| fold change

Graph showing the molecular functions, as defined by the gene ontology database, over-represented in the set of genes with a significant ($p<0.05$) fold change of >|2.0| in *Pax6*$^{sey/sey}$*.DTy54* compared with *Pax6*$^{+/+}$*.DTy54*. Transcriptional domain coverage is calculated as the number of transcripts in each significantly over-represented theme expressed as a percentage of the number of transcripts annotated by at least one significantly over-represented theme. The number of genes in each category is given in bold.

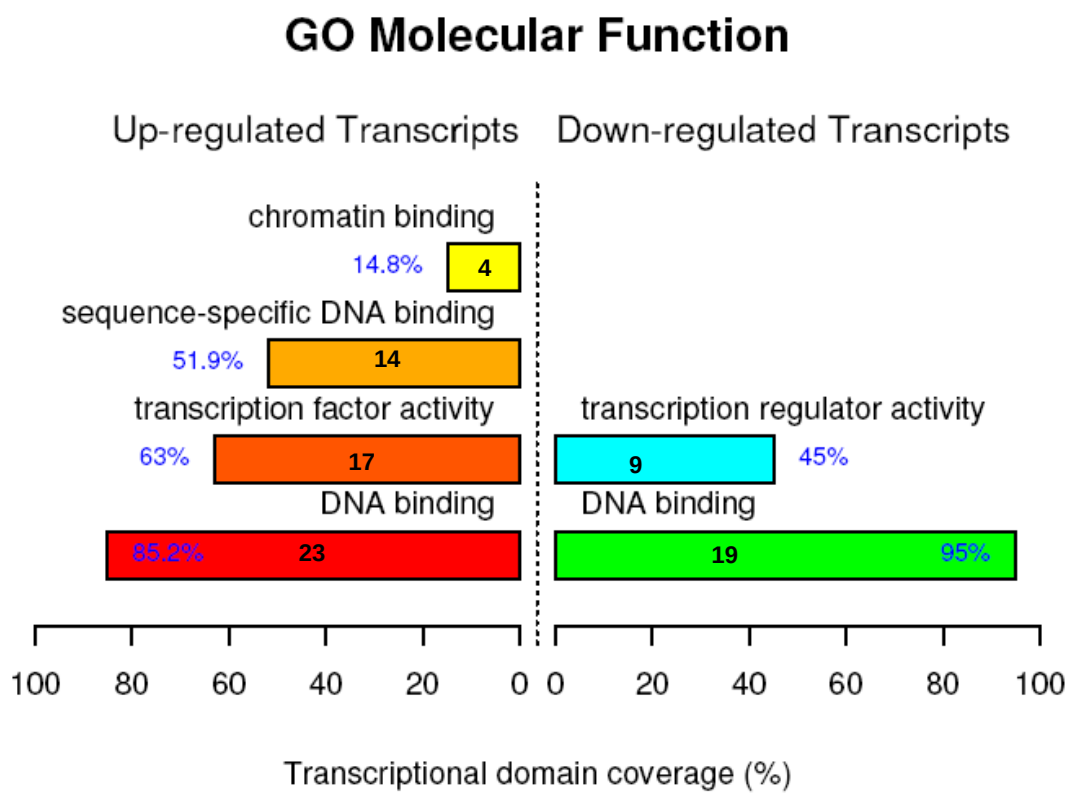
GO Molecular Function
Up-regulated Transcripts
Down-regulated Transcripts
chromatin binding
14.8%
4
sequence-specific DNA binding
51.9%
14
transcription factor activity
63%
17
DNA binding
85.2%
23
transcription regulator activity
9
45%
DNA binding
19
95%
100
80
60
40
20
0
0
20
40
60
80
100
Transcriptional domain coverage (%)

Figure 5.8

Figure 5.9: KEGG analysis for genes with >|2.0| fold change

Graph showing the processes and pathways, described in the Kyoto encyclopaedia of genes and genomes, over-represented in the set of genes with a significant ($p<0.05$) fold change of >|1.5| in *Pax6*$^{sey/sey}$*.DTy54* compared with *Pax6*$^{+/+}$*.DTy54*. Transcriptional domain coverage is calculated as the number of transcripts in each significantly overrepresented theme expressed as a percentage of the number of transcripts annotated by at least one significantly over-represented theme. The number of genes in each category is given in bold.

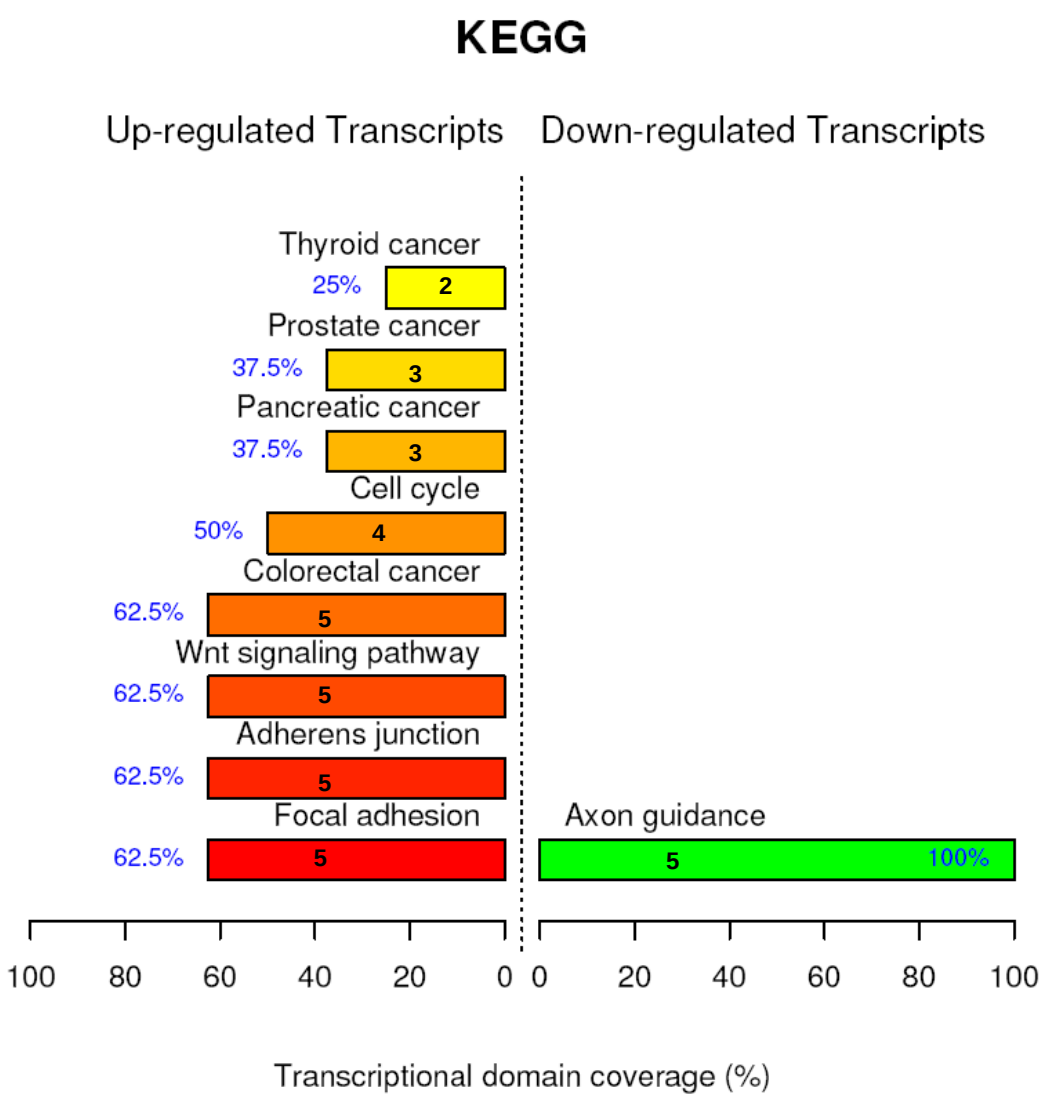
KEGG
Up-regulated Transcripts
Down-regulated Transcripts
Thyroid cancer
25%
2
Prostate cancer
37.5%
3
Pancreatic cancer
37.5%
3
Cell cycle
50%
4
Colorectal cancer
62.5%
5
Wnt signaling pathway
62.5%
5
Adherens junction
62.5%
5
Focal adhesion
62.5%
5
Axon guidance
5
100%
100
80
60
40
20
0
0
20
40
60
80
100
Transcriptional domain coverage (%)

Figure 5.9

is highly similar to the profile of genes showing a fold change >|1.5|, with the exception of metal ion and transition metal ion binding both of which are absent when the analysis is restricted to genes with a fold change >|2|. Analysis of KEGG pathways identified a second cell adhesion pathway as up-regulated among genes with a higher fold change, with genes involved in focal adhesion as well as adherens junction formation over-represented (Fig. 5.9). Axon guidance was the only over-represented KEGG pathway in the down-regulated gene set, with TGFβ signalling no longer over-represented when genes with a down-regulation between 1.5 and 2 fold are excluded from the analysis.

5.2.5 Analysis of all significantly regulated genes

Due to the volume of data produced by microarray experiments it can be easy to under analyse the results by focusing exclusively on genes that have large changes in expression levels and ignoring smaller changes that are none the less significant. In an attempt to avoid this pitfall, all genes showing a significant change in expression were analysed, regardless of the magnitude of that change (Appendices A and B). It is important to bear in mind that even small changes in gene expression can produce large downstream effects and also that large changes that occur in subsets of cells within the dissected tissue can be masked.

To determine if genes with small, but significant changes in expression at the PSPB have a similar functional profile to genes with a significant fold change >|1.5|, the set of all genes with adjusted p-values <0.05, were analysed, regardless of the magnitude of their fold change. This analysis produced results that were, with some exceptions, the same as those obtained using fold change cut-offs of either 1.5 or 2. Down-regulated transcripts showed an over-representation of genes involved in the biological processes of dephosphorylation, asymmetric protein localisation and the ovulation cycle; three categories not identified when the analysis was carried out using either a 1.5 or 2 fold change cut-off (Fig. 5.10). Analysis of molecular functions identified a number of functions, including cyclase and helicase activity, only over-represented when all significantly up-regulated transcripts were examined (Fig. 5.11). The KEGG pathway “one carbon pool by folate”, which provides the

Figure 5.10: GO analysis of biological processes for all genes with a significant change in expression

Graph showing the top 12 over-represented biological processes in the set of all genes with a significant ($p<0.05$) change in expression in *Pax6*$^{sey/sey}$*.DTy54* compared with *Pax6*$^{+/+}$*.DTy54* for both up- and down-regulated genesets, as defined by the gene ontology database. Transcriptional domain coverage is calculated as the number of transcripts in each significantly overrepresented theme expressed as a percentage of the number of transcripts annotated by at least one significantly over-represented theme. The number of genes in each category is given in bold.

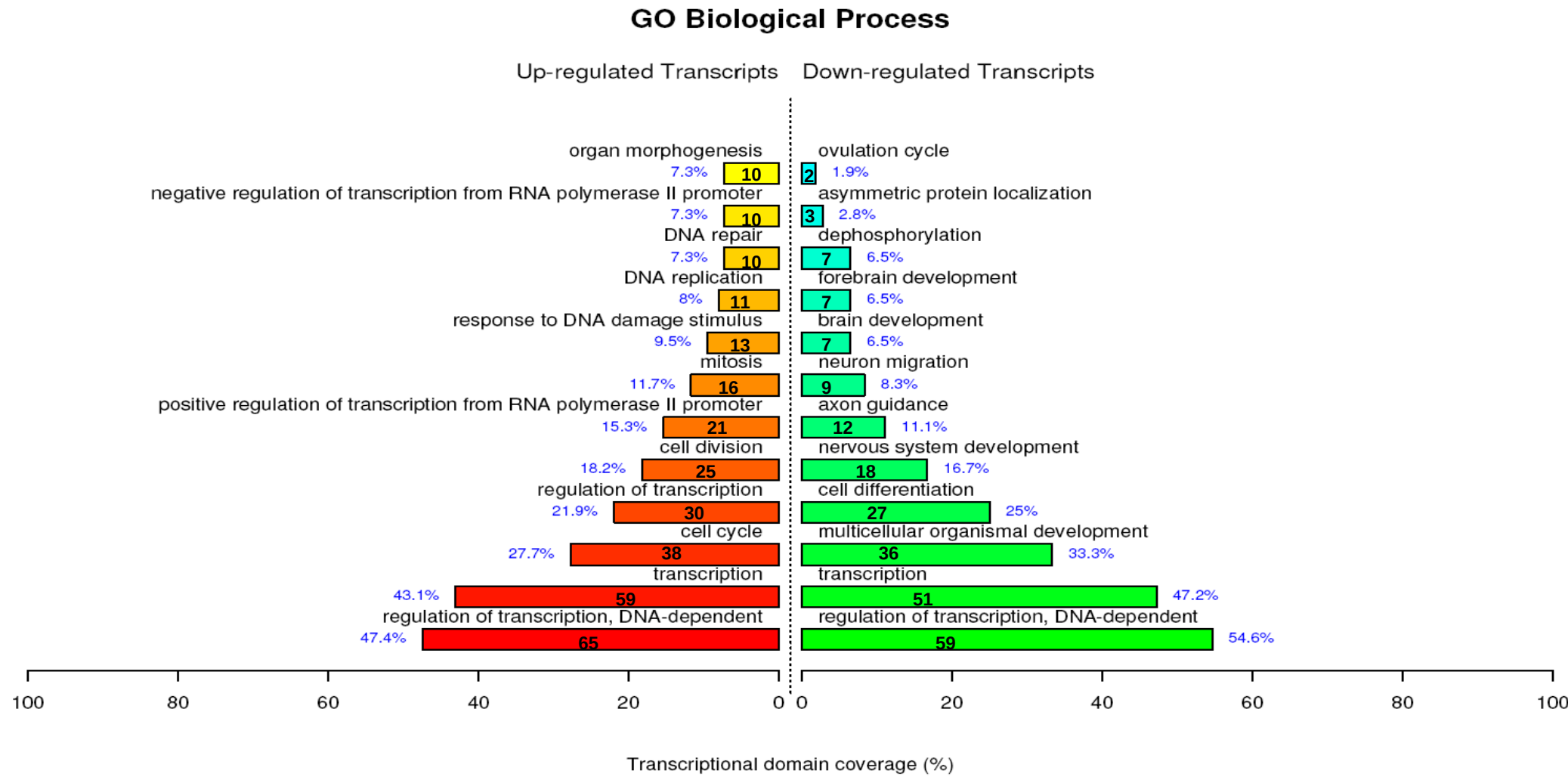
GO Biological Process
Up-regulated Transcripts
Down-regulated Transcripts
organ morphogenesis
7.3%
10
negative regulation of transcription from RNA polymerase II promoter
7.3%
10
DNA repair
7.3%
10
DNA replication
8%
11
response to DNA damage stimulus
9.5%
13
mitosis
11.7%
16
positive regulation of transcription from RNA polymerase II promoter
15.3%
21
cell division
18.2%
25
regulation of transcription
21.9%
30
cell cycle
27.7%
38
transcription
43.1%
59
regulation of transcription, DNA-dependent
47.4%
65
ovulation cycle
2
1.9%
asymmetric protein localization
3
2.8%
dephosphorylation
7
6.5%
forebrain development
7
6.5%
brain development
7
6.5%
neuron migration
9
8.3%
axon guidance
12
11.1%
nervous system development
18
16.7%
cell differentiation
27
25%
multicellular organismal development
36
33.3%
transcription
51
47.2%
regulation of transcription, DNA-dependent
59
54.6%
100
80
60
40
20
0
0
20
40
60
80
100
Transcriptional domain coverage (%)

Figure 5.10

Figure 5.11: GO analysis of molecular functions for all genes with a significant change in expression

Graph showing the molecular functions, as defined by the gene ontology database, over-represented in the set of all genes with a significant ($p<0.05$) change in expression in *Pax6*$^{sey/sey}$*.DTy54* compared with *Pax6*$^{+/+}$*.DTy54*. Transcriptional domain coverage is calculated as the number of transcripts in each significantly over-represented theme expressed as a percentage of the number of transcripts annotated by at least one significantly over-represented theme. The number of genes in each category is given in bold.

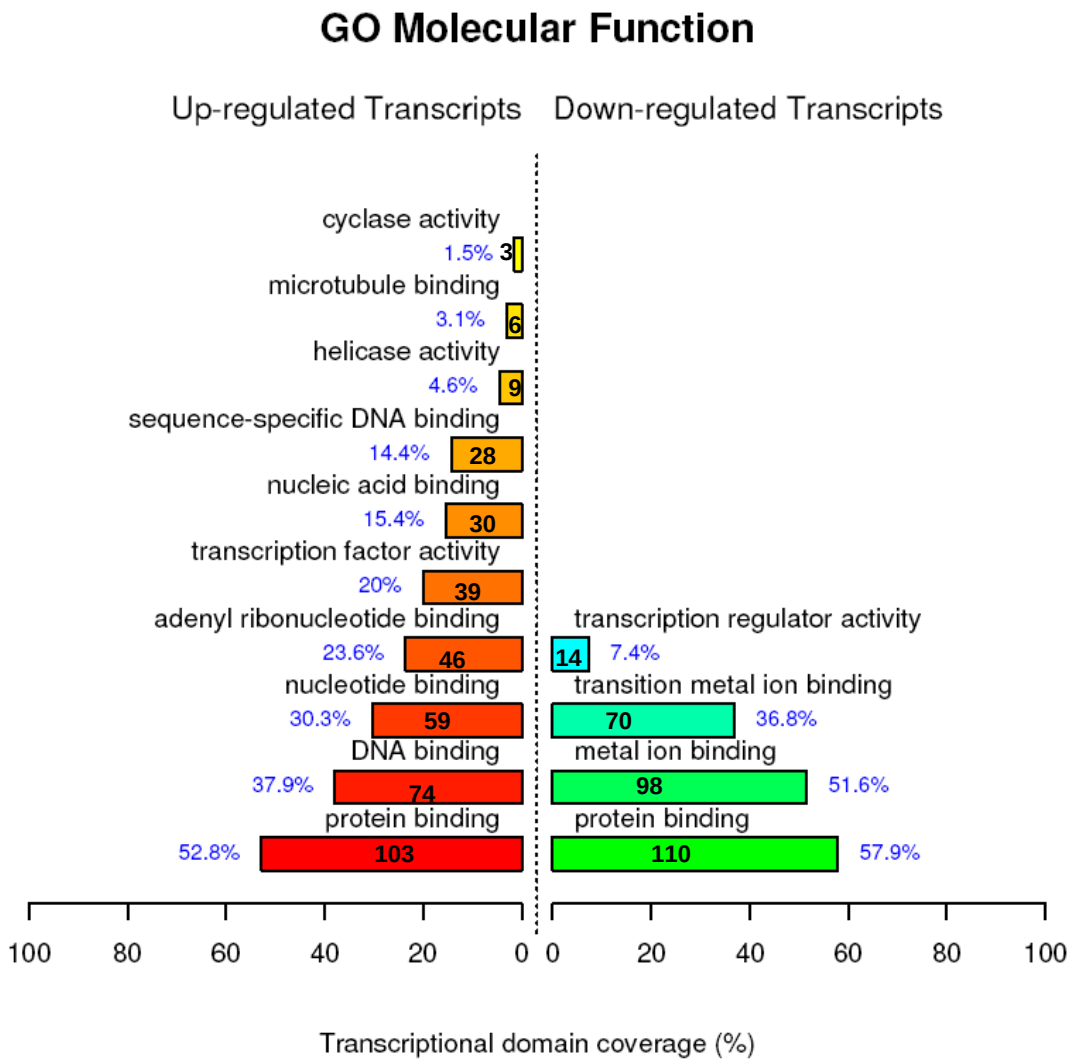
GO Molecular Function
Up-regulated Transcripts
Down-regulated Transcripts
cyclase activity
1.5%
3
microtubule binding
3.1%
6
helicase activity
4.6%
9
sequence-specific DNA binding
14.4%
28
nucleic acid binding
15.4%
30
transcription factor activity
20%
39
adenyl ribonucleotide binding
23.6%
46
nucleotide binding
30.3%
59
DNA binding
37.9%
74
protein binding
52.8%
103
transcription regulator activity
14
7.4%
transition metal ion binding
70
36.8%
metal ion binding
98
51.6%
protein binding
110
57.9%
100
80
60
40
20
0
0
20
40
60
80
100
Transcriptional domain coverage (%)

Figure 5.11

Figure 5.12: KEGG analysis for all genes with a significant change in expression

Graph showing the processes and pathways, described in the Kyoto encyclopaedia of genes and genomes, over-represented in the set of all genes with a significant ($p<0.05$) change in expression in *Pax6*$^{sey/sey}$*.DTy54* compared with *Pax6*$^{+/+}$*.DTy54*. Transcriptional domain coverage is calculated as the number of transcripts in each significantly overrepresented theme expressed as a percentage of the number of transcripts annotated by at least one significantly over-represented theme. The number of genes in each category is given in bold.

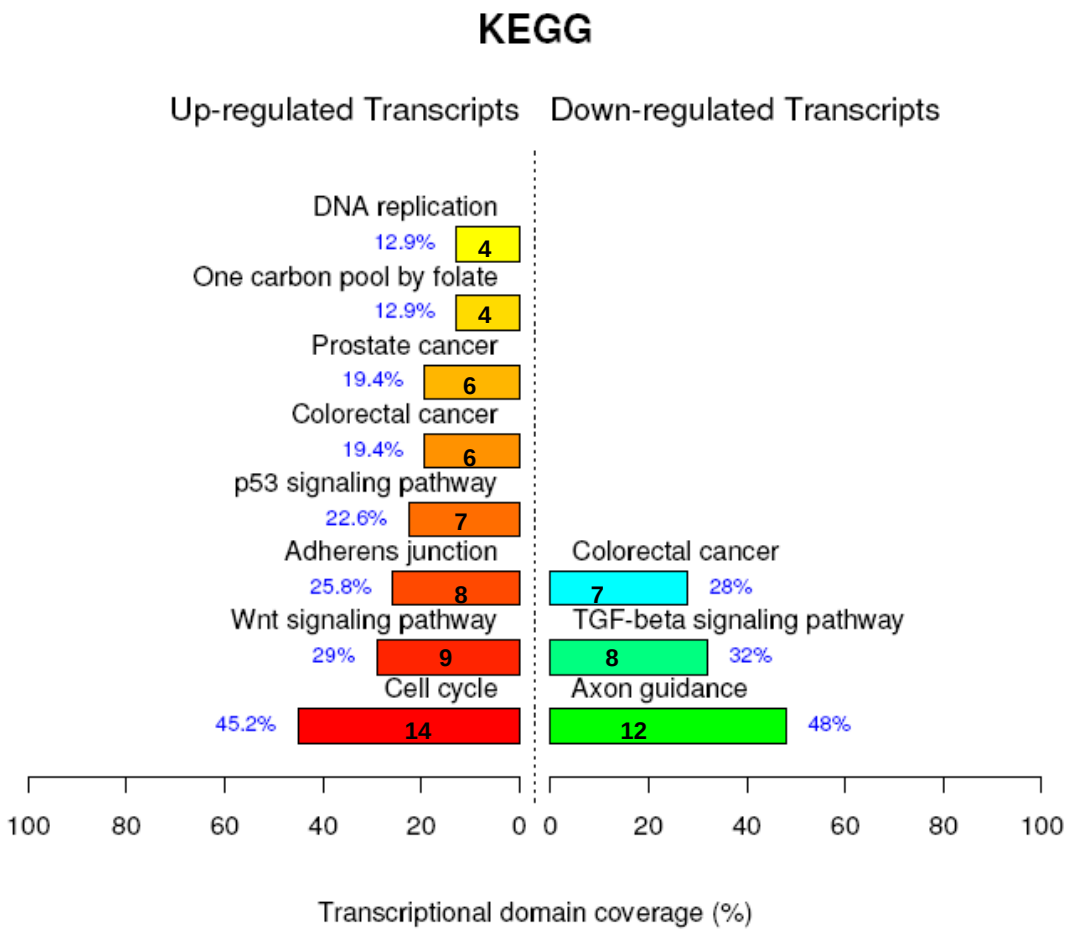
KEGG
Up-regulated Transcripts
Down-regulated Transcripts
DNA replication
12.9%
4
One carbon pool by folate
12.9%
4
Prostate cancer
19.4%
6
Colorectal cancer
19.4%
6
p53 signaling pathway
22.6%
7
Adherens junction
25.8%
8
Wnt signaling pathway
29%
9
Cell cycle
45.2%
14
Colorectal cancer
7
28%
TGF-beta signaling pathway
8
32%
Axon guidance
12
48%
100
80
60
40
20
0
0
20
40
60
80
100
Transcriptional domain coverage (%)

Figure 5.12

one-carbon groups for the *de novo* synthesis of purines and pyrimidines, is also uniquely identified when this gene-set is analysed (Fig. 5.12). The colorectal cancer pathway is identified as over-represented among the up-regulated transcripts, regardless of the fold change cut-off used, but when all significantly changed transcripts are analysed this pathway was also over-represented in the down-regulated gene-set. An overview of the overlap of themes identified as over-represented using different fold change cut-offs is shown for the up-regulated transcripts in Figure 5.13 and for the down-regulated transcripts in Figure 5.14.

5.3 Discussion

5.3.1 Comparison with genes previously identified as regulated by *Pax6*

The microarray data presented here correlates well with previously identified *Pax6* targets half of which were found to show a similar change in expression that was deemed statistically significant. Given that the published literature used for comparison was reporting on changes in gene expression throughout the telencephalon and at a variety of ages between E9.5 and E16.5, it is unsurprising that there are a number of discrepancies when compared with the results of this microarray experiment. Indeed among the genes where there are discrepancies between the microarray data and previously published literature there are only 2 which are directly comparable on the basis of age (*Six3*; Stoykova *et al.,* 2000 and *Sfrp2*; Muzio *et al.,* 2002).

Age is not the only factor that may be contributing to the differences in the observed changes in expression. As the RNA samples used for this microarray experiment were extracted from a small population of cells at the PSPB, changes in expression occurring outwith these cells will not be detected. Expression of *Six3* is mainly confined to postmitotic cells in the ventral telencephalon and as these cells were largely excluded from the microarray experiment it is unsurprising that the measured change in expression for this gene does not correspond with that found by Stoykova *et al.,* (2000). Normal expression of *Six3* in the mantle zone of the LGE extends dorsally into the mantle zone of the ventral pallium in $Pax6^{sey/sey}$ embryos. The use of RNA from samples enriched for Pax6 positive cells from the PSPB, means that the

Figure 5.13: Summary of the degree of correspondence between over-represented themes in the up-regulated geneset using different criteria to define the genes of interest

The top row lists the over-represented themes uniquely identified when different criteria were used to define the genes of interest. From left to right: All genes with a significant increase in expression, genes with a significant up-regulation of >1.5 fold and genes with a significant up-regulation of >2.0 fold. The middle row lists over-represented themes common to all significantly up-regulated genes and genes with an up-regulation of >1.5 fold (on the left) and themes common to genes with a significant up-regulation of either >1.5 or >2.0 fold (on the right). The bottom row lists the themes found to be over-represented in the up-regulated geneset regardless of which criteria were used to define the genes of interest.

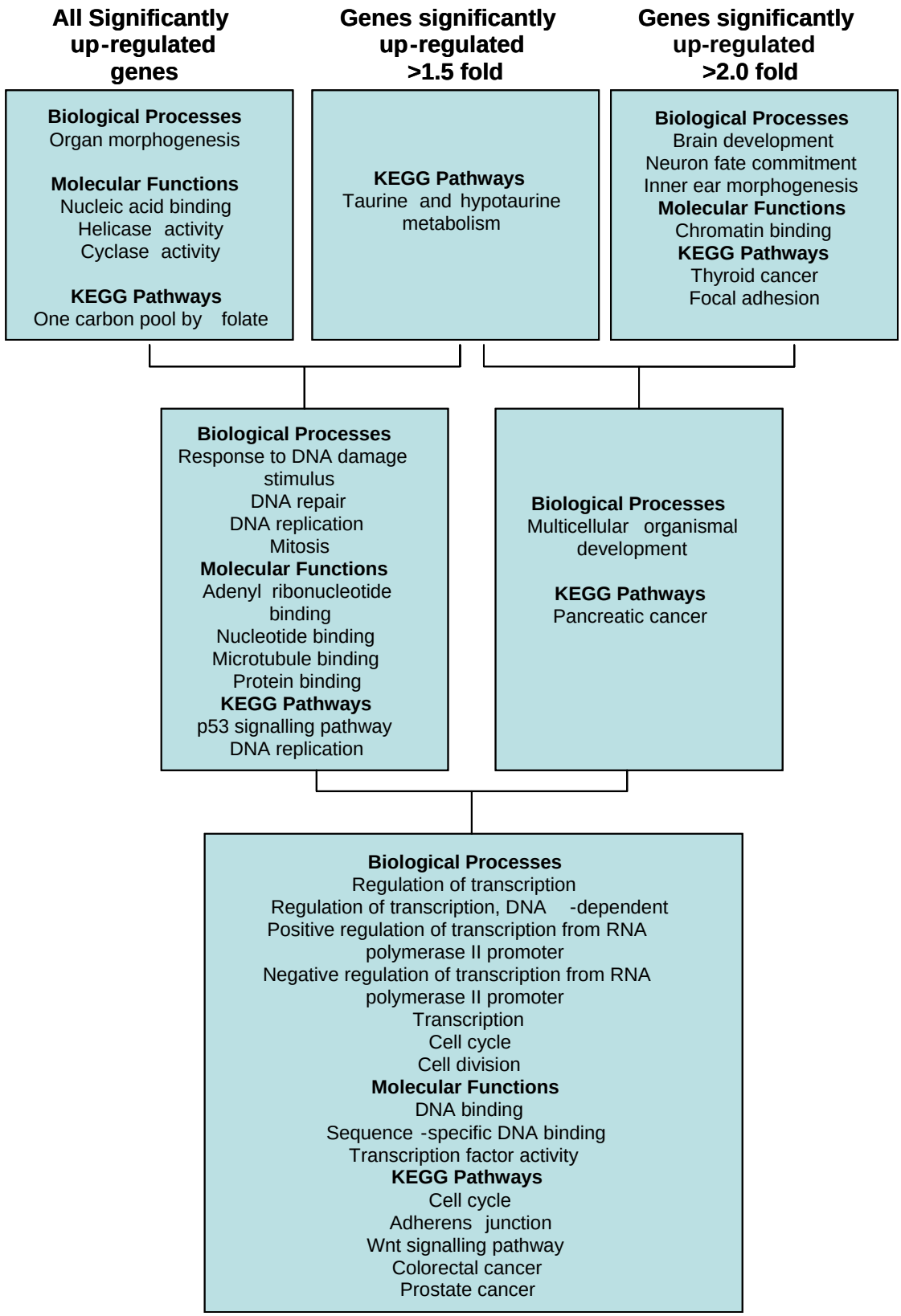
All Significantly up-regulated genes
Genes significantly up-regulated >1.5 fold
Genes significantly up-regulated >2.0 fold
Biological Processes
Organ morphogenesis
Molecular Functions
Nucleic acid binding
Helicase activity
Cyclase activity
KEGG Pathways
One carbon pool by folate
KEGG Pathways
Taurine and hypotaurine metabolism
Biological Processes
Brain development
Neuron fate commitment
Inner ear morphogenesis
Molecular Functions
Chromatin binding
KEGG Pathways
Thyroid cancer
Focal adhesion
Biological Processes
Response to DNA damage stimulus
DNA repair
DNA replication
Mitosis
Molecular Functions
Adenyl ribonucleotide binding
Nucleotide binding
Microtubule binding
Protein binding
KEGG Pathways
p53 signalling pathway
DNA replication
Biological Processes
Multicellular organismal development
KEGG Pathways
Pancreatic cancer
Biological Processes
Regulation of transcription
Regulation of transcription, DNA -dependent
Positive regulation of transcription from RNA polymerase II promoter
Negative regulation of transcription from RNA polymerase II promoter
Transcription
Cell cycle
Cell division
Molecular Functions
DNA binding
Sequence -specific DNA binding
Transcription factor activity
KEGG Pathways
Cell cycle
Adherens junction
Wnt signalling pathway
Colorectal cancer
Prostate cancer

Figure 5.13

Figure 5.14: Summary of the degree of correspondence between over-represented themes in the down-regulated geneset using different criteria to define the genes of interest

The top row lists the over-represented themes uniquely identified when different criteria were used to define the genes of interest. From left to right: All genes with a significant decrease in expression, genes with a significant down-regulation of >1.5 fold and genes with a significant down-regulation of >2.0 fold. The middle row lists over-represented themes common to all significantly down-regulated genes and genes with a down-regulation of >1.5 fold (on the left) and themes common to genes with a significant down-regulation of either >1.5 or >2.0 fold (on the right). The bottom row lists the themes found to be over-represented in the down-regulated geneset regardless of which criteria were used to define the genes of interest.

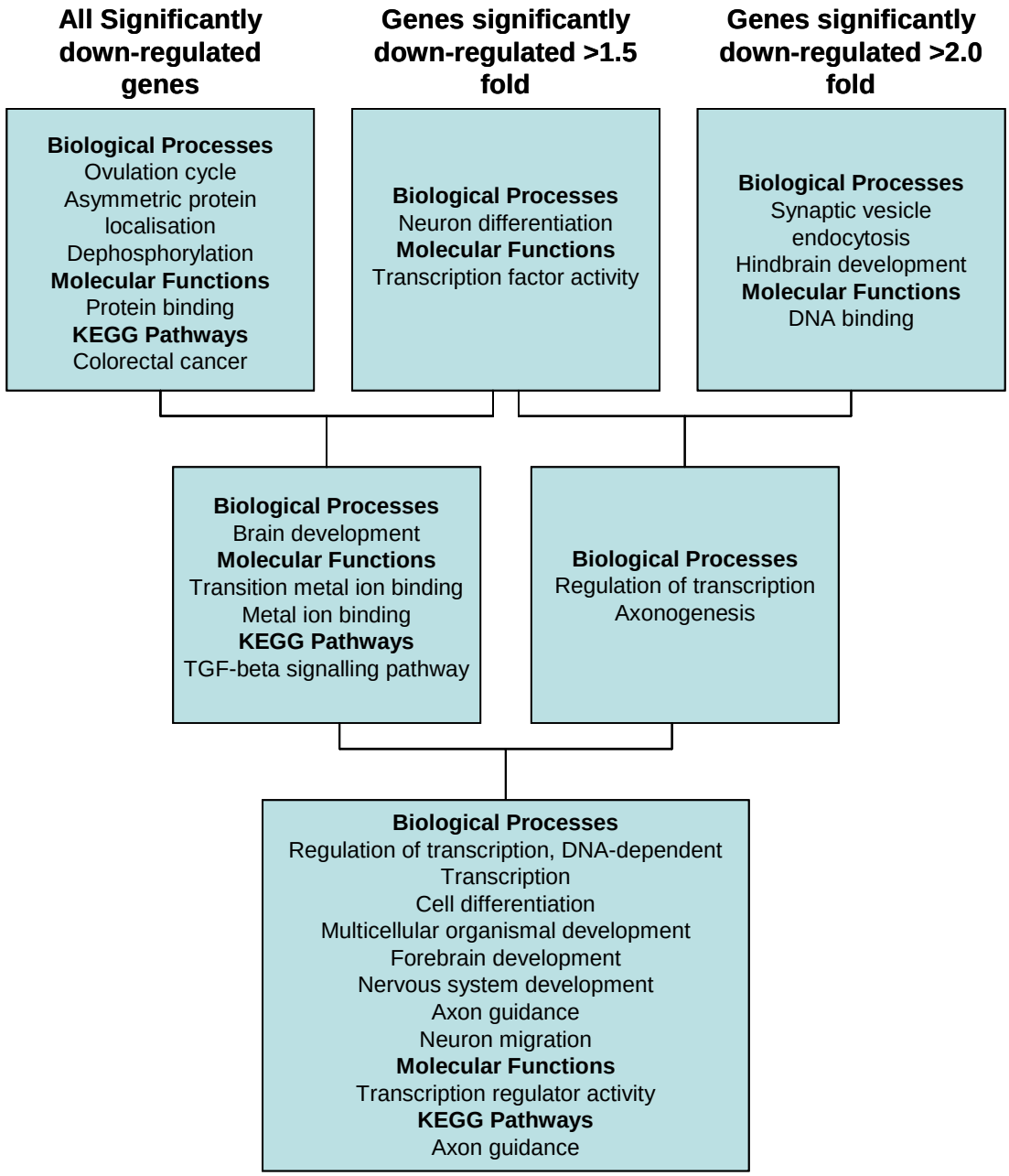
All Significantly down-regulated genes
Genes significantly down-regulated >1.5 fold
Genes significantly down-regulated >2.0 fold
Biological Processes
Ovulation cycle
Asymmetric protein localisation
Dephosphorylation
Molecular Functions
Protein binding
KEGG Pathways
Colorectal cancer
Biological Processes
Neuron differentiation
Molecular Functions
Transcription factor activity
Biological Processes
Synaptic vesicle endocytosis
Hindbrain development
Molecular Functions
DNA binding
Biological Processes
Brain development
Molecular Functions
Transition metal ion binding
Metal ion binding
KEGG Pathways
TGF-beta signalling pathway
Biological Processes
Regulation of transcription
Axonogenesis
Biological Processes
Regulation of transcription, DNA-dependent Transcription
Cell differentiation
Multicellular organismal development
Forebrain development
Nervous system development
Axon guidance
Neuron migration
Molecular Functions
Transcription regulator activity
KEGG Pathways
Axon guidance

Figure 5.14

mantle zone cells showing this up-regulation of *Six3* would have been largely excluded from the microarray analysis.

The failure to detect a significant change in the expression of *Sfrp2* at the PSPB is less easily explained. According to the previously published data *Sfrp2* expression is essentially abolished at the PSPB in the absence of Pax6 (Kim *et al.,* 2001; Muzio *et al.,* 2002); but microarray analysis of this region shows no down-regulation of expression. It is possible however that *in situ* hybridization for *Sfrp2* does not provide an accurate indication of its expression levels as data from real time RT-PCR analysis, described in chapter 4, suggest that the gene is much more widely expressed in the telencephalon than previously reported. By real time RT-PCR, higher levels of *Sfrp2* were detected in the dorsal telencephalon than at the PSPB, although according to published *in situ* hybridization results *Sfrp2* expression is confined to the PSPB. Assuming these RT-PCR results are accurate, this suggests that significant amounts of *Sfrp2* expression go undetected by *in situ* hybridization.

It seems likely that both the tissue under investigation and the age of that tissue contribute to the difference in the reported change in expression of the membrane bound protein *Odz* compared to that measured at the PSPB. In contrast to the 1.7 fold up-regulation measured in this experiment Visel *et al.,* (2007) reported a down-regulation of *Odz* in $Pax6^{sey/sey}$ embryos at E15.5. Their study, however, was focused on the developing cortical plate and they do not report on what is happening at the PSPB. It is therefore entirely possible that *Odz* is up-regulated at the PSPB in $Pax6^{sey/sey}$ at E12.5 and is then down-regulated in more dorsal regions at later stages of development.

Emx2 also shows a significant change in expression at the PSPB in the opposite direction to that previously reported in $Pax6^{sey/sey}$ embryos (Muzio *et al.,* 2002). At E11 *Emx2* is up-regulated in the developing cortex; however in the wildtype *Emx2* is only expressed at very low levels adjacent to the PSPB and when it is up-regulated in $Pax6^{sey/sey}$ embryos the region of up-regulation does not extend into the ventral pallium and so would not be detected in this microarray experiment. Due to the very

low levels of *Emx2* expression at the PSPB, any down-regulation in this region would be very difficult to detect by *in situ* hybridization.

5.3.2 Comparison with results of a recently published array

The initial most striking difference between the two sets of array data compared here is in the numbers of *Pax6* targets identified. The study by Holm *et al.,* (2006) found only 114 genes with a change in expression of >|1.5| fold, whereas analysis of the *Pax6* expressing cells at the PSPB identified 462 significantly regulated genes with that magnitude of fold change. There are a number of potential reasons for this. The two studies were carried out using different microarray platforms (Affymetrix and Agilent) and difficulties have been reported when comparing data across platforms and across laboratories (Li *et al.,* 2002; Tan *et al.,* 2003). The recent MicroArray Quality Control (MAQC) project was a large scale study designed to accurately assess the reproducibility of microarray results, across both different laboratories and microarray platforms (MAQC Consortium, 2006). One aspect of this project was the comparison of one-colour and two-colour platforms which were found to show a high degree of reproducibility (Patterson *et al.,* 2006), suggesting that it is not unreasonable to compare microarray studies from different laboratories carried out using different microarray platforms.

If discrepancies arising from the use of different microarray platforms are accepted to be small, then the differences in the number of identified target genes must be accounted for by other means. One potential reason for this difference is that the RNA samples used in this study were from cells sorted to enrich for the *Pax6* positive population. It is possible that many of the changes in expression seen here occur specifically in cells that normally express high levels of *Pax6*. Such changes in expression would have been diluted in the study by Holm *et al.* due to the inclusion of RNA from adjacent *Pax6* negative tissue and so the measured fold change may have fallen below the 1.5 fold cut off used. It is also possible that cells in the *Pax6* negative tissue may show a fold change in the opposite direction to that seen in *Pax6* positive cells, resulting in an overall change of zero when the expression level is measured across the whole tissue. The inclusion of RNA from

Pax6 negative tissue would also explain why some of the genes identified as downstream of *Pax6* by Holm *et al.* were not identified in this study. Genes whose expression level is changed in cells that would not normally express *Pax6* are unlikely to be identified in this study as the experimental design was such that these cells were largely excluded from the population of interest before RNA extraction (see chapter 4, Fig. 4.5 and 4.6). In spite of the differences in the two datasets there is still a remarkable degree of correspondence between them, strongly suggesting that both experiments are accurately identifying genes downstream of *Pax6* expression.

Given the differences in the design of the two experiments a complete correspondence between the two datasets was not to be expected. Indeed the degree of correspondence observed here is quite remarkable. There were, however, a number of genes that showed a change in expression at the PSPB that was in the opposite direction to that measured by Holm *et al.* (2007). *Arl4* was significantly down-regulated 1.465 fold at the PSPB, but showed an up-regulation of almost two fold in the cortex. *Arl4* has recently been shown, *in vitro*, to have a role in cell adhesion through recruitment to the plasma membrane of one of the major activators of the cell adhesion molecule Arf6 (Hofmann *et al.,* 2007). Changes in cell adhesion have been documented in $Pax6^{sey/sey}$ embryos at E12.5, specifically in dorsal as opposed to ventral telencephalon (Stoykova *et al.,* 1997; Tyas *et al.,* 2003). It is possible, as the PSPB is at the interface between dorsal and ventral regions, that there may be different changes occurring here compared with more dorsal regions. As FACS was used to enrich for the *Pax6* expressing population at the PSPB, and therefore for progenitor cells, another possibility is that the difference is due to different changes occurring in progenitor versus differentiating cells. This may also explain the significant down-regulation of *Tmem163* at the PSPB compared to the up-regulation seen in the cortex and the large up-regulation of *Slc15a2* which was found to be down-regulated in the cortex.

5.3.3 Over-represented themes in the microarray data

The microarray data was analysed using a number of different criteria to identify genes of interest. The following three groups were examined: 1) genes with a significant change in expression of >|1.5| fold; 2) genes with a significant fold change >|2.0| and 3) all genes with a statistically significant change in expression. These three sets of genes were analysed to identify over-represented GO terms and KEGG pathways. This analysis produced very consistent results with a number of themes over-represented across all gene-sets. The important role played by P*ax6* in controlling gene expression in the developing forebrain is emphasised in the results. Transcription factors and their regulators make up the greatest proportion of genes in both the up- and down-regulated gene sets, clearly underlining the position of *Pax6* as a master regulator of transcription via the regulation of other transcription factors. Many of the general processes of neural development are significantly down-regulated in the absence of Pax6 demonstrating the potent neurogenic effect of the gene.

A variety of other themes were identified as either up- or down-regulated in the absence of Pax6 at the PSPB. Some of these, such as the cell cycle and cell adhesion, were expected given what is already known of role of *Pax6* in the developing telencephalon, while others provide new insights into *Pax6* function. Some of these unexpected themes included cancer pathways, DNA repair and signalling and metabolic pathways, the biological significance of which are discussed below. Another highly over-represented function was protein binding, but a closer examination of the individual genes in this group revealed that the majority of them were transcription factors. As the activity of many transcription factors is regulated through the binding of co-factors it is not altogether surprising that a gene-set highly enriched in transcription factors would show an over-representation of genes involved in protein binding.

5.3.3.1 Cell cycle

Cell cycle processes are prominent themes in the up-regulated gene set. This is consistent with the important role of *Pax6* in regulating cell cycle progression in the

cortical ventricular zone (Warren *et al.,* 1999; Estivill-Torrus *et al.,* 2002; Quinn *et al.,* 2007). While alterations in the cell cycle are well documented in *Pax6*$^{sey/sey}$, the data from this experiment provides the opportunity to examine more closely the genetic changes underlying this phenotype and if a particular stage of the cell cycle is affected more than others. The up-regulated genes appear to be dispersed through all stages of the cell cycle as can be seen on the KEGG diagram of this pathway (Fig. 5.15; genes in red are significantly up-regulated). Many more genes than those represented in this figure are involved in the cell cycle, as many genes are not annotated in the KEGG database. Combining annotations from both the KEGG and GO databases identifies a wide range of cell cycle related functions and processes over-represented among up-regulated genes.

Genes such as *polymerase* and members of the minichromosome maintenance complex which are involved in DNA replication are significantly up-regulated. There is also an over-representation of genes with helicase function. As helicases are required for unravelling the DNA double helix these genes would clearly have an important role to play during DNA replication. Further evidence that *Pax6* plays a significant role in regulating DNA replication is provided by the observed up-regulation of genes involved in the production of the dNTPs required for this process (the metabolic pathway is described below). Genes which act later in the cell cycle also lie downstream of *Pax6*. These include genes involved in chromosome condensation and nucleosome assembly, with seven members of the histone cluster family of genes significantly up-regulated. A number of microtubule binding proteins, such as *Mapre1* and *Nusap1*, are also significantly up-regulated. These genes have a role in the organisation of the mitotic spindle, the correct alignment of chromosomes during mitosis and in cytokinesis (Green *et al.,* 2005; Ribbeck *et al.,* 2007; Raemaekers *et al.,* 2003).

Overall the data suggests that at E12.5 in *Pax6*$^{sey/sey}$ embryos, there is an increase in cell cycling in the region of the PSPB. This may be caused either by an increase in the proportion of cells undergoing mitosis or a shortening of cell cycle length. Recent results published by Quinn *et al*., (2007) found no evidence of a shortening of

Figure 5.15: Diagram of genes involved in the cell cycle

The genes involved in the different stages of the cell cycle and their interactions with each other, as annotated in the KEGG database, are outlined here. Genes identified in this study as being significantly up-regulated in the absence of Pax6 are show in red. Image taken from the website of the KEGG database (www.genome.jp/kegg).

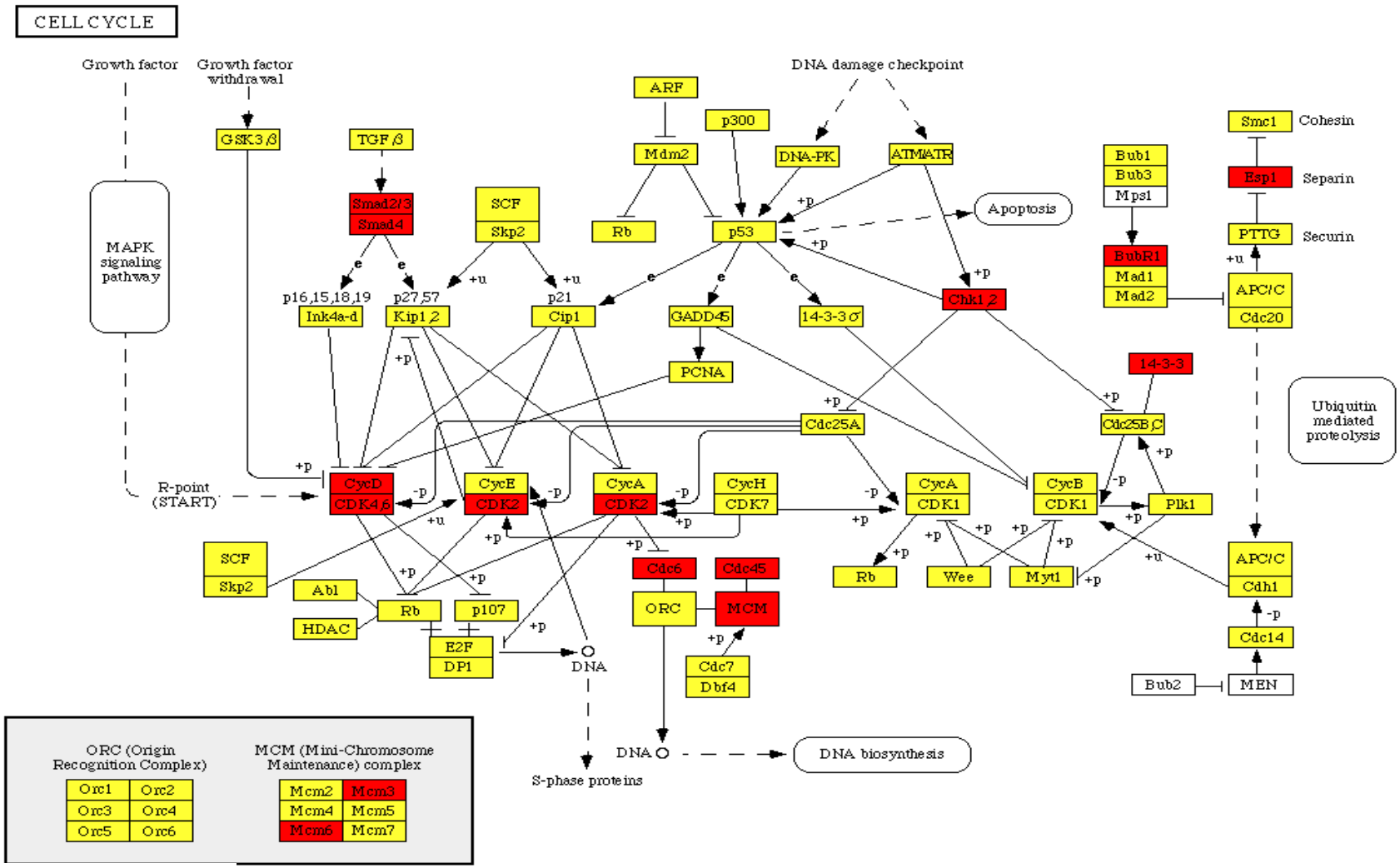
CELL CYCLE
Growth factor
Growth factor withdrawal
GSK3β
TGFβ
MAPK signaling pathway
Smad2/3
Smad4
SCF
Skp2
ARF
p300
Mdm2
DNA-PK
ATM/ATR
DNA damage checkpoint
Rb
p53
Apoptosis
Bub1
Bub3
Mps1
BubR1
Mad1
Mad2
Smc1
Cohesin
Esp1
Separin
PTTG
Securin
APC/C
Cdc20
p16,15,18,19
Ink4a-d
p27,57
Kip1,2
p21
Cip1
GADD45
14-3-3σ
Chk1,2
PCNA
14-3-3
Ubiquitin mediated proteolysis
Cdc25A
Cdc25B,C
R-point (START)
CycD
CDK4,6
CycE
CDK2
CycA
CDK2
CycH
CDK7
CycA
CDK1
CycB
CDK1
Plk1
SCF
Skp2
Abl
HDAC
Rb
p107
E2F
DP1
Cdc6
Cdc45
ORC
MCM
Cdc7
Dbf4
DNA
Rb
Wee
Myt1
APC/C
Cdh1
Cdc14
Bub2
MEN
DNA
DNA biosynthesis
S-phase proteins
ORC (Origin Recognition Complex)
Orc1
Orc2
Orc3
Orc4
Orc5
Orc6
MCM (Mini-Chromosome Maintenance) complex
Mcm2
Mcm3
Mcm4
Mcm5
Mcm6
Mcm7
G1
S
G2
M

Figure 5.15

the cell cycle in the neocortex of *Pax6*$^{sey/sey}$ embryos at this age. It is possible, given their unique position at the boundary between dorsal and ventral telencephalon, that the cells analysed here respond differently, in terms of cell cycle kinetics, to a loss of Pax6 compared with cells located more dorsally in the developing cortex. Given the large number of cell cycle related genes identified here it seems likely that many of them may be indirect targets of *Pax6*, something which cannot be determined from this study. It would be interesting however, to determine how many of these genes are direct *Pax6* targets, either by ChIP analysis or by using bioinformatics approaches to search for *Pax6* binding sites in the regulatory sequences of these genes.

5.3.3.2 Cancer pathways

Pax6 has been shown to be expressed in human tumour cells derived from tumours of the colon and bladder (Salem *et al.,* 2000). Over-expression of *Pax6* can also cause the development of pancreatic tumours in mice (Yamaoka *et al.,* 2000). In spite of this evidence that *Pax6* can act as an oncogene, the identification of prostate, pancreatic, thyroid and colorectal cancer pathways as being up-regulated in the developing forebrain seems at first glance to make little sense. Indeed, if anything, one might expect cancer pathways to be down-regulated in the absence of functional Pax6. It is important to bear in mind however that these pathways have been identified because a number of the genes involved in the pathways are up-regulated and not necessarily the pathway itself, as genes may have very different roles in different tissues and at different stages of development. Indeed a closer examination of the actual genes involved in these cases shows that all of the genes identified as being part of these pathways are also part of one or more of the other pathways over-represented among the up-regulated transcripts. For example *CyclinD1*, involved in all the cancer pathways identified, is also involved in the cell cycle and in the Wnt and p53 signalling pathways. Similarly *Smad 2* and *4*, involved in colorectal and pancreatic cancers, also have a role in the cell cycle, adherens junctions and the Wnt signalling pathway. The fact that genes involved in the colorectal cancer pathway are over-represented in both the up- and down-regulated transcripts when all significantly altered genes are considered also suggests that these pathways are over-

represented here through having many genes in common with other pathways which are regulated by *Pax6*.

5.3.3.3 Signalling pathways

Analysis of the microarray data on the basis of the KEGG annotations of the regulated genes identified the TGFβ and Wnt signalling pathways as over-represented. This was surprising given that there was no indication of an over-representation of signalling molecules in the results from GO analysis. A closer examination of the members of the Wnt signalling pathway which are up-regulated in *Pax6*$^{sey/sey}$ reveals that the genes in question are, for the most part, localised to the nucleus and are not, in themselves, signalling molecules. Of the seven genes in this pathway that are up-regulated by >1.5 fold four of them, *Smad1* and *2* and *CyclinD1* and *2*, have a role in cell cycle regulation. This suggests that the identified up-regulation of the Wnt signalling pathway may be an artefact of more general changes in the expression of cell cycle regulators. Alternatively, given that inhibitors of Wnt signalling have been shown to be down-regulated in the *Pax6*$^{sey/sey}$ (Kim *et al.,* 2001; Muzio *et al.,* 2002) it may be that the cell cycle changes seen in these embryos are due, in part at least, to an increase in Wnt signalling.

The down-regulation of members of the TGFß signalling pathway was not unexpected as *Pax6* has been shown to be downstream of the BMP family of TGFß signalling molecules (Timmer *et al.,* 2002). It is surprising however that *TGFβ2* and *BMP receptor type 1b* are themselves significantly downregulated in *Pax6*$^{sey/sey}$ suggesting that there may be a feedback loop between *Pax6* and this signalling pathway.

5.3.3.4 Metabolic pathways

The data presented here identifies two metabolic pathways as being over-represented among genes up-regulated at the PSPB in the absence of Pax6. Taurine and hypotaurine metabolism is over-represented among genes with a >1.5 fold increase in expression in *Pax6*$^{sey/sey}$. Taurine is the most abundant amino acid in the mammalian brain and hypotaurine is an intermediary product of taurine biosynthesis;

cysteine is converted first to cysteine sulfinic acid (CSA) then to hypotaurine and finally to taurine (for review see Dominy *et al.,* 2004). Two enzymes have been isolated from brain tissue that can catalyse the conversion of CSA to hypotaurine – glutamic acid decarboxylase (Gad) and cysteine sulfinic acid decarboxylase (Csad). *In vitro* investigations of Gad activity, however, reveal that it has a very low affinity for CSA and only efficiently converts CSA to hypotaurine when CSA is present at much higher concentrations than are normally found *in vivo*; its catalysis of this reaction is also inhibited in the presence of glutamic acid for which Gad has a much higher affinity (Tappaz *et al.,* 1992).

The members of the taurine and hypotaurine metabolic pathway found to be up-regulated in this study were *Gad1* and *2*. Given that Gad is not thought to be important for normal physiological taurine biosynthesis it seems likely that these genes are up-regulated for other reasons. Given the increase in interneuron migration to the cortex in *Pax6*$^{sey/sey}$ it is likely that their role in the production of gamma amino butyric acid is more important here. If this pathway was truly up-regulated in response to a loss of Pax6 then other members of the pathway might be expected to show a trend towards up-regulation, even if this did not reach statistical significance. Upon investigation however, other enzymes in the pathway were found to show a trend in the opposite direction. *Cysteine dioxygenase*, which catalyses the conversion of cysteine to CSA, was slightly down-regulated (fold change = -1.238; adjusted p-value=0.096), and *Csad* also showed a decrease in expression which was approaching significance (fold change = -1.712; adjusted p-value=0.058). Given this, it seems highly unlikely that Pax6 plays a role in regulating the taurine and hypotaurine metabolic pathway.

The second metabolic pathway identified as over-represented in the up-regulated gene-set is "one carbon pool by folate". This pathway provides the one-carbon groups critical for the *de novo* synthesis of purines and pyrimidines. It is important in the regulation of cellular dNTP levels and therefore in DNA synthesis and cell cycle progression. Cells grown in the absence of folate, the substrate of this pathway, show a decrease in intercellular pools of nucleotides and this was

associated with a delay in cell cycle progression (James *et al.,* 1993). Given the degree of up-regulation of the cell cycle processes in the array data it is perhaps unsurprising that the metabolic process required to provide the raw materials for DNA replication is also up-regulated. Four key enzymes in this pathway are significantly up-regulated in *Pax6*$^{sey/sey}$, two of them with a fold change greater than 1.5, suggesting that this may represent an important mode of cell cycle regulation for *Pax6*. The significant up-regulation of a number of genes coding for enzymes with cyclase activity also supports a role for *Pax6* in regulating cellular levels of dNTPs.

5.3.3.5 Themes unrelated to telencephalic development

A number of themes were identified as over-represented that are entirely unrelated to telencephalic development. When a fold change of >|2.0| is used to identify genes of interest, inner ear morphogenesis is over-represented in the up-regulated gene-set, while hindbrain development is over-represented among down-regulated genes. The identification of hindbrain development is not particularly surprising as a) many genes involved in forebrain development might reasonably be expected to have a role in the development of other parts of the brain and b) *Pax6* is expressed in the hindbrain and may regulate the expression of a similar set of genes in this region. Indeed the two genes in this group are *Ngn1* and *Tbr1*, both of which have well established roles in forebrain development.

The three genes identified as playing a part in inner ear morphogenesis are all transcription factors and are present in many of the other over-represented groups. As a given transcription factor can be involved in the development of a range of tissues it is easy to understand how the type of analysis used here might result in the identification of certain terms as over-represented where the over-representation is simply an artefact of the type of genes being investigated. This would also explain why the ovulation cycle was over-represented in the down-regulated gene-set when all significantly regulated genes were considered. The genes in this group, *Nhlh2* and *BMP receptor type 1b*, are both present in many of the other over-represented categories.

5.3.4 A closer look at some genes whose regulation by *Pax6* may be particularly relevant at the PSPB

While a number of genes identified in this study have previously been reported to show alterations in expression in the absence of Pax6, many novel *Pax6* targets have also been identified. Some of these genes are reported to be involved in processes like interneuron migration and axon guidance, which are severely disrupted in *Pax6*$^{sey/sey}$ embryos. Therefore they could potentially provide interesting insights into the role of *Pax6* at the PSPB. Among these is *doublecortin-like kinase* (*Dclk*), a microtubule associated protein that has been shown to be involved in the radial migration of cortical neurons (Deuel *et al.,* 2006; Koizumi *et al.,* 2006) and in cortical interneuron migration (Fricourt *et al.,* 2007). Inactivation of *Dclk*, by RNA interference in brain slices, causes a delay in the migration of interneurons from the ganglionic eminences and fewer calbindin positive interneurons reach the cortex of *Dclk*$^{-/-}$ mice (Friocourt *et al.,* 2007).

Given this phenotype it is surprising that *Dclk* is down-regulated in this study, as *Pax6*$^{sey/sey}$ mice have been shown to have an increase in the number of interneurons migrating to the cortex (Chapouton *et al.,* 1999). One possible explanation for this would be that different subtypes of interneurons are affected differently in *Pax6*$^{sey/sey}$ embryos with some subtypes showing a decrease in migration and others showing a large increase, resulting in an overall increase in the total number of cortical interneurons. A delay in the migration of calbindin positive interneurons in *Pax6* mutant mice has also been reported (Jiménez *et al*., 2002). This study found that at E13 calbindin positive cells were completely absent from the developing cortex of *Pax6*$^{sey/sey}$ embryos, but that by E16 numbers had recovered to levels seen in wildtype controls. This finding would be consistent with the *Dclk*$^{-/-}$ phenotype described by Friocourt *et al.* (2007).

Lhx6, the gene with the largest up-regulation is this study, is normally expressed in the MGE and in interneurons where it is essential for their normal migration from the ganglionic eminences to the cortex (Alifragis *et al.,* 2004; Liodis *et al.,* 2007). Although its up-regulation here could be due to the presence of more migrating

interneurons in the vicinity of the PSPB in *Pax6*$^{sey/sey}$ this seems unlikely because a) at E12.5 interneurons are only beginning to reach the PSPB and enter the cortex and b) interneurons would not be expressing GFP and so would have been excluded from the experiment during cell sorting. A study by Kroll and O'Leary (2005) suggests that dorsal telencephalic progenitors ectopically expressing ventral marker genes in *Pax6*$^{sey/sey}$ produce interneurons characteristic of the LGE. Although they found no evidence that *Lhx6* expressing interneurons, characteristic of the MGE, were being produced by these cells, even a very small number of *Lhx6* positive cells could cause *Lhx6* expression to appear up-regulated on the microarray given the absence of *Lhx6* expression in this area in the wildtype.

Chapter 6 – Validation of Candidate *Pax6* Target Genes Identified by Microarray

6.1 Introduction

It is important to validate the accuracy of microarray data, particularly when the number of biological replicates in an experiment is small as this makes statistical analysis of the data less robust. Validation steps allow the identification of genes for which a significant change in expression was measured due to artefact. These genes can then be eliminated from further investigation. There are a variety of ways in which validation can be carried out. The overall performance of an array study can be validated by comparison with previously published literature to determine if genes known to show a change in expression in the condition under investigation have been successfully identified. Experimental validation of the gene expression measurements can also be carried out. *In situ* hybridization can provide useful information about the spatial expression pattern of a gene of interest and may also confirm large changes in expression levels. As it is not a quantitative technique however, small changes in expression levels may go undetected. The failure of *in situ* hybridization to confirm a change in expression identified by microarray is therefore not evidence that the change in question is due to artefact and would need to be supported by experiments using more quantitative techniques. The most common quantitative methods used for validation of microarray data are real time RT-PCR and northern blotting (see Chuaqui *et al.,* 2002 for a review of microarray validation methods).

6.2 Results

The delays encountered in generating the RNA samples for the microarray experiment meant that the amount of validation that could be carried out was limited due to time constraints. Validation of the performance of the microarray experiment by comparison with the literature on *Pax6* was carried out and is described in the previous chapter. Experimental verification by *in situ* hybridization of a small number of genes, showing large changes in expression in $Pax6^{sey/sey}$ compared to wildtype, is described here.

Figure 6.1: *Ngn2* expression

In situ hybridization for *Ngn2* expression in the telencephalon of $Pax6^{+/+}$ (A and B) and $Pax6^{sey/sey}$ (C and D) embryos at E12.5 is shown. B and D are high power images of the boxed areas in A and C respectively. *Ngn2* is widely expressed in the diencephalon and in the VZ of the dorsal telencephalon in wildtype where it has a sharp boundary of expression at the PSPB (dashed red line in B). In $Pax6^{sey/sey}$ *Ngn2* expression is retracted away from the PSPB – note the distance between the dashed red line indicating the normal extent of *Ngn2* expression and the dashed blue line indicating its new expression boundary in D. Ctx, cortex; di, diencephalon; lge, lateral ganglionic eminence. Scale bars: 100µm in A and C; 50µm in B and D

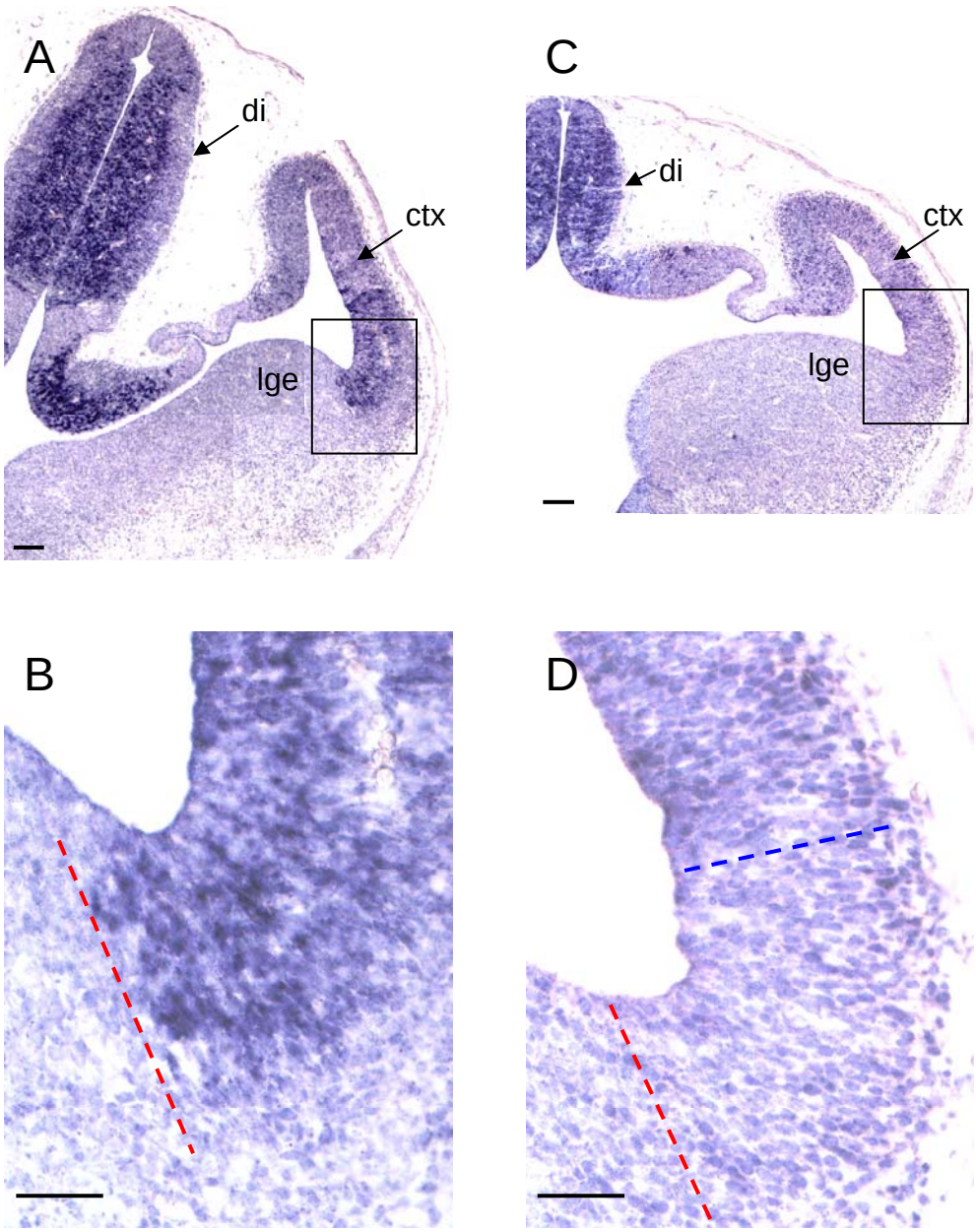

Figure 6.1

6.2.1 *Ngn2*

Ngn2 was the most highly down-regulated gene on the microarray with a fold change of –10.241 (adjusted p-value=0.014). *In situ* hybridization analysis of *Ngn2* expression in coronal sections at E12.5 confirms this down-regulation at the PSPB (Fig. 6.1). In the wildtype *Ngn2* can be seen to be widely expressed in the VZ of the dorsal telencephalon with a sharp boundary of expression at the PSPB (Fig. 6.1 A and B). In contrast in *Pax6*$^{sey/sey}$, expression of *Ngn2* is retracted dorsally away from the PSPB (Fig. 6.1 C and D). *Ngn2* is also expressed at lower levels in the dorsal telencephalon of *Pax6*$^{sey/sey}$ compared with wildtype.

6.2.2 *Lhx6*

The gene with the greatest up-regulation in expression on the microarray was *Lhx6* with a fold change of 15.439 (adjusted p-value=0.008). This change can also be seen by *in situ* hybridization (Fig 6.2). *Lhx6* is normally expressed in postmitotic cells of the MGE and in the interneurons migrating from this tissue to the cortex (Alifragis *et al.,* 2004; Liodis *et al.,* 2007). It is not normally expressed in the region of the PSPB, except where it is present in interneurons crossing the boundary en route to the cortex. This pattern of expression can be clearly seen by *in situ* hybridization (Fig. 6.2 A-C). The level of expression of *Lhx6* in the MGE of *Pax6*$^{sey/sey}$ embryos can be seen to be much higher than in the wildtype and expression can also be seen extending into the LGE (Fig. 6.2 D). A number of very strongly labelled cells can be seen in that part of the tissue that would have been included in the dissection of the PSPB (arrows in Fig. 6.2 E and F).

6.2.3 *Gsh2*

Gsh2 was another gene that was significantly up-regulated at the PSPB (fold change=2.906; adjusted p-value=0.012). Validation by *in situ* hybridization confirms this up-regulation of expression (Fig. 6.3). Ectopic expression of *Gsh2* dorsal to its normal boundary of expression at the PSPB can also be seen in *Pax6*$^{sey/sey}$ embryos. *Gsh2* is normally expressed throughout the VZ of the MGE and LGE, with a sharp boundary at the PSPB (dashed red line in Fig. 6.3 B). In the absence of Pax6, *Gsh2* expression is up-regulated throughout its normal telencephalic expression domain

Figure 6.2: *Lhx6* expression

In situ hybridization for *Lhx6* expression in the telencephalon of $Pax6^{+/+}$ (A-C) and $Pax6^{sey/sey}$ (D-F) embryos at E12.5 is shown. The labelled boxed areas in A and D correspond to the areas shown in B, C, E and F. In $Pax6^{+/+}$ *Lhx6* is expressed in post-mitotic cells of the MGE (A) and is absent from the region of the PSPB (B and C). In $Pax6^{sey/sey}$ *Lhx6* can be seen to be expressed at much higher levels in the MGE (D). Many *Lhx6* positive cells can also be seen in the LGE (D). A number of strongly labelled cells are present at the ventral extremity of the PSPB (arrows in E and F). Ctx, cortex; lge, lateral ganglionic eminence; mge, medial ganglionic eminence. Scale bars: 100µm A and D; 50µm in B, C, E and F

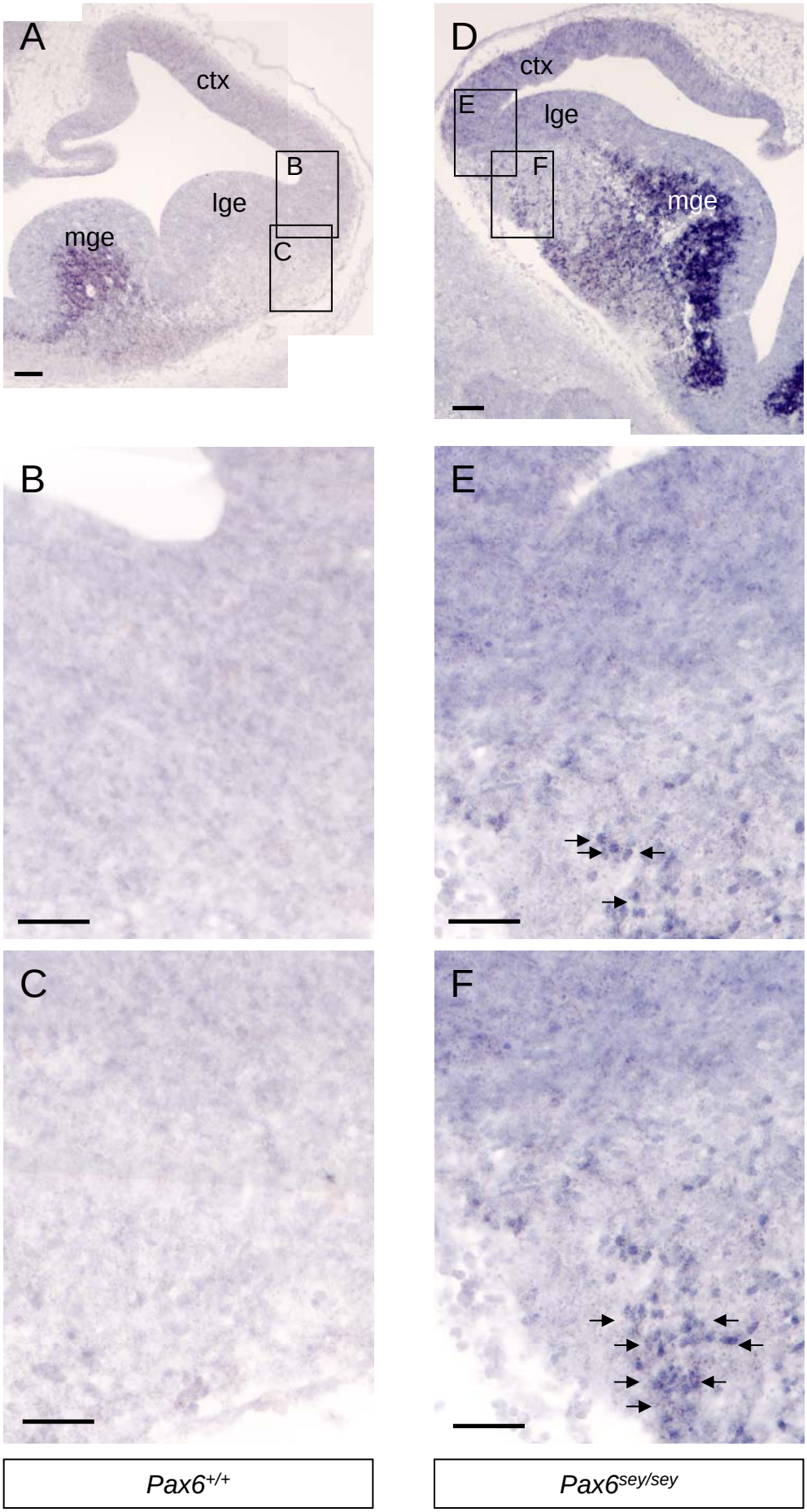

Figure 6.2

Figure 6.3: *Gsh2* expression

In situ hybridization for *Gsh2* expression in the telencephalon of $Pax6^{+/+}$ (A and B) and $Pax6^{sey/sey}$ (C and D) embryos at E12.5 is shown. B and D are high power images of the boxed areas in A and C respectively. In $Pax6^{+/+}$ *Gsh2* is expressed in the VZ of the medial and lateral ganglionic eminences (A) and has a sharp expression boundary at the PSPB (dashed red line in B). By comparison VZ cells of the ganglionic eminences express *Gsh2* at much higher levels in $Pax6^{sey/sey}$ (C). Ectopic expression of Gsh2 can also be seen in $Pax6^{sey/sey}$ embryos, with strongly labelled cells located dorsal to its normal boundary of expression (dashed red line in D). The new expression boundary is indicated by the dashed blue line. Ctx, cortex; lge, lateral ganglionic eminence; mge, medial ganglionic eminence. Scale bars: 100μm in A and C; 50μm in B and D

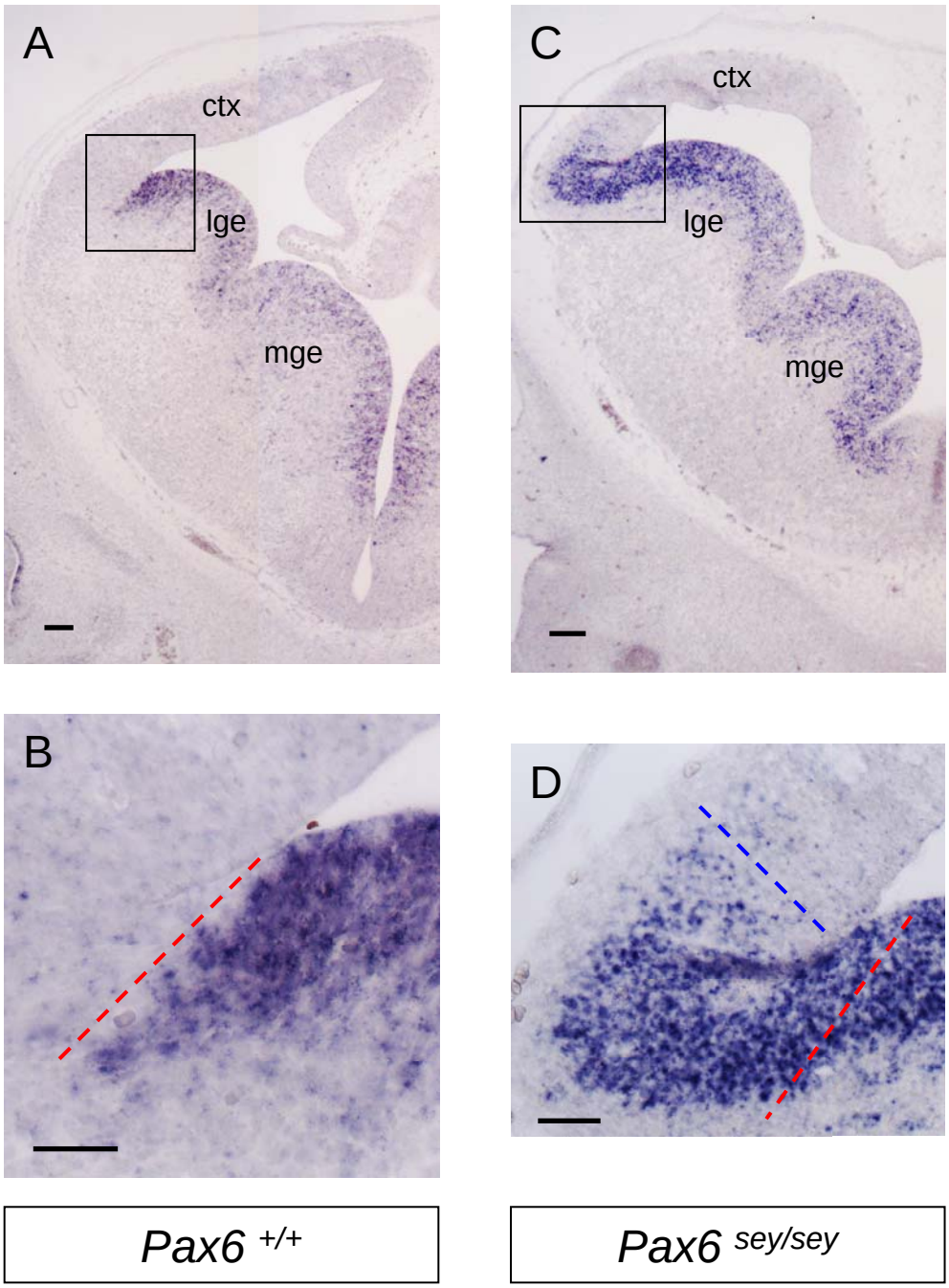

Figure 6.3

and is also ectopically expressed at high levels in VZ cells on the dorsal side of the PSPB (Fig. 6.3 C and D).

6.3 Discussion

The data presented here confirms the changes in expression of *Ngn2* and *Gsh2* measured by microarray at the PSPB in *Pax6*$^{sey/sey}$ compared to wildtype embryos. The down-regulation of *Ngn2*, and the dorsal retraction of its boundary of expression away from the PSPB in *Pax6*$^{sey/sey}$ embryos, is well documented (Toresson *et al.,* 2000; Stoykova *et al.,* 2000; Yun *et al.,* 2001; Heins *et al.,* 2002; Stenman *et al.,* 2003). The up-regulation of *Gsh2* and the expansion of its area of expression to include more dorsal regions in the absence of functional Pax6 are also in accordance with previously published data (Toresson *et al.,* 2000; Yun *et al.,* 2001; Stenman *et al.,* 2003).

While levels of *Lhx6* have been reported to be increased in *Pax6*$^{sey/sey}$ embryos (Stoykova *et al.,* 2000), that increase was not seen at the PSPB but in the MGE and extending into the LGE. Cells from the MGE would have been excluded from the samples investigated by microarray and so any increase in expression in these cells could not have been identified. The results shown here suggest that the large increase in *Lhx6* measured on the microarray is due to a small number of cells, expressing the gene at very high levels and located sufficiently close to the PSPB to have been included in the dissection. As *Lhx6* is not normally expressed in this region, the presence of even a few highly expressing cells in the sample would be sufficient to give a large fold change measurement.

These *Lhx6*-positive cells labelled close to the PSPB in *Pax6*$^{sey/sey}$ embryos lie in a region where the number of *Pax6* expressing cells is relatively small. It is important to determine if these cells do co-express *Pax6* and *Lhx6*. Double *in situ* hybridization for *Pax6* and *Lhx6* expression would allow confirmation that the *Lhx6* positive cells in this region also express *Pax6*. If this does not prove to be the case a possible explanation for the failure to remove these cells from the microarray samples during sorting could be the imperfect correlation between Pax6 and GFP

expression seen in the ventral telencephalon and described in chapter 3. Indeed analysis of Pax6 expression in cells sorted by FACS demonstrates that not all of the strongly GFP-positive cells, isolated by FACS for analysis by microarray, express Pax6, although they may have expressed it previously (Chapter 4, Fig. 4.6).

Chapter 7 – Discussion and Future Work

7.1 Review of the preceding chapters

This thesis has described the validation of the *DTy54* mouse line, a transgenic reporter line designed for the investigation of the role of *Pax6* during development. The GFP-reporter system has been shown here to accurately report the majority of Pax6 expression, although there are some discrepancies between Pax6 and GFP expression patterns, particularly at later stages of development, and it is important to consider these differences carefully when designing experiments using $DTy54^{+}$ animals. Two main issues, as described in chapter 3, were identified. Firstly, in some cells the protein half-life for tauGFP appears to be longer than for Pax6. This is most clearly seen in the cortex at E15.5. Secondly, there appears to be a difference in the regulation of expression from the transgene compared with the endogenous *Pax6* locus when *Pax6* is expressed in post-mitotic cells, as seen in the thalamus and ventral telencephalon.

The successful use of $DTy54^{+}$ animals to investigate the role of *Pax6* at the PSPB is described in chapters 4 and 5. TauGFP expression allowed the accurate dissection of the PSPB and the subsequent enrichment for the *Pax6* expressing population of cells in this region by FACS. Microarray analysis of RNA extracted from these cells, isolated from $Pax6^{+/+}.DTy54^{+}$ and $Pax6^{sey/sey}.DTy54^{+}$ embryos at E12.5, allowed the identification of genes that lie downstream of *Pax6* expression in this region of the telencephalon. Validation of the changes in gene expression that occur in the absence of functional Pax6, measured by microarray, for *Ngn2*, *Gsh2*, and *Lhx6* is described in chapter 6. *In situ* hybridization confirms the large down-regulation of *Ngn2* at the PSPB and the up-regulation of *Gsh2* and *Lhx6*.

Unfortunately, due to time constraints, I was unable to carry out a thorough validation of the microarray data. Work is currently being carried out by others to complete the validation experiments both by examining a larger number of candidate genes by *in situ* hybridization and by measuring the levels of expression of these genes at the PSPB by real time RT-PCR. These steps are particularly important

given the small number of biological replicates used for the microarray experiment (n=3 for each condition).

7.2 The role of *Pax6* at the PSPB

It is clear from the analysis of the genes that show a change in their expression at the PSPB in response to a loss of functional Pax6 that *Pax6* plays a variety of important roles in the development of this region of the telencephalon. An outline of the processes and molecular pathways influenced by *Pax6* expression is shown in figure 7.1. Some of the *Pax6*-regulated genes involved in these processes and their possible significance in terms of the development of the PSPB are discussed in detail below.

7.2.1 Neurogenesis

Pax6 is a strong promoter of neurogenesis and so the down regulation of this process in the absence of functional Pax6 is unsurprising. The action of *Pax6* in neurogenesis is mediated through a variety of transcription factors and their regulators. These genes are significantly over-represented in the down-regulated set of genes. Many of these transcription factors, including *Ngn2*, *Neurod1*, *Neurod2* and *Neurod6*, have been shown to be involved in nervous system development and in cell, and more specifically neuron, differentiation. *Neurod1* and *Neurod2* can cause premature differentiation of neuronal precursors when ectopically expressed in *Xenopus* embryos (Lee *et al.,* 1995; McCormick *et al.,* 1996). In these embryos *Neurod1* and *2* are also capable of converting ectoderm cells into neurons. *Neurod1*, *2*, and *6* are expressed in highly overlapping patterns in the developing CNS of rats (Schwab *et al.,* 1998). Analysis of *Neurod6*$^{-/-}$ mice however shows no obvious defects in neruonal development suggesting that *Neurod6* function may be largely compensated for by *Neurod1* and *2* (Schwab *et al.,* 1998).

Neurod1 has been shown to be required for the normal differentiation of granule cells in the cerebellum and hippocampus with these cells severely depleted in the absence of *Neurod1* (Miyata *et al.,* 1999). Mice lacking both *Neurod1* and *Neurod6* show a more severe hippocampal phenotype and although granule cell precursors are produced in these mice, these cells fail to undergo terminal differentiation (Schwab

Figure 7.1: Summary of the roles of *Pax6* at the PSPB

Pax6-regulated processes at the PSPB are outlined. Genes involved in the processes circled in red are over-represented among the genes down-regulated in response to a loss of Pax6 at the PSPB. Processes circled in blue on the other hand are over-represented in the set of genes up-regulated at the PSPB when Pax6 is lost. Dashed arrows indicate processes whose alteration may mediate, at least in part, the effect that loss of Pax6 has on another process. Some of the key regulated genes are also indicated.

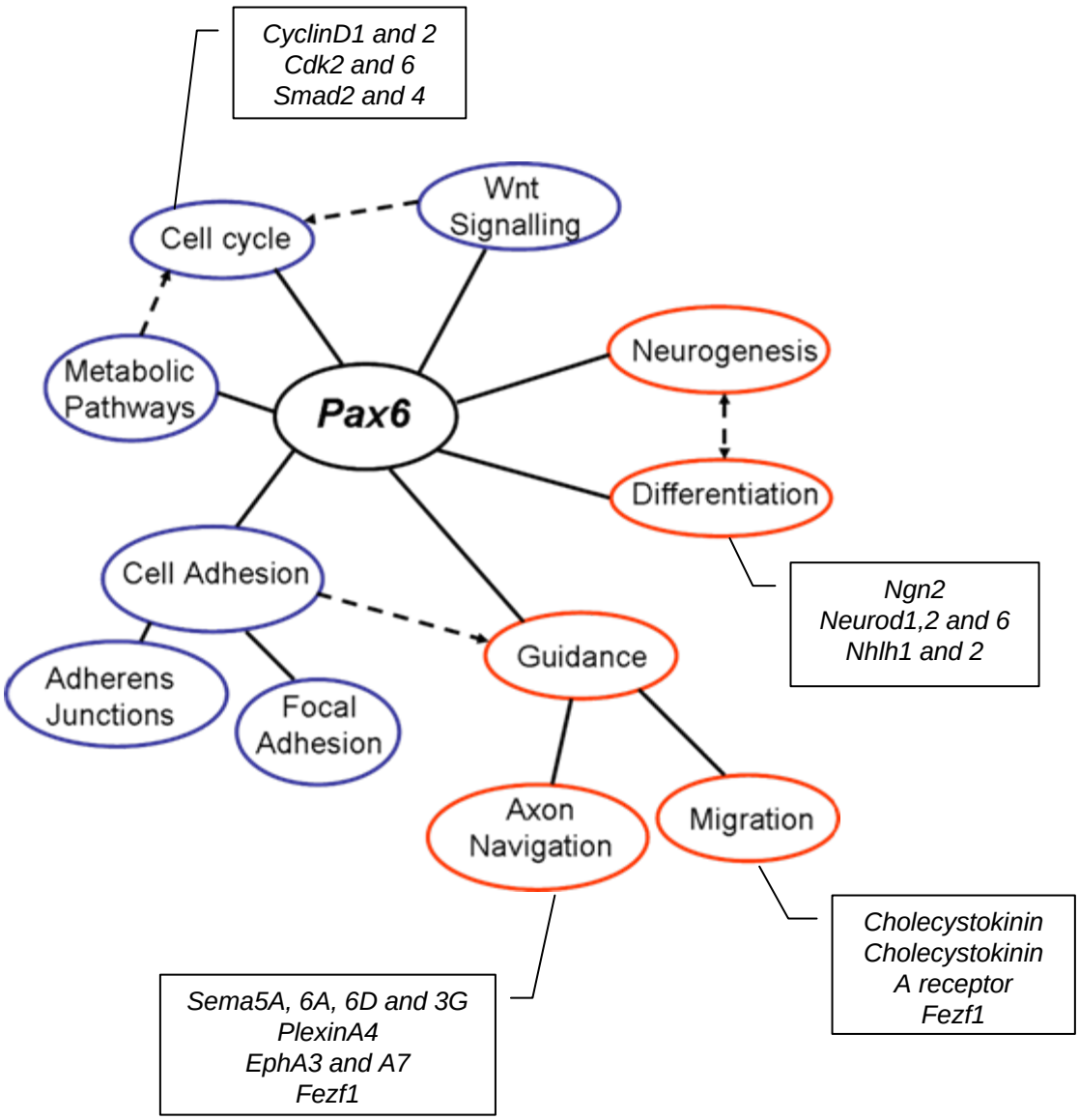
CyclinD1 and 2
Cdk2 and 6
Smad2 and 4
Wnt Signalling
Cell cycle
Metabolic Pathways
Pax6
Neurogenesis
Differentiation
Ngn2
Neurod1,2 and 6
Nhlh1 and 2
Cell Adhesion
Adherens Junctions
Focal Adhesion
Guidance
Axon Navigation
Migration
Cholecystokinin
Cholecystokinin A receptor
Fezf1
Sema5A, 6A, 6D and 3G
PlexinA4
EphA3 and A7
Fezf1

Figure 7.1

et al., 2000). *Neurod2*$^{-/-}$ mice develop normally until about postnatal day 14 (P14; Olson *et al.,* 2001). Analysis of *Neurod2*$^{-/-}$ mice aged between P14 and P21 found that brain areas where *Neurod2* is normally expressed showed higher rates of apoptosis and were smaller than in wildtype controls. The cerebella of these mutants also showed a decrease in expression of genes that support the survival of granule cells (Olson *et al.,* 2001). It is possible that many of the neurogenic roles of *Pax6* are mediated by *Ngn2* as the expression of *Neurod* family members has been shown to lie downstream of *Ngn2* expression (Mattar *et al.,* 2008).

7.2.2 Cell cycle

A range of processes involved in all aspects of the cell cycle are significantly over-represented in the genes up-regulated at the PSPB in *Pax6*$^{sey/sey}$ embryos. Genes involved in everything from DNA replication to chromosome condensation and the formation of the mitotic spindle are all present. It seems clear from the microarray data that the cell cycle is highly up-regulated at the PSPB in response to the loss of Pax6. Given that there is a concurrent down-regulation of genes with a role in differentiation it is likely that the dividing cells are undergoing self-renewal rather than dividing to produce neurons. An analysis of cell cycle kinetics in the E12.5 cortex by Quinn *et al.,* (2007) found no difference between wildtype and *Pax6*$^{sey/sey}$ embryos. This suggests that the up-regulation of cell cycle genes found in this study may be unique to the cells of the PSPB. Measurement of the cell cycle kinetics specifically at this boundary region would help clarify this.

7.2.2.1 Metabolic pathways

The over-representation of genes in the metabolic pathway "one carbon pool by folate", which is essential for the synthesis of the purines and pyrimidines necessary for DNA replication, identifies a novel mechanism by which *Pax6* may influence cell cycle kinetics. If *Pax6* normally represses the expression enzymes required in this pathway then DNA replication and hence cell division will be limited due to a decrease in the intercellular pools of nucleotides.

7.2.2.2 Wnt signalling

Analysis of the genes involved in the Wnt signalling pathway that are up-regulated at the PSPB in the absence of Pax6 suggests that this pathway may provide another means by which *Pax6* can regulate the cell cycle. Of the nine significantly up-regulated genes in this pathway, six of them have a role in the cell cycle (Fig. 7.2). Genes common to both the Wnt signalling pathway and the cell cycle also show large changes in their level of expression in *Pax6*$^{sey/sey}$ embryos with *Smad2*, *Lef1*, *CyclinD1* and *CyclinD2* all having fold changes greater than 2.

7.2.3 Axon guidance and cell migration

Members of the key axon guidance gene families are represented in the down-regulated geneset, including 2 Eph receptors (*EphA3*and *A7*), 4 members of the semaphorin family (*Sema5A*, *6A*, *6D* and *3G*), *Cxcl12*, *PlexinA4* and *Robo2*. Semaphorins comprise a large family of both secreted and transmembrane guidance molecules. Of the semaphorins that are down-regulated at the PSPB in the absence of Pax6, three code for transmembrane proteins while the fourth, *Sema3G*, produces a secreted molecule. Only one of the semaphorins identified in this experiment, *Sema5A*, has previously been reported to be down-regulated in *Pax6*$^{sey/sey}$ embryos (Jones *et al.,* 2002). The down-regulation of *PlexinA4* is also interesting in the context of this family of guidance molecules as it has been shown to mediate signalling by both secreted and transmembrane semaphorins (Suto *et al.,* 2005).

It is possible that some of these axon guidance molecules also play a role in the guidance of neuron migration. *Cxcl12*, for example, has been demonstrated to have a role in guiding migrating interneurons to their correct locations in the cortex (Tiveron *et al.,* 2006; Li *et al.,* 2008). *Sema6A* has also been shown to have a role in migration during development of the cerebellum where it initiates the radial migration of granule cells (Kerjan *et al.,* 2005). The behaviour of cerebellar granule cells is altered in *Pax6*$^{sey/sey}$ embryos (Swanson *et al.,* 2005) so it is possible that this phenotype is mediated in part by *Pax6* regulation of *Sema6A*.

Figure 7.2: Diagram of genes involved in the Wnt signalling pathway

The genes involved in the Wnt signalling pathway and their interactions with each other, as annotated in the KEGG database, are outlined here. Genes identified in this study as being significantly up-regulated in the absence of Pax6 are show in red. Image taken from the website of the KEGG database (www.genome.jp/kegg).

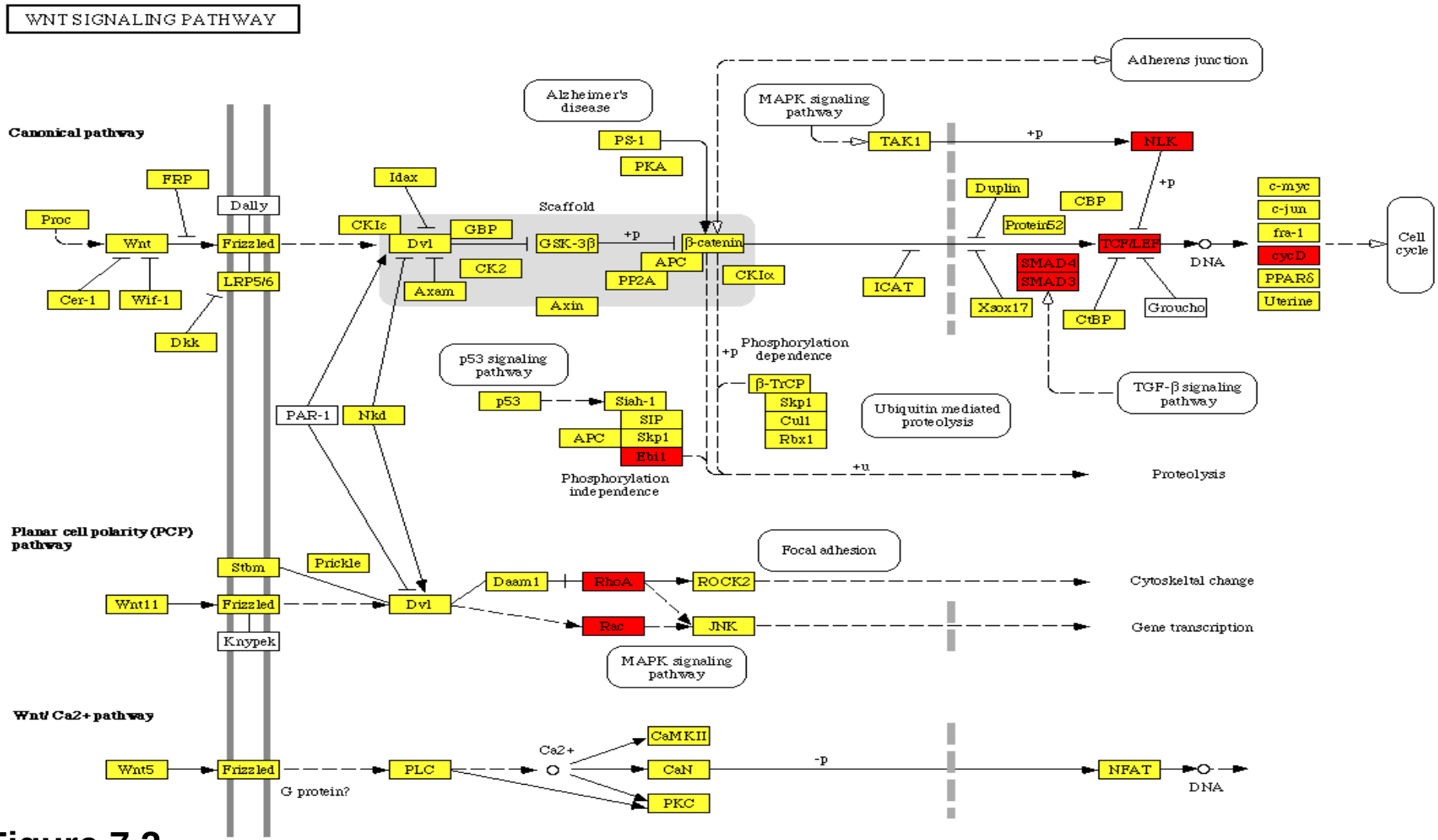
WNT SIGNALING PATHWAY
Canonical pathway
Planar cell polarity (PCP) pathway
Wnt/ Ca2+ pathway
Adherens junction
Alzheimer's disease
MAPK signaling pathway
PS-1
PKA
TAK1
NLK
FRP
Dally
Idax
Proc
Wnt
Frizzled
CKIε
Dvl
GBP
Scaffold
GSK-3β
β-catenin
APC
CK2
Axam
PP2A
Axin
CKIα
Duplin
CBP
Protein52
TCF/LEF
DNA
c-myc
c-jun
fra-1
cycD
PPARδ
Uterine
Cell cycle
LRP5/6
Cer-1
Wif-1
Dkk
ICAT
SMAD4
SMAD3
Xsox17
CtBP
Groucho
TGF-β signaling pathway
p53 signaling pathway
+p
Phosphorylation dependence
β-TrCP
Skp1
Cul1
Rbx1
Ubiquitin mediated proteolysis
p53
Siah-1
SIP
APC
Skp1
Ebi1
Phosphorylation independence
+u
Proteolysis
PAR-1
Nkd
Stbm
Prickle
Wnt11
Frizzled
Knypek
Dvl
Daam1
RhoA
ROCK2
Rac
JNK
Focal adhesion
Cytoskeltal change
Gene transcription
MAPK signaling pathway
Wnt5
Frizzled
G protein?
PLC
Ca2+
CaMKII
CaN
PKC
-p
NFAT
DNA

Figure 7.2

The down-regulation of semaphorins at the PSPB, whose expression in the developing telencephalon is as yet unreported, provides new insights into how *Pax6* may be regulating axon guidance in this region. A detailed analysis of the expression patterns of these genes in the telencephalon of both wildtype and *Pax6*$^{sey/sey}$ embryos is clearly warranted. Knowing how the expression of these genes changes in the absence of Pax6 will hopefully allow a deeper understanding of both the normal development of the axonal tracts of the forebrain and how this development can be disrupted. An investigation of the expression of the semaphorin receptor *PlexinA4* would also be useful in achieving this aim.

Pax6 is important in regulating both the radial migration of neurons to the cortical plate and the tangential migration of interneurons from the ganglionic eminences to the cortex (Schmahl *et al.,* 1993; Carić *et al.,* 1997; Chapouton *et al.,* 1999). An increase in the number of interneurons crossing the PSPB to enter the cortex in the absence of Pax6 has been reported (Chapouton *et al.,* 1999). Given this, one might expect to see an increase in the levels of expression of genes involved in migration in *Pax6*$^{sey/sey}$ embryos rather than the decrease measured in this study. It is possible, however, that as interneurons migrate in the intermediate and marginal zones to reach their final destinations that the genes guiding this migration were not identified in this study as the majority of post-mitotic cells were excluded from the population under investigation. There is also convincing evidence to suggest that the increase in the number of interneurons seen in *Pax6*$^{sey/sey}$ is due not to an increase in migration but to a respecification of progenitor cells at the PSPB to a more ventral fate resulting in the ectopic production of interneurons (Kroll and O'Leary, 2005). It seems likely therefore that the genes involved in migration that are down-regulated here may regulate either radial migration or the migration of cells from the PSPB to the amygdala along the lateral cortical stream (Carney *et al.,* 2006).

In spite of the confusion as to which cells are being affected in terms of migration by the changes in gene expression measured at the PSPB, this study does identify novel genes through which *Pax6* regulation of migration may be mediated. *Cholecystokinin* (*Cck*) and *cholecystokinin A receptor* (*Cckar*) were perhaps the most

surprising genes to be identified. Although there is a large body of literature on the role of *Cck* in the regulation of the neuroendocrine system and the regulation of food intake (for review see Chandra and Liddle, 2007; Valassi *et al.,* 2008), knowledge about its role during embryonic development of the forebrain is much more limited. A role for *Cck* and *Cckar* in the migration of gonadotrophin-releasing hormone-1 neurons has been reported (Giacobini *et al.,* 2004), however the expression of these genes in an area other than the neuroendocrine system suggests they may have a more general role in the regulation of migration during development and it would be interesting to investigate this further.

The zinc finger gene *Fezf1* is also down-regulated at the PSPB in response to a loss of Pax6 and has been shown to have a role in both migration and axon guidance in the developing brain (Hirata *et al.,* 2004; 2006a; Chen *et al.,* 2005). *Fezf1* homozygous mutants produce fewer thalamocortical axons and these do not project normally to the cortex (Hirata *et al.,* 2004). The projections from layer 5 cortical neurons also display axon targeting defects in these mice (Chen *et al.,* 2005), while in the developing olfactory bulbs defects in both axonal projections and the migration of interneuron precursors have been observed (Hirata *et al.,* 2006a). A role for *Fezf1* in boundary formation has also been demonstrated in the diencephalon where it helps to establish the zona limitans intrathalamica (Hirata *et al.,* 2006b). As the PSPB fails to form correctly in $Pax6^{sey/sey}$ embryos the identification of genes with a previously reported role in boundary formation warrants further investigation. Given its variety of roles in telencephalic development it is likely that the loss *Fezf1* may contribute to a number of aspects of the PSPB phenotype seen in $Pax6^{sey/sey}$ embryos.

7.2.3.1 Cell adhesion

It is possible that the up-regulation of genes with a role in the formation of adherens junctions and focal adhesions may contribute to the axon guidance phenotype seen in $Pax6^{sey/sey}$ embryos. Cells that form tighter intercellular connections may be more tightly packed and this could create a less permissive environment for axons to navigate through. Indeed the cells of the PSPB have been reported to be more tightly

packed in *Pax6*$^{sey/sey}$ compared to wildtype embryos at E15.5 and E18.5 (Jones *et al.,* 2002).

7.2.4 Framework for *Pax6* Function at the PSPB

The importance of maintaining the correct spatio-temoporal expression pattern of *Pax6* for the normal development of the telencephalon has been well established (Schmahl *et al.,* 1993; Carić *et al.,* 1997; Götz *et al.,* 1998; Estivill-Torrus *et al.,* 2002; Manuel *et al.,* 2007; Quinn *et al.,* 2007). During cortical neurogenesis *Pax6* helps to regulate the cell cycle kinetics of the cortical progenitor cells in which it is expressed, and these are altered by changes in the levels of Pax6 (Estivill-Torrus *et al.,* 2002; Manuel *et al.,* 2007; Quinn *et al.,* 2007). The orderly radial migration of newly born neurons also relies on Pax6 to maintain the normal morphology of the radial glial cells which guide the movement of these neurons to their correct locations in the cortical plate (Anton *et al.,* 1996; Carić *et al.,* 1997; Götz *et al.,* 1998). At the PSPB *Pax6* has been shown to act with *Gsh2* in a cross-repressive manner to establish a sharp boundary of gene expression separating the very different histogenetic fields of the dorsal and ventral telencephalon (Toresson *et al.,* 2000; Yun *et al*., 2001; Carney *et al.,* 2009). The breakdown of the regulation of axon guidance and cell migration has also been demonstrated at the PSPB in *Pax6*$^{sey/sey}$ embryos (Chapouton *et al.,* 1999; Pratt *et al.,* 2000; Hevner *et al.,* 2002; Jones *et al.,* 2002; Carney *et al.,* 2006). The microarray data presented in this thesis provides further evidence to support these roles for *Pax6* during neurogenesis while adding to the current body of literature by identifying novel targets for the *Pax6* regulation of these complicated processes. The role of *Pax6* as a high level transcription factor that acts via the regulation of a wide range of other transcription factors is also demonstrated by the large numbers of transcription factors present in both the up- and down-regulated gene sets.

An analysis of the microarray data generated in this study suggests that, at the PSPB, the predominant role of *Pax6* is to promote exit from the cell cycle and differentiation along a neural lineage. The loss of functional Pax6 results in massive up-regulation of genes involved in all aspects of the cell cycle with a concurrent

down-regulation of markers of differentiation and neurogenesis (a small subset of the cell cycle genes affected are shown in Fig. 5.15). This indicates that progenitor cells at the PSPB may continue to undergo self-renewal when they lack the neurogenic stimulus provided by *Pax6* expression. Further support of this is provided by the observed down-regulation of markers of the SVZ and early cortical plate such as *Tbr2*, *Neurod6* and *Lhx9* suggesting that there is an absence/reduction of progression of differentiation from VZ to SVZ and hence to a cortical plate identity when functional Pax6 is lost in these cells. As there is convincing evidence that the cell cycle kinetics of progenitor cells in the dorsal pallium of $Pax6^{sey/sey}$ embryos are unaltered at E12.5 (Quinn *et al.,* 2007), it is likely that this represents an action of *Pax6* that is specific to the distinct set of progenitors located adjacent to the PSPB at this stage.

It is clear from the significant changes in the expression of genes involved in axon guidance and cell migration that *Pax6* also contributes to the specialised nature of the PSPB as an important developmental boundary across which movement is tightly regulated. Both these developmental processes are over-represented in the down-regulated gene set. The concurrent over-representation of genes with a role in regulating cell adhesion in the up-regulated gene set is also of note in this context as the level of adhesion between cells can be important in providing a permissive environment through which to migrate/navigate. As this data was collected from E12.5 embryos it is likely that the contribution of guidance molecules is not as large as it might be at later stages as at this age interneurons are only beginning to cross the PSPB and the majority of axons have yet to reach the boundary. The over-representation of these biological processes at this early stage emphasise the important role played by *Pax6* in establishing the functional as well and the gene expression components of the PSPB. The down-regulation of genes involved in cell migration may also be contributed to by the reduction in differentiation to a neural fate with a concurrent decrease in migration away from the VZ towards the pial surface.

The data presented here demonstrates that *Pax6* is involved in a number of important processes at the PSPB. It seems likely however that at E12.5 the key role for *Pax6* in this region is to maintain the progression of VZ cells from self-renewal to the production of cells of a neural lineage by promoting cell cycle exit and neurogenesis.

7.3 Conclusion

This study has identified a number of novel *Pax6* target genes whose expression is altered at the PSPB in response to a loss of functional Pax6. The roles of these genes are such that they are likely to contribute to the PSPB phenotype seen in $Pax6^{sey/sey}$ embryos. Further analysis of these genes will help to elucidate how *Pax6* functions in establishing this important developmental boundary and how defects in the formation of the PSPB contribute to the errors in axon guidance and migration that are prominent components of the *Sey* phenotype.

References

Alifragis, P., Liapi, A. and Parnavelas, J. G. (2004). Lhx6 Regulated the Migration of Cortical Interneurons from the Ventral Telencephalon But Does Not Specify their GABA Phenotype. *J Neurosci* **24.** 5643-5648.

Anderson, S. A., Eisenstat, D. D., Shi, L. and Rubenstein, J. L. R. (1997). Interneuron migration from basal forebrain to neocortex: dependence on Dlx genes. *Science* **278.** 474-476.

Anderson, S. A., Marín, O., Horn, C., Jennings, K. and Rubenstein, J. L. R. (2001). Distinct cortical migrations from the medial and lateral ganglionic eminences. *Dev* **128.** 353-363.

Andrews G. L. and Mastick G. S. (2003) R-cadherin is a Pax6-regulated, growth-promoting cue for pioneer axons. J Neurosci. 23:9873-80

Angevine, J. B. and Sidman, R. L. (1961). Autoradiographic Study of Cell Migration during Histogenesis of Cerebral Cortex in the Mouse. *Nature* **192.** 766-768.

Anton, E. S., Cameron, R. S. and Rakic, P. (1996). Role of Neuron-Glial Junctional Domain Proteins in the Maintenance and Termination of Neuronal Migration across the Embryonic Cerebral Wall. *J Neurosci* **16.** 2283-2293.

Arai, Y., Funatsu, N., Numayama-Tsuruta, K., Nomura, T., Nakamura, S and Osumi, N. (2005). Role of Fabp7, a downstream gene of Pax6, in the maintenance of neuroepithelial cells during early embryonic development of the rat cortex. *J Neurosci* **25.** 9752-9761.

Ashfield R., Enriquez-Harris, P. and Proudfoot, N. J. (1991). Transcriptional termination between the closely linked human complement genes C2 and Factor B: common termination factor for C2 and c-myc? *EMBO* **10.** 4197-4207.

Ashfield, R., Patel, A. J., Bossone, S. A., Brown, H., Campbell, R. D., Marcu, K. B. and Proudfoot, N. J. (1994). MAZ-dependent termination between closely spaced human complement genes. *EMBO* **13.** 5656-5667.

Assimacopoulos, S., Grove, E. A. and Ragsdale, C. W. (2003). Identification of a *Pax6*-Dependent Epidermal Growth Factor Family Sgnaling Source at the Lateral Edge of the Embryonic Cerebral Cortex. *J Neurosci* **23.** 6399-6403.

Bamiou, D.-E., Musiek, F. E., Sisodiya, S. M., Free, S. L., Davies,R. A., Moore,

A., van Heyningen, V. and Luxon, L. M. (2004) Deficient Auditory Interhemispheric Transfer in Patients with *PAX6* Mutations. *Ann Neurol* **56.** 503-509.

Benjamini, Y. and Hochberg, Y. (1995). Controlling the False Discovery Rate: a Practical and Powerful Approach to Multiple Testing. *J R Statist Soc* **57.** 289-300.

Bishop, K. M., Goudreau, G. and O'Leary, D. D. M. (2000). Regulation of Area Identity in the Mammalian Neocortex by Emx2 and Pax6. *Science* **288.** 344-349.

Bishop K. M., Rubenstein, J. L. R. and O'Leary, D. D. M. (2002). Distinct Actions of Emx1, Emx2, and Pax6 in Regulating the Specification of Areas in the Developing Neocortex. *J Neurosci* **22.** 7627-7638.

Bopp, D., Burri, M., Baumgartner, S., Frigerio, G. and Noll, M. (1986). Conservation of a Large Protein Domain in the Segmentation Gene *paired* and in Functionally Related Genes of Drosophila. *Cell* **47.** 1033-1040.

Bopp, D., Jamet, E., Baumgartner, S., Burri, M., Noll, M. (1989). Isolation of two tissue specific Drosophila paired box genes, Pox meso and Pox neuro. *EMBO J* **8.** 3447-3457.

Braisted, J. E., Tuttle, R. and O'Leary, D. D. M. (1999). Thalamocortical Axons Are Influenced by Chemorepellent and Chemoattractant Activities localized to Decision Points along Their Path. *Dev Biol* **208.** 430-440.

Brunjes, P. C., Fisher, M. and Grainger, R. (1998). The small-eye mutation results in abnormalities in the lateral cortical migratory stream. *Dev Brain Res* **110.** 121-125.

Bulfone, A., Puelles, L., Porteus, M. H., Frohman, M. A., Martin, G. R. and Rubenstein, J. L. (1993). Spatially restricted expression of Dlx-1, Dlx-2 (Tes-), Gbx-2, and Wnt-3 in the embryonic day 12.5 mouse forebrain defines potential transverse and longitudinal segmental boundaries. *J Neurosci* **13.** 3155-3172.

Callaerts, P., Halder, G. and Gehring, W. J. (1997). PAX-6 in development and evolution. *Annu Rev Neurosci* **20.** 483-532.

Campbell, K. (2003). Dorsal-ventral patterning in the mammalian telencephalon. *Curr Opin Neurobiol* **13.** 50-56.

Carić D., Gooday, D., Hill, R. E., McConnell, S. K. and Price D. J. (1997). Determination of the migratory capacity of embryonic cortical cells lacking the transcription factor Pax-6. *Development* **124.** 5087-5096.

Carney, R. S. E., Alfonso, T. B., Cohen, D., Dai, H., Nery, S., Stoica, B., Slotkin, J. Bregman, B. S., Fishell, G. and Corbin, J. G. (2006). Cell Migration along the Lateral Cortical Stream to the Developing Basal Telencephalic Limbic System. *J Neurosci* **26.** 11562-11574.

Carney, R. S. E., Cocas, L. A., Hirata, T., Mansfield, K. and Corbin, J. G. (2009). Differential Regulation of Telencephalic Pallial-Subpallial Boundary Patterning by *Pax6* and *Gsh2*. *Cerebral Cortex* **19.** 745-759.

Caubit X, Tiveron MC, Cremer H, Fasano L. (2005). Expression patterns of the three Teashirt-related genes define specific boundaries in the developing and postnatal mouse forebrain. *J Comp Neurol* **486.** 76-88.

Chandra, R. and Liddle, R. A. (2007). Cholecystokinin. *Curr Opin Endocrinol Diabetes Obes* **14.** 63-67.

Chapouton, P., Gärtner, A. and Götz, M. (1999). The role of Pax6 in restricting cell migration between developing cortex and basal ganglia. *Development* **126.** 5569-5579.

Chen, J.-G., Rašin, M.-R., Kwan, K. Y. and Šestan, N. (2005). Zfp312 is required for subcortical axonal projections and dendritic morphology of deep-layer pyramidal neurons of the cerebral cortex. *PNAS* **102.** 17792-17797.

Chuaqui, R. F., Bonner, R. F., Best, C. J., Gillespie, J. W., Flaig, M. J., Hewitt, S. M., Phillips, J. L., Krizman, D. B., Tangrea, M. A., Ahram, M. Linehan, W. M., Knezevic, V. and Emmert-Buck, M. R. (2002). Post-analysis follow-up and validation of microarray experiments. *Nat Genet* **32.** Suppl:509-514.

Cleveland, W. S. (1979). Robust Locally Weighted Regression and Smoothing Scatterplots. *J American Stat Assoc* **74.** 829-836.

Davis, J., Duncan, M. K., Robison, W. G. Jr. and Piatigorsky, J. (2003). Requirement for Pax6 in corneal morphogenesis: a role in adhesion. *J Cell Sci* **116.** 2157-2167.

De Carlos, J. A., López-Mascaraque, L. and Valverde F. (1996). Dynamics of Cell Migration from the Lateral Ganglionic Eminence in the Rat. *J Neurosci* **16.** 6146-6156.

Deng, D. R., Djalais, S., Höltje, M., Grosse, G., Stroh, T., Voigt, I., Kusserow, H., Theuring, F., Ahnert-Hilger, G. and Hörtnagl, H. (2007). Embryonic and postnatal development of the serotonergic raphe system and its target regions in the 5-HT1A receptor deletion of overexpressing mouse mutants. *Neurosci* **147.** 388-402.

Deuel, T. A. S., Liu, J. S., Corbo, J. C., Yoo, S.-Y., Rorke-Adams, L. B. and Walsh, C. A. (2006). Genetic Interactions between Doublecortin and Doublecortin-like Kinase in Neuronal Migration and Axon Outgrowth. *Neuron* **49.** 41-53.

Deutsch, U., Dressler, G. R., and Gruss, P. (1988). *Pax 1*, A Member of a Paired Box Homologous Murine Gene Family, Is Expressed in Segmented Structures during Development. *Cell* **53.** 617-625.

Dominy, F., Eller, S. and Dawson, R. Jr. (2004). Building Biosynthetic Schools: Reviewing Compartmentation of CNS Taurine Synthesis. *Neurochem Res* **29.** 97-103.

Duparc RH, Boutemmine D, Champagne MP, Tétreault N, Bernier G. (2006). Pax6 is required for delta-catenin/neurojugin expression during retinal, cerebellar and cortical development in mice. *Dev Biol* **300.** 647-655.

Easter, S. S. Jr., Ross, L. S. and Frankfurter, A. (1993). Initial Tract Formation in the Mouse Brain. *J Neurosci* **13.** 285-299.

Edwards, D. (2003). Non-linear normalization and background correction in one-channel cDNA microarray studies. *Bioinformatics* **19.** 825-833.

Efron, B. and Tibshirani, R. (2002). Empirical Bayes Methods and False Discovery Rates for Microarrays. *Genetic Epidemiology* **23.** 70-86.

Elvidge, G. (2006). Microarray expression technology: from start to finish. *Pharmacogenomics* **7.** 123-134.

Engelkamp, D., Rashbass, P, Seawright, A. and van Heyningen, V. (1999). Role of *Pax6* in development of the cerebellar system. *Development* **126.** 3585-3595.

Ericson, J., Muhr, J., Jessell, T. M. and Edlund, T. (1995). *Sonic hedgehog*: a common signal for ventral patterning along the rostrocaudal axis of the neural tube. *Int J Dev Biol* **39.** 809-816.

Estivill-Torrús, G., Vitalis, T., Fernández-Llebrez, P. and Price, D. J. (2001). The transcription factor Pax6 is required for development of the diencephalic dorsal midline secretory radial glia that form the subcommissural organ. *Mech Dev* **109.** 215-224.

Estivill-Torrus, G., Pearson, H., van Heyningen, V., Price, D. J., and Rashbass, P. (2002). Pax6 is required to regulate the cell cycle and the rate of progression from symmetrical to asymmetrical division in mammalian cortical progenitors. *Development* **129.** 455-466.

Faedo, A., Quinn, J. C., Stoney, P., Long, J. E., Dye, C., Zollo, M. Ruenstein, J. L. R., Price, D. J. and Bulfone, A. (2004). Identification and Characterization of a Novel Transcript Down-Regulated in Dlx1/Dlx2 and Up-Regulated in Pax6 Mutant Telencephalon. *Dev Dyn* **231.** 614-620.

Fernandes, M., Gutin, G., Alcorn, H., McConnell, S. K. and Hébert, J. M. (2007). Mutations in the BMP pathway in mice support the existence of two molecular classes of holoprosencephaly. *Dev* **134.** 3789-3794.

Fotaki, V., Yu, T., Zaki P. A., Mason, J. O. and Price, D. J. (2006). Abnormal Positioning of Diencephalic Cell Types in Neocortical Tissue in the Dorsal Telencephalon of Mice Lacking Functional Gli3. *J Neurosci* **26.** 9282-9292.

Friocourt, G., Liu, J. S., Antypa, M., Rakić, S., Walsh, C. A. and Parnavelas, J. G. (2007). Both Doublecortin and Doublecortin-Like Kinase Play a Role in Cortical Interneuron Migration. *J Neurosci* **27.** 3875-3883.

Fuccillo, M., Rallu, M., McMahon, A. P. and Fishell, G. (2004). Temporal requirement for hedgehog signaling in ventral telencephalic patterning. *Development* **131.** 5031-5040.

Fukuchi-Shimogori, T. and Grove, E. A. (2001). Neocoretx Patterning by the Secreted Signaling Molecule FGF8. *Science* **294.** 1071-1074.

Furuta, Q., Piston, D. W. and Hogan, B. L. M. (1997). Bone morphogenetic proteins (BMPs) as regulators of dorsal forebrain development. *Dev* **124.** 2203-2212.

Galindo-Mireles, D., Meyer, G., Castañeyra-Perdomo, A. and Ferres-Torres, R. (1985). Cortical projections of the nucleus centralis superior and the adjacent reticular tegmentum in the mouse. *Brain Res* **330.** 343-348.

Giacobini, P., Kopin, A. S., Beart, P. M., Mercer, L. D., Fasolo, A. and Wray, S. (2004). Cholecystokinin modulated migration of gonadotropin- releasing hormone-1 neurons. *J Neurosci* **24.** 4737-4748.

Glaser, T., Lane, J. and Housman, D. (1990). A Mouse Model of the Aniridia-Wilms Tumor Deletion Syndrome. *Science* **250.** 823-827.

Götz, M., Stoykova, A. and Gruss, P. (1998). *Pax6* controls radial glia differentiation in the cerebral cortex. *Neuron* **21**, pp. 1031–1044.

Gradwhol, G., Fode, C. and Guillemot, F. (1996). Restricted expression of a novel murine atonal-related bHLH protein in undifferentiated neural precursors. *Dev Biol* **180.** 227-241.

Green, R. A., Wollman, R., Kaplan, K. B. (2005). APC and EB1 function together in mitosis to regulate spindle dynamics and chromosome alignment. *Mol Biol Cell* **16.** 4609-1622.

Grindley, J. C., Davidson, D. R. and Hill, R. E. (1995). The role of Pax-6 in eye and nasal development. *Development* **121.** 1433-1442.

Grindley, JC, Hargett, LK, Hill, RE, Ross, A., and Hogan BLM (1997). Disruption of Pax6 function in mice homozygous for the *Pax6*$^{Sey\text{-}Neu}$ mutation produces abnormalities in the early development and regionalization of the diencephalon. Mech. Devel., 64, 111-126

Grove, E. A., Tole, S., Limon, J., Yip, L. and Ragsdale, C. W. (1998). The hem of the embryonic cerebral cortex is defined by the expression of multiple *Wnt* genes and is compromised in *Gli3*-deficient mice. *Development* **125.** 2315-2325.

Guillemot, F. and Joyner, A. L. (1993). Dynamic expression of the murine Achaete-Scute homologue Mash-1 in the developing nervous system. *Mech Dev* **42.** 171-185.

Hallonet M, Hollemann T, Wehr R, Jenkins NA, Copeland NG, Pieler T, Gruss P. (1998). Vax1 is a novel homeobox-containing gene expressed in the developing anterior ventral forebrain. *Dev* **125.** 2599-2610.

Hébert, J. M., Mishina, Y. and McConnell, S. K. (2002). BMP Signaling Is Required Locally to Pattern the Dorsal Telencephalic Midline. *Neuron* **35.** 1029-1041.

Heins, N., Malatesta, P. Cecconi, F., Nakafuku, M., Tucker, K. L., Hack, M. A., Chapouton, P., Barde, Y., and Götz, M. (2002). Glial cells ineverate neurons: the role of the transcription factor Pax6. *Nature Neurosci* **5.** 308-315.

Hevner RF, Miyashita-Lin E, Rubenstein JL. (2002) Cortical and thalamic axon pathfinding defects in Tbr1, Gbx2, and Pax6 mutant mice: evidence that cortical and thalamic axons interact and guide each other. J Comp Neurol. 447:8-17.

Hill, R. E., Favor, J., Hogan, B. L., Ton, C. C., Saunders, G. F., Hanson, I. M., Prosser, J., Jordan, T., Hastie, N. D. and van Heyningen, V. (1991). Mouse small eye results from mutations in a paried-like homeobox-containing gene. *Nature* **354.** 522-525.

Hirata, T., Suda, Y., Nakao, K., Narimatsu, M., Hirano, T. and Hibi, M. (2004). Zinc finger gene fez-like functions in the formation of subplate neurons and thalamocortical axons. *Dev Dyn* **230.** 546-556.

Hirata, T., Nakazawa, M., Yoshihara, S., Miyachi, H., Kitamura, K., Yoshihara, Y. and Hibi, M. (2006a). Zinc-finger gene Fez in the olfactory sensory neurons regulates development of the olfactory bulb non-cell-autonomously. *Dev* **133.** 1433-1443.

Hirata, T., Nakazawa, M., Muraoka, O., Nakayama, R., Suda, Y. and Hibi, M. (2006b). Zinc-finger genes Fez and Fez-like function in the establishment of diencephalon subdivisions. *Dev* **133.** 3993-4004.

Hofmann, I., Thompson, A., Sanderson, C. M. and Munro, S. (2007). The Arl4 family of small G proteins can recruit the cytohesin Arf6 exchange factors to the plasma membrane. *Curr Biol* **17.** 711-716.

Hogan, B. L., Horsburgh, G., Cohen, J., Hetherington, C. M., Fisher, G. and Lyon M. F. (1986). Small eyes (Sey): a homozygous lethal mutation on chromosome 2 which affects the differentiation of both lens and nasal placodes in the mouse. *J Embryol Exp Morphol* **97.** 95-110.

Hogan, B. L., Hirst E. M., Horsburgh, G., Hetherington, C. M. (1988). Small eye (Sey): a mouse model for the genetic analysis of craniofacial abnormalities. *Development* **103.** Suppl: 115-119.

Holcman, D., Kasatkin, V. and Prochiantz, A. (2007). Modeling homeoprotein intercellular transfer unveils a parsimonious mechanism for gradient and boundary formation in early brain development. *J Theoretical Biol* **249.** 503-517.

Holm, P. C., Mader, M. T., Haubst, N., Wizenmann, A., Sigvardsson, M. and Götz, M. (2007). Loss- and gain-of-function analyses reveal targets of Pax6 in the developing mouse telencephalon. *Mol Cell Neurosci* **34.** 99-119.

Hornung, J.-P. (2003). The human raphe nuclei and the serotonergic system. *J Chem Neuroanat* **26.** 331-343.

Inoue, T., Tanaka, T., Takeichi, M., Chisala, O., Nakamura, S. and Osumi, N. (2001). Role of cadherins in maintaining the compartment boundary between the cortex and striatum during development. *Development* **128.** 561-569.

James, S. J., Miller, B. J., Cross, D. R., McGarrity, L. J. and Morris, S. M. (1993). The essentiality of folate for the maintenance of deoxynucleotide precursor pools, DNA synthesis, and cell cycle progression in PHA-stimulated lymphocytes. *Environ Health Perspect* **101.** Suppl 5: 173-178.

Jiménez, D., López-Mascaraque, L., De Carlos, J. A. and Valverde, F. (2002). Further studies on cortical tangential migration in wild type and Pax-6 mutant mice. *J Neurocytology* **31.** 719-728.

Joliot, A., Trembleau, A., Raposo, G., Calvet, S., Volovitch, M. and Prochiantz, A. (1997). Association of Engrailed homeoproteins with vesicles presenting caviolae-like properties. *Dev* **124.** 1865-1875.

Joliot, A., Maizel, A., Rosenberg, D., Trembleau, A., Dupas, S., Volovitch, M. and Prochiantz, A. (1998). Identification of a signal sequence necessary for the unconventional secretion of Engrailed homeoprotein. *Curr Biol* **8.** 856-863.

Jones, L., López-Bendito, G., Gruss, P., Stoykova, A. and Molnár, Z. (2002). *Pax6* id required for the normal development of the forebrain axonal connections. *Development* **129.** 5041-5052.

Jun, S., and Desplan, C. (1996). Cooperative interactions between paired domain and homeodomain. *Development* **122.** 2639-2650.

Kamme, F., Salunga, R., Yu, J., Tran, D. T., Zhu, J., Lou, L., Bittner, A., Guo, H. Q., Miller, N., Wan, J. and Erlander, M. (2003). Single-cell microarray analysis in hippocampus CA1: demonstration and validation of cellular heterogeneity. *J Neurosci* **23.** 3607-3615.

Kawano, H., Fukuda T, Kubo K, Horie M, Uyemura K, Takeuchi K, Osumi N, Eto K, Kawamura K. (1999) Pax-6 is required for thalamocortical pathway formation in fetal rats. *J Comp Neurol* **408.** 147-160.

Kerjan, G., Dolan, J., Haumaitre, C., Schneider-Maunoury, S., Fujisawa, H., Mitchell, K. J. and Chédotal, A. (2005). The transmembrane semaphorin Sema6A controls cerebellar granule cell migration. *Nat Neurosci* **11.** 1516-1524.

Kim, A. S., Anderson, S. A., Rubenstein J. L. R., Lowenstein, D. H. and Pleasure, S. J. (2001). Pax-6 regulates expression of SFRP-2 and Wnt-7b in the developing CNS. *J Neurosci* **21.** RC132

Kim, J. and Lauderdale, J. D. (2006). Analysis of Pax6 expression using a BAC transgene reveals the presence of a paired-less isoform of Pax6 in the eye and olfactory bulb. *Dev Biol* **292.** 486-505.

Kleinjan, D. A., Seawright, A., Childs, A. J. and van Heyningen, V. (2004). Conserved elements in Pax6 intron 7 involved in (auto)regulation and alternative transcription. *Dev Biol* **265.** 462-477.

Kleinjan, D. A., Seawright, A., Mella, S., Carr, C. B., Tyas, D. A., Simpson, T. I., Mason, J. O., Price, D. J. and van Heyningen, V. (2006). Long-range downstream enhancers are essential for Pax6 expression. *Dev Biol* **299.** 563-581.

Koizumi, H., Tanaka, T. and Gleeson J. G. (2006). *Doublecortin-like kinase* Functions with *doublecortin* to Mediate Fiber Tract Decussation and Neuronal Migration. *Neuron* **49.** 55-66.

Kroll, T.T. and O'Leary, D.D. (2005). Ventralized dorsal telencephalic progenitors in Pax6 mutant mice generate GABA interneurons of a lateral ganglionic eminence fate. *Proc. Natl. Acad. Sci. U. S. A.* **102**. 7374–7379.

Kuschel, S., Rüther, U. and Theil, T. (2003). A disrupted balance between Bmp/Wnt and Fgf signalling underlies the ventralization of the *Gli3* mutant telencephalon. *Dev Biol* **260.** 484-495.

Landsberg, R. L., Awatramani, R. B., Hunter, N. L., Farago, A. F.,

DiPietrantonio, H. J., Rodriguez, C. I. and Dymecki, S. M. (2005). Hindbrain Rhombic Lip is Comprised of Discrete Progenitor Cell Populations Allocated by Pax6. *Neuron* **48.** 933-947.

Lang, D., Powell, S. K., Plummer, R. S., Young, K. P. and Ruggeri, B. A. (2007). PAX genes: Roles in development, pathophysiology and cancer. *Biochem Pharmacol* **73.** 1-14.

Lee, J. E., Hollenberg, S. M., Snider, L., Turner, D. L., Lipnick, N. and Weintraub, H. (1995). Conversion of *Xenopus* Ectoderm into Neurons by NeuroD, a Basic Helix-Loop-Helix Protein. *Science* **268.** 836-844.

Lee, S. M. K., Tole, S., Grove, E. and McMahon, A. P. (2000). A local Wnt-3a signal is required for development of the mammalian hippocampus. *Dev* **127.** 457-467.

Levers, T. E., Edgar, J. M. and Price, D. J. (2001). The Fates of Cells Generated at the End of Neurogenesis in Developing Mouse Cortex. *J Neurobiol* **48.** 265-277.

Li, J., Pankratz, M. and Johnson, J. (2002). Differential gene expression patterns revealed by oligonucleotide versus long cDNA arrays. *Toxicol Sci* **69.** 383-390.

Li, G., Adesnik, H., Li, J., Long, J., Nicoll, R. A., Rubenstein, J. L. R. and Pleasure, S. J. (2008). Regional Distribution of Cortical Interneurons and Development of Inhibitiory Tone Are Regulated by Cxcl12/Cxcr4 Signaling. *J Neurosci* **30.** 1085-1098.

Liang, P. and Pardee, A. B. (1992). Differential Display of Eukaryotic Messenger RNA by Means of the Polymerase Chain Reaction. *Science* **257.** 967-970.

Liodis, P, Denaxa, M., Grigoriou, M., Akufo-Addo, C., Yanagawa, Y. and Pachnis, V. (2007). *Lhx6* Activity Is Required for the Normal Migration and specification of Cortical Interneuron Subtypes. *J Neurosci* **27.** 3078-3089.

Lipshutz, R. J., Fodor, S. P. A., Gingeras, T. R. and Lockhart, D. J. (1999). High density synthetic oligonucleotide arrays. *Nature Genet (Suppl)* **21.** 20-24.

Luo, Z. and Geschwind, D. H. (2001). Microarray Applications in Neuroscience. *Neuorbiol Disease* **8.** 183-193.

Machon, O., Backman, M., Machonova, O., Kozmik, Z., Vacik, T., Andersen, L. and Krauss, S. (2007). A dynamic gradient of Wnt signaling controls initiation of

neurogenesis in the mammalian cortex and cellular specification in the hippocampus. *Dev Biol* **311.** 223-237.

Maizel, A. Bensaude, O., Prochiantz, A. and Joliot, A. (1999). A short region of its homeodomain is necessary for Engrailed nuclear export and secretion. *Dev* **126.** 3183-3190.

Maizel, A., Tassetto, M., Filhol, O., Cochet, C., Prochiantz, A. and Joliot, A. (2002). Engrailed homeoprotein secretion is a regulated process. *Dev* **129.** 3545-3553.

Manuel, M. and Price, D. J. (2005). Role of Pax6 in forebrain regionalization. *Brain Res Bull* **66.** 387-393.

Manuel, M., Georgala, P.A., Carr, C.B., Chanas, S., Kleinjan, D.A., Martynoga, B. Mason, J.O., Molinek, M., Pinson, J., Pratt, T., Quinn, J.C., Simpson, T.I., van Heyningen, V., West, J.D and Price, D.J. (2007). Controlled overexpression of Pax6 in vivo negatively autoregulates the Pax6 locus, causing cell-autonomous defects of late cortical progenitor proliferation with little effect on cortical arealization. *Dev* **134.** 545-555.

MAQC Consortium (2006). The MicroArray Quality Control (MAQC) project shows inter- and intraplatform reproducibility of gene expression measurements. *Nat Biotech* **24.** 1151-1161.

Marin-Padilla, M. (1978). Dual Origin of the Mammalian Neocortex and Evolution of the Cortical Plate. *Anat. Embryol.* **152.** 109-126.

Marsh, E. D., Minarcik, J., Campbell, K., Brooks-Kayal, A. R. and Golden, J. A. (2008). FACS-Array Gene Expression Analysis During Early Development of Mouse Telencephalic Interneurons. *Develop Neurobiol* **68.** 434-445.

Mastick, G. S., Davis, N. M., Andrews, G. L. and Easter, S. S. Jr. (1997). Pax-6 functions in boundary formation and axon guidance in the embryonic mouse forebrain. *Development* **124.** 1985-1997.

Matsunaga, E, Araki, I. and Nakamura, H. (2000). Pax6 defines the di-mesencephalic boundary by repressing En1 and Pax2. *Dev* **127.** 2357-2365.

Matsunami, H. and Takeichi, M. (1995). Fetal brain subdivisions defined by R- and E-cadherin expressions: evidence for the role of cadherin activity in region-specific, cell-cell adhesion. *Dev Biol* **172.** 466-478.

McCormick, M. B., Tamimi, R. M., Snider, L., Asakura, A., Bergstrom, D. and Tapscott, S. J. (1996). *neuroD2* and *neuroD3*: Distinct Expression Patterns and Transcriptional Activation Potentials within the *neuroD* Gene Family. *Mol Cell Biol* **16.** 5792-5800.

McWhirter, J. R., Goulding, M., Weiner, J. A., Chun, J. and Murre, C. (1997). A novel fibroblast growth factor gene expressed in the developing nervous system is a downstream target of the chimeric homeodomain oncoprotein E2A-Pbx1. *Dev* **124.** 3221-3232.

Medina, L., Legaz, I., Gonza'lez, G., De Castro, F., Rubenstein, J. L. R. and Puelles, L. (2004). Expression of *Dbx1*, *Neurogenin 2*, *Semaphorin 5A*, *Cadherin 8*, and *Emx1* Distinguish Ventral and Lateral Pallial Histogenetic Divisions in the Developing Mouse Claustroamygdaloid Complex. *J Comp Neurol* **474.** 504-523.

Mitchell, T. N., Free, S. L., Williamson, K. A., Stevens, J. M., Churchill, A. J., Hanson, I. M., Shorvon S. D., Moore, A. T., van Heyningen, V. and Sisodiya, S. M. (2003). Polymicrogyria and Absence of Pineal Gland Due to *PAX6* Mutation. *Ann Neurol* **53.** 658-663.

Miyata, T., Maeda, T. and Lee, J. E. (1999). NeuroD is required for differentiation of the granule cells in the cerebellum and hippocampus. *Genes Dev* **13.** 1647-1652.

Miyata, T., Kawaguchi1, A., Saito, K., Kawano1, M., Muto T. and Ogawa, M. (2004). Asymmetric production of surface-dividing and non-surface dividing cortical progenitor cells. *Dev* **131.** 3133-3145.

Monuki, E. S., Porter, F. D. and Walsh C. A. (2001). Patterning of the dorsal Telencephalon and Cerebral Cortex by a Roof Plate-Lhx2 Pathway. *Neuron* **32.** 591-604.

Morris, C. M. and Wilson, K. E. (2004). High throughput approaches in neuroscience. *Int J Devl Neurosci* **22.** 515-522.

Muzio, L., DiBenedetto, B., Stoykova, A., Boncinelli, E., Gruss, P. and Mallamaci, A. (2002). Emx2 and Pax6 Control Regionalisation of the Pre-neuronogenic Cortical Primordium. *Cerebral Cortex* **12.** 129-139.

Nadarajah, B., Brunstrom, J. E., Grutzendler, J. Wong, R. O. and Pearlman A. L. (2001). Two modes of radial migration in early development of the cerebral cortex. *Nat Neurosci* **4.** 143-150.

Neyt, C., Welch, M., Langston, A., Kohtz, J. and Fishell, G. (1997). A Short-Range Signal Restricts Cell Movement between Telencephalic Proliferative Zones. *J Neurosci* **17.** 9194-9203.

Noctor, S. C., Flint, A. C., Weissman, T. A., Dammerman, R. S. and Kriegstein, A. R. (2001). Neurons derived from radial glial cells establish radial units in neocortex. *Nature* **409.** 714-719.

Noctor, S. C., Flint, A. C., Weissman, T. A., Wong, W. S., Clinton, B. K. and Kriegstein, A. R. (2002). Dividing Precursor Cells of the Embryonic Cortical Ventricular Zone have Morphological and Molecular Characteristics of Radial Glia. *J Neurosci* **22.** 3161-3173.

Noctor, S. C., Martínez-Cerdeno, V., Ivic, L. and Kriegstein, A. R. (2004). Cortical neurons arise in symmetric and asymmetric division zones and migrate through specific phases. *Nature Neurosci* **7.** 136-144.

Nural H. F. and Mastick G. S. (2004). Pax6 guides a relay of pioneer longitudinal axons in the embryonic mouse forebrain. *J Comp Neurol*. **479.** 399-409.

Olson, J. M., Asakura, A., Snider, L., Hawkes, R., Strand, A., Stoeck, J., Hallahan, A., Pritchard, J. and Tapscott, S. J. (2001). NeuroD2 Is Necessary for Development and Survival of Central Nervous System Neurons. *Dev Biol* **234.** 174-187.

Orian, A. (2006). Chromatin profiling, DamID and the emerging landscape of gene expression. *Curr Opin Genetics and Dev* **16.** 157-164.

Orlando, V. (2000). Mapping chromosomal proteins *in vivo* by formaldehyde-crosslinked-chromatin immunoprecipitation. *TIBS* **25.** 99-104.

Patterson, T. A., Lobenhofer, E. K., Fulmer-Smentek, S. B., Collins, P. J., Chu, T.-Z., Bao, W., Fang, H., Kawasaki, E. S., Hager, J., Tikhonova, I. R., Walker, S. J., Zhang, L., Hurban, P., de Longueville, F., Fuscoe, J. C., Tong, W., Shi, L. and Wolfinger, R. D. (2006). Performance comparison of one-color and two-color platforms within the MicroArray Quality Control (MAQC) project. *Nat Biotech* **24.** 1140-1150.

Piñon, M. C., Touc, T. C., Ashery-Paden, R., Molnár, Z. and Stoykova, A. (2008). Altered Molecular Regionalization and Normal Thalamocortical Connections in Cortex-Specific *Pax6* Knock-Out Mice. *J Neurosci* **28.** 8724-8734.

Porteus, M. H., Bulfone, A., Liu, J.-K., Puelles, L., Lo, L.-C. and Rubenstein, J. L. R. (1994). Dlx-2, MASH-1, and MAP-2 Expression and Bromodeoxyuridine Incorporation Define Molecularly Distinct Cell Populations in the Embryonic Mouse Forebrain. *J Neurosci* **14.** 6370-6383.

Pratt, T., Vitalis, T., Warren, N., Edgar, J. M., Mason, J. O., and Price, D. J. (2000). A role for Pax6 in the normal development of dorsal thalamus and its cortical connections. *Development* **127.** 5167-5178.

Pratt, T., Quinn, J. C., Simpson, T. I., West, J. D., Mason, J. O. and Price, D. J. (2002). Disruption of early events in thalamocortical tract formation in mice lacking the transcription factors Pax6 or Foxg1. *J Neurosci* **22.** 8523-8531.

Puelles, L and Rubenstein, J. L. R. (1993). Expression patterns of homeobox and other putative regulatory genes in the embryonic mouse forebrain suggest a neuromeric organization. *Trends Neurosci* **16.** 472-479.

Puelles, L and Rubenstein, J. L. R. (2003). Forebrain gene expression domains and the evolving prosomeric model. *Trends Neurosci* **26.** 469-476.

Puelles, L., Kuwana, E., Puelles E., Rubenstein, J. L. (1999). Comparison of the mammalian and avian telencephalon from the perspective of gene expression data. *Eur J Morphol* **37.** 139-150.

Quinn, J. C., West, J. D. and Hill, R. E. (1996). Multiple functions for *Pax6* in mouse eye and nasal development. *Genes & Dev* **10.** 435-446.

Quinn, J. C., Molinek, M., Martynoga, B. S., Zaki, P. A., Faedo, A., Bulfone, A., Hevner, R. F., West, J. D. and Price, D. J. (2007). Pax6 controls cerebral cortical cell number by regulating exit from the cell cycle and specifies cortical cell identity by a cell autonomous mechanism. *Dev. Biol* **302.** 50-65.

Quiring, R., Walldorf, U., Kloter, U. and Gehring, W. J. (1994). Homology of the *eyeless* Gene of *Drosophila* to the *Small eye* gene in Mice and *Aniridia* in Humans. *Science* **265.** 785-789.

Raemaekers, T., Ribbeck, K., Beaudouin, J., Annaert, W., Van Camp, M., Stockmans, I., Smets, N., Bouillon, R., Ellenberg, J. and Carmeliet, G. (2003). NuSAP, a nover microtubule-associated protein involved in mitotic spindle organization. *J Cell Biol* **162.** 1017-1029.

Ragsdale, C. W. and Grove, E. A. (2001). Patterning the mammalian cerebral cortex. *Curr Opin Neurobiol* **11.** 50-58.

Rakic, P. (1974). Neurons in Rhesus Monkey visual cortex: Systematic Relation between Time of Origin and Eventual Disposition. *Science* **183.** 425-427.

Rallu, M., Machold, R., Gaiano, N., Corbin, J. G., McMahon, A. P. and Fishell, G. (2002). Dorsoventral patterning is established in the telencephalon of mutants lacking both Gli3 and Hedgehog signaling. *Development* **129.** 4963-4974.

Rash, B. G. and Grove, E. A. (2007). Patterning the Dorsal Telencephalon: A Role for Sonic Hedgehog? *J Neurosci* **27.** 11595-11603.

Ren, B., Robert, F., Wyrick, J. J., Aparicio, O., Jennings, E. G., Simon, I., Zeitlinger, J., Schreiber, J., Hannett, N., Kanin, E., Volkert, T. L., Wilson, C. J., Bell, S. P. and Young, R. A. (2000). Genome-Wide Location and Function of DNa Binding Proteins. *Science* **290.** 2306-2309.

Ribbeck, K., Raemaekers, T., Carmeliet, G. and Mattaj, I. W. (2007). A role for NuSAP in linking microtubules to mitotic chromosomes. *Curr Biol* **17.** 230-236.

Roelink, H., Porter, J. A., Chiang, C., Tanabe, Y., Chang, D. T., Beachy, P. A. and Jessell, T. M. (1995). Floor Plate and Motor Neuron Induction by Different Concentrations of the Amino-Terminal Cleavage Product of Sonic Hedgehog Autoproteolysis *Cell* **81.** 445-455.

Rossant, J. and Tam, P. P. L. (2002). Mouse Development. Patterning, Morphogenesis, and Organogenesis. San Diego, Academic Press.

Roth, W., Wild-Bode, C., Platten, M., Grimmel, C., Melkonyan, H. S., Dichgans, J. and Weller, M. (2000). Secreted Frizzled-related proteins inhibit motility and promote growth of human malignant glioma cells. *Oncogene* **19.** 4210-4220.

Rubenstein, J. L. R., Martinez, S., Shimamura, K. and Puelles, L. (1994). The Embryonic Vertebrate Forebrain: The Prosomeric Model. *Science* **266.** 578-580.

Salem, C. E. Markl, I. D. C., Bender, C. M., Gonzales, F. A., Jones, P. A. and Liang, G. (2000). *Pax6* methylation and ectopic expression in human tumor cells. *Int J Cancer* **87.** 179-185.

Sander, M. Neubüser, A., Kalamaras, J., Ee, H. C., Martin, G. R. and German, M. S. (1997). Genetic analysis reveals that PAX6 is required for normal

transcription of pancreatic hormone genes and islet development. *Genes and Dev* **11.** 1662-1673.

Schedl, A., Ross, A., Lee, M., Engelkamp, D., Rashbass, P., van Heyningen, V. and Hastie, N. D. (1996). Influence of *PAX6* Gene Dosage on Development: Overexpression Causes Severe Eye Abnormalities. *Cell* **86.** 71-82.

Schena, M., Shalon, D., Davis, R. W. and Brown, P. O. (1995). Quantitative Monitoring of Gene Expression Patterns with a Complementary DNA Microarray. *Science* **270.** 467-470.

Schmahl, W., Knoedlseder, M., Favor, J. and Davidson, D. (1993). Defects of neuronal migration and the pathogenesis of cortical malformations are associated with Small eye (Sey) in the mouse, a point mutation at the Pax-6-locus. *Acta Neuropathol.* **86**. 126 -135.

Schmid, T., Krüger, M. and Braun, T. (2007). NSCL-1 and -2 control the formation of precerebellar nuclei by orchestrating the migration of neuronal precursor cells. *J Neurochem* **102.** 2061-2072.

Schroeder, A., Mueller, O., Stocker, S., Salowsky, R., Leiber, M., Grassman, M., Lightfoot, S., Menzel, W., Granzow, M. and Ragg, T. (2006). The RIN: an RNA integrity number for assigning integrity values to RNA measurements. *BMC Mol Biol* **7.** 3.

Schuurmans C, Armant O, Nieto M, Stenman JM, Britz O, Klenin N, Brown C, Langevin LM, Seibt J, Tang H, Cunningham JM, Dyck R, Walsh C, Campbell K, Polleux F, Guillemot F. (2004). Sequential phases of cortical specification involve Neurogenin-dependent and -independent pathways. *EMBO J* **23.** 2892-2902.

Schwab, M. H., Druffel-Augustin, S., Gass, P., Jung, M., Klugmann, M. Bartholomae, A., Rossner, M. J. and Nave, K.-A. (1998). Neuronal Basic Helix-Loop-Helix Proteins (NEX, neuroD, NDRF): Spatiotemporal Expression and Targeted Disruption of the NEX Gene in Transgenic Mice. *J Neurosci* **18.** 1408-1418.

Schwab, M. H., Bartholomae, A., Heimrich, B., Feldmeyer, D., Druffel-Augustin, S., Goebbels, S., Naya, F. J., Zhao, S., Frotscher, M., Tsai, M.-J. and Nave, K.-A. (2000). Neuronal Basic Helix-Loop-Helix Proteins (NEX and

BETA2/Neuro D) Regulate Terminal Granule Cell Differentiation in the Hippocampus. *J Neurosci* **20.** 3714-3724.

Scott, M. R. D., Westphal, K.-H. and Rigby, P. W. J. (1983). Activation of Mouse Genes in Transformed Cells. *Cell* **34.** 557-567.

Shimamura, K. and Rubenstein, J. L. (1997). Inductive interactions direct early regionalization of the mouse forebrain. *Dev* **124.** 2709-2718.

Shimogori, T., Banuchi, V., Ng, H. Y., Strauss, J. B. and Grove, E. A. (2004). Embryonic signaling centers expressing BMP, WNT and FGF proteins interact to pattern the cerebral cortex. *Dev* **131.** 5639-5647.

Simon, R. M., Korn, E. L., McShane, L. M., Radmacher, M. D., Wright, G. W. and Zhao, Y. (2003). Design and Analysis of DNA Microarray Investigations. DNA Microarray Technology. New York, Springer.

Simpson, T. I. and Price, D. J. (2002). Pax6; a pleiotropic player in development. *BioEssays* **24.** 1041-1051.

Sisodyia, S. M., Free, S. L., Williamson, K. A., Mitchell, T. N., Willis, C., Stevens, J. M., Kendall, B. E., Shorvon, S. D., Hanson, I. M., Moore, A. T. and van Heyningen V. (2001). *PAX6* haploinsufficiency causes cerebral malformation and olfactory dysfunction in humans. *Nat Genet* **28.** 214-216.

Slonim, D. K. (2002). From patterns to pathways: gene expression data analysis comes of age. *Nat Genet* **32.** (Suppl) 502-508.

Smith, D. G., Clemens, J., Crede, W., Harvey, M. and Gracely, E. J. (1987). Impact of Multiple Comparisons in Randomized Clinical Trials. *American J Med* **83.** 545-550.

Stenman, J., Yu, R. T., Evans, R. M. and Campbell, K. (2003). *Tlx* and *Pax6* co-operate genetically to establish the pallio-subpallial boundary in the embryonic mouse telencephalon. *Development* **130.** 1113-1122.

St-Onge, L., Sosa-Pineda, B. Chowdhury, K., Mansouri, A. and Gruss P. (1997). *Pax6* is required for differentiation of glucagon-producing α-cells in mouse pancreas. *Nature* **387.** 406-409.

Storm, E. E., Garel, S., Borello, U., Hébert, J. M., Martinez, S., McConnell, S. K., Martin, G. R. and Rubenstein, J. L. R. (2006). Dose-dependent functions of Fgf8 in regulating telencephalic patterning centers. *Dev* **133.** 1831-1844.

Stoykova, A., Fritsch, R., Walther, C. and Gruss, P. (1996). Forebrain patterning defects in *Small eye* mutant mice. *Development* **122.** 3453-3465.

Stoykova, A., Götz, M., Gruss, P. and Price, J. (1997). *Pax6*-dependent regulation of adhesive patterning, *R-cadherin* expression and boundary formation in developing forebrain. *Development* **124.** 3765-3777.

Stoykova, A., Treichel, D., Halonet, M. and Gruss, P. (2000). *Pax6* Modulates the Dorsoventral Patterning of the Mammalian Telencephalon. *J Neurosci* **20.** 8042-8050.

Sugiyama, S., Di Nardo, A. A., Aizawa, S., Matsuo, I., Volovitch, M., Prochiantz, A. and Hensch, T. K. (2008). Experience-Dependent Transfer of Otx2 Homeoprotein into the Visual Cortex Activates Postnatal Plasticity. *Cell* **134.** 508-520.

Suto, F., Ito, K., Uemura, M., Shimizu, M., Shinkawa, Y., Sanbo, M., Shinoda, T., Tsuboi, M., Takashima, S., Yagi, T. and Fujisawa, H. (2005). Plexin-a4 mediates axon-repulsive activities of both secreted and transmembrane semaphorins and plays roles in nerve fiber guidance. *J Neurosci* **14.** 3628-3637.

Swanson, D. J., Tong, Y. and Goldowitz, D. (2005). Disruption of cerebellar granule cell development in the Pax6 mutant, Sey mouse. *Brain Res Dev Brain Res* **160.** 176-193.

Szybalski, W. (1985). Universal restriction endonucleases: designing novel cleavage specificities by combining adapter oligodeoxynucleodite and enzyme moieties. *Gene* **40.** 169-173.

Talamillo, A., Quinn, J. C., Collinson, J. M. Carić, D., Price, D. J., West, J. D. and Hill, R. E. (2003). Pax6 regulates regional development and neuronal migration in the cerebral cortex. *Dev Biol* **255.** 151-163.

Tamamaki, N., Fujimori, K. E. and Takauji, R. (1997). Origin and Route of Tangentially Migrating Neurons in the Developing Neocortical Intermediate Zone. *J Neurosci* **17.** 8313-8323.

Tan, P. K., Downey, T. F., Spitznagel, E. L. Jr., Xu, P. Fu, D., Dimitrov, D. S., Lempicki, R. A., Raaka, B. M. and Cam, M. C. (2003). Evaluation of gene expression measurements from commercial microarray platforms. *Nucleic Acids Res* **31.** 5676-5684.

Tappaz, M., Almarghini, K., Legay, F. and Remy, A. (1992). Taurine Biosynthesis Enzyme Cysteine Sulfinate Decarboxylate (CSD) from Brain: The Long and Tricky Trail to Identification. *Neurochem Res* **17.** 849-859.

Taverner, N. V., Smith, J. C. and Wardle, F. C. (2004). Identifying transcriptional targets. *Genome Biol* **5.** 210.

Theil, T., Aydin, S., Koch, S., Grotewold, L. and Rüther, U. (2002). Wnt and Bmp signalling cooperatively regulate graded *Emx2* expression in the dorsal telencephalon. *Dev* **129.** 3045-3054.

Timmer, J. R., Wang, C. and Niswander, L. (2002). BMP signaling patterns the dorsal and intermediate neural tube via regulation of homeobox and helix-loop-helix transcription factors. *Dev* **129.** 2459-2472.

Tiveron MC, Rossel M, Moepps B, Zhang YL, Seidenfaden R, Favor J, König N, Cremer H. (2006). Molecular interaction between projection neuron precursors and invading interneurons via stromal-derived factor 1 (CXCL12)/CXCR4 signaling in the cortical subventricular zone/intermediate zone. *J Neurosci* **26.** 13273-13278.

Tole, S., Ragsdale, C. W., Grove, E. A. (2000). Dorsoventral patterning of the telencephalon is disrupted in the mouse mutant extra-toes(J). *Dev Biol* **217.** 254-265.

Ton, C. C. T., Hirvonen, H., Miwa, H., Weil, M. M., Monaghan, P., Jordan, T., van Heyningen, V., Hastie, N. D., Meijers-Heijboer, H., Drechsler, M., Royer-Pokora, B., Collins, F., Swaroop, A., Strong, L. C. and Saunders, G. F. (1991). Positional Cloning and Characterization of a Paired Box- and Homeobox-Containing Gene from the Aniridia Region. *Cell* **67.** 1059-1074.

Ton, C. C. T., Miwa, H. and Saunders, G. F. (1992). *Small eye* (*Sey*): Cloning and Characterization of the Murine Homolog of the Human Aniridia Gene. *Genomics* **13.** 251-156.

Toresson, H., Potter, S. S. and Campbell, K. (2000). Genetic control of dorsal-ventral identity in the telencephalon: opposing roles for *Pax6* and *Gsh2*. *Development* **127.** 4361-4371.

Torres-Munoz, J. E., Van Waveren C., Keegan, M. G., Bookman, R. J. and Petito, C. K. (2004). Gene expression profiles in microdissected neurons from human hippocampal subregions. *Brain Res Mol Brain Res* **127.** 105-114.

Tyas, D. A., Pearson, H., Rashbass, P. and Price, D. J. (2003). Pax6 Regulates Cell Adhesion during Cortical Development. *Cerebral Cortex* **13.** 612-619.

Tyas, D. A., Simpson, T. I., Carr, C. B., Kleinjan, D. A., van Heyningen, V., Mason, J. O. and Price, D. J. (2006). Functional conservation of *Pax6* regulatory elements in humans and mice demonstrated with a novel transgenic reporter mouse. *Dev Biol* **6.**

Vagner, S., Galy, B. and Pyronnet, S. (2001). Irresistible IRES. *EMBO reports* **2.** 893-898.

Valassi, E., Scacchi, M. and Cavagnini, F. (2008). Neuroendocrine control of food intake. *Nutr Metab Cardiovasc Dis* **18.** 158-168.

van der Kooy, D. and Kuypers, H. G. J. M. (1979). Fluorescent Retrograde Double Labeling: Axonal Branching in the Ascending Raphe and Nigral Projections. *Science* **204.** 873-875.

van der Meer-de Jong, R., Dickinson, M. E., Woychik, R. P., Stubbs, L., Hetherington, C. and Hogan, B. L. M. (1990). Location of the Gene Involving the Small Eye Mutation on Mouse Chromosome 2 Suggests Homology with Human Aniridia 2 (AN2). *Genomics* **7.** 270-275.

van Steensel, B., Delrow, J. and Henikoff, S. (2001). Chromatin profiling using targeted DNA adenine methyltransferase. *Nat Genetics* **27.** 304-308.

Velculescu, V. E., Zhang, L., Vogelstein, B. and Kinzler, K. W. (1995). Serial Analysis of Gene Expression. *Science* **270.** 484-487.

Visel A, Carson J, Oldekamp J, Warnecke M, Jakubcakova V, Zhou X, Shaw CA, Alvarez-Bolado G, Eichele G. (2007). Regulatory pathway analysis by high-throughput in situ hybridization. *PLoS Genet* **10.** 1867-1883.

Walther, C. and Gruss, P. (1991). Pax-6, a murine paired box gene, is expressed in the developing CNS. *Development* **113.** 1435-1449.

Warren, N. Caric, D. Pratt, T., Clausen, J. A., Asavaritikrai, P., Mason, J. O., Hill, R. E. and Price, D. J. (1999). The Transcription Factor, *Pax6*, is Required for Cell Proliferation and Differentiation in the Developing Cerebral Cortex. *Cerebral Ctx* **9.** 627-635.

Waterhouse, B. D., Mihailoff, G. A., Baack, J. C. and Woodward, D. J. (1986). Topographical Distribution of Dorsal and Median Raphe Neurons Projecting to

Motor, Sensorimotor, and Visual Cortical Areas in the Rat. *J Comp Neurol* **249.** 460-476.

Wilson, S. W. and Rubenstein, J. L. R. (2000). Induction and Dorsoventral Patterning of the Telencephalon. *Neuron* **28.** 641-651.

Yamaoka, T. Yano, M., Yamada, T., Matsushita, T., Moritani, M., Ii, S., Yoshimoto, K. and Itakura, M. (2000). Diabetes and pancreatic tumours in transgenic mice expressing Pax6. *Diabetologia* **43.** 332-339.

Yang, Y. H., Dudoit, S., Luu, P., Lin, D. M., Peng, V., Ngai, J. and Speed, T. P. (2002). Normalization for cDNA microarray data: a robust composite method addressing single and multiple slide systematic variation. *Nucleic Acids Res* **30.** e15.

Yonaha, M. and Proudfoot, N. J. (2000). Trascriptional termination and coupled polyadenylation *in vitro*. *EMBO*. **19.** 3770-3777.

Yun, K., Potter, S. and Rubenstein, J. L. R. (2001). *Gsh2* and *Pax6* play complementary roles in dorsoventral patterning of the mammalian telencephalon. *Dev* **128.** 193-205.

Zhu, Y., Li, H., Zhou, L., Wu, J. Y. and Rao, Y. (1999). Cellular and Molecular Guidance of GABAergic Neuronal Migration from an Extracortical Origin to the Neocortex. *Neuron* **23.** 473-485.

Up-regulated Genes

Appendix A

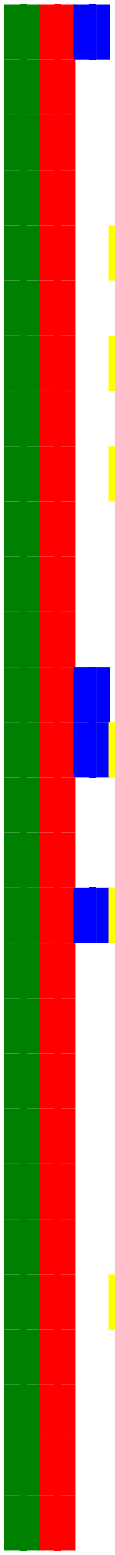

Gene	Fold Change	p-value	Adjusted p-value
Lhx6	15.439	5.82E-06	0.008
Smad2	9.677	4.26E-05	0.014
Titf1	7.406	1.02E-06	0.005
Mpped2	7.186	3.93E-05	0.014
Gpr177	5.060	4.51E-06	0.007
Btbd9	4.658	1.84E-05	0.012
Asb4	4.502	7.89E-07	0.004
Rbbp4	4.146	1.66E-04	0.025
Calb1	3.614	8.34E-05	0.018
Lhx8	3.538	4.55E-05	0.014
Ube2s	3.006	8.41E-04	0.045
Nkx6-2	2.910	3.02E-07	0.004
Gsh2	2.906	1.75E-05	0.012
Ascl1	2.888	2.22E-05	0.012
Arfl4	2.729	3.36E-06	0.007
B230215L15Rik	2.725	1.38E-04	0.023
Dlx1	2.715	3.35E-05	0.013
MGC73635	2.709	2.27E-05	0.012
Fxc1	2.623	8.08E-07	0.004
Hist1h1e	2.621	4.52E-05	0.014
Hnrpa0	2.601	5.70E-04	0.039
Dek	2.548	2.84E-04	0.030
Ube2s	2.548	7.86E-04	0.044
Peg3	2.536	2.19E-04	0.028
Chmp4b	2.533	4.02E-05	0.014
Glcci1	2.527	3.96E-06	0.007
Raly	2.491	1.47E-04	0.024
Glcci1	2.465	5.18E-05	0.015

Up-regulated Genes

Appendix A

Gene	Fold Change	p-value	Adjusted p-value
2810417H13Rik	2.459	1.60E-04	0.024
BC059842	2.457	2.96E-06	0.007
Dlx2	2.454	4.80E-05	0.014
Mpped2	2.431	4.08E-05	0.014
Hnrpa0	2.418	2.27E-05	0.012
Atbf1	2.396	7.58E-04	0.043
Zic3	2.385	3.67E-05	0.014
5830457O10Rik	2.360	7.51E-05	0.017
Uhrf1	2.357	2.91E-04	0.031
Ccnd2	2.351	7.68E-04	0.044
Prrx1	2.349	2.34E-05	0.012
Sox2	2.319	8.40E-04	0.045
Dlx6os1	2.289	8.58E-04	0.045
Ccnd1	2.279	1.26E-04	0.022
Taf15	2.237	8.24E-05	0.018
Mcm6	2.227	2.53E-04	0.029
Hist1h4d	2.202	2.48E-04	0.029
Rac1	2.197	3.42E-04	0.032
Igf1r	2.147	7.57E-05	0.017
Lxn	2.146	7.47E-05	0.017
Lef1	2.145	6.18E-05	0.017
Tmem123	2.136	4.56E-05	0.014
Mki67	2.134	1.40E-04	0.023
Gad2	2.120	4.45E-04	0.036
Actb	2.114	3.62E-04	0.032
Lmnb1	2.104	4.28E-04	0.035
Hist1h2ak	2.096	7.28E-04	0.043
Lsr	2.095	3.12E-04	0.031
Klhl13	2.082	1.06E-03	0.050

Up-regulated Genes

Appendix A

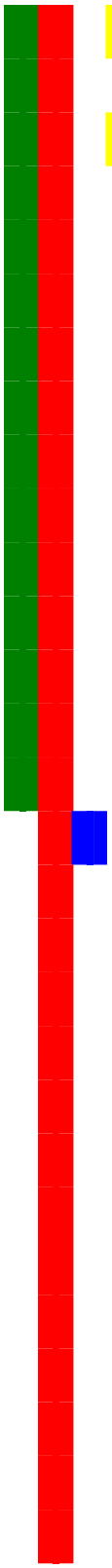

Gene	Fold Change	p-value	Adjusted p-value
Zic4	2.063	2.66E-04	0.030
Cdca7	2.059	1.59E-04	0.024
Sulf2	2.053	2.41E-04	0.029
Tmem16a	2.047	4.64E-07	0.004
Gucy1a3	2.046	2.06E-04	0.027
Sox6	2.046	6.14E-04	0.040
Stk33	2.039	8.74E-06	0.009
Slco3a1	2.038	2.00E-04	0.027
Asb4	2.023	1.77E-05	0.012
Pmch	2.014	4.81E-04	0.037
Hmx3	2.007	1.07E-03	0.050
Notch1	2.006	1.14E-04	0.021
4930506M07Rik	2.004	2.78E-04	0.030
Glo1	2.002	8.57E-05	0.018
Dnmt1	2.001	1.06E-03	0.050
Dlx6os1	1.994	7.83E-05	0.017
Gucy1a3	1.992	9.17E-06	0.009
Melk	1.991	9.75E-06	0.009
Ches1	1.987	7.19E-04	0.043
Slc18a2	1.975	1.26E-05	0.010
Grb10	1.971	1.54E-04	0.024
Hist1h2af	1.963	3.36E-04	0.032
Ywhaz	1.962	2.03E-04	0.027
Casc5	1.959	3.53E-04	0.032
Mapre1	1.957	4.77E-04	0.037
Slc18a2	1.956	4.88E-05	0.014
Arvcf	1.955	9.37E-04	0.047
Smad4	1.950	9.88E-05	0.019
Ptges3	1.949	7.73E-04	0.044

Up-regulated Genes

Appendix A

Gene	Fold Change	p-value	Adjusted p-value
Nucks1	1.924	9.47E-04	0.047
Rbp1	1.912	5.11E-04	0.038
Kifc1	1.910	5.31E-04	0.038
Espl1	1.907	5.65E-04	0.039
Dlx5	1.903	5.16E-04	0.038
Thoc4	1.900	7.32E-04	0.043
Gucy1b3	1.899	3.60E-06	0.007
Top2a	1.897	5.18E-05	0.015
Ccdc5	1.897	2.36E-04	0.029
Clstn2	1.895	9.53E-04	0.047
Spag5	1.894	6.86E-05	0.017
Msi2	1.880	1.96E-04	0.027
Hist1h2ai	1.880	7.44E-04	0.043
Plagl2	1.875	7.84E-06	0.009
Gpr88	1.874	1.42E-04	0.023
Cks1b	1.873	4.40E-04	0.035
Sox9	1.871	3.08E-04	0.031
Uhrf1	1.871	1.30E-04	0.022
ENSMUST00000076113	1.861	4.87E-04	0.037
Epha4	1.861	3.35E-04	0.032
Phgdh	1.855	4.65E-04	0.036
Aph1a	1.853	2.16E-05	0.012
Syt1	1.851	4.75E-04	0.036
LOC627585	1.850	1.05E-03	0.050
Arrdc4	1.850	1.51E-04	0.024
Atbf1	1.847	6.72E-04	0.041
Tspan7	1.840	1.21E-04	0.022
Tcof1	1.838	9.44E-04	0.047
Aldh1a3	1.837	1.69E-04	0.025

Up-regulated Genes

Appendix A

Gene	Fold Change	p-value	Adjusted p-value
Hspa4	1.833	4.04E-04	0.034
Rnaseh2a	1.831	2.13E-04	0.028
Prrx1	1.829	7.08E-05	0.017
Nusap1	1.827	4.34E-05	0.014
S100pbp	1.824	1.23E-04	0.022
Glo1	1.824	9.07E-05	0.018
Rhoa	1.822	6.09E-04	0.040
Kif15	1.820	4.02E-05	0.014
Slc10a4	1.814	2.78E-05	0.013
Cdk6	1.812	2.48E-04	0.029
B130054P17	1.809	3.57E-06	0.007
Ubtf	1.801	7.28E-04	0.043
2410025L10Rik	1.799	3.43E-04	0.032
Cdca2	1.796	4.24E-05	0.014
Slc10a4	1.793	9.08E-05	0.018
Smc2	1.779	3.05E-05	0.013
Ung	1.779	4.51E-05	0.014
Nuf2	1.774	6.26E-05	0.017
Sfrs9	1.773	2.92E-04	0.031
Hoxa9	1.772	1.57E-05	0.011
5730410E15Rik	1.770	7.34E-05	0.017
Tyms	1.765	2.07E-04	0.027
Slc25a13	1.756	3.32E-05	0.013
Hmgn2	1.756	1.95E-04	0.027
Tanc1	1.753	3.14E-04	0.031
Nkx2-2	1.751	1.33E-04	0.022
Mcm3	1.742	8.04E-04	0.044
Gga1	1.739	7.79E-04	0.044
5730437N04Rik	1.738	8.13E-05	0.018

Up-regulated Genes

Appendix A

Gene	Fold Change	p-value	Adjusted p-value
Hist1h1b	1.738	4.88E-04	0.037
Tacc3	1.736	3.23E-04	0.032
Pdlim1	1.735	3.56E-05	0.014
Nrxn3	1.730	7.92E-04	0.044
Ebf1	1.725	3.56E-04	0.032
Tmcc3	1.719	1.53E-04	0.024
Tcfap2e	1.715	2.24E-04	0.028
Taf1	1.714	6.60E-05	0.017
Pask	1.712	1.24E-04	0.022
Pdzrn3	1.710	8.88E-04	0.046
D1Ertd471e	1.710	4.17E-04	0.034
ENSMUST00000092884	1.708	2.91E-04	0.031
Nrip1	1.706	9.80E-04	0.048
Csrp1	1.703	4.06E-05	0.014
Hs6st2	1.703	4.15E-05	0.014
Wnk1	1.702	2.46E-04	0.029
Eif2c2	1.700	6.29E-04	0.040
Hist1h2aa	1.698	3.99E-04	0.034
Atad2	1.694	4.98E-04	0.037
Rxfp3	1.694	1.25E-05	0.010
Mcm3	1.693	5.27E-04	0.038
2410015N17Rik	1.692	7.16E-04	0.043
Dtl	1.691	3.73E-05	0.014
Baz2a	1.690	7.41E-04	0.043
Kif20a	1.689	3.26E-04	0.032
Slc16a1	1.688	3.74E-04	0.033
Foxp2	1.688	6.84E-04	0.042
Hspa12a	1.683	3.29E-04	0.032
Slc16a1	1.678	2.69E-04	0.030

Up-regulated Genes

Appendix A

Gene	Fold Change	p-value	Adjusted p-value
Smoc1	1.677	3.73E-05	0.014
Gad1	1.677	1.66E-04	0.025
Cenpq	1.673	2.12E-04	0.028
Nts	1.671	4.15E-04	0.034
Myb	1.667	3.27E-05	0.013
Ypel4	1.667	7.79E-05	0.017
Rbp1	1.664	5.81E-04	0.039
Bub1b	1.661	1.06E-03	0.050
AU020206	1.660	7.94E-04	0.044
Hist2h2aa1	1.657	8.46E-04	0.045
Col18a1	1.652	5.25E-04	0.038
Ranbp1	1.648	6.25E-04	0.040
Grip1	1.647	5.19E-04	0.038
Tpx2	1.646	3.73E-04	0.033
Rnd3	1.643	9.52E-04	0.047
Sulf2	1.643	2.90E-04	0.031
Kpna2	1.643	1.01E-03	0.049
NAP102645-1	1.642	6.14E-04	0.040
Ntn1	1.634	4.33E-05	0.014
Ckap5	1.634	4.51E-04	0.036
BC085271	1.632	3.12E-04	0.031
Cdh22	1.627	4.70E-04	0.036
Tmpo	1.627	2.40E-04	0.029
Esco2	1.627	2.95E-05	0.013
Chaf1b	1.625	9.21E-04	0.047
Pdk1	1.623	9.50E-05	0.019
Onecut2	1.620	3.94E-04	0.034
Smc2	1.619	3.61E-04	0.032
BX513654	1.617	2.21E-04	0.028

Up-regulated Genes

Appendix A

Gene	Fold Change	p-value	Adjusted p-value
Zfp668	1.617	6.16E-04	0.040
Rif1	1.616	5.72E-04	0.039
Gtf2h1	1.607	3.18E-04	0.032
Zc3h11a	1.604	1.99E-04	0.027
5730590G19Rik	1.603	2.21E-05	0.012
Vwc2	1.601	5.57E-05	0.016
Exoc6b	1.599	1.36E-04	0.023
Tiam2	1.598	2.65E-04	0.030
Hoxb3	1.597	2.06E-05	0.012
Rprm	1.596	8.01E-04	0.044
Lmo1	1.591	3.28E-04	0.032
Cenpb	1.590	3.00E-04	0.031
NAP028759-1	1.590	6.67E-04	0.041
Tcf19	1.587	2.76E-04	0.030
Klhdc4	1.587	2.19E-04	0.028
Slc12a2	1.585	1.44E-04	0.023
Dnajb6	1.579	7.29E-04	0.043
Rad54l	1.578	2.76E-04	0.030
Cdc6	1.576	3.47E-05	0.014
Ranbp2	1.573	4.18E-04	0.034
Nol8	1.572	6.62E-04	0.041
Rffl	1.572	7.61E-05	0.017
Myb	1.568	6.49E-05	0.017
Upf1	1.566	7.57E-04	0.043
Bmper	1.562	3.51E-04	0.032
2610528E23Rik	1.562	5.66E-04	0.039
Ddx6	1.560	4.49E-04	0.036
Frap1	1.559	1.04E-03	0.050
Prrx1	1.558	5.80E-05	0.016

Up-regulated Genes

Appendix A

Gene	Fold Change	p-value	Adjusted p-value
Rffl	1.557	6.13E-04	0.040
Ogg1	1.557	2.62E-04	0.030
Hells	1.554	8.15E-04	0.044
Hook3	1.547	1.01E-03	0.049
Thrap3	1.547	1.57E-04	0.024
3110006E14Rik	1.547	8.90E-04	0.046
Mthfd2	1.543	1.96E-04	0.027
Ttrap	1.542	7.58E-04	0.043
Olig2	1.542	2.41E-04	0.029
LOC666704	1.539	1.04E-03	0.050
Eif1a	1.539	1.93E-04	0.027
Kif7	1.539	4.14E-05	0.014
S100a10	1.538	1.14E-04	0.021
1500003O22Rik	1.537	1.07E-04	0.020
Mrps5	1.534	1.18E-04	0.021
Accn1	1.534	4.02E-04	0.034
Fgf14	1.534	4.19E-05	0.014
Arhgap11a	1.533	1.12E-04	0.021
Timeless	1.533	6.68E-04	0.041
2600005C20Rik	1.532	3.61E-05	0.014
Usf1	1.532	6.68E-04	0.041
Cenpp	1.532	9.20E-04	0.047
Sox9	1.530	6.42E-04	0.041
Nphp1	1.529	7.71E-04	0.044
Gm784	1.529	9.39E-05	0.018
Rrm2	1.528	8.15E-04	0.044
Jarid2	1.527	2.22E-04	0.028
Nat13	1.523	5.71E-04	0.039
Ncapg	1.521	2.97E-04	0.031

Up-regulated Genes

Appendix A

Gene	Fold Change	p-value	Adjusted p-value
Hist1h4d	1.521	8.24E-04	0.045
Oip5	1.521	7.33E-04	0.043
Tac1	1.519	1.60E-04	0.024
Pprc1	1.519	2.41E-04	0.029
Fancl	1.519	2.73E-04	0.030
Cdk2	1.516	1.04E-04	0.020
Olig1	1.509	5.55E-04	0.039
Pola2	1.507	8.92E-05	0.018
Hip2	1.506	9.24E-05	0.018
Sfi1	1.505	9.16E-04	0.047
Chek1	1.501	6.27E-05	0.017
Fkbp8	1.498	5.92E-04	0.040
Asf1b	1.498	5.79E-04	0.039
Lima1	1.495	8.44E-04	0.045
2810416G20Rik	1.494	4.74E-04	0.036
Plscr1	1.494	1.14E-04	0.021
Rcl1	1.493	8.85E-04	0.046
Tmem48	1.492	1.33E-04	0.022
Ankrd43	1.491	3.13E-05	0.013
Mnd1	1.491	4.56E-05	0.014
Tlk1	1.490	6.60E-04	0.041
AK032303	1.489	9.00E-04	0.047
5830446M03Rik	1.486	6.05E-04	0.040
8430408O14	1.485	3.48E-04	0.032
Nlk	1.483	7.94E-04	0.044
Dusp7	1.483	5.61E-04	0.039
Vax1	1.483	1.66E-04	0.025
Rras2	1.482	3.22E-04	0.032
Gins3	1.474	1.53E-04	0.024

Up-regulated Genes

Appendix A

Gene	Fold Change	p-value	Adjusted p-value
Ubqln4	1.471	1.15E-04	0.021
Trerf1	1.470	2.54E-04	0.029
Mettl5	1.470	2.54E-04	0.029
Tbl1x	1.467	4.19E-04	0.034
Rbm28	1.465	9.97E-04	0.049
Zfp179	1.464	2.51E-04	0.029
Zfp469	1.464	6.67E-04	0.041
Prkar2a	1.458	4.21E-04	0.034
Pitpnb	1.455	6.14E-04	0.040
4930442E04Rik	1.454	1.31E-04	0.022
Tnrc15	1.454	8.31E-04	0.045
Ube1l2	1.453	7.41E-04	0.043
Fgd1	1.452	2.45E-04	0.029
Spef1	1.450	2.82E-04	0.030
Cenpl	1.447	5.76E-04	0.039
Papd1	1.444	9.81E-04	0.048
ENSMUST00000050565	1.442	2.33E-04	0.029
Nol3	1.441	3.82E-04	0.033
Has3	1.439	7.06E-04	0.043
Tor1b	1.438	1.02E-03	0.049
Setd8	1.437	4.14E-04	0.034
Fbln1	1.433	8.60E-04	0.045
Rif1	1.431	2.37E-04	0.029
Tmtc2	1.430	7.98E-04	0.044
Utp14a	1.430	8.93E-05	0.018
Top2a	1.430	7.13E-05	0.017
Rpsa	1.430	3.34E-04	0.032
Nap1l5	1.427	4.64E-04	0.036
E2f7	1.425	6.42E-04	0.041

Up-regulated Genes

Appendix A

Gene	Fold Change	p-value	Adjusted p-value
Nkx2-3	1.425	2.19E-04	0.028
Luc7l2	1.424	5.98E-04	0.040
Onecut1	1.424	7.94E-05	0.017
Gpt2	1.422	1.07E-03	0.050
Elovl5	1.420	4.32E-04	0.035
Mmp17	1.419	2.68E-04	0.030
C330016O10Rik	1.416	6.48E-04	0.041
Trp53i13	1.416	4.36E-04	0.035
Cdc6	1.416	2.20E-04	0.028
Dhfr	1.416	4.60E-04	0.036
Ash1l	1.416	5.95E-04	0.040
Mgat4c	1.411	7.92E-04	0.044
Lars	1.410	5.17E-04	0.038
Arhgef1	1.410	9.82E-05	0.019
U2af2	1.409	2.29E-04	0.029
Ric3	1.408	3.90E-04	0.033
Slc39a9	1.408	8.66E-04	0.046
Slc35f1	1.404	4.66E-04	0.036
Zranb3	1.402	5.92E-04	0.040
ENSMUST00000103201	1.402	8.56E-04	0.045
TC1637709	1.400	4.17E-04	0.034
Foxp2	1.398	1.03E-03	0.049
Pbx1	1.397	2.09E-04	0.028
Chka	1.396	5.39E-04	0.038
Cx3cl1	1.395	7.81E-04	0.044
Lgi2	1.395	2.99E-04	0.031
Lef1	1.394	3.25E-04	0.032
Vstm2	1.392	1.54E-04	0.024
Nudt4	1.391	6.34E-04	0.040

Up-regulated Genes

Appendix A

Gene	Fold Change	p-value	Adjusted p-value
Recql4	1.391	7.16E-04	0.043
E130304F04Rik	1.389	5.09E-04	0.038
Cdc45l	1.387	3.53E-04	0.032
Ckap2l	1.386	5.35E-04	0.038
Sub1	1.386	9.07E-04	0.047
3110001I20Rik	1.385	5.72E-04	0.039
Shh	1.385	5.17E-04	0.038
Stox2	1.380	1.06E-03	0.050
Foxo1	1.380	3.88E-04	0.033
Napb	1.379	5.85E-04	0.040
Dclre1a	1.377	8.40E-04	0.045
Chd1l	1.375	3.62E-04	0.032
Siae	1.372	1.98E-04	0.027
Shmt1	1.371	5.52E-04	0.039
Col18a1	1.371	3.10E-04	0.031
Ednrb	1.368	3.73E-04	0.033
Sgol2	1.368	1.76E-04	0.025
AK017340	1.367	6.00E-04	0.040
B2m	1.367	3.71E-04	0.033
Ptpru	1.366	1.07E-03	0.050
Pms1	1.364	5.76E-04	0.039
Ptch1	1.360	7.39E-04	0.043
Rab3b	1.359	7.00E-04	0.042
5730437N04Rik	1.354	6.47E-04	0.041
Senp8	1.352	7.11E-04	0.043
Usp24	1.351	7.84E-04	0.044
Casc5	1.351	1.87E-04	0.027
Ada	1.349	4.96E-04	0.037
Helb	1.347	6.58E-04	0.041

Up-regulated Genes

Appendix A

Gene	Fold Change	p-value	Adjusted p-value
Calb2	1.345	5.90E-04	0.040
Cmtm7	1.342	9.90E-04	0.049
Il16	1.342	3.37E-04	0.032
Clstn2	1.341	3.65E-04	0.032
Akap13	1.338	2.71E-04	0.030
Gnb4	1.338	8.01E-04	0.044
Nfe2l2	1.334	7.47E-04	0.043
Rapgef6	1.332	2.31E-04	0.029
Ccdc90a	1.332	3.72E-04	0.033
AU017455	1.332	9.79E-04	0.048
Dsn1	1.331	6.23E-04	0.040
Itm2a	1.330	8.87E-04	0.046
U2af2	1.327	7.70E-04	0.044
Casp7	1.323	7.81E-04	0.044
Hrasls3	1.320	3.58E-04	0.032
Ddx21	1.318	4.60E-04	0.036
Dcbld2	1.317	3.28E-04	0.032
Zfp324	1.317	3.56E-04	0.032
Sass6	1.316	3.60E-04	0.032
Cenpl	1.314	9.26E-04	0.047
Lhfp	1.309	9.30E-04	0.047
ENSMUST00000031768	1.308	6.61E-04	0.041
Calu	1.306	9.62E-04	0.048
Slc9a3r1	1.306	7.82E-04	0.044
Troap	1.302	5.59E-04	0.039
Pdxk	1.301	6.03E-04	0.040
Frmd6	1.300	4.64E-04	0.036
Slitrk3	1.297	8.67E-04	0.046
Fn1	1.297	1.06E-03	0.050

Up-regulated Genes

Appendix A

Gene	Fold Change	p-value	Adjusted p-value
D430042O09Rik	1.296	8.44E-04	0.045
Gsg2	1.294	8.27E-04	0.045
Bambi	1.293	9.59E-04	0.048
B3bp	1.290	9.75E-04	0.048
Tob2	1.288	7.32E-04	0.043
Ankrd43	1.275	8.15E-04	0.044

Down-regulated Genes

Appendix B

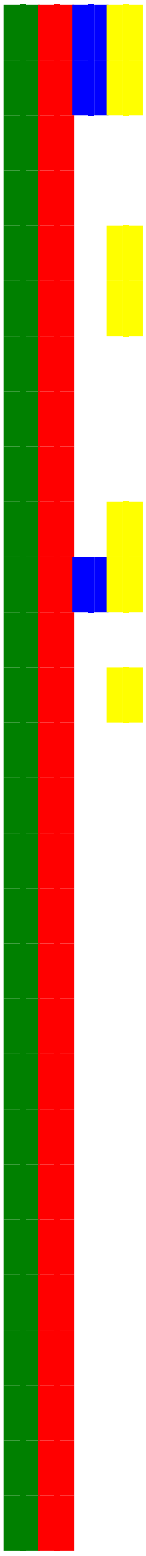

Gene	Fold Change	p-value	Adjusted p-value
Neurog2	-10.241	3.95E-05	0.014
Neurod6	-6.816	8.01E-06	0.009
BC020078	-6.408	4.59E-05	0.014
Prdm8	-6.185	2.47E-05	0.012
Tcfap2c	-5.648	3.71E-05	0.014
Slc1a3	-5.288	3.46E-05	0.014
Nhlh1	-5.151	1.61E-06	0.005
TC1651696	-5.053	3.03E-05	0.013
TC1574886	-4.645	6.06E-04	0.040
Lhx9	-4.633	3.41E-06	0.007
Eomes	-4.549	6.83E-06	0.009
Has2	-3.848	7.49E-06	0.009
Uncx4.1	-3.834	1.35E-06	0.005
Sema6d	-3.801	1.17E-05	0.009
Nrn1	-3.726	2.78E-06	0.007
Chst8	-3.696	4.07E-06	0.007
Slc17a6	-3.686	2.19E-05	0.012
Rabgap1l	-3.666	2.11E-05	0.012
Celsr1	-3.637	1.75E-04	0.025
3110035E14Rik	-3.531	3.06E-05	0.013
Sim1	-3.478	7.61E-04	0.043
Synpr	-3.415	5.49E-06	0.008
Olfm1	-3.320	2.09E-05	0.012
C030019F02Rik	-3.266	1.16E-04	0.021
Pcdh9	-3.136	7.48E-04	0.043
3110009O07Rik	-3.076	4.31E-07	0.004
Mmp14	-2.961	5.62E-05	0.016
AK140658	-2.938	1.44E-06	0.005

Down-regulated Genes

Appendix B

Gene	Fold Change	p-value	Adjusted p-value
Tmem46	-2.925	3.49E-05	0.014
Pcdh9	-2.892	2.53E-05	0.012
Neurod1	-2.885	2.14E-06	0.007
Fezf1	-2.867	2.57E-05	0.012
Cbln2	-2.861	2.10E-05	0.012
Neurod2	-2.792	3.02E-05	0.013
Plxna4	-2.701	2.04E-05	0.012
Drbp1	-2.690	6.86E-05	0.017
Slc17a6	-2.683	2.76E-06	0.007
Acpl2	-2.663	3.30E-05	0.013
Abhd4	-2.646	5.35E-04	0.038
Bhlhb4	-2.643	2.68E-04	0.030
BC056349	-2.624	2.53E-06	0.007
Prdm16	-2.623	7.72E-04	0.044
Epha3	-2.612	6.75E-05	0.017
4933402J24Rik	-2.608	7.98E-07	0.004
Abtb2	-2.579	1.61E-05	0.012
Amph	-2.568	1.12E-05	0.009
Rwdd3	-2.533	6.11E-05	0.017
Sorbs2	-2.531	2.12E-05	0.012
D10Ertd610e	-2.529	1.26E-04	0.022
2810406K13Rik	-2.512	5.88E-06	0.008
A830082K12Rik	-2.479	1.06E-05	0.009
C630002B14Rik	-2.478	9.76E-06	0.009
Cbfa2t2	-2.471	3.56E-04	0.032
Kctd15	-2.470	8.02E-05	0.018
Nhlh2	-2.464	9.92E-06	0.009
Arpp21	-2.439	4.80E-06	0.008
Cck	-2.432	1.24E-06	0.005

Down-regulated Genes

Appendix B

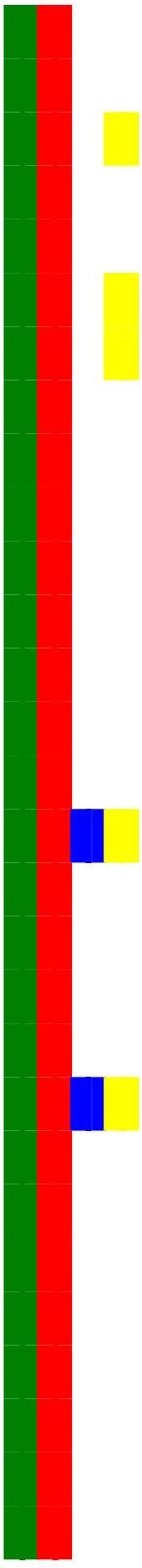

Gene	Fold Change	p-value	Adjusted p-value
Fjx1	-2.411	3.41E-04	0.032
AK081101	-2.403	6.67E-07	0.004
Epha3	-2.402	6.09E-06	0.008
TC1662444	-2.382	1.97E-04	0.027
Tnik	-2.377	2.34E-06	0.007
Serpini1	-2.377	7.66E-05	0.017
Rlbp1	-2.368	7.29E-05	0.017
NAP032887-1	-2.360	3.61E-04	0.032
Galnt14	-2.356	1.07E-05	0.009
Wdr47	-2.348	1.04E-04	0.020
Dmrta1	-2.325	2.35E-04	0.029
Itm2b	-2.306	5.04E-05	0.015
D12Ertd553e	-2.301	1.13E-05	0.009
Nr2f1	-2.262	7.02E-05	0.017
Serinc5	-2.258	1.28E-05	0.010
Tbr1	-2.250	1.91E-04	0.027
Ppp1r14a	-2.243	2.27E-04	0.028
D430039N05Rik	-2.238	2.76E-04	0.030
C130076O07Rik	-2.236	2.18E-05	0.012
X68951	-2.223	1.07E-05	0.009
Pde1b	-2.221	1.42E-05	0.011
Trak1	-2.219	1.23E-04	0.022
C130038G02Rik	-2.208	4.11E-04	0.034
Osbpl5	-2.199	4.74E-05	0.014
2610203C20Rik	-2.194	7.71E-04	0.044
Ryr3	-2.193	2.61E-07	0.004
Actr3b	-2.190	3.76E-05	0.014
Cbln2	-2.175	1.89E-05	0.012
Prss23	-2.169	5.89E-04	0.040

Down-regulated Genes

Appendix B

Gene	Fold Change	p-value	Adjusted p-value
BC026657	-2.169	1.85E-04	0.026
BC043118	-2.168	2.65E-05	0.012
CB590425	-2.145	3.56E-05	0.014
2310010M24Rik	-2.145	1.07E-05	0.009
Cxcl12	-2.129	2.38E-05	0.012
Lrrn3	-2.122	6.98E-05	0.017
Tmem163	-2.121	5.58E-04	0.039
Ppp1r1a	-2.111	2.50E-05	0.012
Glrx2	-2.108	6.55E-05	0.017
Cttnbp2	-2.108	1.14E-05	0.009
2610100L16Rik	-2.107	2.90E-04	0.031
Cbln2	-2.107	1.46E-05	0.011
6620401M08Rik	-2.102	1.42E-04	0.023
A830023I12Rik	-2.101	1.06E-03	0.050
Sema3g	-2.096	4.66E-05	0.014
Crkrs	-2.091	1.04E-04	0.020
Ppp2r2b	-2.090	3.09E-04	0.031
Stxbp1	-2.087	2.75E-04	0.030
Mfap4	-2.087	1.03E-04	0.020
Clk1	-2.086	2.42E-04	0.029
Bmf	-2.080	4.41E-06	0.007
Helt	-2.067	5.94E-05	0.016
D11Bwg0517e	-2.061	2.69E-05	0.013
Ppp2r2b	-2.054	7.88E-05	0.017
Spsb4	-2.045	1.01E-03	0.049
AK081751	-2.033	9.06E-05	0.018
Abcg1	-2.021	6.99E-06	0.009
Cdh4	-2.003	2.50E-05	0.012
Bhlhb5	-2.000	1.40E-04	0.023

Down-regulated Genes

Appendix B

Gene	Fold Change	p-value	Adjusted p-value
Sema5a	-1.995	3.25E-05	0.013
Dusp4	-1.991	8.89E-05	0.018
Tspan14	-1.981	2.85E-04	0.030
4933402J24Rik	-1.980	1.95E-05	0.012
Slc16a2	-1.966	7.06E-04	0.043
Rab6b	-1.959	6.07E-04	0.040
1300018I17Rik	-1.955	4.36E-04	0.035
Ndrg4	-1.947	4.38E-05	0.014
Dhrs4	-1.940	8.60E-05	0.018
Fbxo6	-1.938	6.93E-05	0.017
9630041G16Rik	-1.938	6.86E-06	0.009
Lhx9	-1.935	3.55E-04	0.032
Rpap1	-1.915	9.38E-05	0.018
TC1708996	-1.913	4.06E-04	0.034
Cyp51	-1.907	1.24E-04	0.022
Glrx2	-1.905	1.56E-04	0.024
Ptprd	-1.904	5.18E-05	0.015
Nfia	-1.898	3.40E-04	0.032
B230315N10Rik	-1.893	5.63E-04	0.039
Cntn2	-1.891	8.09E-05	0.018
Olfr74	-1.883	3.55E-04	0.032
Itm2b	-1.878	1.92E-04	0.027
LOC434179	-1.873	6.91E-04	0.042
Rkhd3	-1.865	2.74E-04	0.030
A730054J21Rik	-1.865	1.19E-04	0.021
Prdm15	-1.861	2.75E-04	0.030
CK347075	-1.852	5.09E-04	0.038
Scrt2	-1.850	3.08E-04	0.031
Hs3st3b1	-1.850	9.44E-04	0.047

Down-regulated Genes

Appendix B

Gene	Fold Change	p-value	Adjusted p-value
Dgkq	-1.850	5.12E-04	0.038
St18	-1.849	6.76E-04	0.041
Pcdh8	-1.847	2.69E-04	0.030
F2r	-1.845	7.97E-04	0.044
Plcd1	-1.840	1.88E-04	0.027
4931408A02Rik	-1.838	5.49E-04	0.039
5330426P16Rik	-1.830	9.80E-06	0.009
1190002H23Rik	-1.829	2.87E-04	0.031
Unc45a	-1.828	4.90E-04	0.037
3732412D22Rik	-1.827	1.39E-04	0.023
Traf4	-1.826	5.89E-04	0.040
Ndrg1	-1.825	5.39E-05	0.015
Zfp740	-1.821	4.78E-04	0.037
Ankib1	-1.819	7.34E-04	0.043
Wdr22	-1.818	6.74E-06	0.009
9830124H08Rik	-1.815	6.12E-04	0.040
4933427D14Rik	-1.814	7.01E-04	0.042
Rhbdl3	-1.811	1.45E-04	0.023
Pik3r3	-1.807	2.39E-04	0.029
Cttnbp2	-1.807	1.49E-04	0.024
Phlda1	-1.804	5.80E-04	0.039
Abca1	-1.803	7.61E-05	0.017
Ebf3	-1.802	4.17E-05	0.014
Eif4a2	-1.799	1.61E-04	0.024
Egr1	-1.790	6.32E-04	0.040
Edg2	-1.789	3.33E-05	0.013
Tbc1d23	-1.784	4.31E-04	0.035
1500041B16Rik	-1.780	9.28E-05	0.018
Tmem56	-1.778	2.29E-05	0.012

Down-regulated Genes

Appendix B

Gene	Fold Change	p-value	Adjusted p-value
Kcnn2	-1.777	8.60E-04	0.045
Baz2b	-1.776	5.29E-04	0.038
Rab8b	-1.767	1.53E-04	0.024
Wasf2	-1.767	3.67E-04	0.032
Slc4a10	-1.766	9.01E-06	0.009
Scube1	-1.764	8.44E-04	0.045
Sema6d	-1.762	9.20E-05	0.018
Sesn1	-1.761	6.52E-04	0.041
Dcamkl1	-1.757	8.40E-05	0.018
Gadd45a	-1.757	4.59E-04	0.036
Lrp11	-1.756	1.06E-03	0.050
Atp13a2	-1.755	3.92E-04	0.033
Zfyve27	-1.751	6.15E-04	0.040
Mzf6d	-1.747	2.62E-04	0.030
Hdac9	-1.743	3.92E-05	0.014
Gramd1b	-1.742	7.33E-04	0.043
Clk4	-1.736	5.37E-04	0.038
TC1650853	-1.733	2.88E-04	0.031
Dusp26	-1.730	1.55E-04	0.024
ENSMUST00000096347	-1.730	5.96E-04	0.040
5730409E15Rik	-1.729	4.07E-05	0.014
Cckar	-1.728	2.66E-04	0.030
C130076O07Rik	-1.728	2.74E-04	0.030
Ivd	-1.725	3.04E-04	0.031
BB180072	-1.715	2.18E-04	0.028
5031425E22Rik	-1.715	2.58E-05	0.012
LOC436154	-1.709	3.21E-04	0.032
Syt4	-1.707	6.44E-05	0.017
Id4	-1.706	7.22E-04	0.043

Down-regulated Genes

Appendix B

Gene	Fold Change	p-value	Adjusted p-value
Prkce	-1.706	7.72E-04	0.044
Kcnn2	-1.699	3.87E-04	0.033
NAP006594-001	-1.698	4.39E-04	0.035
LOC668644	-1.697	2.29E-04	0.029
Cotl1	-1.696	7.32E-04	0.043
Aplp1	-1.696	1.05E-03	0.050
Prei4	-1.695	1.61E-04	0.024
Clk4	-1.692	1.87E-05	0.012
NAP007437-001	-1.690	6.73E-05	0.017
AK038660	-1.689	7.25E-04	0.043
Tcte1	-1.687	3.02E-04	0.031
Has2	-1.686	7.58E-05	0.017
Foxk2	-1.683	6.45E-04	0.041
Ppp1r3g	-1.683	7.30E-05	0.017
BC029127	-1.677	4.45E-04	0.036
Cntnap2	-1.674	6.70E-04	0.041
Kcnn2	-1.674	3.95E-04	0.034
Ift81	-1.674	3.74E-04	0.033
Mapre2	-1.673	3.69E-04	0.033
NAP026611-1	-1.672	1.91E-04	0.027
Cyp26b1	-1.670	5.26E-04	0.038
Mszf33	-1.669	4.66E-04	0.036
Slc25a27	-1.668	9.38E-04	0.047
Napa	-1.666	8.32E-05	0.018
2310026E23Rik	-1.666	3.05E-04	0.031
Slc26a11	-1.664	7.74E-05	0.017
EG382421	-1.661	7.32E-05	0.017
Id2	-1.660	7.16E-04	0.043
Tspyl4	-1.660	3.22E-04	0.032

Down-regulated Genes

Appendix B

Gene	Fold Change	p-value	Adjusted p-value
Pcdh9	-1.656	2.16E-05	0.012
Dixdc1	-1.654	7.05E-05	0.017
Frmd5	-1.653	4.91E-04	0.037
Slc30a10	-1.651	7.36E-05	0.017
AK038173	-1.650	5.66E-04	0.039
Gramd1b	-1.649	5.71E-04	0.039
Rgs3	-1.649	2.36E-04	0.029
BC003993	-1.647	2.10E-04	0.028
1500011B03Rik	-1.647	3.04E-04	0.031
C230098O21Rik	-1.646	7.44E-04	0.043
Rhbdl3	-1.646	8.23E-05	0.018
2810409K11Rik	-1.645	2.31E-04	0.029
Bmpr1b	-1.644	5.96E-05	0.016
AI504432	-1.643	2.46E-05	0.012
Araf	-1.642	3.50E-04	0.032
Casp9	-1.641	7.43E-05	0.017
Kcnn2	-1.640	5.60E-04	0.039
NAP102548-1	-1.640	7.56E-04	0.043
LOC433801	-1.637	2.56E-04	0.030
Cog3	-1.637	3.62E-04	0.032
Mtap4	-1.637	9.17E-04	0.047
Sharpin	-1.637	8.75E-04	0.046
Rbm4b	-1.632	3.99E-04	0.034
LOC671029	-1.632	6.21E-04	0.040
Kcnn2	-1.631	6.57E-04	0.041
4931428F04Rik	-1.626	1.04E-03	0.050
Negr1	-1.625	8.27E-04	0.045
Jag1	-1.625	3.34E-04	0.032
Cul1	-1.621	7.15E-04	0.043

Down-regulated Genes

Appendix B

Gene	Fold Change	p-value	Adjusted p-value
LOC435970	-1.619	4.09E-04	0.034
Mszf81	-1.618	7.44E-04	0.043
Dcamkl1	-1.615	4.41E-04	0.035
NAP049942-1	-1.615	3.92E-04	0.033
Fbxl7	-1.614	3.20E-05	0.013
Serping1	-1.611	9.21E-04	0.047
Mterfd3	-1.609	1.07E-03	0.050
4922502B01Rik	-1.608	6.53E-05	0.017
Map1lc3b	-1.608	6.50E-04	0.041
AI836758	-1.606	7.53E-04	0.043
Cdc42ep4	-1.604	1.03E-03	0.049
AK039003	-1.600	8.84E-05	0.018
Chn2	-1.599	1.07E-03	0.050
BC021611	-1.599	1.05E-03	0.050
Polrmt	-1.597	8.79E-04	0.046
Arih1	-1.596	4.15E-04	0.034
Cugbp2	-1.594	3.61E-04	0.032
Emx2	-1.594	1.64E-04	0.025
1700025G04Rik	-1.588	4.57E-04	0.036
AB010317	-1.587	3.59E-04	0.032
Nxph1	-1.587	3.78E-04	0.033
Clk4	-1.586	3.10E-04	0.031
Slc39a11	-1.585	2.16E-04	0.028
Cntnap2	-1.585	4.54E-04	0.036
Dnajb6	-1.585	1.38E-04	0.023
Emx1	-1.584	5.01E-04	0.038
Rnf146	-1.584	1.02E-03	0.049
Slc25a27	-1.583	2.67E-04	0.030
E030049G20Rik	-1.583	1.32E-04	0.022

Down-regulated Genes

Appendix B

Gene	Fold Change	p-value	Adjusted p-value
Nkd1	-1.582	2.97E-04	0.031
Cd200	-1.582	3.97E-04	0.034
Tgfb2	-1.581	5.25E-04	0.038
Capza1	-1.581	8.65E-04	0.046
Tmcc1	-1.580	1.84E-04	0.026
EG667885	-1.580	3.82E-04	0.033
D10627	-1.579	1.02E-03	0.049
2900062L11Rik	-1.579	1.75E-04	0.025
Trappc3	-1.575	1.96E-04	0.027
Ddhd1	-1.573	1.82E-05	0.012
Efcbp2	-1.572	1.93E-04	0.027
Mapk7	-1.569	8.81E-04	0.046
Crmp1	-1.568	3.64E-04	0.032
Gamt	-1.567	4.58E-04	0.036
6720467C03Rik	-1.565	5.74E-05	0.016
Khdrbs2	-1.563	8.34E-04	0.045
Pts	-1.562	5.91E-04	0.040
Kcnn2	-1.560	7.27E-04	0.043
Hnrph1	-1.560	1.04E-03	0.050
Gamt	-1.560	2.69E-04	0.030
Adnp	-1.556	1.28E-04	0.022
Zfp74	-1.554	1.08E-04	0.020
Pla2g4b	-1.554	3.04E-04	0.031
Pepd	-1.551	6.72E-04	0.041
Sesn1	-1.550	4.88E-05	0.014
Smad7	-1.549	1.98E-04	0.027
6620401M08Rik	-1.543	5.26E-04	0.038
Nfil3	-1.542	1.00E-03	0.049
Mknk1	-1.541	6.94E-04	0.042

Down-regulated Genes

Appendix B

Gene	Fold Change	p-value	Adjusted p-value
Pkia	-1.539	1.31E-04	0.022
9430025M13Rik	-1.538	7.11E-05	0.017
Prokr1	-1.537	9.09E-05	0.018
Atf2	-1.535	2.77E-04	0.030
Pcdh9	-1.535	1.72E-04	0.025
Cyfip2	-1.534	2.04E-04	0.027
Prei4	-1.532	3.12E-04	0.031
4933426M11Rik	-1.531	4.86E-04	0.037
Galk2	-1.531	6.08E-04	0.040
Mafb	-1.528	9.98E-04	0.049
Slc2a13	-1.526	8.54E-05	0.018
AW208599	-1.524	7.08E-04	0.043
Rnf146	-1.524	1.53E-04	0.024
5730507N06Rik	-1.524	5.13E-04	0.038
Sema6a	-1.524	2.88E-05	0.013
Crtac1	-1.522	3.59E-04	0.032
5330438D12Rik	-1.520	7.57E-04	0.043
Mar-04	-1.518	1.38E-04	0.023
Zfp51	-1.518	5.33E-04	0.038
Nudt6	-1.517	4.33E-04	0.035
Mrcl	-1.515	3.49E-04	0.032
Atp2a2	-1.515	6.19E-04	0.040
Odc1	-1.513	5.79E-04	0.039
Gamt	-1.511	4.86E-04	0.037
Rb1cc1	-1.511	7.16E-04	0.043
Lcorl	-1.510	2.06E-04	0.027
BC043301	-1.508	1.93E-04	0.027
Zfp553	-1.502	1.03E-03	0.049
LOC631232	-1.502	9.79E-04	0.048

Down-regulated Genes

Appendix B

Gene	Fold Change	p-value	Adjusted p-value
Nckap1	-1.499	2.54E-04	0.029
3110023B02Rik	-1.499	6.07E-04	0.040
Gcg	-1.499	5.24E-04	0.038
Lypd6	-1.498	1.99E-04	0.027
EG631624	-1.497	3.98E-04	0.034
AK052115	-1.496	1.09E-04	0.020
A930009L07Rik	-1.495	2.19E-04	0.028
Setd6	-1.494	1.61E-04	0.024
Tbc1d19	-1.491	4.78E-04	0.037
Pgm2l1	-1.491	2.96E-04	0.031
Tnik	-1.491	1.03E-04	0.020
Gabrg2	-1.488	4.46E-04	0.036
A930038C07Rik	-1.487	6.66E-04	0.041
Pnrc1	-1.486	7.91E-04	0.044
Hspa4l	-1.485	1.79E-04	0.026
TC1653326	-1.483	6.84E-04	0.042
4932442K08Rik	-1.483	7.01E-04	0.042
Mlstd2	-1.482	2.38E-04	0.029
9330132A10Rik	-1.476	5.69E-04	0.039
Brms1l	-1.475	5.12E-04	0.038
Olfr450	-1.470	3.53E-04	0.032
Wdr44	-1.469	1.03E-04	0.020
Chrna6	-1.469	8.87E-04	0.046
Elavl2	-1.467	1.68E-04	0.025
LOC638058	-1.466	9.14E-04	0.047
Ryr1	-1.466	2.27E-04	0.028
Arl4a	-1.465	3.96E-04	0.034
Chgb	-1.464	1.07E-03	0.050
TC1666853	-1.463	2.93E-04	0.031

Down-regulated Genes

Appendix B

Gene	Fold Change	p-value	Adjusted p-value
NAP000001-064	-1.462	5.33E-04	0.038
D86419	-1.462	9.26E-04	0.047
Syt16	-1.459	3.47E-04	0.032
Nab2	-1.458	2.14E-04	0.028
6330439K17Rik	-1.457	1.28E-04	0.022
1190002N15Rik	-1.454	5.16E-04	0.038
6720475J19Rik	-1.453	3.44E-04	0.032
Rufy3	-1.451	8.58E-04	0.045
AK086756	-1.451	2.32E-04	0.029
Cxcl12	-1.449	1.05E-03	0.050
Ywhae	-1.446	3.12E-04	0.031
Zfp422-rs1	-1.443	8.06E-04	0.044
Gamt	-1.443	9.12E-04	0.047
Gipr	-1.442	7.58E-05	0.017
Ryr1	-1.442	6.21E-04	0.040
Rab6	-1.440	8.06E-04	0.044
Prss12	-1.440	6.38E-05	0.017
Igsf11	-1.439	4.52E-04	0.036
LOC195531	-1.439	7.39E-04	0.043
D10Bwg1379e	-1.438	3.91E-04	0.033
Btbd3	-1.436	9.35E-04	0.047
Chd9	-1.434	3.29E-04	0.032
TC1709027	-1.432	1.05E-03	0.050
2810426N06Rik	-1.431	2.79E-04	0.030
Gabrg2	-1.431	4.36E-04	0.035
Fbxo11	-1.425	1.05E-03	0.050
Smad3	-1.425	3.54E-04	0.032
Hmgn3	-1.423	2.62E-04	0.030
Plcl4	-1.422	3.55E-04	0.032

Down-regulated Genes

Appendix B

Gene	Fold Change	p-value	Adjusted p-value
TC1775183	-1.422	6.90E-04	0.042
Mtus1	-1.421	6.48E-04	0.041
Fcho2	-1.421	1.69E-04	0.025
Plxna4	-1.420	3.19E-04	0.032
Pde1c	-1.420	3.02E-04	0.031
Egr3	-1.419	5.66E-04	0.039
Steap1	-1.418	7.28E-04	0.043
Zfp85-rs1	-1.417	5.80E-04	0.039
Lrrcc1	-1.417	9.74E-05	0.019
Tmco3	-1.416	1.06E-03	0.050
Plch1	-1.416	3.23E-04	0.032
Otud7a	-1.416	6.21E-04	0.040
Btbd10	-1.416	9.01E-04	0.047
Lrrc4c	-1.415	8.77E-04	0.046
Tasp1	-1.412	8.75E-04	0.046
Wdr20a	-1.412	7.76E-04	0.044
Tspan32	-1.412	1.59E-04	0.024
Sypl	-1.411	1.03E-03	0.049
Kbtbd9	-1.410	2.69E-04	0.030
Zcchc2	-1.409	1.05E-03	0.050
Plcxd2	-1.409	5.98E-04	0.040
Pip5k1c	-1.408	6.19E-04	0.040
AK133399	-1.408	5.24E-04	0.038
Igsf21	-1.408	8.62E-04	0.045
Ccdc80	-1.408	3.38E-04	0.032
Ptpre	-1.406	1.98E-04	0.027
BC002059	-1.405	5.08E-04	0.038
Zfp95	-1.405	8.18E-04	0.044
Srr	-1.405	6.10E-04	0.040

Down-regulated Genes

Appendix B

Gene	Fold Change	p-value	Adjusted p-value
Zfp758	-1.403	9.36E-04	0.047
Slc7a7	-1.403	3.78E-04	0.033
LOC634588	-1.403	9.42E-04	0.047
CJ326049	-1.399	2.55E-04	0.029
Adamts3	-1.399	3.88E-04	0.033
Ghitm	-1.397	6.87E-04	0.042
Ubox5	-1.397	1.01E-03	0.049
TC1635888	-1.395	3.19E-04	0.032
Spnb2	-1.395	5.19E-04	0.038
Taf1a	-1.395	9.94E-04	0.049
Map4k3	-1.395	9.15E-04	0.047
A130090K04Rik	-1.395	3.38E-04	0.032
Apc2	-1.392	9.03E-04	0.047
NAP102683-1	-1.392	9.74E-04	0.048
Pak7	-1.392	5.03E-04	0.038
Tmem176b	-1.391	5.40E-04	0.038
Zfp1	-1.391	8.57E-04	0.045
Tns3	-1.391	2.03E-04	0.027
1200016B10Rik	-1.389	8.19E-04	0.044
Spock2	-1.389	7.61E-04	0.043
D330050I23Rik	-1.388	4.73E-04	0.036
NAP048198-1	-1.386	8.30E-04	0.045
Trim9	-1.386	8.10E-04	0.044
Vps53	-1.384	8.33E-04	0.045
Fgf13	-1.381	9.49E-04	0.047
Syn2	-1.380	9.64E-04	0.048
Dusp14	-1.379	9.22E-04	0.047
Kit	-1.378	4.04E-04	0.034
Prr15	-1.378	1.63E-04	0.024

Down-regulated Genes

Appendix B

Gene	Fold Change	p-value	Adjusted p-value
Wwc1	-1.375	4.32E-04	0.035
Spcs3	-1.374	3.70E-04	0.033
Ng23	-1.374	7.14E-04	0.043
Lrch2	-1.373	6.70E-04	0.041
Robo2	-1.373	2.61E-04	0.030
Fzd10	-1.372	9.16E-04	0.047
4933435A13Rik	-1.371	3.37E-04	0.032
C130081A10Rik	-1.371	9.91E-04	0.049
Dscr6	-1.369	6.15E-04	0.040
Epha7	-1.368	1.41E-04	0.023
Olfr56	-1.368	5.20E-04	0.038
4930432O21Rik	-1.366	6.27E-04	0.040
Pcdhb17	-1.365	9.49E-04	0.047
1300010F03Rik	-1.365	4.62E-04	0.036
LOC433801	-1.364	5.14E-04	0.038
Osbpl8	-1.363	8.12E-04	0.044
ENSMUST00000036296	-1.362	5.39E-04	0.038
Gpr75	-1.362	9.05E-04	0.047
BC065397	-1.362	2.32E-04	0.029
Wdr37	-1.361	2.70E-04	0.030
Edg2	-1.361	8.59E-04	0.045
BB456595	-1.360	8.40E-04	0.045
A530058N18Rik	-1.359	2.22E-04	0.028
Cnot8	-1.358	5.44E-04	0.039
Prss34	-1.357	8.99E-04	0.047
1700047I17Rik	-1.355	7.75E-04	0.044
Sh3yl1	-1.354	1.06E-03	0.050
Bpnt1	-1.350	2.48E-04	0.029
8430426H19Rik	-1.350	5.87E-04	0.040

Down-regulated Genes

Appendix B

Gene	Fold Change	p-value	Adjusted p-value
Dnajc6	-1.350	8.29E-04	0.045
Pro25G	-1.347	1.03E-03	0.049
3732412D22Rik	-1.347	2.96E-04	0.031
Tmem163	-1.346	4.08E-04	0.034
Sox13	-1.341	7.08E-04	0.043
Pigg	-1.341	9.74E-04	0.048
Pvr	-1.340	2.09E-04	0.028
1810011O10Rik	-1.339	4.55E-04	0.036
Plfr	-1.337	5.90E-04	0.040
Zfp263	-1.336	6.62E-04	0.041
Ppp1r3d	-1.336	2.20E-04	0.028
LOC434179	-1.333	1.05E-03	0.050
Tkt	-1.330	1.03E-03	0.049
Tnik	-1.329	5.56E-04	0.039
AI452195	-1.328	6.66E-04	0.041
Rsu1	-1.326	1.06E-03	0.050
4933407L21Rik	-1.326	7.08E-04	0.043
Hhat	-1.325	7.87E-04	0.044
Zdhhc8	-1.324	9.48E-04	0.047
TC1640689	-1.323	6.92E-04	0.042
AK078994	-1.317	5.27E-04	0.038
Grrp1	-1.316	1.01E-03	0.049
Adcyap1	-1.311	9.92E-04	0.049
5730508B09Rik	-1.306	6.18E-04	0.040
Elovl7	-1.303	9.35E-04	0.047
AI585793	-1.301	5.53E-04	0.039
Cadps2	-1.298	6.25E-04	0.040
BC049806	-1.295	7.35E-04	0.043
Zbtb6	-1.294	7.96E-04	0.044

Down-regulated Genes

Appendix B

Gene	Fold Change	p-value	Adjusted p-value
Spats1	-1.292	6.16E-04	0.040
2310002A05Rik	-1.288	9.15E-04	0.047
Arl8b	-1.285	9.93E-04	0.049
Chl1	-1.282	9.15E-04	0.047
Olfr1519	-1.278	9.66E-04	0.048
NP431110	-1.276	6.37E-04	0.040
9430091E24Rik	-1.275	7.52E-04	0.043
Srr	-1.274	7.71E-04	0.044
Spats1	-1.271	9.64E-04	0.048
Pfkfb2	-1.270	1.06E-03	0.050
3021401N23Rik	-1.268	8.85E-04	0.046